



University  
of Glasgow

Roccisana, Jennifer (2010) *The role of mVps45 in regulating GLUT4 trafficking in 3T3L1 adipocytes*. PhD thesis.

<http://theses.gla.ac.uk/2334/>

Copyright and moral rights for this thesis are retained by the author

A copy can be downloaded for personal non-commercial research or study, without prior permission or charge

This thesis cannot be reproduced or quoted extensively from without first obtaining permission in writing from the Author

The content must not be changed in any way or sold commercially in any format or medium without the formal permission of the Author

When referring to this work, full bibliographic details including the author, title, awarding institution and date of the thesis must be given

# **THE ROLE OF mVPS45 IN REGULATING GLUT4 TRAFFICKING IN 3T3L1 ADIPOCYTES**

A thesis submitted to the  
FACULTY OF BIOMEDICAL AND LIFE SCIENCES

For the degree of  
DOCTOR OF PHILOSOPHY

By  
Jennifer Roccisana

Division of Molecular and Cellular Biology  
Faculty of Biomedical and Life Sciences  
University of Glasgow

September 2010

## Abstract

Insulin stimulates glucose transport in fat cells by inducing the movement of glucose transporters (Glucose transporter-4) from specialised storage vesicles to the plasma membrane. Insulin resistant individuals and those with Type II Diabetes exhibit impairment in the ability of insulin to stimulate glucose transport. The molecular mechanisms of glucose transporter-4 trafficking in adipocytes are an important focus in understanding the underlying etiology of this disease.

Glucose transporter-4 (GLUT4) recycles between the plasma membrane and intracellular stores in the absence of insulin using a complex intracellular pathway. This involves two intracellular cycles: one is the prototypical endosomal system, the other a specialised cycle involving the trans-Golgi network and a sub-set of intracellular vesicles called GSVs (the slow cycle). Understanding the control of the entry into this second cycle is the subject of this thesis. In particular, the work in this thesis will examine the role of Syntaxin 16 and its cognate Sec1/Munc18 protein mammalian Vps45 (mVps45).

The regulation of Syntaxin 16 has not been fully elucidated and understanding the role of Syntaxin 16 in SNARE complex regulation and subsequent control of GLUT4 traffic into the slow cycle requires an understanding of its cognate binding partner Sec1/Munc18 (SM) protein, mammalian Vps45 (mVps45).

The absolute levels of both Syntaxin 16 and mVps45 were quantified and found to be present in 3T3-L1 adipocytes in roughly stoichiometric amounts. IP experiments also showed the ability of mVps45 to interact with Syntaxin 16 in the absence of insulin.

Using the model eukaryote *Saccharomyces cerevisiae*, we found that mVps45 could complement for the deletion of Vps45p. Assays for CPY secretion showed that mVps45 is able to complement for the loss of Vps45p function in the trafficking of carboxypeptidase Y (CPY). Additionally, mVps45 mutants were made that correspond to yeast mutants made previously in the lab and were tested for homology of function.

Depleting 3T3-L1 adipocytes of mVps45 showed alterations in the levels of GLUT4 protein as well as the protein levels of Syntaxin 16, IRAP, and Rabenosyn. Insulin-stimulated deoxyglucose uptake was also profoundly decreased upon depletion of mVps45. Further experiments using mVps45 depleted cells show that these cells lose their sensitivity to insulin and that the loss of mVps45 in these cells causes GLUT4 to have the inability to enter the slow cycle.

Taken together, these findings demonstrate that mVps45 has a role in allowing GLUT4 entry into the slow cycle.

# Table of Contents

<b>Abbreviations .....</b>	<b>16</b>
<b>Chapter 1</b>	
<b>1. INTRODUCTION .....</b>	<b>23</b>
<b>1.1 Diabetes and the Role of Insulin .....</b>	<b>23</b>
1.1.1 Endemic problem of Diabetes.....	23
1.1.2 Function of insulin.....	24
<b>1.2 Trafficking of GLUT4 .....</b>	<b>27</b>
1.2.1 Intracellular location of GLUT4 .....	28
1.2.2 Generation and function of glucose storage vesicles.....	30
1.2.3 Membrane trafficking .....	34
<b>1.3 SNAREs .....</b>	<b>35</b>
1.3.1 Classification of SNAREs .....	36
1.3.2 Structure of SNAREs .....	38
1.3.3 The Syntaxins.....	39
1.3.4 The SNARE Hypothesis .....	43
1.3.5 SNAREs involved in GLUT4 traffic to the plasma membrane.....	43
1.3.6 SNAREs in intracellular traffic and the role of Syntaxins 6 and 16.....	43
<b>1.4 SM Proteins.....</b>	<b>45</b>
1.4.1 Regulation of SNARE Complex formation .....	46
1.4.2 Munc18c and the regulation of Glucose Transport .....	51
<b>1.5 mVps45.....</b>	<b>53</b>
1.5.1 mVps45 as a Class D SM Protein.....	53
1.5.2 Syntaxin 16.....	54
1.5.3 The role of mVps45 in binding to Syntaxin 16 .....	54
1.5.4 The yeast homolog Vps45p .....	55
<b>1.6 The Yeast Model .....</b>	<b>56</b>
1.6.1 Yeast metabolism and the Endocytic pathway .....	57
1.6.2 The Secretory Pathway .....	58
1.6.3 Membrane fusion and homology to the Mammalian System .....	59
1.6.4 The Syntaxin homolog Tlg2p .....	60
<b>1.7 Hypothesis .....</b>	<b>60</b>
<b>1.8 Aims.....</b>	<b>61</b>

## Chapter 2

<b>2. MATERIALS AND METHODS .....</b>	<b>65</b>
<b>2.1 Materials.....</b>	<b>65</b>
2.1.1 Common Reagents and Suppliers .....	65
2.1.2 Computer Software.....	67
2.1.3 Primers .....	67
2.1.4 Plasmids .....	68
2.1.5 <i>E. coli</i> Strains.....	69
2.1.6 <i>S. cerevisiae</i> Strains .....	69
2.1.7 Cell Culture materials, media, solutions and cell lines ...	70
2.1.8 Primary Antibodies.....	71
2.1.9 Secondary Antibodies.....	72
2.1.10 General Solutions .....	73
<b>2.2 DNA Methods .....</b>	<b>75</b>
2.2.1 Generation of target DNA and sequencing .....	75
2.2.2 Amplification of target DNA by PCR .....	75
2.2.3 Agarose gel electrophoresis .....	76
2.2.4 Gel Extraction of DNA.....	76
2.2.5 A Tail reaction and TA Cloning .....	77
2.2.6 Restriction Digestion.....	77
2.2.7 Ligation .....	77
2.2.8 Transformation of <i>E. Coli</i> .....	78
2.2.9 Small and large scale DNA isolation.....	79
2.2.10 Determination of DNA concentration .....	80
<b>2.3 Protein Methods.....</b>	<b>81</b>
2.3.1 Protein purification by Nickel NTA Method .....	81
2.3.2 Protein purification with thrombin cleavage .....	81
2.3.3 Trichloroacetic Acid precipitation .....	82
2.3.4 Immunoprecipitation .....	82
2.3.5 SDS Gel Electrophoresis and transfer to Nitrocellulose.....	83
2.3.6 Western blotting.....	84
2.3.7 Coomassie staining .....	85
2.3.8 Protein concentration determination (MicroBCA).....	85
<b>2.4 Cell Culture Methods.....</b>	<b>86</b>
2.4.1 Growth, trypsinisation and passage of cells.....	86
2.4.2 Freezing down and resurrection of cells .....	87
2.4.3 Cell treatment and preparation of homogenates.....	88
2.4.4 Glucose Transport Assay .....	89
2.4.5 Confocal Microscopy and staining .....	91
<b>2.5 Virus Generation and Expression .....</b>	<b>92</b>
2.5.1 Construction of shRNA .....	92
2.5.2 Ligation into retroviral vector.....	93
2.5.3 Transfection into EcoPack2-293 and virus collection.....	94
2.5.4 Determining viral titer in NIH3T3 cells.....	95

2.5.5	Infection of adipocytes and subsequent differentiation ..	95
2.5.6	Recycling Assay using HA-GLUT4-GFP cells.....	95
2.5.7	Subcellular Fractionation .....	96
2.5.8	The Budding Assay.....	97
2.5.9	Iodixanol Gradients.....	98
<b>2.6</b>	<b>Yeast Methods .....</b>	<b>98</b>
2.6.1	Construction of plasmid by homologous recombination.....	98
2.6.2	Transformation of plasmids into yeast cells .....	99
2.6.3	Plasmid Rescue.....	100
2.6.4	Construction of mutants by site-directed mutagenesis	100
2.6.5	Preparation of yeast lysates for SDS-PAGE.....	101
2.6.6	Invertase Assay- TCA precipitation method.....	101
2.6.7	CPY Invertase Assay- Colorimetric method.....	102
2.6.8	Complementation by spot plate method .....	102

## Chapter 3

<b>3.</b>	<b>ENDOGENOUS LEVELS OF SYNTAXIN 16 AND mVPS45 IN ADIPOCYTES .....</b>	<b>105</b>
<b>3.1</b>	<b>Introduction.....</b>	<b>105</b>
3.1.1	The location of Syntaxin 16 and mVps45 .....	105
3.1.2	Interactions between Syntaxin 16 and mVps45.....	105
3.1.3	The effects of insulin stimulation on endogenous levels of Syntaxin 16, mVps45 and their interaction....	105
<b>3.2</b>	<b>Aims.....</b>	<b>106</b>
<b>3.3</b>	<b>Results.....</b>	<b>106</b>
3.3.1	Construction and purification of mVps45 .....	106
3.3.2	The Purification of Syntaxin 16 .....	108
3.3.3	Changes in intracellular protein levels upon 3T3L1 cell differentiation .....	109
3.3.4	Expression of Syntaxin 16 in Adipocytes .....	112
3.3.5	Expression of mVps45 in Adipocytes.....	113
3.3.6	Levels of Syntaxin 16 and mVps45 in Fibroblasts .....	115
3.3.7	Levels of Syntaxin 16 and mVps45 in Rat Primary Cells .....	116
3.3.8	Analysis of Endogenous Syntaxin 16 and mVps45 expression using the standard curve method and calculation of copy number per cell.....	118
3.3.9	The Co-Immunoprecipitation of Syntaxin 16 and mVps45.....	120
<b>3.4</b>	<b>Discussion .....</b>	<b>121</b>

## Chapter 4

<b>4. THE YEAST MODEL IN UNDERSTANDING mVPS45 FUNCTION .....</b>	<b>125</b>
<b>4.1 Introduction .....</b>	<b>125</b>
4.1.1 Homology between yeast and mammalian Vps45 .....	125
4.1.2 Complementation between the behaviour of Vps45p and mVps45 .....	125
4.1.3 Use of yeast mutants to screen for mVps45 function..	126
<b>4.2 Aims .....</b>	<b>126</b>
<b>4.3 Results .....</b>	<b>126</b>
4.3.1 Construction of the rat recombinant .....	126
4.3.2 Expression of the recombinant in yeast cells .....	128
4.3.3 Construction of yeast mutants.....	129
4.3.4 Expression of the recombinant and yeast mutants in wildtype and delete cells .....	130
4.3.5 CPY Assay- TCA Precipitation.....	131
4.3.6 CPY Invertase Assay- Colorimetric Assay .....	133
4.3.7 Spot Plate Complementation .....	134
4.3.8 Expression of Tlg2p in mVps45 mutants.....	139
<b>4.4 Discussion.....</b>	<b>141</b>

## Chapter 5

<b>5. GENERATION OF mVPS45 KNOCKDOWN AND EXPRESSION OF INTRACELLULAR FACTORS IN 3T3L1 ADIPOCYTES .....</b>	<b>144</b>
<b>5.1 Introduction.....</b>	<b>144</b>
<b>5.2 Aims.....</b>	<b>145</b>
<b>5.3 Results.....</b>	<b>145</b>
5.3.1 Construction of shRNA targets .....	145
5.3.1.1 GFP control of transfection.....	147
5.3.2 Immunoblots of mVps45 knockdown .....	148
5.3.3 Immunoblots of the intracellular environment .....	150
5.3.4 Confocal Images of GLUT4 Translocation .....	157
5.3.5 Glucose Transport Assays.....	159
5.3.6 Budding Assay.....	165
5.3.7 Recycling Assay with HA-GLUT4-GFP .....	167
5.3.8 Subcellular Fractionation .....	169
5.3.9 Iodixanol Gradients.....	170

5.4 Discussion .....	172
<b>Chapter 6</b>	
6. CONCLUSIONS AND FUTURE DIRECTIONS .....	177
6.1 Endogenous levels and binding of Syntaxin 16 and mVps45.....	178
6.2 Yeast Model of Vps45 mutants and Complementation .....	179
6.3 Effects of mVps45 knockdown on the intracellular environment.....	180
<b>Bibliography .....</b>	<b>183</b>

## List of Tables

Table 1.1 - Classification of SNAREs .....	39
Table 2.1.3- Primers.....	67
Table 2.1.4- Plasmids .....	68
Table 2.1.5- <i>E. coli</i> Strains .....	69
Table 2.1.6- <i>S. cerevisiae</i> Strains .....	69
Table 2.1.7- Cell Lines .....	71
Table 2.1.8- Primary Antibodies .....	71
Table 2.1.9- Secondary Antibodies .....	72
Table 3.1 - Quantification of SNARE protein levels.....	119

## List of Figures

### Chapter 1

Figure 1.1-	GLUT4 is the glucose transporter involved in Glucose Uptake.....	30
Figure 1.2-	The slow recycling pathway .....	32
Figure 1.3-	The distribution of SNAREs in the adipocyte .....	38
Figure 1.4-	The closed and open conformations of the syntaxins ...	40
Figure 1.5-	SNARE structure has functional consequences.....	40
Figure 1.6-	The SNARE hypothesis .....	41
Figure 1.7-	SM proteins bind to their cognate t-SNARE .....	49
Figure 1.8a-	The functional role of SM proteins in regulating membrane fusion.....	50
Figure 1.8b-	SM Modes of Binding.....	50
Figure 1.9-	Insulin may trigger GLUT4 translocation through the regulatory role of Munc18c.....	52
Figure 1.10-	The endocytic and secretory pathways in yeast.....	58
Figure 1.11-	Sorting of GLUT4 into the slow recycling pathway may be mVps45 dependent .....	61

### Chapter 3

Figure 3.1-	The construction of pCMV-mVps45 .....	107
Figure 3.2-	The Purification of mVps45 .....	108
Figure 3.3-	The Purification of Syntaxin 16 .....	109
Figure 3.4-	Oil Red O Staining of Basal Cells .....	110
Figure 3.5-	Differentiation of 3T3-L1 adipocytes causes changes in cellular protein levels.....	111
Figure 3.6-	Quantification of the levels of Syntaxin 16 in	

	membranes from basal cells .....	112
Figure 3.7a-	Quantification of the levels of mVps45 in 3T3-L1 membranes and cytosol from basal cells .....	113
Figure 3.7b-	Quantification of the levels of mVps45 in 3T3-L1 membranes and cytosol from insulin-stimulated cells .....	114
Figure 3.8a-	Quantification of the levels of Syntaxin 16 in 3T3-L1 fibroblast cells .....	115
Figure 3.8b-	Quantification of the levels of mVps45 in 3T3-L1 fibroblast cells.....	116
Figure 3.9a-	Quantification of the levels of Syntaxin 16 in Rat Primary Adipocytes .....	117
Figure 3.9b-	Quantification of the levels of mVps45 in Rat Primary Adipocytes .....	118
Figure 3.10a-	Syntaxin 16 Co-Immunoprecipitates with mVps45.....	120
Figure 3.10b-	mVps45 Co-Immunoprecipitates with Syntaxin 16 .....	121

#### **Chapter 4**

Figure 4.1-	The method of Homologous Recombination allows mammalian Vps45 to be expressed in yeast.....	127
Figure 4.2-	Mammalian Vps45 expression in transformed cells ....	128
Figure 4.3-	HA-tagged mammalian Vps45 expressed in yeast delete cells .....	130
Figure 4.4-	The TCA Secretion Assay .....	132
Figure 4.5-	Secretion of Invertase .....	133
Figure 4.6-	Expression of mVps45 pocket-fill mutants complement the osmotic sensitivity phenotype of Vps45 mutants .....	135
Figure 4.7-	Expression of mVps45 dominant-negative mutants complement the osmotic sensitivity phenotype of Vps45 mutants .....	136
Figure 4.8-	Expression of mVps45 double mutants complement the osmotic sensitivity phenotype of Vps45 mutants...	136

Figure 4.9-	Expression of mVps45 pocket-fill mutants complement the temperature sensitivity phenotype of Vps45 mutants .....	137
Figure 4.10-	Expression of mVps45 dominant-negative mutants complement the temperature sensitivity phenotype of Vps45 mutants .....	138
Figure 4.11-	Expression of mVps45 double mutants complement the temperature sensitivity phenotype of Vps45 mutants .....	138
Figure 4.12-	Expression of mammalian Vps45 stabilises cellular Levels of Tlg2p, the yeast homologue of Syntaxin 16 .....	139

## Chapter 5

Figure 5.1-	Packaging of the shRNA virus using EcoPack2-293 cells .....	147
Figure 5.2-	Viral packaging cells are analysed for transfection efficiency using a GFP reporter plasmid.....	148
Figure 5.3-	mVps45 is knocked down in 3T3-L1 adipocytes .....	149
Figure 5.4a-	The effect of mVps45 depletion on intracellular proteins .....	151
Figure 5.4b-	Densitometric analysis of the effect of mVps45 depletion on intracellular proteins.....	152
Figure 5.5a-	The effect of mVps45 depletion on proteins involved in membrane fusion.....	153
Figure 5.5b-	Densitometric analysis of the effect of mVps45 depletion on proteins .....	154
Figure 5.6-	Proteins involved in membrane fusion .....	155
Figure 5.7-	The effect of mVps45 depletion on differentiation proteins .....	156
Figure 5.8-	GLUT4 is translocated to the plasma membrane in response to Insulin-stimulation .....	158
Figure 5.9a-	Effect of mVps45 depletion by viral targeting on basal and insulin-stimulated deoxyglucose uptake	

in 3T3-L1 adipocytes .....	159
Figure 5.9b- Effect of mVps45 depletion by best viral construct on basal and insulin-stimulated deoxyglucose uptake in 3T3-L1 adipocytes .....	160
Figure 5.10a- Analysis of the maximum glucose transport in wildtype and mVps45 depleted 3T3-L1 adipocytes .....	162
Figure 5.10b- Analysis of the maximal concentration-dependence of Insulin- stimulated deoxyglucose uptake in wildtype and mVps45 depleted 3T3-L1 adipocytes ....	162
Figure 5.11a- Time course of the maximal percentage of the reversal of insulin-stimulated 2-Deoxy-D-Glucose transport in control and mVps45 knockdown 3T3-L1 adipocytes .....	164
Figure 5.11b- Time course of the reversal of Insulin-stimulated 2-Deoxy-D-Glucose Transport in control and mVps45 knockdown 3T3-L1 adipocytes .....	164
Figure 5.12a- Budding of vesicles in Wildtype Cells.....	166
Figure 5.12b- Budding of vesicles in Knockdown Cells.....	166
Figure 5.13a- The Recycling Assay .....	168
Figure 5.13b- The Recycling Assay normalized for HA-GLUT4-GFP Expression .....	168
Figure 5.14- The subcellular distribution of proteins in basal and Insulin-stimulated 3T3-L1 adipocytes depleted of mVps45 .....	169
Figure 5.15- Iodixanol equilibrium gradient sedimentation analysis of wildtype and knockdown 3T3-L1 adipocytes .....	171
 <b>Chapter 6</b>	
Figure 6.1- The effect of mVps45 on GLUT4 sorting into the slow recycling pathway.....	178

## Acknowledgements

I would like to thank my supervisor Professor Gwyn Gould for all the support, patience and advice that he has given me throughout the Ph.D. process.

I would also like to thank Dr. Nia J. Bryant for many helpful discussions, advice and encouragement and everyone in Lab 241, past and present, for their support. In particular, I would like to thank my wonderful friend Dr. Pamela Jane Logan who kept me going with her support, understanding and unwavering friendship.

I must also say a special thanks to Dr. Scott Shanks, who has been a great resource and support throughout this endeavour, Dr. Jolanta Wiejak for excellent advice and several helpful discussions and Mr. Alasdair Boyd for his efforts on the recycling experiment. A special note of gratitude must also go to Mr. Alistair Whitelaw for his tenacity and wisdom. Thanks also to the MacArthur Foundation for funding this studentship.

Finally, profound gratitude must go to my parents, Larry and Alice, who have always encouraged me and instilled in me a deep value for learning.

## **Declaration**

I declare that the work presented in this thesis has been carried out by me, unless otherwise stated. It is entirely of my own composition and has not, in whole, or in part been submitted for any other degree.

Jennifer Roccisana

September 2010

## Abbreviations

2μ	Two Micron
aa	amino acid
amp	ampicillin
APS	Ammonium Persulphate
BME	β-Mercaptoethanol
BSA	Bovine Serum Albumin
°C	degrees Celsius
CaCl <sub>2</sub>	calcium chloride
Cat#	catalog number
cDNA	complementary DNA
C/EBPα	CAAT/enhancer-binding protein alpha
<i>CEN</i>	centromeric
cfu	colony forming units
CPY	carboxypeptidase Y
Cyto	cytosolic
deGlc	2-Deoxy-D-Glucose
DMEM	Dulbecco's modified Eagle Medium
DMF	dimethyl formamide
DMSO	dimethyl sulfoxide
DNA	deoxyribonucleic acid
DNase I	deoxyribonuclease I
dNTP	deoxynucleoside (5')-triphosphate
ds	double-stranded

DTT	Dithiothreitol
<i>E. coli</i>	<i>Escherichia coli</i>
ECL	enhanced chemiluminescence
EDTA	Ethylenediaminetetraacetic Acid
EEA-1	early endosome antigen 1
EtBr	ethidium bromide
EtOH	ethanol
FAS	Fatty Acid Synthase
FCS	Fetal Calf Serum
g	gram
<i>g</i>	gravitational force
GFP	Green Fluorescent Protein
GLUT	Glucose Transporter protein isoform
GSV	GLUT4 storage vesicle
h	hour
H <sub>2</sub> O <sub>2</sub>	Hydrogen peroxide
HA	Influenza hemagglutinin epitope tag
HAc	Acetic Acid
HCl	Hydrochloric Acid
HDM	high density microsome
HEPES	2-[4-(2-Hydroxyethyl)-1-piperazine]ethanesulfonic Acid
His <sub>6</sub>	six histidine residue tag
hrs	hours
HRP	Horse Radish Peroxidase
IBMX	Isobutylxanthine

IgG	Immunoglobulin G
IP	Immunoprecipitation
IPTG	Isopropyl $\beta$ -D-1-thiogalactopyranoside
IRAP	Insulin-responsive aminopeptidase
Kan	Kanamycin
kb	kilobase
kDa	kiloDalton
KCl	potassium chloride
$K_2HPO_4$	dipotassium hydrogen orthophosphate
$KH_2PO_4$	potassium dihydrogen orthophosphate
KOAc	potassium acetate
KOH	potassium hydroxide
KPi	potassium phosphates buffer
KRH	Krebs Ringer HEPES
KRP	Krebs Ringer Phosphate
L	liter
LDM	low density microsome
LiOAc	lithium acetate
LiTE-Sorb	lithium acetate tris EDTA Sorbital
LSB	Laemmli sample buffer
$\mu$	micro
$\mu$ g	microgram
$\mu$ l	microliter

$\mu\text{M}$	micromolar
M	molar
mA	milliamp
mg	milligram
$\text{MgCl}_2$	magnesium chloride
$\text{MgSO}_4$	magnesium sulphate
min	minute, minutes
ml	millilitre
mM	millimolar
MOI	multiplicity of infection
MWCO	molecular weight cut off
nm	nanometers
NaCl	Sodium Chloride
$\text{Na}_2\text{HPO}_4$	disodium hydrogen orthophosphate
$\text{NaN}_3$	Sodium azide
NaOH	Sodium Hydroxide
NCS	Newborn calf serum
NEM	N-ethylmaleimide
NSF	N-ethylmaleimide-sensitive factor
Ni-NTA	Nickel ( $\text{Ni}^{2+}$ )-nitrilotriacetic acid
$\text{OD}_{600}$	optical density at 600nm
ORF	open reading frame
pfu	plaque forming units
P/S	Penicillin/Streptomycin
PBS	Phosphate buffered saline

PBST	Phosphate buffered saline with 0.1% Tween-20
PCR	Polymerase Chain Reaction
PFA	paraformaldehyde
PM	plasma membrane
PMSF	Phenylmethanesulphonylfluoride
PPAR $\gamma$	Peroxisome proliferator activated receptor gamma
PrA	protein A
<i>R. norvegicus</i>	<i>Rattus norvegicus</i>
rpm	revolutions per minute
RT	room temperature (22-25°C)
<i>S. cerevisiae</i>	<i>Saccharomyces cerevisiae</i>
SD	yeast synthetic media, dextrose
SDM	site-directed mutagenesis
SDS	Sodium dodecyl sulphate
SDS-PAGE	Sodium dodecyl sulphate polyacrylamide gel electrophoresis
sec	second
SM	Sec1p/Munc18
SNAP23	23kDa synaptosome-associated protein
SNARE	Soluble NSF attachment protein receptor
SOC	Super Optimal Broth
Sx	Syntaxin
TAE	Tris acetic acid EDTA
<i>Taq</i>	<i>Thermus aquaticus</i>

TB	Terrific Broth
TBS-T	Tris buffered saline with 0.1% Tween-20
TCA	Trichloroacetic Acid
TE	Tris-EDTA
TEMED	N, N, N', N' - Tetramethylethylenediamine
TfR	Transferrin Receptor
TGN	trans-Golgi network
Tlg2p	t-SNARE of the late Golgi compartment 2
Tm	melting temperature
t-SNARE	target SNARE
Tris	2-amino-2-(hydroxymethyl)-1,3-Propanediol
TST	Tris-Saline-Tween
Tween-20	Polyoxyethylene sorbitan Monolaurate
U	Unit
UTR	untranslated region
VPS	Vacuolar protein sorting
v-SNARE	vesicle SNARE
v/v	volume per volume
w/v	weight per volume
X-gal	X-Gal (5-bromo-4-chloro-3-indolyl- $\beta$ -D-galactopyranoside)
YPD	yeast extract, peptone, dextrose
YT	yeast extract, tryptone, NaCl

## **Chapter 1 – Introduction**

# Chapter 1: Introduction

## 1.1 Diabetes and the Role of Insulin

### 1.1.1 Endemic of Diabetes

Diabetes mellitus is a global epidemic affecting approximately 150 million people worldwide, a figure which will double by the year 2025 (DeFronzo, 1992). The majority (90%) of these cases are of the type II form. Type II diabetes is a chronic disease characterised by defective insulin action, a condition known as insulin resistance. The incidence of insulin resistance and Type II diabetes is endemic to a culture that adheres to a high sugar, high fat diet and a sedentary lifestyle.

Insulin resistance places a greater demand on the pancreas to produce insulin leading to hyperinsulinaemia. Insulin stimulates glucose transport into fat and muscle by regulating the translocation of the facilitative glucose transporter GLUT4 from an intracellular store to the cell surface (Birnbaum et al., 1992). Upon binding to its receptor on the surface of fat and muscle cells, insulin initiates a signalling cascade that culminates in changes in the trafficking itinerary of GLUT4, releasing it from its intracellular store and delivering it to the cell surface (Zaid et al., 2008). Individuals with insulin resistance and Type 2 diabetes exhibit defective insulin-stimulated GLUT4 translocation (Birnbaum et al., 1992; Charron et al., 1989) consequently, much effort has gone into defining the trafficking of GLUT4 in adipocytes and muscle.

GLUT4 is a facilitative glucose transporter that transports glucose down its concentration gradient into the cell in an energy-independent manner. It is a membrane protein with 12 transmembrane domains (as shown in Figure 1.1). There are 13 known members of the GLUT family of proteins (GLUT1-13) which can be divided into 3 classes. Class I includes GLUTs 1-4, class II includes GLUTs 5, 7, 9 and 11 and class III includes GLUTs 8, 10, 12 and the proton-myoinositol symporter  $H^+$ -myo-inositol cotransporter (HMIT1) (Joost

and Thorens, 2001). GLUT4 is expressed primarily in striated muscle and adipose tissue and is the major insulin responsive GLUT isoform.

### 1.1.2 Function of Insulin

Insulin is an important hormone involved in metabolism. It has a role in cell growth, differentiation, and the storage of substrates in fat, muscle and the liver. One of its most important roles is in whole body glucose homeostasis (Saltiel and Kahn, 2001). At high plasma glucose concentrations, for example after eating a meal, insulin stimulates the uptake of glucose by adipose and muscle tissue and inhibits glucose production by the liver. Insulin stimulates glucose uptake in adipocytes by stimulating the translocation of GLUT4 glucose transporter molecules from unique intracellular storage site(s) to the cell surface which results in an increase in glucose uptake into the cell. This returns glucose concentrations to their normal levels. In insulin resistance and type II diabetes this normal response to insulin is impaired.

It has been known for more than 30 years that insulin stimulates the translocation of glucose transport activity (Saltiel and Kahn, 2001). Cushman and Wardzala performed detailed studies of D-Glucose inhibitable Cytocholasin-B binding sites which lead to the suggestion that increased numbers of glucose transport systems in the PM in response to insulin stimulation originate in an intracellular membrane pool associated with microsomal membranes (Cushman and Wardzala, 1980). Insulin shifts the distribution of GLUT4 from storage pools toward the PM primarily by elevating its exocytic rate (Zaid et al., 2008). It also modestly reduces the endocytic rate in adipocytes (Blot and McGraw, 2008). Insulin binds to a receptor on the surface of muscle and adipose cells that triggers a cascade of signalling events.

There are two major signalling pathways that have been identified in insulin-regulated GLUT4 translocation (Kanzaki, 2006). These two pathways are the phosphatidylinositol 3-kinase (PI3K)-dependent pathway (Verhey et al., 1995) and the c-Cbl-dependent pathway (Verhey et al., 1995). In both these pathways insulin binds to its heterotetrameric receptor composed of two  $\alpha$  and two  $\beta$  subunits. This results in a conformational change in the receptor, which leads to activation of its tyrosine kinase domains in the intracellular

portion of the  $\beta$  subunits. The receptor is then able to phosphorylate several potential substrates. Furthermore, the binding of insulin to the  $\alpha$ -subunits of the receptor induces the trans-phosphorylation of the  $\beta$ -subunit which causes increased catalytic activity of kinase (Watson et al., 2004). This activated insulin receptor in turn catalyses the tyrosine phosphorylation of a number of intracellular substrates, including the insulin-receptor substrate (IRS) family. The phosphorylated tyrosine of this substrate acts as a docking site for signalling proteins (Czech and Corvera, 1999). These proteins then regulate a myriad of cellular processes including vesicle trafficking, protein synthesis and gene expression (Saltiel and Kahn, 2001). The IRS family of proteins are the most studied intracellular substrates to be phosphorylated by the insulin receptor. They interact with several effector molecules

In the PI3K pathway, the insulin receptor phosphorylates insulin-receptor-substrate (IRS)-1 and IRS-2. It has been found that IRS-1 rather than IRS-2 is required for GLUT4 translocation and glucose uptake (Huang et al., 2005). IRS recruits PI3K to the plasma membrane where it catalyses the production of phosphatidylinositol 3-phosphate (PI3P). IRS-1 binds the regulatory p85 subunit of class I PI3K activating its catalytic p110 subunit (He et al., 2007). The PI3K family phosphorylate the third hydroxyl position of the inositol ring of phosphoinositides. Insulin induced activation of Class I PI3K produces PtdIns(3,4,5)P<sub>3</sub> which then recruits kinases including PKB/Akt via their pleckstrin homology (PH) domain. Downstream of Class I PI3K there lies three major signalling axes, PKB/Akt, atypical PKC and Rac. This brings it in close proximity to the kinase phosphatidylinositol-dependent kinase-1 (PDK-1) which phosphorylates and activates PKB (Gonzalez and McGraw, 2006).

PKB (Akt) is a serine/threonine kinase which requires phosphorylation at two sites (Thr<sup>308</sup> and Ser<sup>473</sup>) for activation. Upon activation by insulin signalling, PKB phosphorylates several substrates in the cell. One downstream target of PKB which is thought to be important in GLUT4 translocation is AS160 (Sakamoto and Holman, 2008). AS160, also known as TBC1D4, is a protein with Rab-GAP (GTPase-activating protein) activity (Kanzaki, 2006). It is thought that PKB phosphorylation of AS160 inhibits its Rab-GAP activity (keeping it in its inactive GDP-bound form) towards Rabs associated with GLUT4 storage vesicles (GSVs) which lead to translocation of GLUT4

(Zeigerer et al., 2002; Zaid et al., 2008). Further work has shown that AS160 is important for intracellular retention of GLUT4 under basal conditions (Verhey et al., 2005).

In-vitro the GAP domain of AS160 acts on Rabs 2A, 8A, 10 and 14 (Ng et al., 2008). Rabs 8A and 14 seem to be the targets of AS160 in muscle cells (Ishikura et al., 2008). However, Ishikura and colleagues have found that Rab 10 is the predominant AS160 target in 3T3-L1 adipocytes (Ishikura et al., 2008). Rabs are considered to be molecular switches, linking signal transduction cascades to molecular effectors including molecular motors. This may indicate that there are cell-specific differences in the insulin signalling pathways regulating GLUT4 translocation. TBC1D1 is also a PKB substrate, highly homologous with AS160. While AS160 has six phosphorylation sites for PKB, TBC1D1 only has two (Thr<sup>590</sup> and Ser<sup>501</sup>) (Ramm et al., 2000). Both AS160 and TBC1D1 can bind 14-3-3 proteins. In fact, 14-3-3 binding to phosphorylated AS160 is essential for GLUT4 translocation (Zaid et al., 2008). It remains to be determined whether TBC1D1 or AS160 (AS160) is the more important PKB target. The major role of insulin is acting on the exocytosis of GLUT4 which has several insulin regulated steps (Zaid et al., 2008). Insulin has the ability to regulate the docking and fusion of GLUT4 vesicles with the plasma membrane (Lizunov et al., 2005) as well as the budding of vesicles from the storage compartment (Xu and Kandror, 2002) and their trafficking to the plasma membrane (Thurmond and Pessin, 2001).

GLUT4 contains several motifs which regulate its localisation and trafficking (Lalioi et al., 2001). The majority of these motifs are found in the N- and C-terminal domains.

In the N-terminus, the FQQI motif has been shown to be important for the internalisation of GLUT4 from the cell surface (Verhey et al., 1995). Other studies have found that this motif may be involved in other aspects of GLUT4 trafficking. FQQI is also involved in entry of newly synthesised GLUT4 into the insulin-responsive compartment (IRC) (Capilla et al., 2007) and the AS160-dependent exit of GLUT4 from the IRC (Capilla et al., 2007). Recent work suggests that the FQQI motif may be involved in the basal retention of GLUT4 (Blot and McGraw, 2008).

The LL motif in the C-terminus of GLUT4 has also been shown to be important for the rapid endocytosis and retention of GLUT4 (Blot and McGraw, 2008). It is thought that the LL motif regulates the transport of internalised GLUT4 out of a fast recycling pathway into the retention pathway (Blot and McGraw, 2008). Several other residues and motifs in the C-terminus are thought to be important for GLUT4 trafficking and tend to be acidic in nature. The last 30 amino acids of the C-terminus are sufficient for the correct localisation of GLUT4 into the IRC (Verhey et al., 1995). A YXXPDEND motif has been shown to be important for the release of GLUT4 from the IRC (Marsh et al., 1995) and a LXXLXPEND motif is essential for insulin-stimulated GLUT4 translocation to the plasma membrane (Marsh et al., 1995). Also a TELEYLGP motif regulates sorting of GLUT4 into a post-endosomal compartment (Shewan et al., 2003). This post-endosomal compartment has been shown to be a subdomain of the TGN enriched with syntaxin 6 and 16 (Shewan et al., 2003). Recently it has been shown that TELEY is required for the full basal retention of GLUT4 and that the trafficking step it is involved in is regulated by AS160 (Blot and McGraw, 2008). Other recent work suggests that the C-terminus of GLUT4 is required for targeting of GLUT4 to a peri-nuclear insulin-responsive vesicle (IRV) donor compartment but is not required for entry into the IRVs (Li et al., 2009).

In addition to the motifs in the N- and C-terminus, other motifs have been discovered which regulate GLUT4 trafficking. The large intracellular loop has been shown to be important for entry of GLUT4 into the IRC (Marsh et al., 1995) and also the AS160-dependent exit of GLUT4 from the IRC. Also a phosphatidic acid binding motif, SQWL in the first intracellular loop of GLUT4 is involved in the insulin-stimulated fusion of GLUT4 vesicles with the plasma membrane (Li et al., 2009).

## 1.2 Trafficking of GLUT4

A crucial facet of insulin is its ability to stimulate glucose transport in fat and muscle cells. This is mediated by the tissue-specific expression of a GLUT isoform (GLUT4) in those cells with unique trafficking and regulatory properties. Below, the key facets of GLUT4 biology will be discussed.

### 1.2.1 Intracellular location of GLUT4

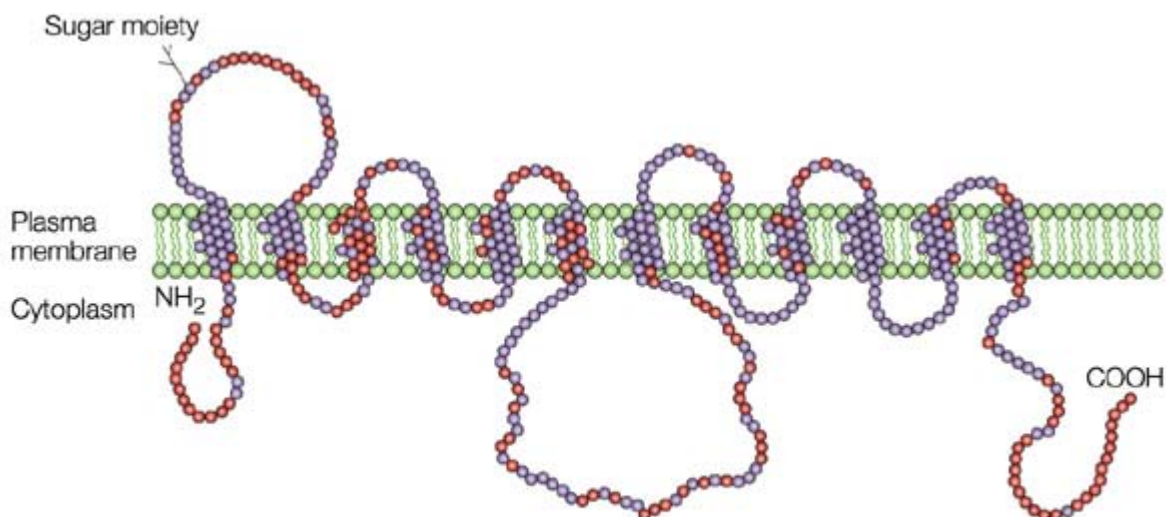
Insulin stimulates glucose transport into fat and muscle by regulating the translocation of the facilitative glucose transporter GLUT4 from an intracellular store to the cell surface (Watson and Pessin, 2007). Upon binding to its receptor on the surface of fat and muscle cells, insulin initiates a signalling cascade that culminates in changes in the trafficking itinerary of GLUT4, releasing it from its intracellular store and delivering it to the cell surface (Watson and Pessin, 2007). Individuals with insulin resistance and Type 2 diabetes exhibit defective insulin-stimulated GLUT4 translocation (Watson et al., 2004), consequently, much effort has gone into defining the trafficking of GLUT4 in adipocytes and muscle.

In the absence of insulin, around 95% of cellular GLUT4 is sequestered within intracellular compartment(s), including specialised GLUT4 storage vesicles (GSVs). Upon insulin stimulation, GSVs traffic to the plasma membrane (PM), resulting in a 10- to 20-fold increase in PM GLUT4 levels. This is achieved by a dramatic increase in the rate constant for exocytosis and a modest inhibition of endocytosis. A working model for GLUT4 trafficking in insulin-sensitive cells based on work from many laboratories is presented in Fig. 1.2.

Intracellular GLUT4 populates two inter-related endosomal cycles. The first (the proto-typical endosomal system) operates between the PM and early endosomes. This is a fast trafficking loop, and in the absence of insulin serves to effectively internalise GLUT4 from the PM (this process is dependent upon two endocytosis motifs within GLUT4). Once in this cycle, GLUT4 is further sorted into a slowly recycling pathway, operating between recycling endosomes, the *trans*-Golgi network (TGN) and GSVs (sorting into this cycle depends upon a distinct signal on the extreme C-terminus of GLUT4). According to this model, insulin mobilises GLUT4 to the cell surface from an intracellular store that moves slowly between the TGN and endosomes in the absence of insulin.

Insulin stimulation of adipose cells causes a net gain in surface GLUT4 that peaks within 10-15 minutes of stimulation, brought about by a robust increase in the rate of GLUT4 exocytosis and a smaller reduction in its

endocytosis (Foster, 2000). In mature adipocytes, GLUT4 is a long lived protein with a half life of approximately 40 hours, so each polypeptide chain is likely to cycle to the PM many times during its lifetime (Ishiki et al., 2005). Hence, Glut4 trafficking to and from the cell surface is controlled by a series of membrane trafficking steps with GLUT4 populating distinct intracellular compartments, all of which are either directly or indirectly in communication with the PM. Insulin acts to change rate constants of endo- and exo-cytosis between these compartments, and so re-distributes GLUT4 to the PM. In the absence of insulin, >95% of GLUT4 is intracellularly sequestered inside the adipocyte or muscle cell. Analysis of this distribution reveals that Glut4 is present within the *trans*-Golgi network, recycling endosomes and transferrin receptor positive (early) endosomes. However, a variety of studies have strongly supported a model in which a portion of Glut4 is sorted into so-called Glut4 Storage Vesicles (GSVs), which function to retain Glut4 within the cell until such time as insulin recruits it to the cell surface. Hence, the model of two inter-related cycles of Glut4 trafficking has evolved from many studies to explain the behaviour of GLUT4 within cells. The argument is that cycle 1 (the prototypical endosomal system) functions to rapidly internalise Glut4 from the cell surface. A subsequent sorting event, which is poorly understood, traffics Glut4 into the TGN/GSV cycle, a slow cycle, which effectively 'traps' Glut4 in an intracellular location. Understanding the role of SNARE proteins in this cycle is the main objective of this thesis.



Nature Reviews | Molecular Cell Biology

### Figure 1.1 GLUT4 is the Glucose Transporter involved in Glucose Uptake

GLUT4 is a Class I Glucose transporter that spans the membrane 12 times. This representation of Class I transporters shows residues specific to GLUT4 in red (Bryant et al., 2002). Insulin regulates glucose transport in muscle and fat cells by stimulating the translocation of GLUT4 from intracellular vesicles to the plasma membrane (Ramm and James, 2005).

### 1.2.2 Generation and function of glucose storage vesicles

GSVs are small insulin-responsive vesicles which are highly enriched in GLUT4 molecules and are characterized by the presence of v-SNAREs (Ishiki and Klip, 2005). VAMP-2 is the primary v-SNARE (Mora and Pessin, 2002) required for fusion of GLUT4 vesicles mobilized by insulin with the PM (Toonen and Verhage, 2003). VAMP-2 interacts with the target SNAREs Syntaxin 4 and 23kDa synaptosomal associated protein (SNAP23) (James, 2005) which are localized to the plasma membrane.

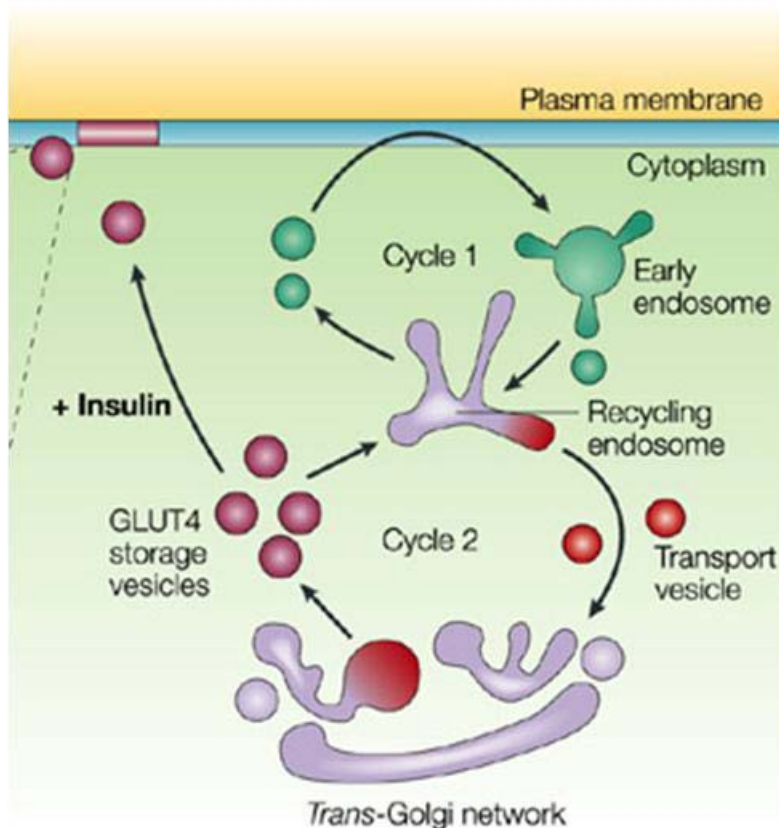
GSVs also contain insulin-responsive aminopeptidase (IRAP) (Martin et al., 2000; Ramm et al., 2000). IRAP traffics in concert with GLUT4 in response to insulin (Bogan and Kandrór, 2010). However, the GSVs are notably lacking in several proteins including TfR, cellubrevin (VAMP3) (Hashiramoto and James, 2000), cellugyrin (synaptogyrin 2) and cation-dependent mannose-6-phosphate receptor (CD-MPR) (Martin et al., 2000). Such observations prompted the notion that GSVs are segregated from the general recycling endosomal system, a thesis supported by chemical ablation of TfR-containing endosomal compartment experiments which argued strongly that GLUT4

within GSVs are separate to endosomal membranes (Livingstone et al., 1996).

The precise mechanism by which the GSVs are formed is not fully known. Sortilin, a major component of GSVs has been shown to be sufficient and essential for GSV formation (Shi and Kandror, 2008). Further work has shown that it is the luminal Vsp10p domain of sortilin which interacts with GLUT4 and IRAP and plays an important role in GSV formation (Shi and Kandror, 2008). Also Golgi-localised  $\gamma$ -ear-containing Arf-binding proteins, GGAs are required for sorting of GLUT4 (Watson et al., 2004) and IRAP (Hou et al., 2007) into GSVs. It has been proposed that the formation of GSVs is driven by mass action, in which the expression of GLUT4, IRAP and sortilin, whose interaction and abundance fill the compartment, largely excludes other molecules (Pilch, 2008). Recently it has been shown that GSVs self assemble during differentiation of 3T3-L1 adipocytes and that luminal interactions of GLUT4 and IRAP have an important role in the assembly of GSVs (Shi et al., 2008).

The specialised GSV compartment is thought to be an important mechanism of basal intracellular retention of GLUT4 and it is thought that GLUT4 in this compartment translocates to the cell surface in response to insulin.

In the basal state, GLUT4 continuously cycles between the PM and an intracellular compartment but at a very slow rate, where 2-5% of the protein is at the plasma membrane with the remainder localized to various intracellular compartments (Mora and Pessin, 2002). In the basal state, GLUT4 vesicles arrive at the PM but do not dock and studies have reported that docking/fusion is an insulin regulated event (Kumarov et al., 2005; Foster and Klip, 2000).



Nature Reviews | Molecular Cell Biology

### Figure 1.2 The slow recycling pathway

This model shows the two recycling pathways in insulin-responsive cells. Cycle 1, the fast pathway, consists of the pathway between the cell surface and the endosomes. In this cycle, insulin shifts GLUT4 from the slow TGN-endosome pathway to translocate to the cell surface at the plasma membrane. The recycling pathway shown in cycle 2 between the TGN and endosomes is known as the slow recycling pathway. All the steps of this pathway are not known. It is in this pathway that GLUT4 is sorted in the TGN and is packaged into GSVs. 90% of GLUT4 is kept in this state under basal conditions. (Bryant et al., 2002)

There have been several models of GLUT4 trafficking proposed to explain the basal exclusion of GLUT4 from the plasma membrane and the high insulin responsiveness of GLUT4 translocation (Pessin et al., 1999; Dugani and Klip, 2005). These models include retention mechanisms, dynamic sorting events and packaging GLUT4 into a more stationary population of secretory-type vesicles or a static specialised compartment.

The retention model predicts that sequences in GLUT4 specifically target GLUT4-containing vesicles away from the recycling endosomes (Lalioi et al.,

2001). These sequences bind to retention receptors found in insulin-responsive cells, for example, TUG (Bogan and Kandror, 2010). Insulin stimulation or competition by retention sequence peptides (Lee and Pilch, 1994), disrupts the interaction between the GLUT4 sequences and the retention receptors, allowing the GLUT4-containing vesicles to enter the recycling endosomal system resulting in translocation to the plasma membrane.

In the dynamic recycling model, the entire complement of GLUT4 eventually recycles to the plasma membrane in the basal state (Martin et al., 2000). GLUT4-containing vesicles undergo a futile cycle of fission and fusion with endosomes (Karylowski et al., 2004) and insulin acts to switch the fusion of these vesicles to the plasma membrane. Insulin promotes two routes for GLUT4 mobilisation towards the plasma membrane, a direct route from the GLUT4-containing vesicles and an indirect one from the GLUT4-containing vesicles via the endosomal recycling system (Ramm et al., 2000; Zeigerer et al., 2002). A variation of this model is that only a fraction of GLUT4 recycles to the plasma membrane in the basal state. There also exists a latent pool of GLUT4 molecules which is never mobilised in response to insulin (Zeigerer et al., 2002). In the secretory vesicle model GLUT4 is localised to both small synaptic-like vesicles as well as larger tubulovesicular compartments. Insulin stimulation results in association and fusion of the vesicles with the plasma membrane (Xu and Kandror, 2002).

These models are not mutually exclusive, nor has one been proven overwhelmingly better than another. Recent work has shown that GLUT4 is regulated by both static and dynamic retention mechanisms (Muretta et al., 2008). It is possible that cell culture conditions can affect GLUT4 trafficking, for example replating 3T3-L1 cells after differentiation inhibits static retention of GLUT4. According to Bryant et al., GLUT4 transport is controlled by all three mechanisms (Bryant et al., 2002). It is proposed that intracellular GLUT4 occupies two inter-related and overlapping endosomal cycles as shown in Figure 1.2. The first is a fast trafficking cycle involving the plasma membrane and early endosomes. In the absence of insulin it is this cycle which internalises GLUT4. Once in the endosome, GLUT4 is further sorted into a slow trafficking cycle involving endosomes, the TGN and GSVs.

It is thought that it is the GLUT4 in these GSVs which translocates to the plasma membrane in response to insulin. Recent data also supports a model in which basal GLUT4 retention involves two intracellular trafficking cycles (Blot and McGraw, 2008).

### 1.2.3 Membrane trafficking

The trafficking of GLUT4 involves the fusion of vesicles with specific membranes which is mediated by target- (t-) and vesicle- (v-) SNAREs (soluble *N*-ethylmaleimide-sensitive factor attachment protein receptors) (Watson et al., 2008). During membrane trafficking or vesicle-mediated transport, vesicles are formed from a donor compartment or membrane. These transport vesicles are then translocated to the target compartment or membrane. Then the vesicles dock and fuse with the target membrane. SNAREs function in the final docking and fusion stages of this process and catalyse the final fusion step (Chen and Scheller, 2001).

Membrane fusion is a two step process: the membranes are brought into close proximity where counteracting electrostatic forces need to be overcome before the lipids of the proximal leaflets can interact. The boundary between the hydrophilic and hydrophobic portion of the bi-layer is destabilized (Jahn et al., 2003). Fusion proceeds by an ordered sequence of steps that includes the merging of the proximal mono-layers, stalk formation, generating of hemi-fusion intermediates and fusion pore opening (Jahn et al., 2003). Intracellular fusion machines are dynamic supra-molecular structures that are assembled upon demand and dismantled as soon as fusion is completed to allow them to be easily and quickly reused. Except for membrane anchored SNAREs, most components are recruited from the cytoplasm. Fusion must be fast enough or of high enough probability to meet the physiological requirements of that trafficking step and fusion must be specific such that vesicles release their contents after encountering the correct target membrane (Shen et al., 2007).

Membrane fusion is controlled by three main protein families, Rab GTPases, SNARE proteins and members of the Sec1/Munc18 (SM) family (Gengyo-Ando et al., 2007). Membrane fusion involves NSF, SNAPs, SNAREs, and SM

proteins (Rizo, 2003). All types of intracellular membrane fusion are believed to share common protein machinery (Dulubova et al., 2002). Transport and fusion are highly compartmentalized phenomena and occur in discreet locations in the cell. Maintaining compartment identity and fusion specificity is particularly important for proteins, which navigate through multiple membrane compartments during their biogenesis, intracellular storage, exocytosis, and retrieval from the plasma membrane such as GLUT4 (Mora and Pessin, 2002). When the intracellular transport vesicle is fused with an intracellular membrane, it first needs to recognize its partner membrane by physical contact in a specific location. This process provides specificity to fusion reactions and is variably called membrane attachment, tethering, or docking (Jahn et al., 2003). After membrane attachment, fusion is initiated by the concerted action of SNARE and SM proteins. After fusion, the transmembrane regions of the SNAREs are present in the same membrane, resulting in cis- complexes that need to be disassembled for reactivation. This reaction is catalyzed by the ATPase NSF with SNAPs as cofactors (Jahn et al., 2003). Internalized molecules can be recycled back from early endosomes or a late recycling compartment to the plasma membrane and can therefore participate in several rounds of exocytosis.

Since my thesis work mainly concerns SNARE proteins and SM proteins, below, I will discuss aspects of SNARE and SM protein biology germane to Glut4 vesicle trafficking.

### **1.3 SNARES**

Insulin-regulated GLUT4-traffic represents a specialised form of membrane trafficking, with GLUT4 being transported between various membrane-bound compartments by means of vesicular transport. Membrane traffic in all eukaryotic cells is controlled by the formation of specific SNARE complexes. Members of the t- (target) family of SNARE proteins mark specific organelles. The formation of complexes between t-SNAREs and their cognate v- (vesicle) SNARE localised to the appropriate donor membrane is sufficient to catalyse bilayer fusion, and the SNAREs have been proposed to impart a degree of specificity on membrane traffic. While there is little doubt that these SNARE interactions control the fusion of the donor and acceptor compartments, the

role of SNAREs in determining specificity is somewhat more controversial. Nonetheless, it is likely that controlling SNARE complex formation enables the cell to regulate membrane traffic, providing an impetus to understand which SNAREs are involved in GLUT4 traffic and how they are regulated.

### 1.3.1 Classification of SNAREs

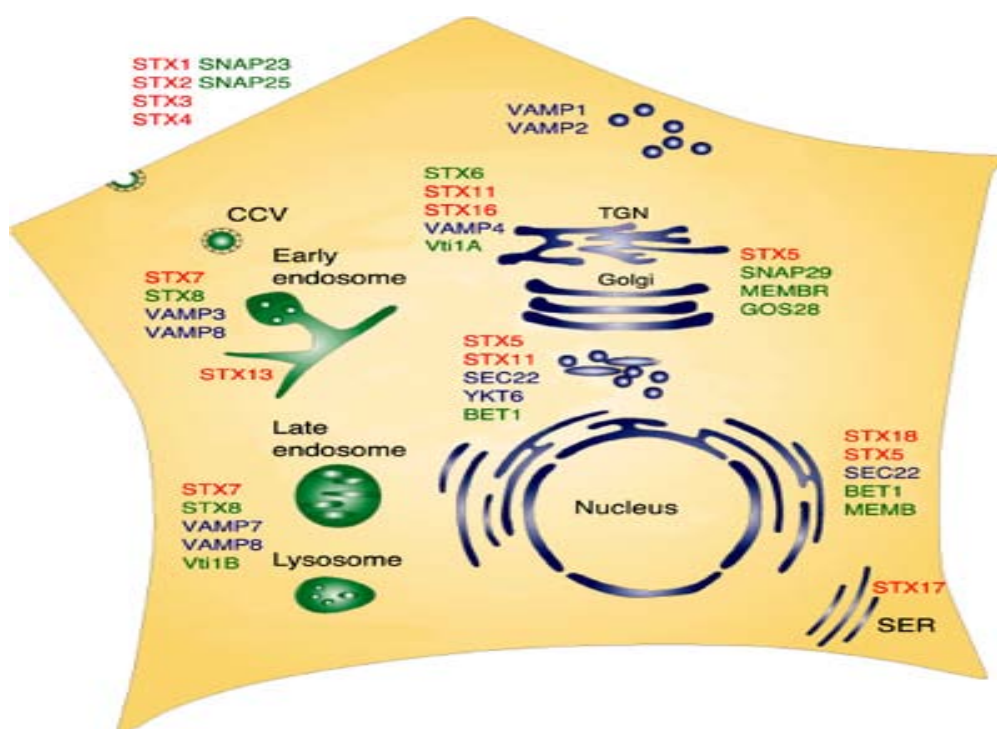
Membrane fusion in eukaryotic cells is thought to be mediated by a highly conserved family of proteins called soluble N-ethyl maleimide sensitive-factor attachment protein receptors (SNAREs) (Yoon et al., 2006). SNAREs are a super-family of small proteins with 24 known members in yeast and more than 35 in mammals (Jahn et al., 2003). SNAREs are highly abundant in the cell and vary widely in size and structure and share only one homologous sequence, the SNARE motif that serves as their defining feature (Jahn et al., 2003). The SNARE motif is an evolutionarily conserved stretch of about 60-70 amino acids arranged in eight heptad repeats, SNARE proteins also usually possess a single trans-membrane anchor domain at their C-terminus connected to the motif by a short linker. Other SNAREs feature hydrophobic post-translational modifications instead of a trans-membrane domain (Gerst, 1999). The SNARE motifs are unstructured and spontaneously assemble into core complexes of high stability that are disassembled by the ATPase chaperone NSF in conjunction with cofactor SNAPs (Gerst, 1999).

SNARE motifs are classified into Qa-, Qb-, Qc-, and R-SNAREs. Based on a highly conserved layer of interacting amino acids (three glutamines and one arginine) in the centre of the helix bundle, the subfamilies are termed Qa-SNAREs (the Syntaxins), Qb- and Qc-SNAREs (homologs of the N- and C-terminal SNARE motifs of SNAP25) and R-SNAREs (VAMPs) (Jahn et al., 2003). SNAREs that carry trans-membrane domains can also be palmitoylated which has been shown to protect SNAREs from degradation (Jahn, 2000).

Monomeric SNAREs are largely unstructured, but when SNAREs combine, the SNARE motifs form helical core complexes of great stability; it is thought that these stable complexes release sufficient energy to catalyse the fusion of two bilayers. These core complexes can withstand conditions such as 80°C temperatures, 8M urea concentrations, and 2% SDS chemical disruption (Brunger, 2006). The core complex is assembled from four parallel alpha

helices and comprises 16 stacked layers of interacting side chains. Each core complex is assembled from one of each of the Qa-, Qb-, Qc-, and R-SNAREs (corresponding to three helices from t-SNAREs and one from the v-SNARE). These layers are largely hydrophobic except for a central zero-layer that contains three highly conserved glutamine residues and one highly conserved arginine residue (Jahn and Scheller, 2006). The zero layer is crucial for dissociation because it recruits the cofactors of NSF.

Complex formation is mediated by the SNARE motifs and is accompanied by large conformational changes (Jahn et al., 2003). The Q-SNARE acceptor complexes bind with the R-SNAREs from the N-terminal end of the SNARE motif towards the C-terminus, with the prevailing concept being that SNAREs 'zipper-up' into the core complex (Sollner et al., 1993).



a

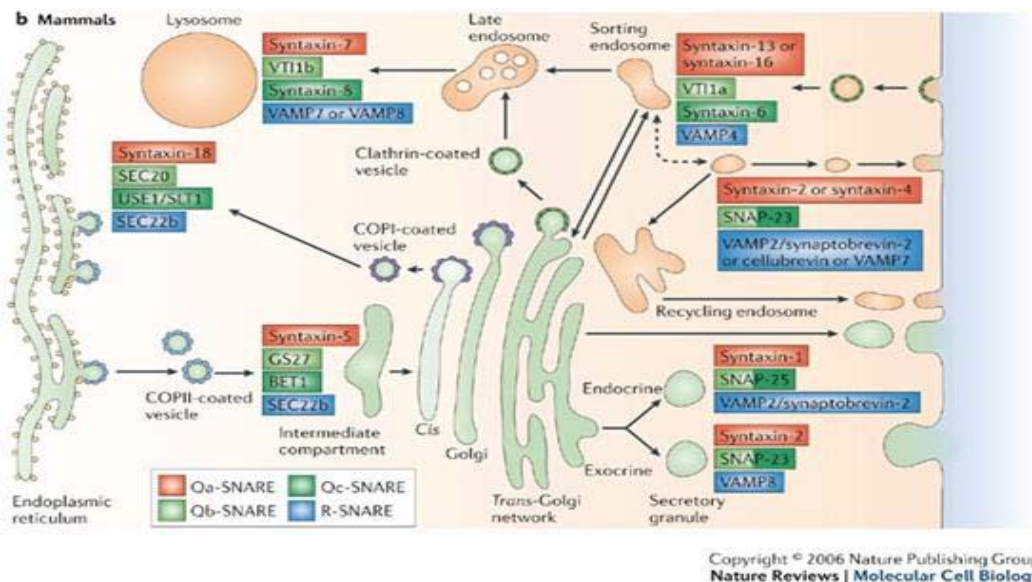


### Figure 1.3 The distribution of SNAREs in the Adipocyte

The adipocyte is highly compartmentalized and each participant in GLUT4 trafficking is localized near to where its action will take place. The Syntaxin 4/SNAP23/VAMP2 complex that occurs in the fast pathway is located at the plasma membrane so that GLUT4 can be translocated to the plasma membrane in response to insulin stimulation. Likewise, Syntaxin 16 is located near the Trans-Golgi Network (TGN) for its role in the slow recycling pathway, as shown in panel a (Chen and Scheller, 2001). Panel B uses the same color scheme to delineate between SNARE types and shows clearly which SNAREs are involved in sorting pathways (Jahn and Scheller, 2006).

#### 1.3.2 Structure of SNAREs

SNAREs have a highly conserved structure (Brunger, 2006). The majority of SNAREs contain three domains, an N-terminal domain, a SNARE domain and a transmembrane domain. The main feature of these proteins is the SNARE domain of around 60 residues, which is found in all SNAREs. This domain consists of heptad repeats which form coiled-coil structures. The structure of the N-terminal domain varies and is involved in a variety of functions. The N-terminal domain of the syntaxin subfamily has a three helical bundle consisting of Ha, Hb and Hc regions. This region can bind to the C-terminal SNARE motif generating a closed conformation, which needs to be opened before assembly into a t-SNARE. The N-terminal region of the subfamily can also be involved in interactions with regulators of SNARE assembly. For example the N-terminus of syntaxin 16 binds to the SM protein mVps45 (Dulubova et al., 2002). Also, the N-terminal can direct intracellular targeting of the SNARE, for example the N-terminal of VAMP4 targets the SNARE to the TGN by a di-leucine motif and an acidic cluster (Burkhardt et al., 2008). SNAREs associated with GLUT4 trafficking in the adipocyte are shown in Figure 1.3 and are listed in Table 1.1.

Mammalian SNARE	Yeast Homologue	SNARE Type	Localization, Role and Tissue Distribution	N-Terminal Domain
Syntaxin 4	N/A	Qa	PM, GLUT4 translocation in muscle/fat, binds Synip	Habc
Syntaxin 13	Pep12p	Qa	EE, RE; EE/RE Fusion, Binds EEA1	Habc
Syntaxin 16	Tlg2p	Qa	Golgi, Endosome to Golgi trafficking,	Habc
Vti1a	Vti1p	Qb	Golgi, TGN; Endosome to Golgi	3-HB
Syntaxin 6	Tlg1p	Qc	TGN, endosomes; TGN to endosome and endosome to Golgi trafficking; binds EEA1	3-HB
SNAP23	Sec9p	Qb/c	PM; GLUT4 translocation to PM	No TMD
VAMP2	N/A	R	Recycling compartments, regulated exocytosis; also synaptobrevin 2	No TMD
VAMP4	N/A	R	TGN; TGN to LE and endosome to Golgi trafficking; binds AP-1	No TMD
VAMP 8	Nyv1p	R	EE, LE; homotypic EE/LE Fusion	No TMD

**Table 1.1 Classification of SNAREs**

SNAREs are required in the trafficking of GLUT4 in the adipocyte. These SNAREs form complexes with one another based on SNARE type. PM: Plasma Membrane, EE: Early endosome, RE: Recycling endosome, TGN: Trans-Golgi Network, LE: Late endosome, TMD: Transmembrane Domain.

### 1.3.3 The Syntaxins

Syntaxins (Qa-SNAREs) are members of the SNARE protein superfamily. Each syntaxin consists of a SNARE motif, a trans-membrane domain (TMD) and an Habc domain. This Habc domain, located in the N-terminal portion of the syntaxin, consists of three alpha helices that fold back on one another (Togneri et al, 2006). Syntaxin homology has been conserved among species with mammals having nearly double the number of syntaxins as yeast. This, however, could be explained by the number of syntaxins with redundancy of function between species. For example, the mammalian Syntaxins 1-4 function at the plasma membrane, while in yeast the only PM syntaxin is Sso1p (Shen et al, 2007). Some syntaxins can exist in both the closed and open conformations (such as Sso1p) and this allows them to specify function. In the closed conformation, the Habc domain folds over and interacts with the SNARE domain which disallows SNARE complex formation (Dulubova et al, 1999) as shown in Figure 1.4. In contrast, there is no contact between the Habc domain and the SNARE domain in the open conformation which allows interaction with the SNARE domains of other SNAREs in order to form a SNARE complex (Dulubova et al, 1999). Figure 1.4 shows this open

conformation arrangement and Figure 1.5 shows the open conformation in relation to the opposing membranes.

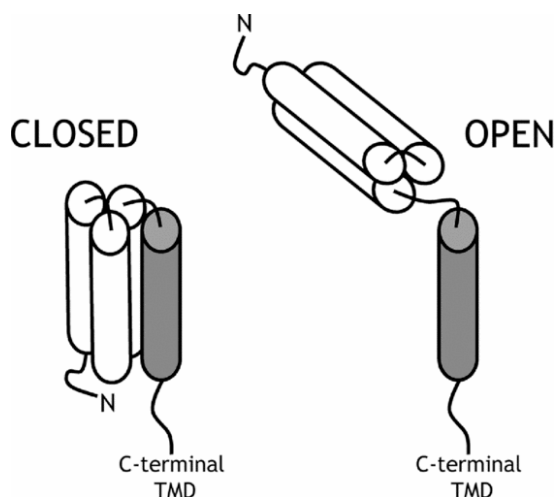
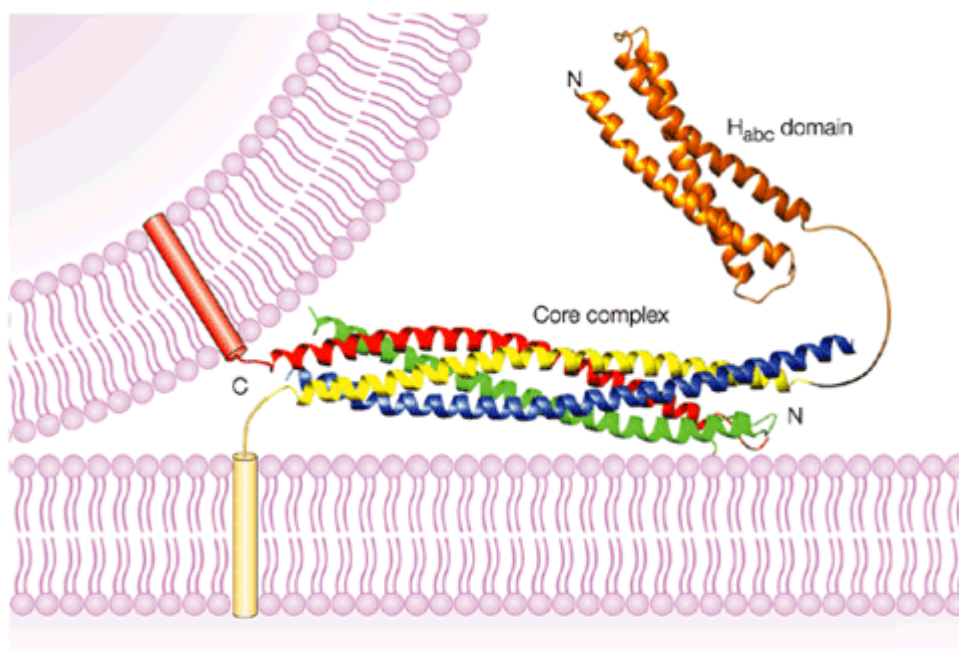


**Figure 1.4 The closed and open conformations of the Syntaxins**

In the closed conformation the Habc domain is folded over and interacts with the SNARE domain, inhibiting SNARE complex formation. In the open conformation the Habc domain does not interact with the SNARE domain, leaving space for SNARE-SNARE interaction and SNARE complex formation. Reproduced with permission from MacDonald C, Munson M, Bryant NJ, 2010, *Biochem Soc Trans*, **38**, Pt 1, 209-12. © the Biochemical Society



Nature Reviews | Neuroscience

**Figure 1.5 SNARE structure has functional consequences**

Syntaxin is in the open conformation where the Habc domain is not folded back against the SNARE domain. (Rizo and Sudhof, 2002)

### 1.3.4 The SNARE Hypothesis

SNARE complex assembly is an essential step in the fusion of vesicles to the plasma membrane (or indeed any membrane fusion step). SNARE proteins that are localized in opposing membranes drive membrane fusion by using the free energy that is released during the formation of a tight four helix bundle, the core complex (Jahn and Scheller, 2006). The SNARE motifs, which precede C-terminal membrane regions of SNARE proteins, form a core complex when a SNARE motif from one membrane (v-SNARE) the donor vesicle, and three from the other membrane (t-SNARE), the target membranes assemble in a parallel arrangement of alpha helices (Dulubova et al., 2002). This proposed explanation of how SNAREs interact is called the SNARE hypothesis (as shown in Figure 1.6).

The vesicle associated v-SNARE engages with its partner t-SNAREs on the target membrane to form a coiled coil that bridges two membranes and facilitates fusion (Yoon et al., 2006). Within the late secretory pathway, individual v- and t-SNAREs can pair with multiple other SNAREs to allow a certain level of crosstalk (Shen et al., 2007). Cognate v- and t-SNAREs form a parallel four helix bundle through coiled-coil domain interactions that may be sufficient to overcome the energetic barrier to membrane fusion (Mora and Pessin, 2002). v- and t-SNAREs are conformationally adaptable and are found in specific places in the cell.

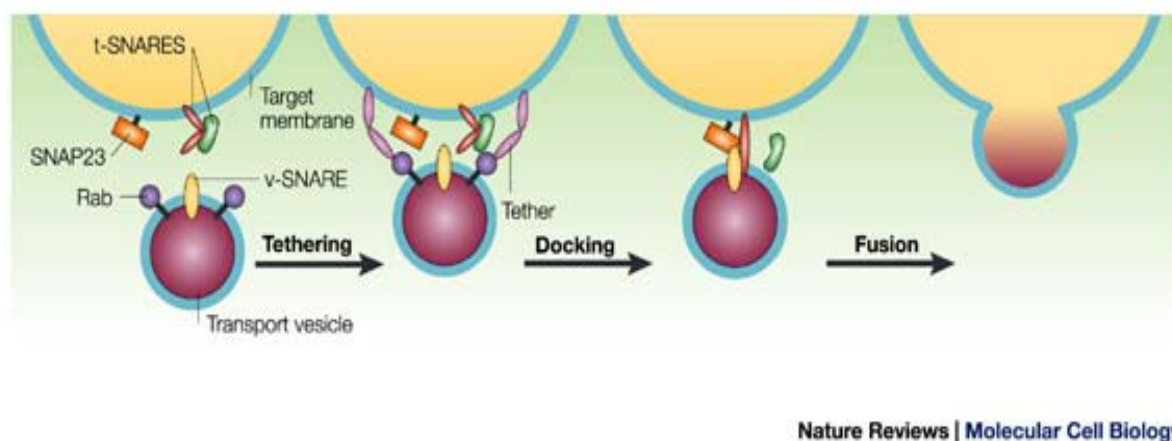


### Figure 1.6 The SNARE Hypothesis

The SNARE hypothesis states that in order for membrane fusion to occur, t-SNAREs on the target membrane, and v-SNAREs on the vesicle membrane must form a SNARE complex, then tether and dock on the target site before ultimately fusing and releasing cargo from the vesicle. (Bryant et al., 2002)

SNARE mediated fusion occurs with an intermediate step called hemi-fusion. Hemi-fusion is a meta-stable membrane structure in which the outer leaflets

are merged while the inner leaflets remain intact. Fusion is blocked if a SNARE trans-membrane domain is replaced by a more flexible lipid anchor or if extra amino acids are inserted between the SNARE motif and the trans-membrane domain (Jahn and Scheller, 2006). After fusion, SNARE complexes are transformed from a trans- to cis- configuration in which all SNAREs of a complex are together in the fused membrane (Gerst, 1999).

SNARE proteins proceed from binary to 7s and then to 20s complexes comprising one v- and one t-SNARE before the fusion of the vesicles to the target membrane (Foster and Klip, 2000). SNAREs alone can induce lipid mixing and complexes are dissociated after fusion so individual SNARE proteins can be recycled to their membranes (Jahn et al., 2003). SNAREs are recycled through dissociation of the core complex which is achieved through N-ethylmaleimide sensitive factor (NSF) (Jahn and Scheller, 2006). During fusion, the trans-complex relaxes to a cis-configuration, cis-complexes are disassembled by NSF and the R- and Q-SNAREs are separated for sorting (Brunger, 2006). Disassembly requires energy which is provided by NSF, a hexameric member of the AAA+ protein family (Jahn and Scheller, 2006). It requires cofactors, soluble NSF attachment proteins ( $\alpha$ -SNAPs) to bind to the SNARE complex and has three distinct domains, two of which contain ATP binding sites (Sollner et al., 1993). The complete dissociation of SNARE complexes might involve several catalytic cycles where NSF has several hydrolysis events which provides the energy for disassembly of the SNAREs (Jahn and Scheller, 2006).

SNAREs return to their donor compartment by intracellular membrane trafficking (Jahn and Scheller, 2006). SNAREs reside not only in the organelle for which they mediate fusion, but they also reside in the membranes of the organelles that are part of their recycling pathway. SNAREs that are involved in trafficking between endoplasmic reticulum (ER) and the Golgi are found in both of these compartments and in the intermediate vesicles (Toonen et al., 2006). The organization of the membrane compartments of eukaryotic cells is therefore likely to arise from numerous layers of regulation, many of which probably occur before the formation of the SNARE complexes that catalyze the final and irreversible step (Jahn and Scheller, 2006). Core regions of SNAREs can interact with SM

proteins mediating Golgi or endocytic membrane fusion (Shen et al., 2007). Mammalian cells encode nearly twice as many SNAREs as yeast and the majority of that increase is concentrated in the endocytic/exocytic pathways (Shen et al., 2007).

### **1.3.5 SNAREs involved in GLUT4 traffic to the plasma membrane**

A substantial body of experimental work has examined the t-SNAREs required for the insulin-stimulated delivery of GLUT4 to the PM, with the general consensus that syntaxin 4 (Sx4) (Qa) and SNAP-23 (Qb,c) are the crucial t-SNAREs for this process. A good deal of experimental evidence now supports this view. For example, homozygotic disruption of the Sx4 gene results in early embryonic lethality, but heterozygote (Sx4 +/-) knockout mice exhibit impaired glucose tolerance, with a 50% reduction in whole-body glucose uptake, a result attributed to a ~50% reduction in insulin-stimulated glucose uptake and GLUT4 translocation in skeletal muscle (Tozzo et al., 1996). Similarly, depletion of either syntaxin 4 or SNAP23 using siRNA has revealed that these PM SNAREs are essential for GLUT4 translocation to the plasma membrane and thus for insulin-stimulated glucose transport (Kawaguchi et al., 2010).

In common with other Qa-SNAREs, Syntaxin 4 is proposed to adopt either of two conformations. The first is a closed conformation whereby the N-terminal Habc helical domain is folded back upon the SNARE motif, thus rendering the latter inaccessible to incoming v-SNAREs. Alternatively, the Habc domain can be moved away from the SNARE domain (the open conformation) in the second conformation thus allowing the formation of productive SNARE complexes. How this regulation is achieved will be discussed further below when discussing SM proteins.

### **1.3.6 SNAREs in intracellular traffic and the role of Syntaxins 6 and 16**

The mechanisms controlling the sorting of GLUT4 into the GSV compartment have received much less attention than the events regulating GLUT4 insertion into the PM. GLUT4 is effectively sorted from recycling endosomes into a slow, futile cycle (cycle 2, in Figure 1.2), which culminates into the sorting of GLUT4 into an insulin-responsive compartment, termed GSVs.

Clearly, if cells are unable to correctly sort GLUT4 into GSVs, then it is likely that insulin-stimulated GLUT4 translocation will be impaired.

The first reported role for an intracellular Syntaxin in GLUT4 sorting was that of Syntaxin 6. Over-expression of a mutant form of Syntaxin 6 which lacked a transmembrane anchor (and thus acting as a 'dominant negative inhibitor' of endogenous Syntaxin 6) was found to result in delayed re-internalisation of GLUT4 from the cell surface upon insulin removal. Although the locus of action of Syntaxin 6 remains to be defined, studies in other systems have suggested that this SNARE acts at the *trans*-Golgi network (TGN), consistent with a role for Syntaxin 6 in sorting into GSVs. This conclusion is further supported by data showing that the recycling of the insulin-responsive aminopeptidase (IRAP; a GSV resident protein) from the cell surface back to GSVs required functional Syntaxin 6 (Perera et al., 2003). The localization of both syntaxin 16 and syntaxin 6 to intracellular membranes in the TGN region suggests that this SNARE complex may control traffic of GLUT4 into or out of the slow recycling pathway and thus regulates the insulin responsiveness of cells (Perera et al., 2003).

Two further studies have strengthened this hypothesis, in this case examining the role of Syntaxin 16 (Sx16) in GLUT4 traffic. Sx16 acts with Syntaxin 6 (Sx6) (and presumably Vti1a or Vti1b) to form a t-SNARE complex. Shewan and colleagues found that Sx16 exhibits a high degree of co-localisation with GLUT4, and further showed that GLUT4 recycled through a sub-domain of the TGN enriched in Sx16 and Sx6 (Shewan et al., 2003). Moreover, Proctor et al further showed that depletion of Sx16 (or over-expression of a dominant negative Sx16 mutant) in adipocytes resulted in reduced insulin-stimulated glucose transport and a reduction in cellular GLUT4 levels (Proctor et al., 2006). Such data suggest that Sx16 acts to facilitate the traffic of GLUT4 into GSVs, and that disruption of this pathway results in mis-targeting of GLUT4 and ultimately a reduction in total cellular GLUT4 levels (Proctor et al., 2006). This data suggest that Syntaxin 16 is required for entry into the slow recycling pathway and hence the GSVs and when this is prevented, GLUT4 levels decline as GLUT4 is mis-targeted into the lysosomal pathway.

There are five different splice variants of Syntaxin 16: 16A, 16B, 16C, 16D and 16H (Dulubova et al., 2002). This study examines the role of Syntaxin 16A since it has been shown to function in GLUT4 trafficking (Proctor et al., 2006).

## 1.4 SM Proteins

SNARE-dependent fusion is a tightly regulated process. How this regulation is achieved is the subject of intense research effort, and recently attention has been focused on the SM (Sec1p/Munc18) proteins. SM proteins are evolutionarily conserved cytosolic proteins known to regulate vesicle fusion in the secretory pathway. The first SM protein was isolated in *Caenorhabditis elegans*. This SM protein, known as *unc-18*, was later joined by the *Saccharomyces cerevisiae* orthologue Sec1p. Later other orthologues were discovered in plants (KEULE), invertebrates (ROP) and mammals (Munc-18) (Rodkey et al., 2008). Moreover, Sec1p isoforms were found in several yeast pathways (Banta et al., 1988).

SM proteins are essential for vesicle trafficking. For example a temperature-sensitive mutant of the yeast SM protein Vps45p causes an accumulation of post-Golgi vesicles (Piper *et al.*, 1994). SM proteins bind to syntaxins and regulate SNARE complex assembly (Toonen and Verhage, 2003; Sudhof and Rothman, 2009). They function to positively regulate SNARE complex assembly by regulating t-SNARE receptivity. SM proteins bind to syntaxins in three different modes (Carpp *et al.*, 2006; Aran *et al.*, 2009; Furgason *et al.*, 2009). In the first mode, the SM protein binds to syntaxin in a closed conformation, preventing the formation of SNARE complexes (Mode 1). In the second mode (Mode 2), the N-terminal lobe of the SM protein binds to the N-terminal peptide of the syntaxin. This mode of binding allows the t-SNARE complex to assemble and then accept the v-SNARE, forming a trans-SNARE complex. SM proteins also bind the trans-SNARE complex. Interaction of the SM protein with the trans-SNARE complex stimulates membrane fusion and adds specificity to membrane trafficking. In addition to a role in SNARE complex assembly, SM proteins have been implicated in stabilisation and transport (Bryant and James, 2001; Carpp et al., 2007).

### 1.4.1 Regulation of SNARE Complex formation

SNARE proteins are subject to a considerable degree of regulation, and a crucial family of regulatory proteins are the members of the Sec1p/Munc18 (SM) family (Dulubova et al., 2002). The SM family is a group of arc-shaped hydrophilic proteins of 650-700 residues which consist of three domains with a major v-shaped cleft in the middle (Toonen and Verhage, 2003). There are four SM proteins in yeast and seven in the human genome. SM proteins interact with specific Qa isoforms, adding a further layer of specificity upon the formation of the SNARE complex. The job of SM proteins may include proofreading SNAREs and preventing promiscuous SNARE pairing (Jahn et al., 2003), but in addition they are thought to regulate the formation of productive SNARE complexes.

Initially, SM proteins were thought to function by binding to the closed conformation of the corresponding syntaxin, and thus inhibiting the formation of the open syntaxin complex and so preventing SNARE complex formation. A good deal of data subsequently showed that SM proteins appeared to play both a positive and negative role in SNARE-dependent membrane fusion, and that the interaction of SM proteins with syntaxin molecules involved more than one 'mode' of binding. SM proteins interact with SNAREs in multiple ways, of particular importance is SM protein binding directly to the N-terminal ~20 residues for the corresponding Qa-SNARE. It should be noted that the binding of an SM to the closed conformation of a syntaxin involves the arch-shaped SM protein 'cradling' the closed Syntaxin (Mode 1); binding to the extreme N-terminus of the (open) syntaxin involves a distinct binding pocket on the opposite face of the SM protein (Mode 2). The structures of several SM/Syntaxin complexes have now been solved and allow the formation of generalised models of these protein/protein interactions. SM proteins have also subsequently been shown to bind intact SNARE complexes (so-called mode 3 binding) with important consequences for the rate of SNARE-dependent fusion.

The function of the N-terminal domain is interesting because some N-terminal domains can reversibly associate with the SNARE motif of the same

SNARE to from a closed conformation which in turn prevents the SNARE motif from forming a complex (Jahn and Scheller, 2006). Other N-terminal domains cannot assume a closed conformation which indicates that this function is non-essential. It has been found that there are four binding modes for which SNAREs will complex with SM proteins. In the first mode, the arch-shaped SM protein wraps over the closed SNARE conformation which provides stability to the interaction (see Figure 1.7a) (Jahn and Scheller, 2006). In the second mode of binding, the SM protein only interacts with the extreme N-terminal end of the Qa-SNARE in a superficial way. In the third mode of binding, the SM protein binds to the Qa-SNARE only when it is part of an assembled SNARE complex. Modes one and two are important in cell trafficking and the second mode, SM-SNARE binding to N-terminal peptides adjacent to the three helix bundle domains of Qa-SNAREs, (as shown in Figure 1.7b) is the most prevalent mode of binding for SM proteins (Rizo, 2003).

In this first mode, the SM protein binds to the individual t-SNARE forming a complex that includes part of the SNARE motif which serves to disable the formation of a SNARE complex (Sudhof and Rothman, 2009). The SM protein clasps a four helix bundle formed within the syntaxin. In addition to the SNARE motif, the syntaxin also contains a three helix bundle that includes a globular N-terminal Habc domain that folds back and binds the helical SNARE motif to form the closed conformation (Dulubova et al, 1999). This mode, shown in Figure 1.7a, is favoured by syntaxins involved in exocytosis.

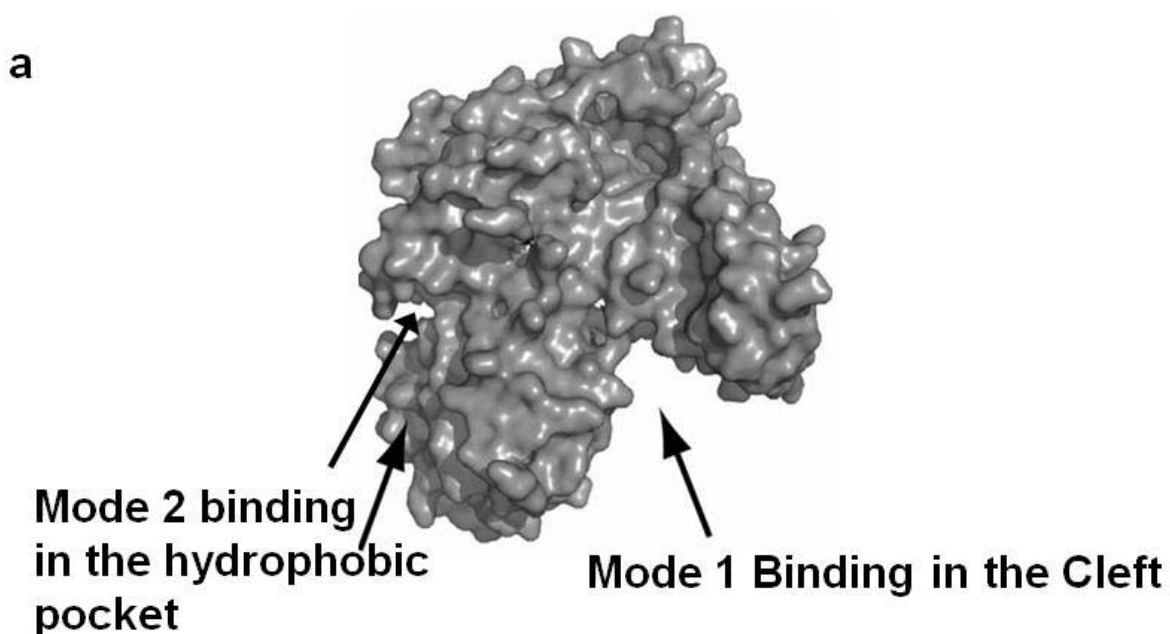
Rothman and colleagues have found that SM proteins are designed to clasp a four helix bundle and this is a general feature of SM proteins (Sudhof and Rothman, 2009). This mode of binding has been suggested as evidence that SM proteins act as negative regulators. However, the second mode of binding also exists to postulate that SM proteins can both negatively and positively regulate binding.

In the second mode of binding, the SM protein is fixed by its N-terminal end to a specific N-terminal peptide of the cognate syntaxin (Yamaguchi et al, 2002). This binding mode, as shown in Figure 1.7b, leaves the body of the SM protein free to fold back onto the SNARE complex to grasp four helices. These four helices must consist of one helix from the v-SNARE and three

helices from the t-SNARE. Shen and colleagues have discovered that this mode may allow SM proteins to organize SNARE complex assembly both spatially and temporally (Shen et al., 2007). This is the mode preferred by SM proteins involved in membrane trafficking events. mVps45 binds to the conserved N-terminal motif of Syntaxin 16 (Dulubova et al., 2002; Yamaguchi et al., 2002) using this mode.

The third mode of binding is compatible with binding syntaxin in either the closed or open conformation. This mode of binding may feature in models where SM proteins do not inhibit SNARE complex assembly. In this model, the SM protein remains bound to the assembled SNARE complex to mediate later events (Munson and Bryant, 2009). Changes to the component partners in Mode 3 binding can result in trafficking defects in mammalian cells.

Of course, others have described a fourth mode of binding via multi-protein complexes. The yeast SM protein Vps33p uses this mode to interact with Vam3p and the C-Vps complex (Sato et al., 2000). These different binding modes might suggest an adaptation to prevent SM proteins from binding to their non-cognate syntaxins and thus preserving specificity of function.



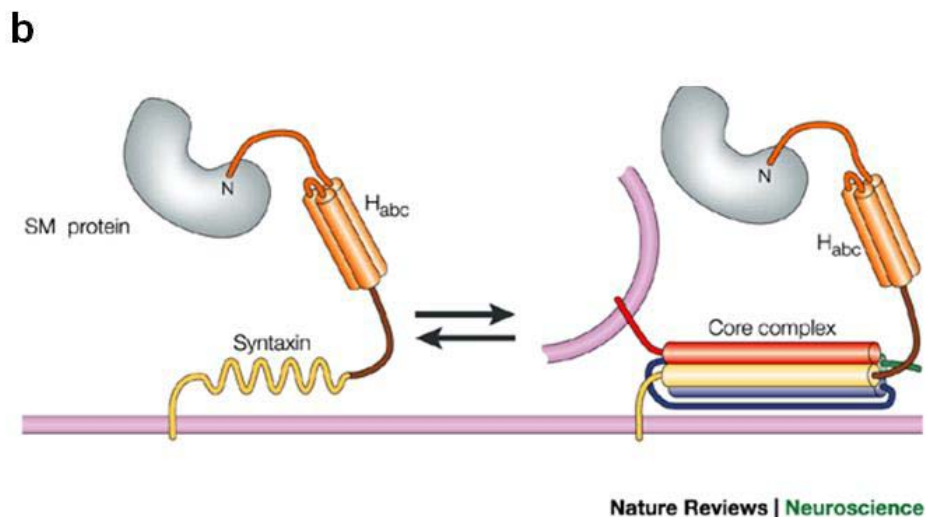
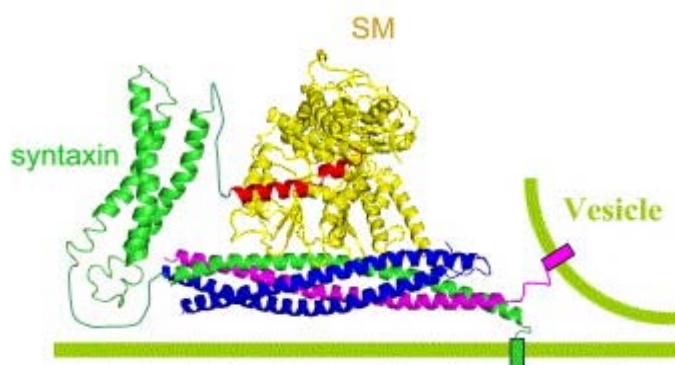


**Figure 1.7 SM proteins bind to their cognate t-SNARE**

a. SM proteins can bind using either Mode 1 or Mode 2 although Mode 2 binding (also shown in b) is the favoured method (Figure a: MacDonald et al., 2010) Reproduced with permission from MacDonald C, Munson M, Bryant NJ, 2010, *Biochem Soc Trans*, **38**, Pt 1, 209-12. © the Biochemical Society. b. In the ER, Golgi, TGN and early endosomes, SM proteins bind to the amino-peptide motif of the corresponding t-SNARE, an example of Mode 2 binding. (Figure b: Rizo and Sudhof, 2002)

Thus, SM proteins can differentiate among syntaxin conformations and facilitate the inter-conversion among conformations to control vesicle fusion (James, 2005). SM proteins cradle syntaxin in its closed conformation and may interact with more than one syntaxin, including non-syntaxin t-SNAREs and v-SNAREs (James, 2005). The small N-terminal domains of SM proteins bind to SNAREs leaving the rest free to function as possible effector domains as shown in Figure 1.8 (Dulubova et al., 2003). SM proteins use multiple epitopes of the SNAREpin and may regulate both the speed and the specificity of a fusion reaction (Shen et al., 2007). Proteins acting upon SM proteins may influence binding to Syntaxins. The loss of activity of each SM protein leads to impaired transport in different systems since deletion of these genes lead to blockage of fusion (Shen et al., 2007).



General role of SM protein:  
Selective activation of cognate SNAREpins

### Figure 1.8a The functional role of SM proteins in regulating membrane fusion

SM proteins bind to the core domains of cognate SNARE complexes as well as the N-terminal peptide of Syntaxin to regulate membrane fusion. Blue: light chain of t-SNARE. Magenta: v-SNARE, Red: N-terminal portion of Syntaxin bound to SM protein (Yellow). (Shen et al., 2007)

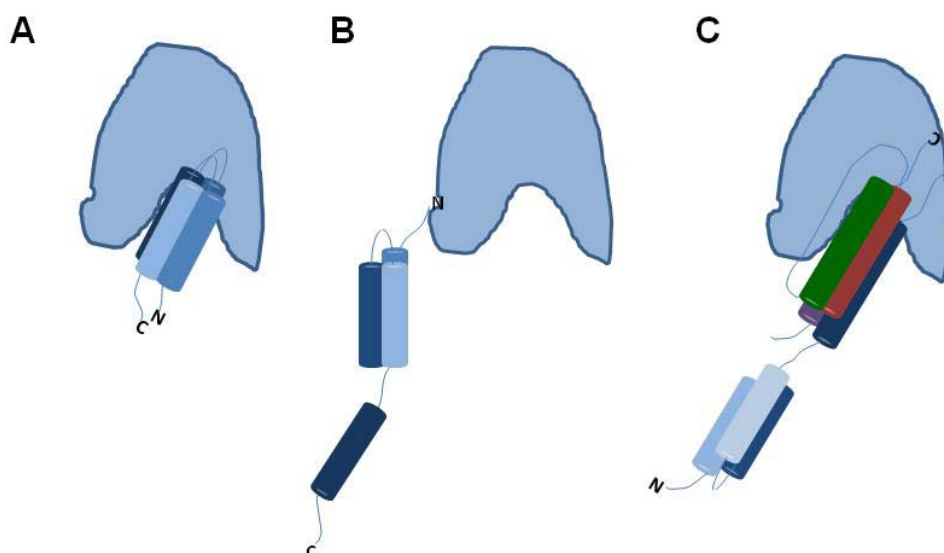


### Figure 1.8b SM Modes of Binding

SM proteins are thought to regulate the specificity of membrane fusion through the interaction with their cognate syntaxin and/or the assembled SNARE complex. This regulation occurs through several possible modes of binding. Mode 1 binding, illustrated in Panel A, occurs when the syntaxin is in the closed conformation (the Habc domain, here depicted in lighter blue colors, is folded back over the SNARE domain, a conserved region here represented by the dark blue color). In this mode of binding, the closed syntaxin interacts with the SM protein through the SM cleft region. Mode 2 binding, illustrated in Panel B, is the preferred mode of binding between mVps45 and Syntaxin 16. In this binding mode, the syntaxin remains in the open conformation with the extreme amino terminus of the protein binding the SM protein in the hydrophobic pocket region rather than in the cleft. This leaves the SNARE domain (dark blue) free to interact with other SNARE domains. Mode 3 binding, illustrated in Panel C, also occurs when a SNARE complex (shown here with the open conformation Qa-SNARE domain in dark blue, Qb- in green, Qc- in red and the R-SNARE in purple) binds with the SM protein in the SM cleft region.

### 1.4.2 Munc18c and the regulation of glucose transport

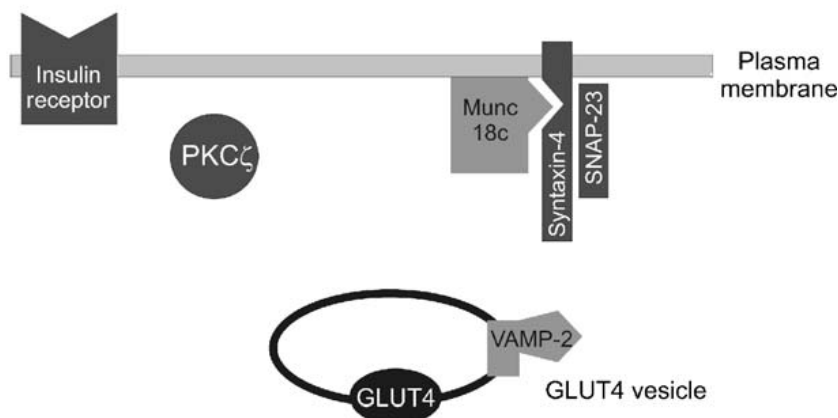
The SM protein that binds to Sx4 is Munc18c, and there is a wealth of evidence that implicates this SM protein in the control of insulin-stimulated GLUT4 translocation to the plasma membrane.

Munc18c is a cytosolic Syntaxin 4 binding protein which is involved in insulin regulated GLUT4 (James, 2005). Munc18c is composed of three domains, a small N-terminal domain, a central domain, and a C-terminal domain arranged in an arch shape. These three domains form a cavity that binds to the closed conformation of the syntaxin. The Habc domain folds back onto the SNARE motif forming a closed conformation that is incompatible with the core complex but is required for Munc18 binding to the closed conformation (Dulubova et al., 2002).

Recent studies have clearly shown that Munc18c can also bind to the open form of Munc18c. Thus, Aran et al have shown that Munc18c can bind a mutant of syntaxin 4 located in the open conformation, this binding (mode 2) mediated by the N-terminus of the syntaxin inserting into a hydrophobic pocket on Munc18c. It is clear that both these forms of interaction between syntaxin 4 and Munc18c are involved in SNARE complex regulation, as is the interaction of Munc18c with the intact SNARE complex (so-called mode 4 binding).

Over-expression of Munc18c (or the expression of mutants within cells) renders 3T3-L1 adipocytes refractory to insulin-stimulated glucose transport, presumably reflecting an imbalance between the SM/Syntaxin pairs within the cell. Indeed, quantification of the levels of Munc18c and Syntaxin 4 revealed that they are present in stoichiometric amounts, so that inhibition of translocation caused by the over-expression of Munc18c can be rescued with increased levels of Syntaxin 4 (Mora and Pessin, 2002). Thus, studying the role of Munc18c (or indeed any SM protein) in vivo has been difficult.

## No insulin



## Insulin

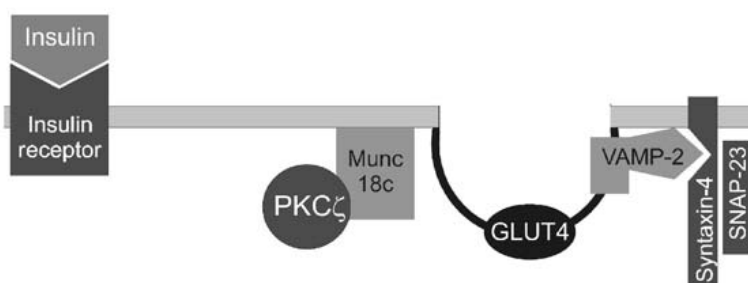


**Figure 1.9 Insulin may trigger GLUT4 translocation through the regulatory role of Munc18c.**

In the absence of insulin, Munc18c binds to the closed conformation of Syntaxin 4, thereby preventing VAMP2 from binding to the t-SNARE. Insulin may induce a conformational change in Munc18c so it is less able to bind Syntaxin 4, allowing VAMP2 to bind to the t-SNARE and form the SNARE complex necessary for GLUT4 translocation to the plasma membrane. (Hodgkinson et al., 2005)

A model for Munc18c function is shown in figure 1.9. Initially, it is thought that Munc18c retains Syntaxin 4 in a closed conformation which renders the syntaxin unable to bind with VAMP-2 and SNAP23 and this change occurs in response to insulin whereby Munc18c may undergo a conformational change that allows interaction between VAMP-2 and Syntaxin 4 (James, 2005; Hodgkinson et al., 2005).

Several studies have suggested that a key facet of insulin action occurs after the arrival of GLUT4 vesicles at the plasma membrane, suggesting that a step after the initial stabilised docking of these vesicles at the cell surface is under acute regulation by insulin. This contention is supported by TIRFM

studies, which show that in the absence of insulin, GLUT4-containing vesicles dock with the cell surface but do not normally proceed to fusion; in contrast, the rate of productive fusion events is dramatically increased by insulin. Moreover, using an elegant cell-free system which recapitulates the final fusion step of GLUT4 vesicles with purified plasma membranes, Koumarov and colleagues showed that the fusion of GLUT4 vesicles with plasma membranes is not constitutively active, but rather is activated ~8-fold by insulin (Koumarov et al., 2005). Such data posit that there is an insulin-dependent 'switch' to fusion competency after docking of GSVs at the plasma membrane. This might involve Munc18c. Homozygous depletion of Munc18c was found to be embryonically lethal, but heterozygous knockout mice (Munc18c(-/+)) exhibited decreased insulin sensitivity in an insulin tolerance test and a >50% reduction in skeletal muscle insulin-stimulated GLUT4 translocation when compared with wild-type mice, strongly supporting the notion that Munc18c is a key regulator of insulin-stimulated GLUT4 translocation. Using adipocytes derived from MEFs from Munc18c -/- mice, Kanda et al showed that GLUT4 translocation is enhanced by the absence of Munc18 (Kanda et al., 2005). Such data suggest that Munc18c inhibits insulin-stimulated externalization of GLUT4, and argues that the disruption of the interaction between Syntaxin 4 and Munc18c in adipocytes might result in enhancement of insulin-stimulated GLUT4 translocation. Consistent with this, over-expression of Munc18c was found to inhibit insulin-stimulated GLUT4 translocation in 3T3-L1 adipocytes, as did peptides designed to inhibit the binding of Munc18c to Sx4. Interestingly, Munc18c was found to inhibit the fusion of artificial liposomes mediated by Sx4/SNAP 23 and VAMP-2 *in vitro*, further supporting the notion of Munc18c inhibiting fusion of GLUT4 vesicles with the plasma membrane (Brandie et al., 2008).

## 1.5 mVps45

### 1.5.1 mVps45 as a Class D SM Protein

Vps45 encodes a 67 kDa homolog of Sec1p. It is peripherally associated with cellular membranes, potentially including Golgi and endosomal membranes, as well as membrane vesicles (Cowles et al., 1994). It is essential for viability and receptor-mediated endocytosis and it has also been shown that

Vps45 is expressed in all tissues of the early embryo of several species including *C. elegans* and *Drosophila* suggesting that it is ubiquitously expressed in development (Gengyo-Ando et al., 2007; Rahajeng et al., 2010).

### 1.5.2 Syntaxin 16

Syntaxin 16 is a member of the syntaxin subfamily of SNAREs (Simonsen et al., 1998). There are five splice variants of Syntaxin 16: Syntaxin A, B, C, D, and H. (Simonsen et al., 1998). The three longest splice variants encode membrane proteins (Syntaxins A, B, and H) but differ in sequence between the first 27 residues and their Habc domains (Dulubova et al., 2002). Syntaxins C and D are truncated versions that lack SNARE and trans-membrane domains (Simonsen et al., 1998). The corresponding yeast homologue to Syntaxin 16A is Tlg2p which has been shown to function in a similar manner (Struthers et al., 2009). Syntaxin 16 is located in the TGN (Simonsen et al., 1998) and is known to be involved in early endosome to TGN transport (Mallard and Tang, 2002). It is required for the efficient retrograde transport of Shiga toxin, cholera toxin, ricin and the mannose 6-phosphate receptor (Amessou et al., 2007). Syntaxin 16 forms a t-SNARE complex with syntaxin 6 and Vti1a (Mallard and Tang, 2002) and also with syntaxin 10 and Vti1a, however the latter complex is not formed in murine cells and is specifically required for the retrograde transport of mannose 6-phosphate receptor. Syntaxin 16 also binds to the SM protein mVps45 (Dulubova et al., 2002) which regulates its assembly into SNARE complexes.

Shewan and colleagues have found that Syntaxin 16 (in concert with Syntaxin 6) is transported to the plasma membrane in response to insulin (Shewan et al., 2003), but to an extent less than that observed for GLUT4.

### 1.5.3 The role of mVps45 in binding to Syntaxin 16

The interaction with mVps45 involves the very N-terminal sequence of Syntaxin 16 (Dulubova et al., 2002). An N-terminal peptide motif, specifically the first half, mediates binding to mVps45, and this short peptide sequence is all that is necessary to complex with Vps45 since this is the only functional region of Syntaxin 16 that is intact in all variants (Dulubova et al., 2003). Differences in the length of the sequence that follows the peptide motif may modulate the interplay between mVps45

binding and core complex formation, but it has now been established that the extreme N-terminus is all that is required to capture Vps45p (Dulubova et al., 2003). Residues outside of the N-peptide region of mammalian Syntaxin 16 increase its affinity for Vps45 (Burkhardt et al., 2008). Moreover, isothermal titration calorimetry has demonstrated that Vps45 binds tightly to the Syntaxin 16 N-peptide but weakly to Syntaxin 16 in the closed conformation (Burkhardt et al., 2008). Studies have indicated that syntaxins do not require their cognate SM protein for correct formation or targeting and that observed lower syntaxin levels in the absence of SM proteins can be explained by impairment in stability at their site of action (Novick and Zerial, 1997).

#### **1.5.4 The yeast homolog Vps45p**

Vps45p is a 67kDa hydrophilic protein characterized as a Class D mutant (Cowles et al., 1994). Class D mutants have large single vacuoles similar in morphology to the wildtype vacuoles in Class A mutants (but much larger and singular) which is in contrast to Class B mutants which display fragmented vacuoles and Class C mutants which do not possess a vacuole (Banta et al., 1998) Class E mutants contain additional compartments along with their vacuole and Class F mutants contain a large single vacuole surrounded by fragmented smaller compartments (Banta et al., 1988). In yeast, Vps45 function is required for the secretion of vacuolar proteins such as Carboxypeptidase Y (CPY) (Cowles et al., 1994). Vps45p, the yeast homolog, has a half time of sixty minutes in wild type cells and may function in vesicle docking or fusion from the Golgi to the endosome (Cowles et al., 1994). The yeast Tlg2p/Vps45p binding is homologous to the mammalian Syntaxin 16/mVps45 binding mode (Carpp et al., 2006). The similarity of the N-terminal sequences of Tlg2p and Syntaxin 16 indicate that Syntaxin 16 could bind to mVps45 by the same mechanism observed for the Tlg2p/Vps45p interaction (Dulubova et al., 2002). The Qa-SNARE Tlg2p cannot form SNARE complexes in strains of yeast that lack the SM protein Vps45p (Jahn and Scheller, 2006). The murine orthologue of Vps45 (mVps45) is functionally interchangeable with human Vps45 (hVps45) showing conservation in mammals (Gengyo-Ando et al., 2007), although it is not clear whether the human or rodent isoforms can compensate for the VPS45 deletion in yeast (see Chapter 4). Loss of Vps45 blocks transport from the Golgi to vacuoles.

In yeast cells deleted for Vps45p, CPY trafficking is defective and the cells are sensitive to osmotic stress and become growth sensitive in non-permissive temperatures (Piper et al., 1994). Vps45p binds to monomeric Tlg2p using mode 3 binding but can also bind to cis-SNARE complexes that contain Tlg2p (mode 4) (Carpp et al., 2006).

It has been found that Vps45p functions in the same Golgi-to-endosome pathway as the Rab-GTPase Vps21p. It is possible that Vac1p couples the interaction of Vps45p and Vps21p by interacting with Vps21p on the vesicle and Vps45p bound to the t-SNARE Pep12p on the endosome. In mammals, rabenosyn-5 may be the functional homologue of Vac1p and couples the interaction of the endosomal GTPase Rab5 with mVps45 (Nielson et al., 2000).

## 1.6 The Yeast Model

Yeast was the first eukaryote where the entire genome sequence was known (Coe et al., 1999). The yeast genome is 12.8 Mb divided into 16 chromosomes, which is 200 times smaller than that in humans but nearly four times bigger than *E. coli*. Taken with the fact that a protein encoding gene is found every two Kb on the yeast genome, yeast can be an ideal model organism for screening biological functions.

Yeast is a eukaryote that can be grown on deficient media and is amenable to classical genetic manipulations. A substantial number of cellular functions are highly conserved from yeast to mammals and corresponding genes can complement one another. The basic functions in yeast that are similar to those in higher eukaryotes include biosynthetic pathways and their regulation, cell division and the cell cycle, DNA replication, recombination and repair, transcriptional regulation and activation, signal transduction pathways and stress responses.

The life cycle of *S. cerevisiae* alternates between diploid and haploid phases and both ploidies exist in stable cultures. Yeast cells have a plasma membrane that folds into the cytosol and a lipid bilayer containing transmembrane proteins. The yeast periplasm outside of the plasma membrane secretes proteins such as invertase that converts sucrose to

glucose and fructose so that they can cross the plasma membrane. In this thesis, yeast is used as a screening mechanism to study the function of Vps45 through functional homology and mutational analysis.

### 1.6.1 Yeast metabolism and the Endocytic pathway

In the endocytic pathway (shown in Figure 1.10), membrane proteins and receptor-associated ligands are targeted to intracellular compartments (Maxfield and McGraw, 2004). At the plasma membrane, proteins are packaged into vesicles and transported to early endosomes and the lysosome for degradation. Alternatively, proteins that are reusable by the cell are recycled back to the plasma membrane. It has been shown that dephosphorylation of t-SNAREs modulates exocytosis and endocytosis in yeast by regulating the assembly of SNARE complexes (Gerst, 1999). Yeast cells lacking the v-SNAREs Snc1p and Snc2p and Tlg1p or Tlg2p t-SNAREs are defective in endocytosis. This is because after the disintegration of the late Golgi cisternae (TGN) some vesicles pass into the endocytic pathway along with newly synthesized vacuolar proteins and TGN syntaxins such as Tlg1p among others and when these molecules are defective they are unable to shuttle into the endocytic pathway. This shuttling is clathrin-dependent and can also be seen in animal cells that form secretory granules where the Tlg1p homologue Syntaxin 6 is removed in clathrin coated vesicles. Endocytosis is regulated by t-SNARE phosphorylation *in vivo*. It is thought that phosphorylation regulates the availability of t-SNAREs to participate in trafficking events.

The endocytic pathway in yeast is not essential. In fact, yeast can survive with only ER and plasma membrane syntaxins along with Sed5p (Cowles et al., 1994). Cowles and others have found that there is a direct transport pathway from the Golgi to the vacuole and the expression of Pep12p is enough to create endosomes. Other studies suggest that endosomes can form by the fusion of endocytic vesicles which with the addition of Pep12p can form structures capable of fusing with vacuoles (Nichols et al, 1998).

Transfer of proteins from the exocytic to the endocytic pathways in yeast is dependent on the late Golgi syntaxins Tlg1p and Tlg2p (Nichols et al., 1998). In relation to this, the v-SNARE Snc1p, which mediates fusion of exocytic vesicles with the PM, is dependent on these syntaxins for its function. After

Snc1p arrives at the PM, it dissociates from the t-SNARE Sso1p and is endocytosed (Pelham, 1999) after which it is recycled to the Golgi. Just as in the mammalian homologues Syntaxin 6 and 16, Tlg1p forms a complex with Tlg2p.

### 1.6.2 The Secretory Pathway

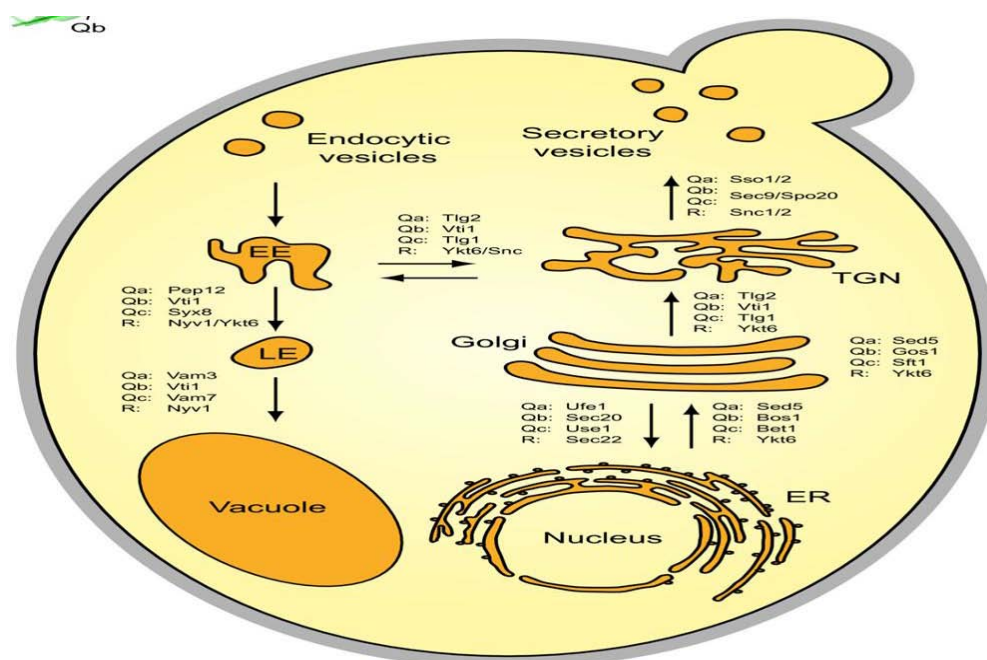


**Figure 1.10 The Endocytic and Secretory Pathways in Yeast**

The endocytic and secretory pathways in yeast are regulated by t-SNAREs and transfer between pathways is dependent on the actions of Tlg1p and Tlg2p, the homologues of Syntaxins 6 and 16 in mammals. Sso1p has been found to be essential for exocytosis at the plasma membrane. (Kienle et al., 2009)

In the secretory pathway newly synthesized membrane proteins and soluble proteins are translocated into the endoplasmic reticulum. The proteins are packaged into vesicles and transported to the Golgi. Once at the Golgi, the proteins move through the Golgi cisternae to the *trans*-Golgi network (TGN). At the TGN, proteins are sorted with soluble proteins being secreted from the cell and membrane proteins exocytosed to the plasma membrane by vesicle fusion. Proteins not destined for other functions are either retained or sorted to the lysosome for degradation.

### 1.6.3 Membrane fusion and homology to the Mammalian System

There are around 20 SNAREs in yeast, eight of which can be considered syntaxins (Pelham, 1999). Two yeast syntaxins, Sso1p and Sso2p are found on the plasma membrane. Pep12p is found on endosomes while Vam3p is found on vacuoles. Ufe1p localizes to the ER and Sed5p is found on early Golgi cisternae. Tlg1p and Tlg2p are also Golgi-associated but localize with late Golgi markers (Pelham, 1999). There are clear homologues of Golgi syntaxins (Sed5p, Tlg1p and Tlg2p) between mammals, nematodes (which have nine syntaxins) and yeast. In yeast, v-SNAREs can bind multiple syntaxins, for example the v-SNARE Vti1p binds five different syntaxins. Further, for v-SNAREs to be used again they must be recycled to their starting point and thus traffic on vesicles in both directions. In addition to this multi-tasking of v-SNAREs, the t-SNARE Sed5p binds to at least seven different SNAREs in at least three separate complexes (Pelham, 1999).

Trafficking routes show several redundancy steps. For example, the v-SNARE Vti1p is thought to be involved in traffic from Golgi to endosomes, Golgi to vacuole and endosomes to Golgi (Pelham, 1999). In the SNARE complex of yeast, the hydrophobic core of the complex is conserved but there are sequence differences on residues located on the solvent-exposed surfaces of the helix bundle (Pelham, 1999). This shows that syntaxin function is not terribly specific and weak interactions with associated effector molecules provide specificity of function rather than the action of individual SNAREs. For example, in both yeast and animal cells fusion of endosomes requires the phosphorylation of phosphatidylinositol molecules to form PI3P (Burd et al., 1997). Docking of the membranes requires the recruitment of a soluble protein which is EEA1 in animal cells and Vac1p in yeast whose binding depends on both Rab5 and PI3P which restricts it to endosomes (Pelham, 1999).

The four yeast SM proteins are Sec1p which controls exocytosis, Sly1p which acts at the Golgi and ER, Vps45p which acts at the TGN, and Vps33p which acts with the HOPS complex to restrict sorting in the vacuole or lysosome (Chen and Scheller, 2001). SM protein sequences are conserved and they have a common fold, but there is enough sequence diversity to allow for functional differences. There is a noted conservation of the SM protein-

syntaxin peptide interaction. In fact, structural similarities of SM proteins and biochemical evidence suggest that Tlg2p residues 1-33 are sufficient for Vps45p interaction (Dulubova et al., 2002).

#### **1.6.4 The Syntaxin homolog Tlg2p**

Tlg2p is localized to the TGN and functions normally as a t-SNARE (Dulubova et al., 2002). Cells deleted for Tlg2p show defective sorting of carboxypeptidase Y (CPY) and Tlg2p is required for the recycling of Snc1p through the early endosome (Abeliovich et al., 1998). Tlg2p complexes with Tlg1p (the syntaxin 6 homologue) and Vti1p (the Vti1a homologue) as well as the v-SNAREs Snc1p and Snc2p (Abeliovich et al., 1998). Like Syntaxin 16, Tlg2p requires phosphorylation in order to complex with other SNAREs (Gurunathan et al., 2002). Vps45p stabilizes the syntaxin Tlg2p and positively regulates SNARE complex formation (Bryant and James, 2001). Vps45p is recruited to the target membrane by binding to the N-terminus of Tlg2p. In fact when Vps45p is deleted in yeast cells, Tlg2p is down-regulated (Bryant and James, 2001).

### **1.7 Hypothesis**

This project tests the hypothesis that when mVps45 interacts with Syntaxin 16 in the absence of insulin, GLUT4 goes into the slow cycle. However, when insulin stimulation occurs, mVps45 does not bind to Syntaxin 16 and GLUT4 is prevented from going into the slow recycling pathway.

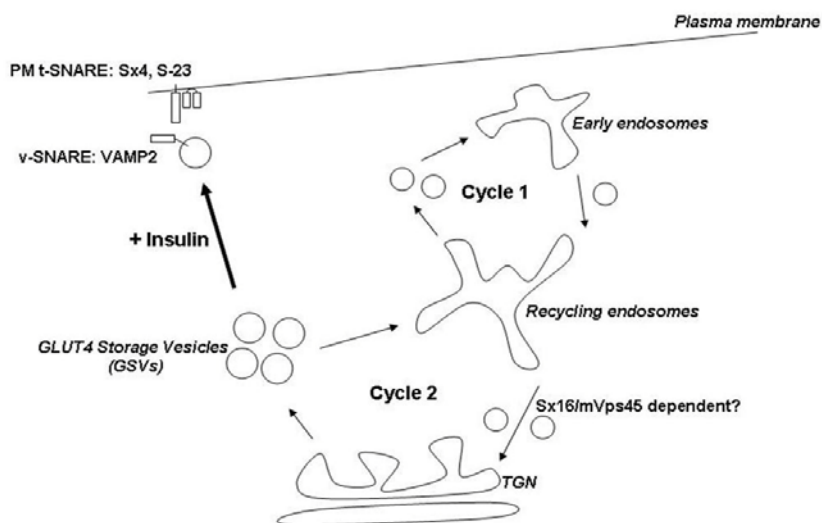


**Figure 1.11 Sorting of GLUT4 into the slow recycling pathway may be mVps45 dependent**

In the cartoon depicted above, mVps45 may have a role in shuttling GLUT4 into the slow recycling pathway in the absence of insulin. mVps45 may act on this pathway via its role in modulating the actions of the t-SNARE Syntaxin 16. The aims of this thesis set out to examine if this is the case. (Reproduced with permission from Gwyn Gould)

## 1.8 Aims

This work is aimed at understanding the mechanism by which insulin regulates glucose transport in adipocytes and specifically the mechanism by which the intracellular sorting of glucose transporters is regulated in adipocytes. This regulation is known to be defective in Type II diabetes and understanding the mechanisms utilised by insulin to achieve this regulation is an important step to developing effective therapies.

Glut4 translocation to the plasma membrane is an essential step in glucose metabolism. Upon insulin stimulation, GLUT4 storage vesicles (GSVs) are rapidly translocated to the plasma membrane where they dock and subsequently fuse, resulting in elevated cell surface GLUT4 levels (see Figure 1.11). In the absence of insulin, GLUT4 is sorted into a slow recycling pathway, operating between recycling endosomes, the trans-Golgi network (TGN) and GSVs. Switching from the fast to the slow pathway creates a pool of GLUT4 in GSVs that can be used rapidly in response to an increase in glucose at the cell surface.

How adipocytes sequester GLUT4 in the slow cycle is poorly understood and this project aims to understand this sorting mechanism at the molecular level. It is known that Syntaxin 16 is required for entry into the slow recycling pathway (Proctor et al., 2006), but little is known about how Syntaxin 16 is regulated in this system. mVps45 is a Sec1/Munc18 (SM) protein that binds to Syntaxin 16 (Cowles et al., 1994) and may control GLUT4 recycling to the GSVs in the slow cycle.

This project tests the hypothesis that when mVps45 interacts with Syntaxin 16 in the absence of insulin, GLUT4 goes into the slow cycle. However, when insulin stimulation occurs, mVps45 does not bind to Syntaxin 16 and GLUT4 is prevented from going into the slow recycling pathway. This hypothesis is testable in a variety of ways.

In Chapter 3 the absolute levels of mVps45 and Syntaxin 16 were quantified in 3T3-L1 fibroblasts and differentiated adipocytes. This is an important starting point in learning baseline information about the intracellular environment. Knowing the endogenous levels of mVps45 and Syntaxin 16 is vital to learning the underlying mechanisms of slow pathway recycling. Quantitative immunoblots with titrated amounts of recombinant protein were assayed for Syntaxin 16 and mVps45. These data indicated the amounts of both Syntaxin 16 and mVps45 in adipocytes both in membrane and cytosolic fractions were present at levels indicated by other studies (Proctor et al., 2006). Similar blots were also performed using insulin stimulated adipocytes and the data compared to basal levels. These measurements of protein expression levels indicated whether Syntaxin 16 and mVps45 were present in stoichiometric amounts. The interaction between Syntaxin 16 and mVps45 was examined by preparing cell lysates from differentiated 3T3-L1 adipocytes in basal and insulin stimulated conditions. These lysates were used to immunoprecipitate Syntaxin 16 and blot for the presence of mVps45. This experiment showed whether Syntaxin 16 and mVps45 interact in the presence of insulin.

One of the few pieces of information known about mVps45 is its homology to the yeast system. In Chapter 4, complementation between the mammalian and yeast systems are the focus. In yeast, the depletion of Vps45 causes

problematic sorting of vacuolar hydrolase Carboxypeptidase Y (CPY). Experiments using this knowledge tested whether mVps45 could complement the yeast VPS45 deletion mutant, and thus whether mVps45 was a true functional homologue. Once complementation was tested, functional assays were then performed. In the event that functional complementation could be demonstrated, the potential to design mutants of mVps45 will be exploited.

In chapter 5, the condition of the intracellular environment in the absence of mVps45 was analysed. It is postulated that this SM protein is the regulator of Syntaxin 16 and thus controls entry of GLUT4 into the slow recycling pathway, so in the absence of mVps45, the corresponding levels of Syntaxin 16 and the progress of GLUT4 both in the presence and absence of insulin were noted. To study this question, adipocytes were depleted of mVps45 by RNAi knockdown. After depletion, glucose metabolism was measured in the presence and absence of insulin to ascertain information about the rate, sensitivity and extent of insulin stimulation. These series of experiments, testing cells after the depletion of mVps45, gave a better understanding of how insulin stimulated transport is changed in the absence of mVps45.

## **Chapter 2 – Materials and Methods**

## Chapter 2: Materials and Methods

### 2.1 Materials

#### 2.1.1 Common Reagents and Suppliers

All reagents were purchased from VWR UK Ltd., Leicestershire UK unless otherwise stated below:

*Ambion, Texas, USA*  
Nuclease Free Water

*BD Biosciences, Oxford UK*  
Syringes  
26 <sup>5</sup>/<sub>8</sub> Gauge Needles

*BDH Laboratory Supplies, Poole, UK*  
Calcium Chloride (CaCl<sub>2</sub>)  
Coomassie Brilliant Blue R-250  
Dipotassium hydrogen phosphate (K<sub>2</sub>HPO<sub>4</sub>)  
Hydrogen Peroxide (H<sub>2</sub>O<sub>2</sub>)  
Magnesium Chloride (MgCl<sub>2</sub>)  
Magnesium Sulfate (MgSO<sub>4</sub>)  
Potassium Chloride (KCl)  
Sodium Chloride (NaCl)  
Tetrasodium pyrophosphate (Na<sub>4</sub>P<sub>2</sub>O<sub>7</sub>)

*Fisher Scientific UK Ltd., Leicestershire, UK*  
Ethanol  
Glycine  
HEPES (N-2-hydroxyethylpiperazine-N' 2-ethane sulphonic acid)  
Potassium dihydrogen phosphate (KH<sub>2</sub>PO<sub>4</sub>)  
Tris Base (tris(hydroxymethyl)aminoethane)

*ForMedium, Norfolk UK*  
Agarose  
Amino Acid Drop-Out Media -URA, -Met  
Peptone  
Tryptone  
Yeast Extract  
Yeast Nitrogen Base without Amino Acids  
Micro Agar

*GE Healthcare, Buckinghamshire, UK*  
Protein A-sepharose beads

*Invitrogen, Paisley UK*  
SOC Media  
Deoxynucleotidetriphosphates (dNTPs)

*Kodak Ltd., Hertfordshire UK*  
X-Ray Film

*New England BioLabs UK Ltd., Hertfordshire UK*  
T4 DNA Ligase  
Restriction endonucleases

*Melford Laboratories Ltd., Suffolk, UK*  
Dithiothreitol (DTT)

*Perkin Elmer, Buckinghamshire, UK*  
2-<sup>3</sup>H]-deoxy-D-glucose

*Pierce, Perbio Science UK Ltd., Cheshire, UK*  
10,000 MWCO slide-a-lyzer

*Premier Brands UK, Staffordshire UK*  
Marvel Low-fat Milk Powder

*Promega, Southampton UK*  
Pfu DNA Polymerase  
Wizard Plus SV miniprep kit

*Qiagen, West Sussex, UK*  
QIAfilter Maxi-plasmid purification kit  
QIAquick Gel Extraction kit  
Nickel-NTA agarose (Ni-NTA beads)

*Roche Diagnostics Ltd., Burgess Hill UK*  
Complete and Complete EDTA-Free protease inhibitor tablets

*Severn Biotech Ltd., Worcestershire UK*  
30% acrylamide/bisacrylamide

*Sigma-Aldrich, Steinheim, Germany*  
5-Amino-2,3-dihydro-1,4-phtalazinedione (luminol)  
Adenosine 5'-triphosphate (ATP)  
Ammonium peroxydisulphate (APS)  
Bovine Serum Albumin (BSA)  
p-Coumaric acid  
Dimethyl sulphoxide (DMSO)  
Disodium hydrogen phosphate (Na<sub>2</sub>HPO<sub>4</sub>)  
Ethylenediamine tetraacetic acid (EDTA)  
Glycerol  
Sodium Fluoride (NaF)  
Sodium hydrogen carbonate (NaHCO<sub>3</sub>)  
Sodium dihydrogen phosphate (NaH<sub>2</sub>PO<sub>4</sub>)  
Sodium orthovanadate (Na<sub>4</sub>VO<sub>3</sub>)  
Sodium dodecyl sulphate (SDS)  
N,N,N',N'-Tetramethylethylenediamine (TEMED)  
Triton X-100  
Tween-20

*Sterilin Limited, Caerphilly UK*

90 mm Petri dishes

*Whatman Plc., Kent UK*  
Protran nitrocellulose

### 2.1.2 Computer Software

Image J V1.41 National Institutes of Health, Bethesda MD, USA

LSM Viewer Carl Zeiss AxioVision LE Rel 4.5 Hertfordshire, UK

Photoshop CS5, Adobe Systems Europe Ltd., Uxbridge, UK

Vector NTI V10.3 Invitrogen, Carlsbad, CA, USA

### 2.1.3 Primers

Primer	Sequence (5'-3')
Vps45 His 5' Forward	GGGCTCCAGCTCGAACGTCCTCTTTGCTGTGAAG
Vps45 His 3' Reverse	GCCCGCGGCCCGTCATCTTCTGCTTGCTGACCT
Vps45 Seq +1 Forward	ATG AAC GTG GTT TTT GCT
Vps45 Seq +500 Forward	CTG AAG AAG TGT CCC ATG
Vps45 Seq +1000 Forward	GGT TGG AGA ACT GTC TCG
Vps45 Seq +1500 Forward	GGA GGA GCC ACC TAT GAA
Vps45 Seq -1713 Reverse	TCA TCT TCT GCT CGC TGA
Vps45 Seq -1200 Reverse	GCT GCT GTG TCG CTC ATA
Vps45 Seq -700 Reverse	GGC CTG ATA TGT CCA CTG
Vps45 Seq -200 Reverse	GCC TTC AGG TGT TTC ATG
Vps45 ShRNA Target 1 132 5' Forward	GATCCGGTATAGTGAGTATGGTCTTTCAAGAGAAGACCAT ACTCACTATACTTTTTTACGCGTG
Vps45 ShRNA Target 1 132 3' Reverse	AATTCACGCGTAAAAAAGGTATAGTGAGTATGGTCTTCTC TTGAAAGACCATACTCACTATAACCG
Vps45 ShRNA Target 2 427 5' Forward	GATCCGCGGTGAATCCACAATTTGTTTTCAAGAGAAACA AATGTGGATTCACCGTTTTTACGCGTG
Vps45 ShRNA Target 2 427 3' Reverse	AATTCACGCGTAAAAACGGTGAATCCACATTTGTTTCTCT TGAAAACAAATGTGGATTCACCGCG
Vps45 ShRNA Target 3 329 5' Forward	GATCCGCAGTAATGTGATCAGCAAGTTCAAGAGACTTGCT GATCACACTACTGTTTTTACGCGTG
Vps45 ShRNA Target 3 329 3' Reverse	AATTCACGCGTAAAAAAGGTATAGTGAGTATGGTCTTCTCT TGAAAGACCATACTCACTATAACCG
Vps45 ShRNA Target 4 1256 5' Forward	GATCCGAGTGGACCTCAGGAGTAAATTCAAGAGATTTACT CCTGAGGTCCACTTTTTTACGCGTG
Vps45 ShRNA Target 4	AATTCACGCGTAAAAAAGTGGACCTCAGGAGTAAATCTCT

1256 3' Reverse	TGAATTTACTCCTGAGGTCCACTCG
Vps45 Yeast Recombinant 5'	GAAGAGGTACAGTGACTTGGTTTTGAGTTAAGGCCATCTT TACTGTATAGAACAAGAAATGAACGTGGTCTTTGCTGTG AAGC
Vps45 Yeast Recombinant 3'	CGAAAAAGTTATATAGATTTATGCCTCATATATAAAATAGA ATTTTAGAATAAGATAATCCTCAAGCGTAATCTGGAACGTC ATATGGATAGGAACCACTGCCATCTCATCTTCTGCTTGC
Vps45 V107R 5'	GTAATGTGATCAGCAAGAGTGACCGGAAGTCCTTGGCTGA AGCTGACG
Vps45 V107R 3'	CGTCAGCTTCAGCCAAGGACTTCCGGTCACTCTTGCTGATC ACATTAC
Vps45 W230R 5'	CATCACCCCACTGCTCAACCAGCGGACATATCAGGCCATGG TCCATG
Vps45 W230R 3'	CATGGACCATGGCCTGATATGTCCGCTGGTTGAGCAGTGG GGTGATG

Construction of mVps45 protein required particular restriction sites to be engineered into the Insert sequence by PCR for ligation into the recombinant vector. These restriction sites are indicated in bold in the Vps45 His primer set. Additionally, synthesis of knockdown targets using shRNA required using specific sequences from the mVps45 CDS, which are also indicated in bold. When mutating the yeast recombinant to make pocket-filled and dominant negative mutants, amino acids were changed in the protein sequence and these changes, all to arginine mutants, are indicated in bold. The pocket-fill mutant V107R, which inhibits binding by steric hindrance, is a valine to arginine mutant at the 107 amino acid in the protein sequence. The dominant-negative mutant W230R, which binds but does not function, is a tryptophan to arginine mutant at the 230 amino acid in the protein sequence. A double mutant was also made by using the pocket-fill mutant as a template and applying SDM with the dominant-negative primers.

#### 2.1.4 Plasmids

Plasmid	Description	Source
RNAi-Ready pSIREN-RetroQ vector	ColE <i>ori</i> Amp <sup>r</sup> Puro <sup>r</sup>	Clontech
RNAi-Ready pSIREN-RetroQ Zs Green	ColE <i>ori</i> Amp <sup>r</sup> Zs Green 1	Clontech
HA-GLUT4-GFP in the pRRL-PGK plasmid	Human GLUT4 cDNA, tagged with GFP at the C-terminus and an HA epitope-tag in the exofacial loop in a vector for producing lentivirus	Dr. Cynthia Mastick, University of Nevada, Reno

	particles	
pCMV-Vps45	Full length cDNA of rat mVps45 in pAlter-Max vector.	Dr. Robert Piper, University of Iowa
pCR2.1-TOPO	ColE <i>ori</i> Amp <sup>r</sup> Kan <sup>r</sup> <i>LacZ</i> <sub>α</sub> , TA Cloning Vector	Invitrogen
pCog70	yEpVPS45 (YEplac195) <i>2u</i> , <i>URA3</i> encoding C-terminally HA-tagged version of <i>S. cerevisiae</i> Vps45p flanked by downstream sequences containing the <i>VPS45</i> promoter and terminator region.	Carpp et al., 2006 Gietz and Sugino, 1988
pQE-30	pUC <i>ori</i> , LacO, Amp <sup>r</sup> , <i>E. coli</i> expression vector	Qiagen
pALA001 (Stx16-PrA)	<i>E. coli</i> expression plasmid encoding C-terminally PrA-tagged truncated version of Syntaxin 16A (Cytosolic residues 1-269)	Alicja Drozdowska

### 2.1.5 *E. coli* Strains

Strain	Genotype	Source
BL-21 (DE3)	F <sup>-</sup> <i>omp</i> T <i>hsdS</i> <sub>B</sub> ( <i>r</i> <sub>B</sub> <sup>-</sup> <i>m</i> <sub>B</sub> <sup>-</sup> ) <i>gal dcm</i> (DE3)	Invitrogen
Fusion Blue	<i>endA1</i> , <i>hsdR17</i> ( <i>r</i> <sub>K12</sub> <sup>-</sup> , <i>m</i> <sub>K12</sub> <sup>-</sup> ), <i>supE44</i> , <i>thi-1</i> , <i>recA1</i> , <i>gyrA96</i> , <i>relA1</i> , <i>lac F</i> '[ <i>proA</i> <sup>+</sup> <i>B</i> <sup>+</sup> , <i>lacI</i> <sup>q</sup> <i>ZΔM15::Tn10</i> ( <i>tet</i> <sup>R</sup> )]	Invitrogen
Top 10	F- <i>mcrA</i> _( <i>mrr-hsdRMS-mcrBC</i> ) <i>φ80lacZ_M15_lacX74 nupG recA1 araD139_(ara-leu)7697 galE15 galK16 rpsL(Str<sub>R</sub>) endA1 λ</i>	Invitrogen
XL-1 Blue	<i>recA1 endA1 gyrA96 thi-1 hsdR17 supE44 relA1 lac</i> [F' <i>proAB lacI</i> <sup>q</sup> <i>ZΔM15 Tn10</i> (Tet <sup>r</sup> )]	Stratagene

### 2.1.6 *S. cerevisiae* Strains

Strain	Genotype	Source
9Dα (SF838-9D)	MATα <i>leu2-3 112 ura3-52 his4-519, ade6, gal2 pep4-3</i>	Rothman, Howald et al., 1989
9DαΔ45 (LCY008)	MATα, <i>ura3-52 leu2-3 112 his4-519, ade6, gal2, pep4-3, vps45Δ::Kan<sup>r</sup></i>	<i>Sma</i> I/ <i>Sph</i> I digested pNOz13 (Bryant and James, 2001) used to disrupt <i>VPS45</i> in SF838-9D

## 2.1.7 Cell Culture materials, media, solutions and cell lines

### Materials

*Cell Culture BD Falcon Plasticware from BD Biosciences, Oxford UK*

10cm culture plates Cat#734-0006

6 well plates Cat#734-0019

12 well plates Cat#734-0055

24 well plates Cat#734-0020

96 well plates Cat#734-0026

*Corning Cell Culture Flasks, Fisher Scientific, Leicestershire UK*

Corning T150 Flasks Cat#430823

### Medium and Reagents

*Invitrogen, Paisley UK*

NCS Cat#16010159

FCS USA Certified Cat#16000-044

Dulbecco's Modified Eagle's Medium (DMEM) Cat#41965

Trypsin Cat#25300054

Optimem Cat#11058021

Lipofectamine 2000 Cat#11668019

*Fisher Scientific UK Ltd., Leicestershire UK*

D-Glucose Cat#G-0400-60

*Novo-Nordisk, Bagsvaerd, Denmark*

Porcine Insulin

*Sigma-Aldrich, Steinheim, Germany*

Cytocholasin B

Dexamethasone

Isobutylxanthine (IBMX)

### Cell Culture Solutions

*HES Buffer, pH 7.4*

250mM Sucrose

20mM HEPES pH 7.4

1mM EDTA

1 Tablet Roche EDTA-Free Protease Cocktail Inhibitor

*IP Buffer*

50mM HEPES, pH 7.5

5mM EDTA

10mM Tetra sodium pyrophosphate

10mM NaF

150mM NaCl

2% (w/v) Protease Inhibitor Cocktail Tablet (Roche)

2mM Sodium Orthovanadate  
 50mM  $\beta$ -Glycerophosphate  
 1mM DTT  
 1% (v/v) Triton X-100

## Cell Lines

Cell Line	Source	Catalog Number
3T3-L1	American Type Culture Collection (ATCC)/LGC Promochem	CL-173
EcoPack 2-293	Clontech	631507
NIH/3T3	ATCC	CRL-1658

## 2.1.8 Primary Antibodies

All antibodies were incubated overnight at 4°C unless otherwise stated

Epitope	Clonality	Host Species	Dilution	Diluent	Source
Actin	Polyclonal (C11)	Rabbit	1:100	5% BSA	Sigma-Aldrich (Cat#A2066)
C/EBP $\alpha$	Polyclonal (14AA)	Rabbit	1:250	5% Milk PBST	Santa Cruz Biotechnology (Cat#sc-61)
$\alpha$ CPY	Monoclonal Clone:10A5	Mouse	1:50	5% Milk TBST	Roeder and Shaw 1996
EEA1	Monoclonal Clone:14	Mouse	1:100	5% Milk TBST	BD Transduction Labs (Cat#610456)
FAS	Monoclonal Clone:23	Mouse	1:250	5% Milk PBST	BD Transduction Labs (Cat#610962)
GAPDH	Monoclonal Clone:6C5	Mouse	1:40,000	5% Milk PBST	Ambion (Cat#AM4300)
GLUT4	Monoclonal Clone:1F8	Mouse	1:500	5% Milk PBST	Cell Signaling (Cat#2213)
HA	Monoclonal Clone:3F10	Rat	1:1000	5% Milk PBST	Roche (Cat#11867423001)
HA.11	Monoclonal Clone:16B12	Mouse	2.5mg/ml WB 1:1000	WB:5% Milk PBST	Covance/Cambridge Biosciences (Cat#MMS-101R)
IRAP	Polyclonal	Rabbit	1:100	5% Milk PBST	Cell Signaling (Cat#3808)
IRAP	Polyclonal (E-14)	Goat	1:100	5% Milk PBST	Santa Cruz Biotechnology (Cat#sc-107642)
Pgk1p	Polyclonal	Rabbit	1:20,000	5% Milk TBST	Piper et. al 1994
PPAR $\gamma$	Monoclonal Clone:E-8	Mouse	1:2000	5% Milk PBST	Santa Cruz Biotechnology

					(Cat#sc-7273)
Rabenosyn-5	Polyclonal	Goat	1:300	5% Milk PBST	Sigma-Aldrich (Cat#SAB2500853)
SNAP23	Polyclonal	Rabbit	1:2000	5% Milk TBST	Synaptic Systems (Cat#111 203)
Syntaxin 4	Polyclonal	Rabbit	1:10,000	5% Milk PBST	Synaptic Systems (Cat#110 042)
Syntaxin 6	Monoclonal Clone:30	Mouse	1:1500	5% Milk PBST	BD Transduction Labs (Cat#610635)
Syntaxin 13	Monoclonal Clone:15G2	Mouse	1:1000	5% Milk PBST	Stressgen (Cat#VAM-SV026)
Syntaxin 16	Monoclonal Clone:148.6	Mouse	1:1000	5% Milk PBST	Synaptic Systems (Cat#110 161)
Syntaxin 16	Polyclonal	Rabbit	4µg/ml	IP Buffer	Synaptic Systems (Cat#110 162)
Transferrin Receptor	Monoclonal Clone:H68.4	Mouse	1:500	5% Milk PBST	Zymed/Invitrogen (Cat#13-6800)
Tubulin	Monoclonal Clone:14C11	Mouse	1:2500	5% BSA TBST	BD Transduction Labs (Cat#629201)
Vps45	Polyclonal	Rabbit	1:1000	5% Milk PBST	Synaptic Systems (Cat#137 002)
Vps45	Polyclonal	Goat	1:200	1%BSA 3% Donkey Serum 2 hours RT	Abcam (Cat#ab40853)
Vps45p (Yeast)	Polyclonal	Rabbit	1:500	5% Milk TBST	Eurogentec aa 14-28, 563-577
Vti1a	Monoclonal Clone:aa.114-217	Mouse	1:1000	5% Milk PBST	BD Transduction Labs (Cat#611220)
Vti1b	Monoclonal Clone:aa. 9-121	Mouse	1:1000	5% Milk PBST	BD Transduction Labs (Cat#611404)

### 2.1.9 Secondary Antibodies

All secondary antibodies were linked to HRP and were used in 1% (w/v) Milk PBST or TBST for 45 minutes at room temperature

Epitope	Host Species	Dilution	Source
Alexa Fluor 488 Donkey	Rat	1:50	Molecular Probes/Invitrogen (Cat#A20218)
Alexa Fluor 594 Donkey	Rabbit	1:50	Molecular Probes/Invitrogen (Cat#A21207)

Mouse IgG	Sheep	1:2500	GE Healthcare (Cat#NA931)
Goat IgG	Swine	1:2000	Caltag (Cat#G50007)
Rabbit IgG	Donkey	1:2500	GE Healthcare (Cat#NA934)
Rat IgG	Goat	1:2000	GE Healthcare (Cat#NA935)

### 2.1.10 General Solutions

#### *Coomassie*

0.05% (w/v) Coomassie brilliant blue R250

50% (v/v) methanol

10% (v/v) acetic acid

#### *Coomassie Destain*

10% (v/v) methanol

10% (v/v) acetic acid

#### *DNA Loading Dye*

2.5% (w/v) Bromophenol Blue

2.5% (w/v) Xylene Cyanole FF

67% (v/v) Ficoll Type 400 (Pharmacia)

#### *ECL reagents*

##### *Solution 1*

100mM Tris-HCl, pH 8.5

2.25mM luminal in 2% (v/v) DMSO

0.4 mM p-coumaric acid in 1% (v/v) DMSO

##### *Solution 2*

100mM Tris-HCl, pH 8.5

0.018% (v/v) H<sub>2</sub>O<sub>2</sub>

#### *KRH Buffer*

20mM NaCl

20mM HEPES-NaOH, pH 7.4

5mM NaHCO<sub>3</sub>

10mM D-Glucose

5mM KCl

1.2mM CaCl<sub>2</sub>

1.2mM MgSO<sub>4</sub>

1.2mM NaH<sub>2</sub>PO<sub>4</sub>

0.1mM L-Arginine

#### *KRP Buffer*

1.28M NaCl

47mM KCl

50mM NaH<sub>2</sub>PO<sub>4</sub>, pH 7.4

12.5 mM MgSO<sub>4</sub>

12.5 mM CaCl<sub>2</sub>

*LiTE-Sorb*

1M LiOAc  
1M Tris, pH7.6  
0.5M EDTA  
2.4M Sorbital

*PBS pH 7.2*

85 mM NaCl  
1.7 mM KCl  
5 mM Na<sub>2</sub>HPO<sub>4</sub>  
0.9 mM KH<sub>2</sub>PO<sub>4</sub>

*Ponceau S*

0.2% (w/v) Ponceau S  
1% (v/v) Glatial acetic acid

*SDS-PAGE Running Buffer*

250 mM glycine  
62 mM Tris Base  
0.1% (w/v) SDS

*4X SDS-PAGE sample buffer*

200mM Tris-HCl, pH 6.8  
8% (w/v) SDS  
40% (v/v) Glycerol  
0.4% (w/v) bromophenol blue  
400mM DTT

*SDS-PAGE Transfer Buffer*

25mM Tris Base  
192 mM Glycine  
20% (v/v) Methanol

*SOC Medium*

2% (w/v) Tryptone  
0.5% (w/v) Yeast Extract  
20mM D-Glucose  
20mM MgSO<sub>4</sub>  
10mM NaCl  
2.5mM KCl  
10mM MgCl<sub>2</sub>

*2YT*

1.6% (w/v) Tryptone  
1% (w/v) Yeast Extract  
0.5% (w/v) NaCl

*TAE*

40mM Tris-Acetate  
1mM EDTA, pH 8.0

*TB*

1.2% (w/v) Tryptone

2.4% (w/v) Yeast Extract  
 0.4% (v/v) Glycerol  
 2.3% (w/v)  $\text{KH}_2\text{PO}_4$   
 12.5% (w/v)  $\text{K}_2\text{HPO}_4$

*TBST*

20 mM Tris-HCl, pH 7.5  
 137 mM NaCl  
 0.1% (v/v) Tween-20

*TST*

50 mM Tris-HCl, pH 7.6  
 150 mM NaCl  
 0.05% (v/v) Tween-20

*YPD*

1% (w/v) Yeast Extract  
 2% (w/v) Peptone  
 2% (w/v) D-Glucose

## 2.2 DNA Methods

### 2.2.1 Generation of target DNA and sequencing

pCMV-Vps45 cDNA was generously provided by Dr. Robert Piper from the University of Iowa. DNA was reconstituted in water from being previously blotted to filter paper. It was then ethanol precipitated, washed and quantitated at  $\text{OD}_{260}$ . This template DNA was then used with the 5' and 3' Vps45 primers (listed in Primers Table) to PCR amplify the target.

### 2.2.2 Amplification of target DNA by PCR

The PCR reaction contained 1X PCR Buffer, 200  $\mu\text{M}$  dNTPs, 1 mM  $\text{MgSO}_4$ , 0.5  $\mu\text{M}$  5' Vps45 Primer, 0.5  $\mu\text{M}$  3' Vps45 Primer (Primer Sequences listed in Section 2.1.2) and 1 unit of Pfx proofreading Taq polymerase (5U/ $\mu\text{l}$ ) to a total volume of 50  $\mu\text{l}$  with Ambion DNase and RNase free water.

Reactions were incubated in a PCR machine and subjected to the following program:

94°C 3 min  
 94°C 1 min  $\curvearrowright$   
 50°C 1 min 30 Cycles  
 68°C 1 min  $\curvearrowleft$   
 68°C 10 min  
 4°C Holding temperature

### 2.2.3 Agarose gel electrophoresis

Amplicons were analysed by agarose gel electrophoresis. Agarose gels were prepared that consisted of 1% (w/v) Agarose in TAE buffer (0.04 M Tris-acetate, 0.001 M EDTA). These gels were stained with a stock solution of 0.625 mg/ml ethidium bromide for a final gel concentration of 0.5 µg/ml. The running buffer was 1X TAE and gels were run under a constant current of 100 mA. DNA ladders were used to assess the size of separated DNA, in particular New England BioLabs Quick-Load 1Kb DNA Ladder (Cat#N0468S) and Quick-load 100 bp DNA ladder (Cat#N0467S).

### 2.2.4 Gel Extraction of DNA

DNA separated on Agarose-TAE gels was excised from the gel using a clean scalpel and the gel slice was weighed. The Qiagen QIAquick Gel Extraction kit was used to extract the DNA from gels. All centrifugations occurred at 12470 x *g* for 1 min. 3 volumes of Buffer QG (Proprietary) were added to every 100 mg of gel and these samples were incubated at 50°C for 10 min with occasional vortexing. This solution, containing a colorimetric pH indicator, ensured that the DNA stayed at the proper pH for adsorption to the membrane. After the gel slice had dissolved into the buffer, 1 gel volume of isopropanol was added to increase the yield of DNA fragments and the sample was mixed before placing in a QIAquick spin column with collection tube. The sample was applied to the column containing a silica-gel membrane and centrifuged. DNA adsorbed to the silica membrane in the presence of high salt concentration while impurities passed through the column and were washed away. An additional  $\frac{1}{2}$  volume of Buffer QG to maintain high salt conditions for maximal adsorption was then added to the tube and centrifuged before the sample was washed in Buffer PE (Proprietary) and centrifuged again. The tube was then centrifuged empty before the spin column was transferred to a fresh eppendorf tube. The DNA was then eluted in water by a final centrifugation step. Water was used since maximal elution occurs at low salt and pH (pH 7.0- 8.5) conditions. The collected DNA was stored at -20°C.

### 2.2.5 A Tail reaction and TA Cloning

10  $\mu$ l of the PCR product was added to a reaction of 1  $\mu$ l (5 Units) Taq polymerase, 1 mM MgCl<sub>2</sub>, 1X Taq Polymerase Buffer and 200  $\mu$ M dATP at 72°C for 20 min. 2  $\mu$ l of this product was then added to 0.5  $\mu$ l of PCR 2.1 Vector and incubated for 5 min at room temperature. 0.5  $\mu$ l 1 M NaCl salt solution was added to the reaction before it was added to 50  $\mu$ l of Top 10 *E. coli* cells, kept on ice for 30 min, then heat shocked for 40 sec at 42°C. After 2 min on ice, 250  $\mu$ l SOC Media was added and tubes were then incubated in a shaking incubator for 90 min at 37°C. Selection of positive colonies was assisted by blue-white colony screening. This screening method used X-Gal (20 mg/ml in N'N'-dimethyl formamide) spread on plates and dried 20 min before plating transformants. Cells were then plated and incubated overnight at 37°C.

Colonies that incorporated the DNA and thus disrupted the ability of the  $\beta$ -galactosidase enzyme to hydrolyse the X-gal substrate appeared white due to the lack of the 5-bromo-4-chloroindole metabolite were selected for downstream applications.

### 2.2.6 Restriction Digestion

DNA was digested overnight at 37°C in a final volume of 20  $\mu$ l. DNA comprised half of this volume while 10% (v/v) of the reaction consisted of 10X restriction digestion buffer specifically designed to work with the restriction enzyme in question. 100X BSA was added to minimize star activity at a concentration of 0.5% (v/v) and the rest of the reaction volume was water. In the case of a double digestion, an additional 10% (v/v) of buffer was used as well as two restriction enzymes at an individual concentration of 0.5% (v/v) and which was added to the reaction last to minimize premature activity.

### 2.2.7 Ligation

Insert and vector DNA was ligated in several experimental ratios depending on the amount of DNA present in each sample as assessed by either

absorbance or examination on an agarose gel using a quantifying ladder. The most common ratio was 1 volume of insert to 3 volumes of vector owing to the smaller size of the insert contributing more molecules per unit volume than the comparatively larger vector. Insert and vector were combined in a 10  $\mu$ l volume that also included 10% (v/v) T4 DNA Ligase Buffer and 10% (v/v) T4 DNA Ligase. If these components did not result in a final volume of 10  $\mu$ l, then the remainder of the volume was made up of water. These reactions were incubated at 16°C in a PCR thermocycler overnight before being transformed into the appropriate *E. coli* cells.

### **2.2.8 Transformation of *E.coli***

DNA and competent cells were individually thawed on ice. Once thawed, the DNA was transferred into the tube containing the competent cells and this tube was incubated on ice for 30 min. The samples were then heat shocked at 42°C for 30 sec and placed immediately on ice for 2 min. SOC media was then added to the tubes and they were incubated in a shaking incubator for 90 min at 37°C. After this incubation, samples were centrifuged at 660 x *g* for 3 min and the supernatants were discarded. Cell pellets were re-suspended in the appropriate volume of SOC and plated on plates containing selective media. These plates were incubated at 37°C overnight.

*E.coli* were made competent for transformation by using the calcium chloride method. Cells were grown overnight in 2YT growth media in a shaking incubator at 37°C. The next day, an O.D.<sub>600</sub> reading was taken and cells diluted in fresh media and grown for several hours to achieve a healthy doubling of cells before they were assessed to be in mid-log phase by having an O.D.<sub>600</sub> of 0.6. Cells were then transferred to chilled centrifuge tubes and centrifuged at 660 x *g* for 10 min at 4°C. The supernatant was discarded and cells were resuspended in ice-cold 0.1 M CaCl<sub>2</sub> before being centrifuged a second time under the same conditions. The pellet was then suspended in storage buffer (0.1 M CaCl<sub>2</sub>, 15% (v/v) glycerol) and the cells were aliquoted on ice into eppendorf tubes before being stored at -80°C.

### 2.2.9 Small and large scale DNA isolation

Cells containing plasmids of interest were grown overnight at 37°C in the appropriate media and harvested by centrifugation at 1060 x *g* for 5 min. Pellets were then subjected to DNA isolation using the Promega Wizard Plus SV DNA Purification System. This system purifies plasmid DNA efficiently from *E. coli* cells with a mutated *EndA* gene. Briefly, cells were re-suspended in Cell Resuspension Solution (50 mM Tris-HCl pH 7.5, 10 mM EDTA, 100 µg/ml RNase A) and Cell Lysis Solution (0.2 M NaOH, 1% (w/v) SDS) was then added to each sample and inverted 4 times to mix. These steps ensure the cells are lysed and the bacterial lysates are at the correct salt concentration and pH to maximize DNA yield. To this mixture, 10 µl of Alkaline Protease Solution (subtilisin Carlsberg, isolated from the bacterium *Bacillus licheniformis*) was added to inactivate endonucleases. The mixture was incubated for 5 min at room temperature, which is enough time to degrade protein contaminants. Neutralization Solution (4.09 M guanidine hydrochloride, 0.759 M potassium acetate, 2.12 M Glacial Acetic Acid) was then added to the samples, reducing them from pH 9 and ending alkaline protease activity. They were centrifuged at 12470 x *g* for 10 min. The supernatant was decanted into specialized flow through collection tubes containing a membrane that bound the DNA and was centrifuged at 12470 x *g* for 1 min. Bound DNA settled onto these specialized membranes were washed twice with Wash Solution (162.8 mM Potassium Acetate, 22.6 mM Tris-HCl pH 7.5, 0.109 mM EDTA pH 8.0) and then the membrane collection inserts were transferred to new eppendorf tubes and the DNA was eluted using Nuclease Free water and stored at -20°C.

To obtain larger yields of isolated DNA, cells containing plasmids of interest were grown for 8 hours at 37°C in the appropriate media and diluted in additional media before being grown overnight at 37°C. These cultures were then harvested at 6000 x *g* for 15 min at 4°C. Pellets were collected and subjected to the Qiagen QIAfilter plamid purification method which used a modified alkaline lysis procedure with a patented anion-exchange-based resin to yield high purity DNA. Briefly, pellets were re-suspended in Buffer P1 (50 mM Tris-HCl pH 8.0, 10 mM EDTA, 100 µg/ml RNase A) and then lysed with Buffer P2 (200 mM NaOH, 1% (w/v) SDS) and incubated at room temperature for 5 min. The proprietary resin filter cartridge was

equilibrated with Buffer QBT (750 mM NaCl, 50 mM MOPS pH 7.0, 15% (v/v) Isopropanol, 0.15% (v/v) Triton X-100). After 5 min incubation, chilled neutralization buffer Buffer P3 (3 M potassium acetate pH 5.5) was added to the lysed culture to stop RNase activity and the cultures were filtered through a specialized tip before being decanted into the equilibrated cartridge. The cleared lysate then passed through the resin of the cartridge by gravity flow so that the released DNA could bind to the resin before the resin was washed twice with Buffer QC (1 M NaCl, 50 mM MOPS pH 7.0, 15% (v/v) isopropanol). This wash removed any remaining RNA or protein contaminants. The bound DNA was then eluted from the resin using Buffer QF (1.25 M NaCl, 50 mM Tris-HCl pH 8.5, 15% (v/v) Isopropanol). DNA was then precipitated by adding 0.7 volumes of isopropanol to the eluate and centrifuging at 15000 x *g* for 30 min at 4°C. The resulting DNA pellet was then washed in 70% (v/v) ethanol and centrifuged at 15000 x *g* for 10 min before air-drying and resuspension in a suitable volume of water followed by storage at -20°C.

After mini-prepping was performed, plasmid DNA was diluted in water and sent with the appropriate sequencing primers to the Sequencing Service at Dundee University (sequencing performed on an Applied Biosystems model 3730 automated capillary DNA sequencer using Applied Biosystems Big-Dye Ver 3.1 chemistry). These sequences were then aligned using the accession number U81160 for *Rattus norvegicus* vesicular transport protein rvps45 mRNA, complete CDS in Vector NTI V10.3.

### **2.2.10 Determination of DNA Concentration**

DNA concentration was quantified by measuring absorbance at 260 nm and the purity of the sample assessed by measuring the 260 nm/280 nm ratio on a spectrophotometer (WPA S2000, Cambridge, UK). Alternatively, an estimate of DNA concentration was obtained by comparing the intensity of DNA bands on agarose gels to the intensity of bands in DNA quantifying ladders of known concentration.

## 2.3 Protein Methods

### 2.3.1 Protein purification by Nickel NTA Method

Plasmids were transformed into BL-21 (DE3) cells and grown in 2YT/Amp (1.6% (w/v) tryptone, 1% (w/v) yeast extract, 0.5% (w/v) NaCl with 50 µg/ml kanamycin and 100 µg/ml ampicillin) culture media overnight at 37°C. These cells were then grown in TB/Amp culture media (1.2% (w/v) tryptone, 2.4% (w/v) yeast extract, 0.4% (v/v) glycerol, 0.017 M KH<sub>2</sub>PO<sub>4</sub>, 0.072 M K<sub>2</sub>HPO<sub>4</sub> with 50 µg/ml kanamycin and 100 µg/ml ampicillin) and grown to mid-log phase of 0.75 O.D.<sub>600</sub> and then induced with 1 M IPTG and incubated overnight at 22°C.

Cultures were then centrifuged at 1060 x *g* for 30 min at 4°C and the pellets were resuspended in 10 ml A<sub>400</sub> (25 mM HEPES, 400 mM KCl, 10% (v/v) glycerol), 1 mM BME, 20 mM imidazole. Lysozyme at a concentration of 100 µg/ml was then added and incubated at 4°C for 20 min with rotation. After 20 min, cells were sonicated 8 times with 20 second intervals on ice and centrifuged at 56420 x *g* for 20 min.

Nickel-NTA beads were washed with A<sub>400</sub> with 1 mM BME and 15 mM imidazole twice and the beads were added to the cleared lysate. The lysate was then incubated with the beads rotating constantly overnight at 4°C. The beads were centrifuged at 560 x *g* for 5 min at 4°C and washed 7 times with A<sub>400</sub> with 1 mM BME and 5 mM imidazole. Protein fractions were eluted with A<sub>200</sub> (25 mM HEPES, 200 mM KCl, 10% v/v glycerol) with 1 mM BME and 500 mM imidazole. Aliquots of the resulting protein were dialyzed using a 10000 MWCO slide-a-lyzer in PBS at 4°C overnight. After dialysis, the protein was loaded on to a 10% SDS-PAGE gel, Coomassie stained and dried.

### 2.3.2 Protein purification with thrombin cleavage

Plasmids were transformed into BL21 (BL-21 DE3, Invitrogen) cells and grown in 2YT/Amp culture medium overnight at 37°C. These transformants were then grown in TB/Amp culture media and grown to a mid-log phase of 0.6 O.D.<sub>600</sub> and then induced with 1 M IPTG and incubated overnight at 22°C.

Cultures were then centrifuged at 1060 x *g* for 30 min at 4°C and the pellets were resuspended in 10 ml PBS with added protease inhibitors (1 tablet of Roche Complete Cocktail Inhibitor). This suspension was then treated with 100 mg/ml Lysozyme and incubated rotating constantly at 4°C for 20 min. After 20 min the cultures were sonicated 8 times at 20 second intervals on ice and centrifuged at 48400 x *g* for 30 min.

IgG Sepharose beads were washed in alternating TST and 0.5 M acetic acid pH 3.4 and the supernatant from the preceding spin was transferred into the packed beads and incubated rotating constantly overnight at 4°C. The lysate was then centrifuged at 560 x *g* for 5 min at 4°C and the beads were washed with TST 10 times. The beads were then eluted with Thrombin Elution Buffer (50 mM Tris pH 8, 150 mM NaCl, 2.5 mM CaCl<sub>2</sub>, 50 U/ml Thrombin) for 40 min at room temperature. The eluate was centrifuged for a final time at 560 x *g* for 5 min at 4°C. The resulting protein was loaded on to a 10% Tris-HCl gel and Coomassie stained and dried.

### **2.3.3 Trichloroacetic Acid precipitation**

Cytosolic fractions of cells were collected from the extraction method described in Section 2.4.3. These fractions were incubated for 5 min at room temperature in the presence of 0.15% (w/v) Deoxycholic acid. They were then vortexed after the addition of 18% (w/v) Trichloroacetic Acid (TCA), incubated on ice for 30 min and centrifuged at 12470 x *g* for 15 min at 4°C. The supernatant was discarded and the pellet was washed in 1 ml of ice-cold Acetone and again centrifuged at 12470 x *g* for 15 min at 4°C. The final pellet was then re-suspended in loading sample buffer and stored at -20°C.

### **2.3.4 Immunoprecipitation**

Cells were cultured in 12 well plates and differentiated on Day 8, as described in Section 2.4.1, serum starved for 2 hrs and then Insulin wells were treated with 1 μM Insulin and Insulin + NEM wells were treated with 50 μM NEM to a final well concentration of 5 μM NEM and 100 nM Insulin for 20 min. Basal wells were left in serum-free media for the duration of the treatments.

Each 12 well plate contained 4 conditions in triplicate: Basal, Basal + NEM, Insulin and Insulin + NEM. After treatment, all wells were washed 3 times in ice-cold 20 mM Tris-HCl, 150 mM NaCl wash buffer. Then, 1 ml Lysis Buffer (20 mM Tris-HCl, 150 mM NaCl, Protease Inhibitor cocktail, 1% (w/v) Thesit (C<sub>12</sub>E<sub>8</sub>), pH 7.4) was added to the wells. NEM wells received 1 ml Lysis Buffer containing an additional 5 mM NEM. Wells were scraped using a Corning Cell Lifter and collected into eppendorf tubes on ice. Lysates were passed 10 times through a 26 <sup>5</sup>/<sub>8</sub>" needle and then incubated on ice for 30 min.

Lysates were then centrifuged at 12470 x *g* for 20 min at 4°C. The supernatants were decanted into fresh tubes and used for immunoprecipitation.

500 µl of each lysate was pre-cleared for 1 hr with washed Protein A beads (50% slurry). Then, either 2 µg (~5µl) of Syntaxin 16 antibody (SY SY #110 162), Vps45 antibody (SY SY #137 002) or Random Rabbit IgG was added, inverted 10 times to mix and incubated on ice for 1 hr. In the meantime, Protein A beads were washed 3 times in IP buffer (50 mM HEPES pH 7.5, 5 mM EDTA, 10 mM sodium pyrophosphate, 10 mM NaF, 150 mM NaCl, EDTA-Free Protease Inhibitor Cocktail, 2 mM β-Glycerophosphate, 1 mM DTT and 1% (v/v) Thesit) as before and 40 µl of beads were then added to the lysate and antibody. Tubes were then rotated overnight at 4°C.

Samples were then centrifuged at 12470 x *g* for 1 min at 4°C, the supernatant discarded and the pellet washed 5 times in 1ml IP Buffer, then 5 times in IP buffer containing 0.1% (v/v) Thesit. After the final wash, pellets were again spun at 12470 x *g* for 1 min at 4°C and the final pellet was resuspended in 2X SDS-PAGE sample loading buffer containing 20 mM DTT, boiled at 95°C for 5 min, cooled on ice and then stored at -20°C.

### **2.3.5 SDS Gel Electrophoresis and transfer to Nitrocellulose**

Proteins were mixed 3:1 with 4X loading sample buffer, heated at 65°C for 5 min, cooled and loaded into wells of 10-12% Tris-HCl SDS-PAGE gels. These gels were 1 mm in thickness and contain a stacking region approximately 2

cm deep consisting of 5% (w/v) Acrylamide/0.136% (w/v) bisacrylamide, 0.25 M Tris-HCl pH 6.8, 0.2% (w/v) SDS polymerized with 0.1% (w/v) APS and 0.05% (v/v) TEMED and a resolving pathway comprising (for 10% gel) 0.75 M Tris-HCl pH 8.8, 0.2% (w/v) SDS, 30% 37.5 acrylamide:5 bisacrylamide polymerized with 0.1% (w/v) APS and 0.05% TEMED. These slab gels were cast using Bio-Rad mini-Protean III gel casting units. Bio-Rad Precision Plus Protein Standards All Blue (Cat#161-0373) were run in one lane of each gel to help determine protein size. Gels were run at 80V constant voltage in tris-glycine running buffer (25 mM Tris-HCl, 250 mM Glycine, 0.1% (w/v) SDS) using the Bio-Rad Protean III system.

Once separated by electrophoresis, gels were then transferred to nitrocellulose using a Bio-Rad mini Protean III trans-blot system. Transfer cassettes were layered with transfer sponges, Whatmann 3MM Filter paper, the gel and Protran 0.45  $\mu$  pore size nitrocellulose membrane and pre-soaked in Transfer Buffer (25 mM Tris-HCl, 192 mM glycine, 20% (v/v) Ethanol). The transfer then occurred at a constant current of 50 mA overnight or 200mA for 2 hrs.

To confirm adequate transfer, membranes were stained with the reversible stain Ponceau S. Briefly, membranes were removed from transfer buffer and washed twice in water before being submersed in Ponceau solution (0.1% (w/v) Ponceau S, 5% (v/v) glacial acetic acid). Membranes were incubated under constant agitation at room temperature for 1 min and then washed once in water to detect the pink protein bands. The stain was reversed in water until the membrane no longer contained any pink dye and the membrane was then subject to western blotting.

### **2.3.6 Western blotting**

Once the transfer was completed, membranes were washed once in TBST for 5 min and blocked in 5% (w/v) Milk TBST for 1 hr. Membranes were then incubated with primary antibody solution containing the primary antibody in 5% (w/v) Milk TBST or 5% (w/v) BSA TBST overnight rotating constantly at 4°C. The blots were then washed 3 times for 10 min each time in TBST before being immersed in secondary antibody solution containing the appropriate HRP conjugated secondary antibody in 0.5% (w/v) Milk TBST or

0.5% (w/v) BSA TBST for 45 min at room temperature. The membranes were then washed 3 times for 10 min each time in TBST before being subjected to the ECL detection system.

Membranes were taken out of wash buffer and immersed in a solution of equal volumes of ECL detection reagent 1 and ECL detection reagent 2 with constant agitation for 1 min. Membranes were then removed, wrapped in clear plastic film, then exposed to film.

Densitometric data was obtained by scanning the films on a Mercury 1200c scanner using Adobe Photoshop software. The intensity of the protein bands on the film was measured by using Image J Software.

Statistical analysis was performed on all assays, including densitometric data. Data was expressed as  $\pm$  SEM. Statistically significant differences were determined using a one or two-tailed student's *t* test (two-sample assuming unequal variance), or one-way and two-way ANOVA where appropriate, with  $p < 0.05$  as significant.

### **2.3.7 Coomassie Staining**

Proteins separated on Tris-HCl gels were visualized by submersing into 100 ml Coomassie Brilliant Blue solution (2.5 g/L Coomassie Brilliant Blue R250 in 45% (v/v) water, 45% (v/v) Methanol, 10% (v/v) glacial acetic acid) for 30 min followed by constant washing in Destain Solution (5% (v/v) Methanol, 10% (v/v) glacial acetic acid) overnight. Gels were then washed once in water and wrapped in cellulose paper, clipped into a drying board and allowed to air dry for 72 hrs.

### **2.3.8 Protein concentration determination (MicroBCA)**

Protein was measured using a 96 well plate method incorporating Pierce MicroBCA solutions as the detection reagent. Protein samples that comprised the sample wells of the plate were diluted to 0.5% of the total well volume in a 96 well Corning CoStar plate. A standard curve that contained points from 0 to 12  $\mu$ g was then produced using 1 mg/ml BSA. To each standard and sample well that contained 100  $\mu$ l volume, and additional 100  $\mu$ l detection reagent was added that consisted of 50% (v/v) of Solution A

(Proprietary alkaline tartrate-carbonate solution), 48% (v/v) of Solution B (Proprietary bicinchonic acid solution) and 2% (v/v) of Solution C (Proprietary copper sulfate solution). Plates were incubated at 37°C for 30 min before being read on a Fluorostar Optima plate reader (BMG LabTech, Aylesbury, UK) at 570 nm. Sample values were then plotted against the standard curve using an Excel program and protein concentrations were calculated.

## 2.4 Cell Culture Methods

### 2.4.1 Growth, trypsinisation and passage of cells

#### *Culture of 3T3-L1 Fibroblasts*

Murine fibroblast 3T3-L1 cells are an L1 continuous substrain of 3T3 (Swiss albino) cells that undergo a pre-adipose to adipose phenotypic conversion upon contact inhibition. They were grown in DMEM (Dulbecco's Modified Eagle's Medium), 10% (v/v) Newborn Calf Serum (NCS), 1% (v/v) Penicillin (10,000 U)/Streptomycin (10,000 U) in Corning T75 75 cm<sup>2</sup> flasks. Cells were cultured at 37°C in a humidified atmosphere of 10% CO<sub>2</sub>. Media was changed every other day until cells reached confluence.

#### *Trypsinization of 3T3-L1 Fibroblasts*

Media was removed from T75 culture flasks and 2 ml 0.5 g/L Trypsin- 0.2 g/L EDTA·4Na was added to the cells. Cells were incubated at 37°C for 5 min and collected in a 15 ml Corning conical tube. Cells were then pelleted in a benchtop centrifuge at 800 x *g* for 5 min. The pellet was then resuspended in 10 ml DMEM/10% (v/v) NCS and re-plated onto plates or flasks.

#### *Differentiation of 3T3-L1 Fibroblasts*

Cells were grown to confluence and differentiated by administering differentiation medium (10% (v/v) FCS, 1% (v/v) Penicillin/Streptomycin (P/S), 0.5 mM 3-isobutyl-1-methylxanthine (IBMX), 1 μM Insulin, 0.25 μM Dexamethasone) 48 hours post-confluence. After an additional 48 hr period, cells were given 1 μM Insulin and cell culture medium was changed every other day in DMEM/10% (v/v) FCS/1% (v/v) P/S until cells are at day 8-12 post differentiation.

### *Collagen Coating Cell Culture Plasticware*

Collagen I (Rat Tail) Invitrogen Cat#A1048301 was sterile filtered using a Millipore 0.22  $\mu\text{m}$  syringe filter and the solution was used to wash the plates leaving a thin film coating. Plates were then dried in a sterile flow hood and irradiated with ultra violet (U.V.) light overnight. Prior to use, plates were washed with serum-free DMEM to remove any traces of excess collagen solution.

## **2.4.2 Freezing Down and Resurrection of Cells**

### *Freezing of Cells*

3T3-L1, NIH3T3, and EcoPack2-293 cells all were frozen down and woken up using the same method. Cells were frozen down when 50-70% confluent by aspirating the growth media and washing the cells once in warm PBS. The PBS was aspirated and Trypsin-EDTA was then applied to the cell culture plates in a volume of 10% of the total culture volume. The plates were then incubated at 37°C for 5 min before swirling the Trypsin solution to detach the cells from the culture dishes. Once cells had fully detached by inspection in a microscope, the cell volume was collected in a tube which was then centrifuged at 500 x  $g$  for 5 min. The supernatant was discarded and the cell pellet was re-suspended in Cell Freezing Media (90% (v/v) FCS, 10% (v/v) DMSO). The solution was then aliquoted into cell freezing vials and incubated in a Nalgene Mr. Frosty containing isopropanol overnight at -80°C before vials were placed in a communal liquid nitrogen tank for long term storage.

### *Resurrection of Cells*

Cells were obtained from liquid nitrogen stocks and rapidly heated in a 37°C water bath until each aliquot was approximately half liquid. The outside of vials were then sterilized with alcohol and the vials were placed into a biological cabinet. The vial contents were transferred to a tube where 10 volumes of additional warmed media were added before being centrifuged at 500 x  $g$ . The supernatant was discarded and the resulting pellet was diluted into the appropriate volume of warmed media and plated in cell culture plastic ware.

### 2.4.3 Cell treatment and preparation of homogenates

#### *Preparation of Whole Cell Homogenates*

Cells were used on Day 8 post-differentiation, serum starved for 2 hrs in serum-free media and some cells were treated with 200 nM Insulin for 20 min. Cells were washed in ice-cold HES buffer and scraped into HES buffer containing inhibitors as described in the preparation of membrane extracts. Cells were then passed 10 times through a 26 5/8" gauge needle and kept on ice for 5 min. Total homogenates were cleared by centrifugation at 500 x *g* for 10 min at 4°C. Supernatants were then collected into fresh eppendorf tubes and quantitated for protein content using the MicroBCA method. Extracts were stored at -20°C.

#### *Preparation of Membrane and Cytosol Extracts*

Cells were used on Day 8 post-differentiation, serum starved for 2 hrs in serum-free media and were left untreated or stimulated with 200 nM Insulin for 20 min. Cells were washed 3 times in ice-cold HEPES/EDTA/Sucrose (HES) Buffer (250 mM Sucrose, 20 mM HEPES pH 7.4, 1 mM EDTA, and 1 tablet/50 ml volume of Roche EDTA-Free Protease Cocktail Inhibitor). Cells were scraped into 400 µl HES Buffer on ice and transferred to eppendorf tubes. Homogenates were then passed 10 times through a 25 gauge needle and kept on ice for 5 min. They were then centrifuged at 500 x *g* for 10 min at 4°C. Supernatants were then collected into fresh ultracentrifuge tubes and centrifuged at 86200 x *g* for 1 hr to generate a total membrane fraction. Cytosolic fractions were then prepared by TCA precipitation of the resulting supernatant and the pellets, which are the membrane fraction, were resuspended in the appropriate volume of HES buffer and protein quantified. Fractions were stored at -20°C.

#### *Preparation of Primary Rat Adipocyte Lysates*

Male Sprague-Dawley (SD) Rats (Charles River, CrI:SD) were sacrificed by isoflurane (2-chloro-2-(difluoromethoxy)-1,1,1-trifluoro-ethane) intoxication and 30 g of epididymal fat was harvested and transferred into 50 ml of Collection Buffer (118 mM NaCl, 5 mM NaHCO<sub>3</sub>, 4.7 mM KCl, 1.2 mM KH<sub>2</sub>PO<sub>4</sub>, 1.2 mM MgSO<sub>4</sub>, 25 mM HEPES, 100 nM Adenosine, 2.5 mM CaCl<sub>2</sub>, 0.2% (w/v) BSA, 3 mM Glucose, final solution pH 7.4 at 37°C). Tissue was then placed

into Digestion Buffer (118 mM NaCl, 5 mM NaHCO<sub>3</sub>, 4.7 mM KCl, 1.2 mM KH<sub>2</sub>PO<sub>4</sub>, 1.2 mM MgSO<sub>4</sub>, 25 mM HEPES, 100 nM Adenosine, 2.5 mM CaCl<sub>2</sub>, 0.2% (w/v) BSA, 3 mM Glucose, 2 mg/ml Collagenase, final solution pH 7.4 at 37°C), dissected to remove blood vessels and connective tissue, and digested under constant agitation in a 37°C shaking water bath for 30 min. After 30 min, 3 volumes of Wash Buffer (118 mM NaCl, 5 mM NaHCO<sub>3</sub>, 4.7 mM KCl, 1.2 mM KH<sub>2</sub>PO<sub>4</sub>, 1.2 mM MgSO<sub>4</sub>, 25 mM HEPES, 100 nM Adenosine, 2.5 mM CaCl<sub>2</sub>, 0.2% (w/v) BSA, final solution pH 7.4 at 37°C) was added to terminate digestion. Tissue was then passed once through a 21" gauge needle and cells were allowed to pass through a mesh sieve that separated the cells from any remaining connective tissues. These adipocytes floated to the top of the wash buffer and were collected into a fresh tube. These cells were then washed 4 times in 10 min intervals in 2 volumes of wash buffer before being collected once more for lysis. Collected cells were then passed through a 26 <sup>5</sup>/<sub>8</sub>" needle 10 times before being centrifuged at 500 x *g* for 10 min at 4°C. The resulting lysate was collected using a 1 <sup>1</sup>/<sub>2</sub>" 18 gauge needle to remove the lysate without disrupting the fat cake that formed on the top of the collection volume. This lysate was then quantitated using the MicroBCA method as described previously, aliquoted and stored at -20°C.

#### **2.4.5 Glucose transport assay**

All glucose transport assays utilized 3T3-L1 cells that were grown in BD Falcon 12-well plates until confluent, and then differentiated using the standard method as described previously. Cells were used on day 8 post-differentiation and all experiments were performed on a hot plate water bath at a constant temperature of 37°C.

##### *Basic Glucose Transport Assay*

Cells were serum-starved for 2 hrs before being washed 3 times in KRP (1.28 M NaCl, 47 mM KCl, 50 mM NaH<sub>2</sub>PO<sub>4</sub>, 1.25 mM MgSO<sub>4</sub>, 1 M CaCl<sub>2</sub>, final solution pH 7.4 at 37°C). The plates were then incubated for 5 min with 6 wells incubated in KRP alone and the other 6 wells incubated in KRP containing 10 μM Cytocholasin B. Of these wells, 3 wells of the 6 incubated in KRP alone were treated with 1 μM Insulin as were 3 wells of the 6 incubated in KRP plus Cytocholasin B. Insulin treatment lasted 30 min, after which time Deoxyglucose solution (2-[<sup>3</sup>H]-deoxy-D-glucose: 50 μM 2-deoxyglucose, 0.5

$\mu\text{Ci}/\text{well}$  Tritium in KRP) was added for 5 min to all wells. After 5 min, plates were washed in ice-cold PBS and allowed to air-dry for 30 min. When plates were sufficiently dry, 1 ml TritonX-100 was added to each well and allowed to stand at room temperature overnight. The next day, the liquid was collected into scintillation vials, covered with scintillation fluid and counted in a scintillation counter (Beckman Coulter LS 6500) along with a sample of the deoxyglucose solution (for total counts) for 3 min per vial.

#### *Dose Response Glucose Transport Assay*

Cells were serum-starved for 2 hrs before being washed 3 times in KRP (1.28 M NaCl, 47 mM KCl, 50 mM  $\text{NaH}_2\text{PO}_4$ , 1.25 mM  $\text{MgSO}_4$ , 1 M  $\text{CaCl}_2$ , final solution pH 7.4 at  $37^\circ\text{C}$ ). The plates were then incubated for 5 min with 6 wells incubated in KRP alone and the other 6 wells incubated in KRP containing 10  $\mu\text{M}$  Cytocholasin B. For each plate, 3 wells incubated in KRP alone and 3 wells incubated in KRP containing Cytocholasin B were treated with one concentration of Insulin, the other half plate were treated exactly the same but with a different concentration of Insulin. Insulin treatment lasted 30 min, after which time Deoxyglucose solution (2- $^3\text{H}$ ]-deoxy-D-glucose: 50  $\mu\text{M}$  2-deoxyglucose, 0.5  $\mu\text{Ci}/\text{well}$  Tritium in KRP) was added for 5 min to all wells. After 5 min, plates were washed in ice-cold PBS and allowed to air-dry for 30 min. When plates were sufficiently dry, 1 ml TritonX-100 was added to each well and allowed to stand at room temperature overnight. The next day, the liquid was collected into scintillation vials, covered with scintillation fluid and counted in a scintillation counter along with a sample of the deoxyglucose solution (for total counts) for 3 min per vial.

#### *Insulin Reversal Glucose Transport Assay*

Cells were washed 3 times in KRP and incubated in KRP alone. 6 wells were treated with 100 nM Insulin for 30 min while the other wells were left untreated. After 30 min, all wells were aspirated and 3 of the insulin treated wells were incubated in KRP alone and 3 were incubated in KRP+ Cytocholasin B. Similarly 3 of the untreated wells were incubated in KRP alone, and 3 were incubated in KRP+Cytocholasin B. Deoxyglucose solution (50  $\mu\text{M}$ ) was added to all wells and the plate was incubated for 3 min before being plunged into ice-cold PBS and allowed to air dry. This plate represented baseline basal and insulin-stimulated conditions.

Subsequently, other plates were washed in KRP and stimulated with 100 nM Insulin for 30 min. Thereafter, the KRP and/or Insulin was removed and the wells repeatedly washed in KRM (1.28 M NaCl, 47 mM KCl, 20 mM MES, 1.25 mM MgSO<sub>4</sub>, 1 M CaCl<sub>2</sub>, final solution pH 6.0 at 37°C) to remove Insulin and 'reverse' Glut4 translocation. This reversal protocol was varied to incubate cells in KRM for times ranging from 5 min to 60 min. After this, cells were washed 3 times in KRP and deoxyglucose uptake was assayed as described above.

After the plates had air-dried, 1ml TritonX-100 was added to each well and allowed to stand at room temperature overnight. The next day, the liquid was collected into scintillation vials, covered with scintillation fluid and counted in a scintillation counter along with a sample of the deoxyglucose solution (for total counts) for 3 min per vial.

#### **2.4.6 Confocal Microscopy and staining**

Cells were grown on collagen-coated borosilicate glass cover slips using the method described previously. After differentiation, cells were serum-starved for 2 hrs in serum-free media and either kept in media or 1 μM Insulin was added to media for 20 min. Cells were then washed with PBS 3 times and fixed in 2% (w/v) paraformaldehyde (p-Formaldehyde 7.5 g/L, 1 M CaCl<sub>2</sub>, 1 M MgCl<sub>2</sub>, in PBS) and left in the dark for 20 min. Cover slips were then washed 3 times in PBS and used for staining.

Cover slips were then washed twice in 20 mM Glycine in PBS and permeabilized in permeabilization media (2% (w/v) BSA, 0.1% (w/v) Saponin, 20 mM Glycine, PBS) for 20 min. Primary antibody was added in permeabilization media for 45 min. Cover slips were then washed in permeabilization media 4 times and the secondary antibody, again in permeabilization media, was applied and the cover slips were incubated for 30 min in the dark. Cover slips were washed 4 times in permeabilization media, and then washed once in PBS before being mounted on microscope slides using Immunomount adhesive. Slides were left overnight at 4°C before being visualized under the confocal microscope. Cover slips were

analysed using a 63X oil immersion objective fitted to a Zeiss Axiovert fluorescence microscope, equipped with a Bio-Rad MRC-600 confocal imaging system. Image sets were processed and overlaid using Adobe Photoshop CS5.

### *Adipocyte staining with Oil Red O*

3T3-L1 cells were grown in Lab-Tek glass chamber slides (Cat#177372, Fisher Scientific) until confluence, differentiated as previously described and used on Day 8 post-differentiation. Cells were then fixed in 10% (v/v) Formalin and incubated at room temperature for 5 min initially. The formalin was then replaced with fresh formalin and incubated at room temperature in the dark for 1 hr. Cells were then washed once in 60% (v/v) isopropanol and wells were left to dry completely. At this time, the Oil Red O working solution (60% (v/v) Oil Red O Stock (8.57 mM Oil Red O (Sigma Cat# O-0625) in isopropanol) 40% (v/v) water) was placed in the wells for 10 min and then washed away with water 4 times before the wells were left to dry. Slides were then dipped for 30 sec in Mayers Hematoxylin (193.64 mM Aluminum Potassium Alum, 16.54 mM Hematoxylin, 2.02 mM Sodium Iodate, 2% (v/v) Glacial Acetic Acid) and then dipped in Ammonium Blue (3% (w/v) Ammonium Hydroxide, pH 10 in water) for 10 sec. Slides were then dried and cover slips were affixed using Immuno-mount adhesive media (Fisher Scientific Cat#1900331). Slides were stored at 4°C before being examined using a light microscope.

## **2.5 Virus Generation and Delivery**

### **2.5.1 Construction of shRNA**

Sequences along the accession number U81160 for *Rattus norvegicus* vesicular transport protein rVps45 mRNA, were used to design shRNA oligonucleotides. 19 base pair sequences were chosen that were not near the start codon or in untranslated regions and that had between 40-60% GC content. 4 sets of target sequences were generated using these criteria and checked for secondary structures and long base runs using the BLAST sequence and the proprietary software from the Promega website. Briefly, the mVps45 sequence was entered into the software which checked base pairings for GC richness, excess internal runs of A and T and strand complementarity. For each target, 2 complementary oligonucleotides were

synthesized with a 5'-BamHI restriction site overhang on the top strand and a 5'-EcoRI restriction site overhang on the bottom strand. The target sense sequence had an added G (Guanine) residue added upstream of the 5'-end as well as a nucleotide hairpin loop sequence (5'-TTCAAGAGA-3'). The target antisense sequence had a terminator sequence of a 5-6 nucleotide poly (T) tract. Each target sequence then consisted of a restriction site (5-6 bases) at the 5' end, 19 bases of sense strand, 7-9 bases of hairpin loop, 19 bases of anti-sense strand, 6 bases of terminator poly (T) and 6 bases of restriction site at the 3' end (for Mlu I digestion). 4 such targets were generated using the rat Vps45 CDS and each target was separated from another by at least 200 base pairs. The oligonucleotides were synthesized by IDT (Integrated DNA Technologies, Germany)

### 2.5.2 Ligation into retroviral vector

Each oligonucleotide was resuspended in TE Buffer (1 M Tris pH 8.0, 100 mM EDTA) to a final concentration of 100  $\mu$ M. Each complementary strand for a target was then combined equally to achieve a 50  $\mu$ M ds oligo. The targets were placed in a PCR machine to anneal with the following program:

95°C 30 sec  
72°C 2 min  
37°C 2 min  
25°C 2 min

These conditions were to allow any secondary structures, including any internal hairpin loops to be removed while promoting intermolecular annealing.

Once annealed, the oligonucleotides were diluted in TE Buffer to a concentration of 0.5  $\mu$ M so that ligation efficiency was not impeded with an extreme molar excess of oligonucleotide. Once diluted, oligonucleotides were used in ligation reactions consisting of linearized pSiren vector (25 ng/ $\mu$ l), 10X T4 DNA Ligase Buffer, BSA (10 mg/ml), Nuclease-free water, and T4 DNA Ligase (400 U/ $\mu$ l). These reactions, including positive and negative controls, were incubated for 3 hours at room temperature.

At the end of the incubation period, 2  $\mu$ l of each ligation reaction was transformed into Fusion Blue competent cells (described in 2.1.4). Cells

were incubated on ice for 5 min and then heat shocked for 30 sec at 42°C. Cells were immediately placed on ice for 2 min and then SOC Media was added before cells were incubated under constant agitation at 37°C for 1 hr. After this incubation, 1/10 of the transformation volume was plated onto 2YT/Ampicillin plates (50 µg/ml) and incubated overnight at 37°C. The next day, 2YT/Ampicillin culture media was inoculated with single colonies from the transfected plates and grown overnight at 37°C in a shaking incubator. The resulting cultures were then mini-prepped using the Promega Wizard SV system as described in 2.2.9. This DNA was then restriction digested using New England BioLabs (NEB) Mlu I overnight at 37°C. This product was then run on 1% (w/v) DNA Agarose gels stained with Ethidium Bromide for visualization. Single bands at approximately 7 Kb were identified as successful clones and sent for sequencing to the University of Dundee sequencing Service. Once sequences were confirmed to be correct, large scale Maxi-preps were performed as described in 2.2.9 and DNA was dispensed into 60 µg aliquots.

### **2.5.3 Transfecting into EcoPack2-293 cells and virus collection**

EcoPack2-293 cells were taken from liquid nitrogen stocks and cultured in collagen-coated Corning T150 Flasks before being sub-cultured into BD Falcon 6-well plates at a density of 30,000 cells per well in Complete media (DMEM, 10% (v/v) FCS, 1 mM Sodium Pyruvate, 1% (v/v) 10000 U/ml P/S). ShRNA constructs were transfected into these viral packaging cells using the Lipofectamine method. Briefly, media on 6-well plates were changed to antibiotic-free media (DMEM, 10% (v/v) FCS, 1 mM Sodium Pyruvate) overnight. The next day 60 µg DNA from shRNA targets was diluted into Optimem and 150 µl of Lipofectamine 2000 reagent was separately diluted into Optimem media. Both dilutions were incubated at room temperature for 5 min before being combined and incubated for an additional 20 min. The complexes were then placed on the 6-well plates and incubated at 37°C for 4 hrs. Plates were then aspirated and fresh Complete Media was applied and plates were incubated for 24 hrs. After 24 hrs, the conditioned media was removed from the cells and fresh Complete media was applied to the cells for a further 24 hrs. The conditioned media was centrifuged at 500 x *g* for 5 min and the supernatant was collected into tubes that were then foiled to obscure light and stored at 4°C. After 48 hrs, the second addition of

Complete Media was similarly processed. It was then pooled with the previous supernatant, treated with 1 mg/ml Polybrene (Hexadimethrine Bromide Sigma Cat# H9268) and stored away from light at 4°C.

#### **2.5.4 Determining viral titer in NIH3T3 cells**

NIH 3T3 cells were plated in 6-well plates at a cell density of 50,000 cells per well in NCS Media (DMEM, 10% (v/v) FCS, 1% (v/v) 10000 U/ml P/S). 6 10-fold serial dilutions of the viral supernatants were then prepared to represent  $10^1$  to  $10^6$  pfu and 1 ml of each dilution was placed on the cells in the representative well. Cells were subjected to antibiotic selection for 2 weeks after infection since a kill curve determined this to be the optimum amount of time. At the end of the 2 weeks, 2 colonies had formed in the  $10^6$  well, indicating that the viral titer was  $2 \times 10^6$  cfu/ml.

#### **2.5.5 Infection of adipocytes and subsequent differentiation**

3T3-L1 fibroblasts were grown in 10 cm plates and infected with 5 ml/plate of  $2 \times 10^6$ /ml cfu virus per target. Plates with cells growing in NCS Media (DMEM, 10% (v/v) Newborn Calf Serum (NCS), 1% (v/v) 10000 U/ml P/S) were aspirated and the normal media was replaced with virus (collected conditioned media). Cells were left in the viral media for 24 hrs and then the media was changed to NCS Media containing 2.5 µg/ml Puromycin dihydrochloride (Sigma Cat#P8833) (NCS/Puromycin). Cells growing in NCS/Puromycin had their media changed 3 times into additional NCS/Puromycin before becoming super-confluent (confluence plus 48 hrs) and then were differentiated as described previously. On day 8 post-differentiation, cells were used for downstream applications, such as whole cell lysates.

#### **2.5.6 Recycling Assay for HA-Tagged GLUT4**

HA-Glut4-GFP cells were cultured in 96 well plates and differentiated as described previously. On day 8, cells were serum starved overnight and then washed into fresh serum-free media. Wells (in triplicate) were incubated with saturating concentration of Alexa-labelled anti-HA monoclonal antibody (a concentration of 2 mg/ml was routinely employed) for times ranging from 0 to 16 hours. After this time, plates were rapidly washed in ice-cold PBS, each well rinsed in 20 mM sodium citrate, pH 4 to remove cell surface

antibody, then washed again in PBS. Fluorescence was read in a microplate reader, assaying for both GFP (total Glut4 levels) and Alexa (internalised anti-HA) signals.

### 2.5.7 Subcellular Fractionation

3T3-L1 pre-adipocytes were grown to confluence in 10 cm plates and differentiated as described previously. On day 8, cells were serum starved for 2 hrs and some cells were treated with 1  $\mu$ M Insulin for 20 min. After treatment, cells were washed 3 times with ice-cold HES Buffer and scraped into HES Buffer that included protease inhibitors. All steps were performed on ice, all re-suspensions involving HES Buffer contained protease inhibitors and all centrifugation steps were conducted at 4°C. Cells were homogenized 10 times through a 26 <sup>5</sup>/<sub>8</sub>" needle and centrifuged at 500 x *g* for 10 min. The pellet was discarded and the Post- Nuclear Supernatant (PNS) was further centrifuged at 9400 x *g* for 12 min.

The pellet from this centrifugation (the M/N) was then re-suspended in HES buffer and again centrifuged at 9400 x *g* for 12 min. This resulting pellet was re-suspended in HES buffer and layered over a high sucrose HES solution containing 1.12 M Sucrose. This layered solution was centrifuged at 56420 x *g* using a swinging bucket rotor (Beckmann SW41) for 1 hr. The interface of the heavy sucrose solution contained the Plasma Membrane Fraction (PM) and was collected from the sucrose gradient. This fraction was diluted with additional HES buffer and centrifuged at 13300 x *g* for 15 min. The resultant pellet, the washed PM was re-suspended in HES buffer and loading sample buffer, heated at 65°C for 5 min and stored at -20°C.

The supernatant from the PNS centrifugation step containing the Cytosol, LDM and HDM was further centrifuged at 13300 x *g* for 17 min. The pellet from this centrifugation was the HDM fraction which was re-suspended in HES Buffer and Loading Sample Buffer, heated at 65°C for 5 min and stored at -20°C. The supernatant from this spin, containing the Cytosol and LDM, was centrifuged at 86200 x *g* for 75 min. The resulting pellet from this centrifugation was the LDM Fraction which was re-suspended in HES Buffer and Loading Sample Buffer, heated at 65°C for 5 min and stored at -20°C. The supernatant was the Cytosolic Fraction and was TCA precipitated as

described previously, then re-suspended in HES Buffer and Loading Sample Buffer, heated at 65°C for 5 min and stored at -20°C. The stored samples were then loaded onto 10% Tris-HCl gels and subjected to Western Blot Analysis.

### 2.5.8 The Budding Assay

3T3-L1 cells were grown to confluence in 10 cm plates and differentiated as described previously. On day 8, cells were serum starved for 2 hrs and then washed twice in Budding Buffer (38 mM Potassium Aspartate, 38 mM Potassium Glutamate, 20 mM MOPS, 5 mM Sodium Carbonate, 2.5 mM Magnesium Sulfate, 5 mM reduced Glutathione and Roche protease cocktail inhibitor tablets, pH 7.2) then scraped into Budding Buffer and passed through a 26 5/8" gauge needle 10 times and centrifuged at 1000 x *g* for 5 min at 4°C. Supernatants resulting from this spin were transferred to fresh tubes and centrifuged at 16000 x *g* for 20 min at 4°C. The pellets were retained and supernatants from this spin were then put into ultracentrifuge tubes and centrifuged at 104300 x *g* for 1 hr at 4°C. During this hour spin, the pellets that were retained were then washed in budding buffer twice by centrifuging them at 16000 x *g* for 1 min at 4°C. These pellets were resuspended in budding buffer and kept on ice during the cytosolic 1 hr spin. After this spin, both membrane and cytosol were analysed for protein content using the MicroBCA method described previously. The ATP regeneration system (800 mM Creatine Phosphate, 500 U/ml Creatine Kinase, 100 mM ATP) was combined with the Cytosol and Membrane protein in a reaction consisting of 250 µg of membrane, 2 mg/ml Cytosol and 0.3% (v/v) ATP Regeneration System. These reactions were then incubated at 37°C for 20 min or 40 min before being centrifuged at 16000 x *g* for 20 min at 4°C. The resultant pellets (the donor fraction) were then re-suspended in Budding Buffer and Loading Sample Buffer (described previously) and heated for 5 min at 65°C. The supernatants were re-centrifuged at 200000 x *g* for 1 hr at 4°C. The pellets from this centrifugation step (the vesicle fraction) were also re-suspended in Budding Buffer and Loading Sample Buffer and heated for 5 min at 65°C. Donor and vesicle fractions were then subjected to SDS-PAGE and Immunoblot analysis.

### 2.5.9 Iodixanol Gradients

LDM membranes (from Subcellular Fractionation experiments) were diluted in 60% (v/v) Iodixanol to a final Iodixanol concentration of 14% (v/v) in HES buffer (250 mM Sucrose, 20 mM HEPES pH 7.4, 1 mM EDTA, and 1 tablet/50 ml volume of Roche EDTA-Free Protease Cocktail Inhibitor) and inverted to mix. The mixture was then heat-sealed into Beckmann Quick Seal polyallomer tubes before being secured into a pre-chilled Beckmann TLN 100 Rotor and centrifuged at 295000 x *g* at 4°C for 1 hr. Fractions were then collected by piercing the top and bottom of the tubes, effectively dislodging the air lock on the sealed tubes, and allowing the fractions to flow by gravity into eppendorf tubes. Fractions were then mixed with Loading Sample Buffer (described previously) and heated to 65°C for 15 min before being loaded onto 10% Tris-HCl SDS-PAGE gels and subjected to Western Blotting.

## 2.6 Yeast Methods

### 2.6.1 Construction of Vps45 plasmid using homologous recombination

pCOG70, driving the overexpression of Vps45p harbouring an HA tag at its carboxy terminus, a generous gift of Dr. Lindsay Carpp, was digested with BamH1 and Sph1 to excise the Vps45p region and linearize the YEpVPS45 *2u* *URA3* vector (Gietz and Sugino, 1998). YEpVPS45 was originally made from subcloning a Vps45 fragment into YEplac195.

A DNA fragment was then PCR amplified using the mammalian DNA received from Dr. Piper (described in 2.2.1) as a template. The PCR reaction contained 1X PCR Buffer, 200 µM dNTPs, 1 mM MgSO<sub>4</sub>, 0.5 µM 5' Vps45 yeast Recombinant Primer, 0.5 µM 3' Vps45 Yeast Recombinant Primer (Primer Sequences listed in Section 2.1.2) and 1 unit of Pfx proofreading polymerase (5U/µl) to a total volume of 50 µl with Ambion DNase and RNase free water.

Reactions were incubated in a PCR machine and subjected to the following program:

94°C 3 min  
 94°C 30 sec  
 48°C 30 sec  
 68°C 4 min 30 sec  
 68°C 10 min  
 4°C Holding temperature

} 30 Cycles

### 2.6.2 Transformation of plasmids into yeast cells

The insert was then homologously recombined with the pCOG70 vector in a ratio of 1:3 vector to insert and added to 100  $\mu$ l of 9D $\alpha$  $\Delta$ 45 cells with 200  $\mu$ l of 70% (v/v) PEG3350. The recombinant solution was heat shocked at 42°C for 20 min and then shaken for 90 min at 30°C. The solution was centrifuged for 3 min at 660 x *g*, the supernatant was then discarded and the resulting pellet resuspended in 100  $\mu$ l of water. This was plated on SD -ura -met plates (SD; 0.67% (w/v) yeast nitrogen base without amino acids, 2% (w/v) glucose, 0.18% (w/v) Synthetic complete amino acid drop-out supplement -ura-met, 2% (w/v) micro agar) and incubated at 30°C for 72 hrs.

9D $\alpha$  and 9D $\alpha$  $\Delta$ 45 cells were made competent for transformation using the Lithium Acetate method (adapted from Gietz). Cells were streaked onto YPD plates and after 72 hours were picked into YPD growth media (1% (w/v) yeast extract, 2% (w/v) peptone, 2% (w/v) glucose) and allowed to grow overnight at 30°C. The next day, an O.D.<sub>600</sub> was taken and cells were diluted to adjust the starting O.D.<sub>600</sub> to 0.25. Cells were allowed to undergo one doubling until they were assessed to be in mid-log phase as verified by an O.D.<sub>600</sub> reading of 0.7. Cells were collected into tubes and centrifuged at 500 x *g* for 2 min. The supernatant was discarded and the resulting pellet was resuspended in 10 ml Lite-Sorb (1 M Lithium Acetate, 1 M Tris pH 7.6, 0.5 M EDTA, 2.4 M Sorbitol) centrifuged again at 500 x *g* for 2 min. The supernatant was discarded and the pellet was suspended in 1 ml of fresh Lite-Sorb before being transferred to eppendorf tubes. These tubes were incubated in a shaking incubator at 30°C for 1 hr. After 1 hr, the tubes were placed on ice for 20 min after which time the cells suspended in Lite-Sorb received an additional volume of Competent Cell Freezing Media (40% (v/v) Glycerol, 0.5% (w/v) NaCl) so that the final composition of buffer on the cells was 50% (v/v) Lite-Sorb and 50% (v/v) Competent Cell Freezing Media. Cells were then aliquoted on ice and frozen at -80°C.

### 2.6.3 Plasmid Rescue

Colonies from transformed plates were picked into a 10 ml overnight culture of SD -ura -met culture media and incubated at 30°C for 14 hrs. The next day, 5 O.D.<sub>600</sub> equivalents were harvested at 3610 x *g* for 2 min. These cells were suspended in Buffer S (100 mM KPO<sub>4</sub> pH 7.2 (KH<sub>2</sub>PO<sub>4</sub> + K<sub>2</sub>HPO<sub>4</sub>), 10 mM EDTA, 50 mM BME, 50 µg/ml Yeast Lytic Enzyme(15 mg/ml Yeast Lytic Enzyme in 50 mM Tris pH 7.7, 1mM EDTA, 50% (v/v) Glycerol) and incubated at 37°C for 30 min. After this incubation, Lysis Buffer (25 mM Tris-HCl pH 7.5, 25 mM EDTA, 2.5% (w/v) SDS) was added, samples were vortexed briefly and incubated at 65°C for 30 min. Then 3 M potassium acetate was added to the samples and they were kept on ice for 10 min. Samples were then centrifuged at 12470 x *g* for 10 min and transferred to new tubes where ethanol was added and they were again incubated on ice for 10 min. After this final incubation, cells were centrifuged at 12470 x *g* for 10 min and washed once in 70% (v/v) ethanol before being air dried and resuspended in water. This DNA was then transformed into XL-1 Blue *E. coli* cells (Stratagene, Cambridge, UK) and plated onto 2YT/Ampicillin plates to select for the correct plasmid.

### 2.6.4 Construction of Vps45p mutants by site directed mutagenesis

Mammalian rat Vps45 homologously recombined into the pCOG70 plasmid and under control of the yeast *VPS45* promoter was used as a template for constructing mutants using site-directed mutagenesis. The mutagenesis reactions contained 1X PCR Buffer, 200 µM dNTPs, 1 mM MgSO<sub>4</sub>, 0.5 µM 5' V107R or W230R Primer, 0.5 µM 3' V107R or W230R (Primer Sequences listed in Section 2.1.2) and 1 unit of Pfx proofreading Taq polymerase (5U/µl) to a total volume of 50 µl with Ambion DNase and RNase free water.

Reactions were incubated in a PCR machine and subjected to the following program:

95°C 2 min  
 94°C 1 min ↖  
 50°C 1 min      18 Cycles  
 68°C 20 min ↘  
 68°C 10 min  
 4°C Holding temperature

Amplicons were then digested with Dpn I (10 U/μl) at 37°C for one hour to digest the non-mutated super-coiled parental DNA. After Dpn I digestion, plasmids were then transformed into XL-1 Blue cells using the transformation protocol described in 2.2.8. Cells were then plated onto 2YT/Amp plates overnight and subsequent colonies that formed were cultured for 14 hrs in 2YT/Amp media, DNA purified using the Promega Wizard system described previously in section 2.2.9, and sent for sequencing to the University of Dundee Sequencing Service. Sequences were aligned using the Vector NTI V10.3 software program.

Yeast colonies containing the correct sequences were then grown overnight at 30°C in selective media (SD-URA-Met), mixed with 10% (v/v) DMSO and aliquoted into cryovials which were stored at -80°C. To wake up these cells, plates containing selective media were streaked with 10 μl of frozen cells and incubated at 30°C for 72 hours before individual colonies were picked and grown overnight at 30°C in selective growth media.

### **2.6.5 Preparation of yeast lysates for SDS-PAGE**

Yeast cells grown overnight in selective medium (SD -ura -met) were diluted in fresh selective medium and grown to mid-log phase as assessed by taking an O.D.<sub>600</sub> of 0.7 and 10 O.D. units/ml were collected and centrifuged at 660 x g for 3 min. The pellets were resuspended in TWIRL Buffer (5% (w/v) SDS, 8M Urea, 10% (v/v) Glycerol, 50 mM Tris pH 6.8 and 0.2% (w/v) Bromophenol Blue, 10% (v/v) B-mercaptoethanol). Cell extracts were then incubated at 65°C for 10 min, cooled and resolved by SDS-PAGE on 10% Tris-HCl acrylamide gels.

### **2.6.6 Invertase Assay- TCA precipitation method**

Cells were grown overnight in 10 ml selective medium (SD -ura -met) cultures, inoculated to an O.D.<sub>600</sub> of 0.2 and allowed to double until reaching an O.D.<sub>600</sub> of 0.7. Cells were then centrifuged at 1060 x g for 5 min.

90% of the supernatant was removed to fresh tubes and 10% (v/v) TCA was added to this sample before being incubated on ice for 1 hr. The supernatant was then centrifuged at 12470 x *g* at 4°C for 10 min to pellet the precipitated secreted proteins. The supernatant from this protein pellet was discarded and the resulting protein was washed twice in ice-cold acetone to eliminate the effects of the TCA and change the pH. The pellets were then resuspended in sample buffer (200 mM Tris-HCl, pH 6.8, 8% (w/v) SDS, 40% (v/v) glycerol, 0.4% (w/v) bromophenol blue, 400 mM DTT, 10% (v/v) BME) using the original doubled optical density so that all samples were equivalent to each other in relation to volume. Samples were then corrected for pH using saturated Tris and boiled at 95°C for 5 min before being stored at -20°C.

### **2.6.7 CPY Invertase Assay- Liquid Colorimetric method**

Cells were grown overnight in 10 ml SD -ura -met culture media and 12 O.D.<sub>600</sub> equivalents were harvested at 1060 x *g* for 2 min. Pellets were resuspended in 94 mM sodium acetate pH 4.9 before being further diluted to a final composition of 75 mM sodium acetate pH 4.9. Cells that were assayed for total activity were lysed 5 times by freeze-thawing in a dry ice/methanol bath and subsequent placement in a 30°C water bath. After freeze-thawing, 5 µl of 20% (v/v) Triton-X100 was added and the samples were vortexed briefly before being placed in a 30°C water bath. When the samples had reached 30°C, 0.5 M sucrose was added and they were incubated in the water bath for 30 min at which time a stop solution of 0.2 M K<sub>2</sub>HPO<sub>4</sub> was added. After the addition of the stop solution, samples were placed in a boiling water bath for 3 min and then placed on ice. Samples were then replaced into the 30°C water bath and Glucostat Reagent (0.1 M potassium phosphate pH 7.0, 1000 U/ml glucose oxidase in PBS, 1 mg/ml HRP, 20 mM NEM, 10 mg/ml O-Dianisidine) was added and allowed to incubate in the water bath for 30 min. After 30 min, 6 N HCl was added to stop the reaction and absorbance measured at 540 nm.

### **2.6.8 Complementation by spot plate method**

Cells were grown overnight in 10 ml selective medium (SD -ura -met) and 10 O.D.<sub>600</sub> equivalents were collected. Samples were then diluted using culture medium to 1, 0.1, 0.01, and 0.001 O.D.<sub>600</sub> equivalents and vortexed to

ensure homogenous dilutions. SD -ura -met plates and SD -ura -met plates that contained 1.5 M KCl were then inoculated using a grid pattern and incubated for 72 hrs at either 30°C or 39.5°C.

## **Chapter 3 - Endogenous Levels of Syntaxin 16 and mVps45 in Adipocytes**

## **Chapter 3: Endogenous Levels of Syntaxin 16 and mVPS45 in Adipocytes**

### **3.1 Introduction**

#### **3.1.1 The location of Syntaxin 16 and mVps45**

Syntaxin 16 is a functional t-SNARE located at the TGN and responsible for early endosomal to TGN transport (Yamaguchi et al., 2002). It forms a SNARE complex with the t-SNAREs Syntaxin 6 and Vti1a and has been shown to translocate to the PM in response to insulin stimulation (Proctor et al., 2006). Vps45 is an SM protein located at the TGN and found to bind to Syntaxin 16 (Dulubova et al., 2002). These proteins are both found at the TGN of 3T3-L1 adipocytes. In this chapter we determine the levels of Syntaxin 16 and mVps45 in the locations where they are found in adipocytes.

#### **3.1.2 Interactions between Syntaxin 16 and mVps45**

Studies in yeast have revealed that the syntaxin 16 homologue Tlg2p binds the yeast SM protein Vps45p (Dulubova et al., 2002) and that this Tlg2p/Vps45p binding mode is conserved in mammalian Syntaxin 16 and mVps45. Syntaxin 16 has been found to bind to mVps45 via an N-terminal peptide motif (Dulubova et al., 2002). In addition, Yamaguchi also found that Syntaxin 16 and mVps45 bind directly to each other (Yamaguchi et al., 2002). This binding interaction implies that SNAREs and SM proteins perform active roles in membrane fusion while forming part of the same complex. In this chapter we assess binding of mVps45 and Syntaxin 16 by immunoprecipitating these proteins.

#### **3.1.3 The effects of insulin stimulation on endogenous levels of Syntaxin 16, mVps45 and their interaction**

Several studies have suggested that the action of Syntaxin 16 may control the insulin-responsiveness of adipocytes. Shewan found that insulin caused a significant redistribution of Syntaxin 16 from intracellular membranes to the PM (Shewan et al., 2003). Perera also found that acute insulin stimulation reduced the phosphorylation state of Syntaxin 16 by nearly half (Perera et al.,

2003) which may regulate GLUT4's ability to enter the GSVs. Furthermore, Proctor and colleagues suggested that Syntaxin 16 functions to control the entry of GLUT4 into the slow recycling pathway which regulates the insulin responsiveness of adipocytes (Proctor et al., 2006).

The effects of insulin stimulation on the action of mVps45 have not been established in the literature and in this chapter, we quantify the levels of mVps45 in insulin-stimulated membrane and cytosol. Similarly, while Dulubova and others have reported the binding mode used by Syntaxin 16 to interact with mVps45 (Dulubova et al., 2002; Yamaguchi et al., 2002), the binding of these partners has not been reported in cells which were insulin-stimulated. In this study, we examine the ability of mVps45 and Syntaxin 16 to bind under insulin-stimulated conditions.

## **3.2 Aims**

This first chapter investigates two important questions relating to the hypothesis that mVps45 interacts with Syntaxin 16 in the absence of insulin which allows GLUT4 to traffic into the slow cycle, shown in Figure 1.2. First, quantification experiments in fibroblasts, differentiated 3T3-L1 adipocytes and rat primary adipocytes answer the question of whether mVps45 and Syntaxin 16 are present in stoichiometric amounts. The chapter goes on to answer the question of whether insulin stimulation alters the interaction between Syntaxin 16 and mVps45. Immunoprecipitation experiments are used to determine if the interaction of Syntaxin 16 and mVps45 is regulated by insulin.

## **3.3 Results**

### **3.3.1 Construction and purification of mVps45**

mVps45 recombinant protein was synthesized using a protein expression vector designed to express mammalian Vps45 in bacteria. This construct was made by PCR amplifying the full length cDNA of rat mVps45 from the plasmid pCMV-Vps45 (generously donated by Dr. Piper, a plasmid containing the full length mVps45 in pALTER-MAX, see appendix for plasmid maps) as a template

and utilising the primer set Vps45 His (see Materials and Methods for sequence) in which restriction sites for Kpn I and Sph I were engineered. This PCR product was cloned into the TA shuttle vector pCR2.1 (see appendix for plasmid map). Once successfully incorporated into the shuttle vector, clones were selected and the resulting DNA was then digested with Kpn I and Sph I (restriction sites known to be in the MCS of the destination protein expression vector pQE-30). This product was ligated into the 6X His-tagged protein expression vector pQE-30 and expressed in BL-21 (DE3) cells from which the expressed protein was purified as described in Materials and Methods. Figure 3.1 illustrates this process.

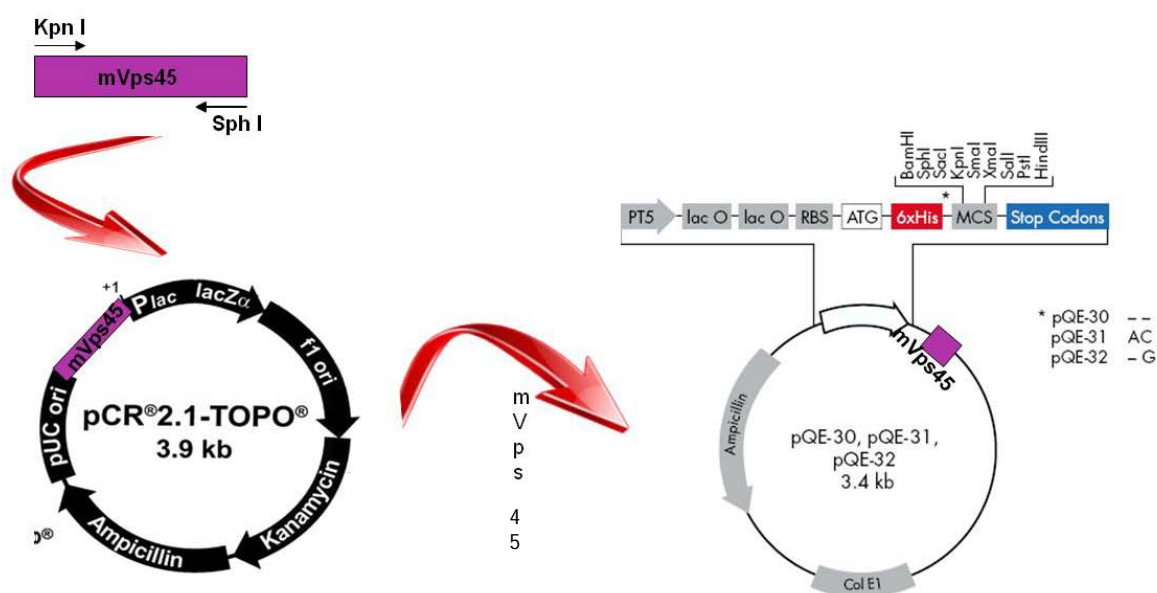


### Figure 3.1 The Construction of pCMV-mVps45

Rat mVps45 was PCR amplified using primers engineered to clone into the N-terminal His-tagged expression vector pQE-30. The PCR product was A-tailed and subcloned into the TA shuttle vector pCR2.1 before being ligated into pQE-30. The construct was transformed into BL-21 (DE3) *E. coli* cells and purified using a Nickel-NTA method. Additional details of pCR2.1 and pQE-30 can be found in the Appendix.

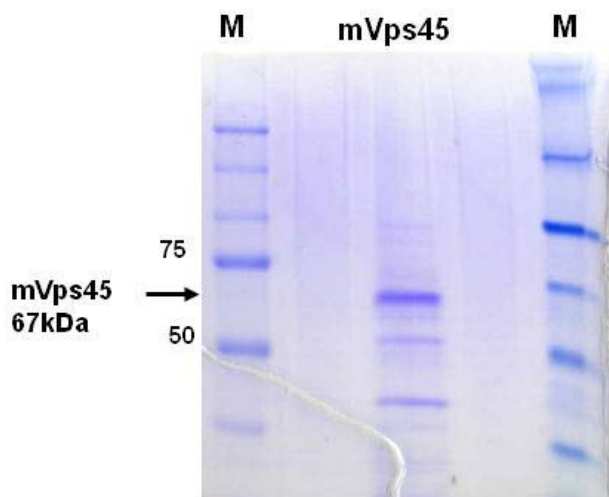


### Figure 3.2 The Purification of mVps45

mVps45 was purified using the Nickel-NTA method as described in Section 2.3.1. The protein was run on an SDS-PAGE gel and Coomassie stained. Lane 1: Marker, Lane 3: mVps45 (25  $\mu$ g) purified and shown to run at 67 kDa, Lane 5: Marker.

This recombinant protein was subjected to SDS-PAGE which was then Coomassie stained to assess yield and that the protein was properly synthesized. As Figure 3.2 shows, mVps45 was found to be at the correct molecular weight of 67 kDa and yielded a major band with only minor degradation products (which could be removed by dialysis).

### 3.3.2 Purification of Syntaxin 16

After the synthesis of mVps45, the SM protein studied in this work, recombinant protein of its cognate syntaxin was also necessary to study functional interactions. Syntaxin 16 was expressed in bacteria from the plasmid pALA001 (a protein-A tagged version of Syntaxin 16A, see section 2.1.4) as described in Materials and Methods. As Figure 3.3 illustrates, protein run on an SDS-PAGE gel yields a major band just above the 25 kDa molecular weight marker, corresponding to the molecular weight of Syntaxin 16 (32 kDa).

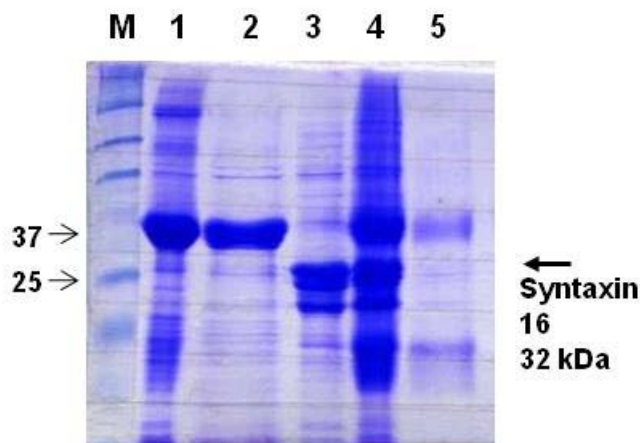


**Figure 3.3 The Purification of Syntaxin 16**

Marker, Lane 1: Syntaxin 16-PrA bound to beads, Lane 2: Syntaxin 16-PrA cleaved from beads, Lane 3: Syntaxin 16 cleaved from Protein A Tag, Lane 4: Residual protein A tag, Lane 5: Beads alone. Each lane is loaded with 20  $\mu$ g total protein. Additional information about pALA001 in pETDuet-1 can be found in the Appendix.

### 3.3.3 Changes in Intracellular Protein Levels upon 3T3L1 Cell Differentiation

After synthesis of mVps45 and Syntaxin 16 recombinant protein for use as tools in understanding more about the interaction of mVps45 and Syntaxin 16, the target cell under study, the 3T3-L1 adipocyte, was assessed for differences in differentiation. First, we looked at basic morphological changes in the cells upon differentiation under basal conditions. Oil Red O staining revealed that fibroblasts assumed the same basic morphology as other fibroblast lineages. However, when these fibroblasts were exposed to differentiation factors such as methylisobutylxanthine (IBMX or MIX), dexamethasone, insulin and serum, they differentiate into a phenotype resembling mature white fat cells. While induction is necessary to convert these fibroblasts into adipocytes, it is not required to maintain these cells as adipocytes which can be taken as evidence that gene upregulation is the cause of this phenotypic change. MIX, a phosphodiesterase inhibitor, is thought to function through increasing cAMP accumulation and has been shown to increase C/EBP- $\beta$  expression which is required for subsequent PPAR $\gamma$  expression. Dexamethasone, a synthetic glucocorticoid which induces PPAR $\gamma$  expression is also necessary to activate genes required for the adipocyte conversion. Insulin, in supraphysiological concentrations which do not increase the number of differentiated adipocytes but accelerates the accumulation of

lipid, and serum which contributes growth factors are also necessary for induction. CCAAT-enhancer binding protein- $\alpha$  (C/EBP $\alpha$ ) and Peroxisome proliferator-activated receptor  $\gamma$  (PPAR $\gamma$ ) transactivate adipocyte specific genes and the substances used for induction directly affect the activation of these two molecules. Committed pre-adipocytes undergo clonal expansion and growth arrest prior to differentiation but studies have shown that it is the growth arrest rather than any contact inhibition that is vital for differentiation to occur (Gregoire et al., 1998).

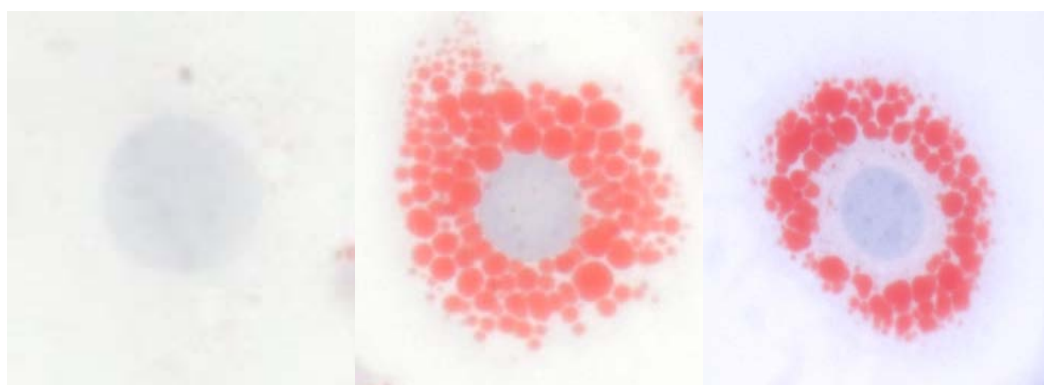


**Figure 3.4 Oil Red O Staining of basal cells.**

3T3-L1 adipocytes are a useful cell line for studying adipocyte biology because they are rapidly converted from a fibroblast-like cell lineage to a differentiated adipocyte phenotype. Differentiation requires the fibroblasts to be incubated with Insulin and other co-factors such as IBMX and dexamethasone in the presence of serum to shuttle cells into the adipocyte phenotype where they progressively accumulate lipid droplets. Shown here, 3T3-L1 fibroblasts share the same morphology of other fibroblast cells. Once differentiated, they exhibit the behaviours of adipocytes and collect lipid in their vacuole after they have undergone clonal expansion and growth arrest. In KD cells, lipid accumulation is decreased compared to wildtype. In this figure: L-R: Fibroblast, WT differentiated 3T3-L1, KD differentiated 3T3-L1. Cells were fixed onto slides, stained with Oil Red O and counterstained with Mayer's hematoxylin and imaged under a light microscope under 63X Oil magnification.

In Figure 3.4, basic fibroblast morphology is clear in the left panel. However, upon induction with differentiation agents, fibroblasts assume an adipocyte phenotype and lipid rapidly accumulates. Oil red O staining shows these accumulated lipids in red in the middle panel of Figure 4.3 (the nucleus has been counterstained as a positional landmark in blue). Interestingly, knockdown of mVps45 in fibroblasts that were later differentiated into adipocytes shows a slight decrease in the size and number of lipid droplets (shown in the right panel, Figure 3.4), the effects of mVps45 knockdown will be discussed in detail in Chapter 5.

After assessing the basic morphological changes in basal cells when fibroblasts are converted to adipocytes by Oil Red O staining, fibroblasts and adipocytes were made into lysates and were subjected to immunoblot analysis. mVps45, Syntaxin 16 and GLUT4 protein levels were analysed in Figure 3.5 for changes upon differentiation. As shown in the top panel of Figure 3.5, GLUT4 is not present in fibroblasts but is expressed in differentiated adipocytes. Shewan and colleagues have reported that 3T3-L1 cells have a characteristic ability to form insulin responsive GLUT4 compartments after adipocyte differentiation (Shewan et al., 2003). Shewan found that the levels of Syntaxin 16 increased more than 2.5 fold upon differentiation. Here, in the third panel of Figure 3.5, we report similar results.

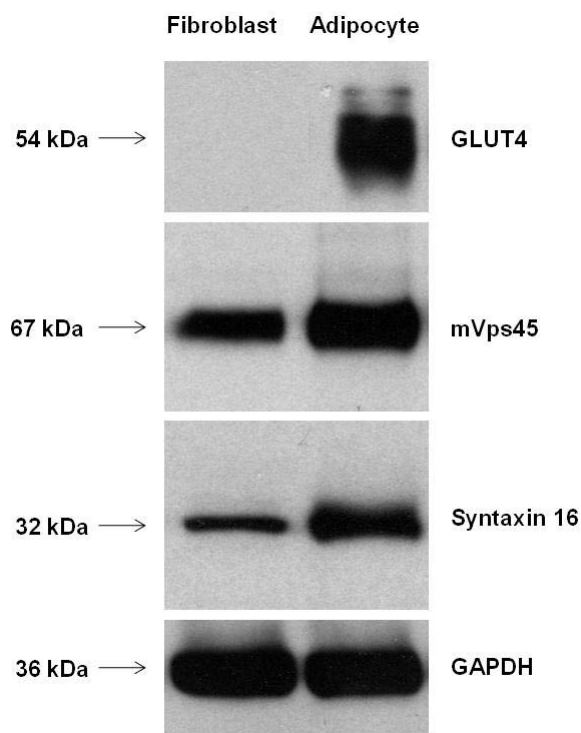


**Figure 3.5 Differentiation of 3T3-L1 Adipocytes causes changes in cellular protein levels**

Two sets of 3T3-L1 fibroblasts were grown until 70% confluent. For the first set, whole cell lysates were prepared as described in Materials and Methods and immunoblotted for the proteins GLUT4, mVps45, Syntaxin 16 and GAPDH. For the second set, cells were allowed to divide until growth arrest resulting from contact inhibition, then differentiated as described previously into mature adipocytes. Whole cell lysates were then prepared from these adipocytes. Fibroblast and adipocyte samples (25 micrograms) were separated on SDS-PAGE gels and immunoblotted for the above proteins. The data above are typical of several experiments of this type.

We also assessed the differences in mVps45 levels upon adipocyte differentiation in an effort to discover whether the SM protein binding partner for this t-SNARE would also increase in a similar manner. Here, in the second

panel of Figure 3.5 we show that mVps45 does increase upon adipocyte differentiation but not with the same fold increase as Syntaxin 16. Later in this chapter, this finding becomes apparent when discussing whether mVps45 and Syntaxin 16 are present in stoichiometric amounts. GAPDH was used as a loading control.

### 3.3.4 Expression of Syntaxin 16 in Adipocytes

Once expression in adipocytes had been analysed and compared to levels in fibroblasts, quantification of these levels was performed. As mentioned above, Syntaxin 16 in basal adipocytes shows an increase in expression levels when compared to fibroblasts. These levels were quantified in Figure 3.6 by comparing known quantities of differentiated basal membrane from 3T3-L1 adipocytes (20 and 50  $\mu$ gs) against a standard curve of microgram quantities of recombinant Syntaxin 16 (described in Section 3.3.2 and shown in Figure 3.3). Figure 3.6 also shows immunoblots of GLUT4, the glucose transporter involved in glucose uptake, and mVps45, the binding partner of Syntaxin 16. GAPDH was used as a loading control.

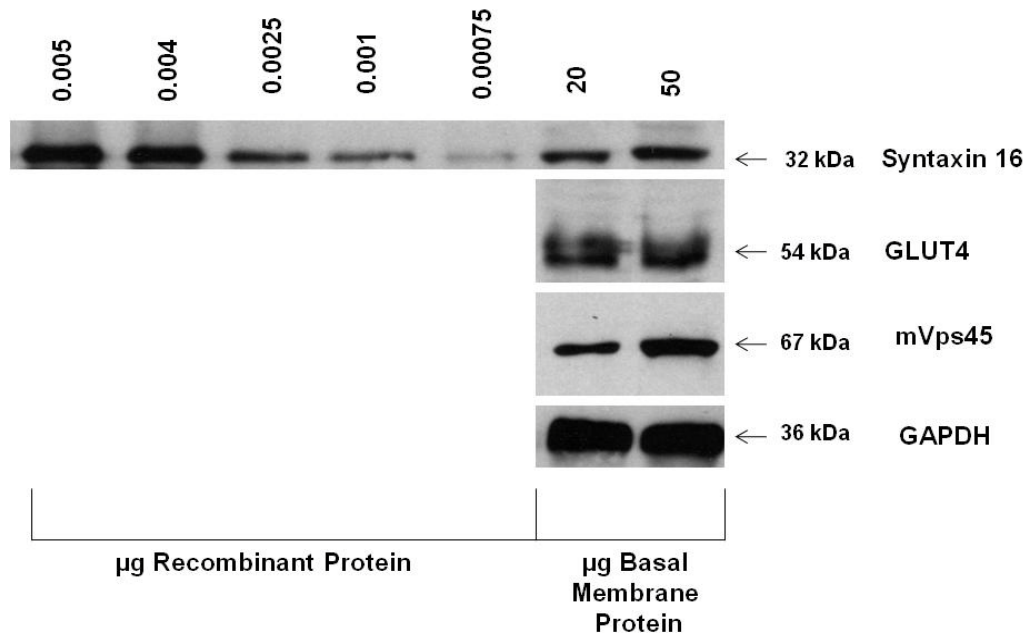


**Figure 3.6 Quantification of the levels of Syntaxin 16 in membranes from basal cells.** Syntaxin 16 recombinant protein was purified as previously described and loaded in known amounts onto SDS-PAGE gels in a dose-dependent manner. This standard curve was later used to quantify the amount of Syntaxin 16 present in basal differentiated 3T3-L1 membrane protein. Also shown are representative immunoblots of known amounts of 3T3-L1 membranes. The antibodies used are indicated along with the approximate position of the molecular weight marker at the right of the figure. Data from one representative immunoblot with each antibody is shown, repeated three times with different samples of 3T3-L1 adipocyte membranes.

The information gained from this quantitation experiment is reported in Table 3.1 both as copies of Syntaxin 16 per microgram of membrane protein and copy number per cell.

### 3.3.5 Expression of mVps45 in Adipocytes

After quantifying the levels of Syntaxin 16 in basal membranes, the levels of mVps45 in basal membranes were also examined. Unlike Syntaxin 16, a t-SNARE that is membrane bound, mVps45 is present both in membranes and cytosol in differing amounts depending on insulin stimulation. In Figure 3.7a, basal levels of mVps45 both in the cytosol and in membranes were quantified using the same method as before. A standard curve using recombinant mVps45 protein (discussed in Section 3.3.1 and shown in Figure 3.2) in known microgram quantities (the same values as in the Syntaxin 16 standard curve) was used to quantify 20 and 50  $\mu\text{g}$  quantities of both basal cytosol and basal membrane fractions from 3T3-L1 adipocytes. In the basal state, mVps45 is expressed at lower levels in the cytosol compared to levels in basal membranes. The quantification data is listed in Table 3.1.

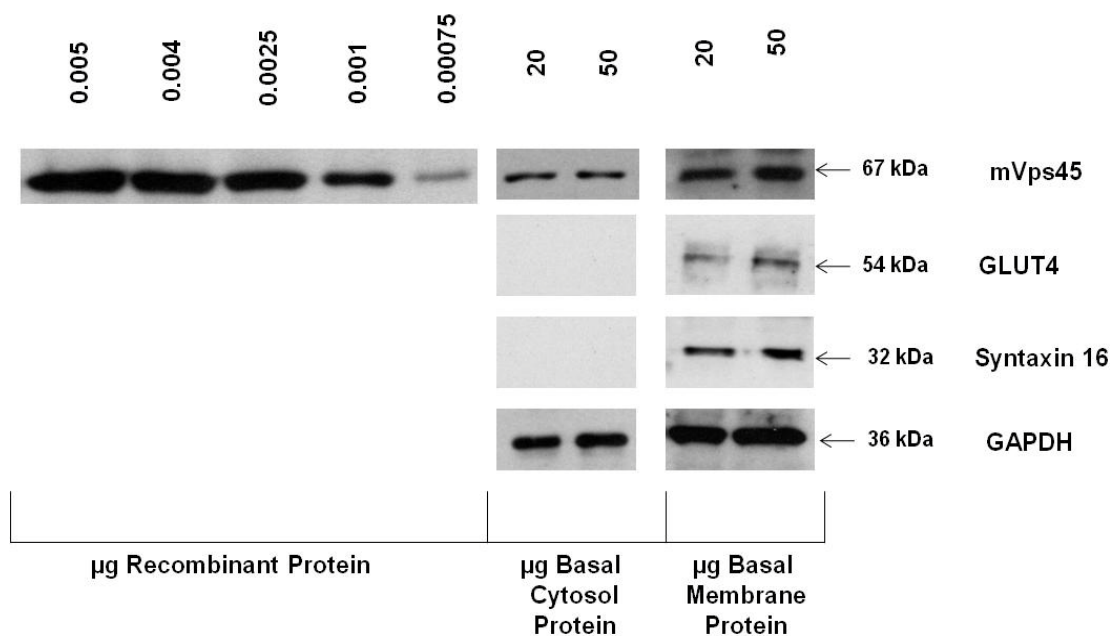


**Figure 3.7a Quantification of the levels of mVps45 in 3T3-L1 membranes and cytosol from basal cells.**

mVps45 recombinant protein was purified as previously described and loaded in known amounts onto SDS-PAGE gels in a dose-dependent manner. This standard curve was later used to quantify the amount of mVps45 present in basal differentiated 3T3-L1 membrane protein as well as basal cytosol fractions. Also shown are representative immunoblots of known amounts of 3T3-L1 membranes and cytosol. The antibodies used are indicated along with the approximate position of the molecular weight marker at the right of the figure. Data from one

representative immunoblot with each antibody is shown, repeated three times with different samples of 3T3-L1 adipocyte membrane and cytosol extract. Note that for the mVps45 samples, all samples were loaded on the same gel, but are presented above as different exposures for clarity.

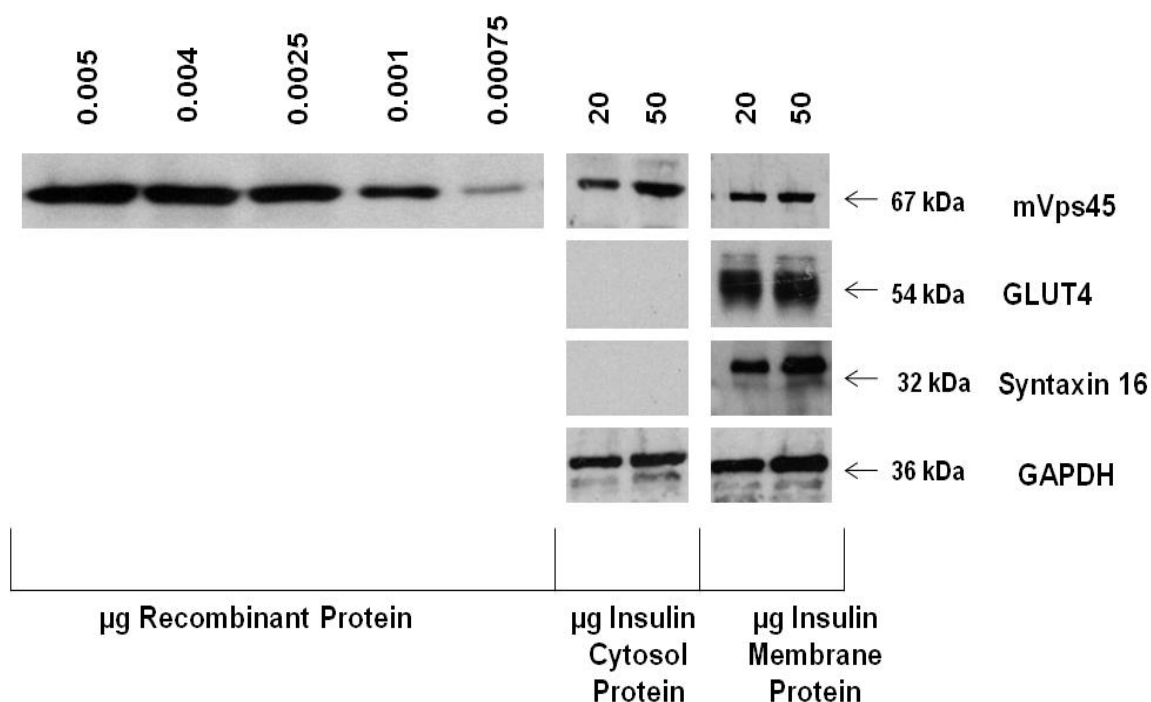


**Figure 3.7b Quantification of the levels of mVps45 in 3T3-L1 membranes and cytosol from Insulin-stimulated cells**

mVps45 recombinant protein was purified as previously described and loaded in known amounts onto SDS-PAGE gels in a dose-dependent manner. This standard curve was later used to quantify the amount of mVps45 present in insulin-stimulated differentiated 3T3-L1 membrane protein as well as insulin-stimulated cytosol. Also shown are representative immunoblots of known amounts of 3T3-L1 membranes and cytosol. The antibodies used are indicated along with the approximate position of the molecular weight marker at the right of the figure. Data from one representative immunoblot with each antibody is shown, repeated three times with different samples of insulin-stimulated 3T3-L1 adipocyte membrane and cytosol extract. Note that for the mVps45 samples, all samples were loaded on the same gel, but are presented above as different exposures for clarity.

In Figure 3.7b, adipocytes were stimulated with 1 $\mu$ M Insulin for 20 min and cytosol and membrane fractions were prepared. A standard curve of known quantities of mVps45 recombinant protein was used to compare 20 and 50  $\mu$ g quantities of insulin-stimulated cytosol and membrane protein from 3T3-L1 adipocytes. In the insulin-stimulated state, it would appear that there is a slight increase in the amount of mVps45 present in the cytosol. This increase could be explained by the role of mVps45 in translocation events. It is important to note that in both the basal (Figure 3.7a) and insulin-stimulated state, GLUT4 and Syntaxin 16 are not present in the cytosolic fraction. Data from this experiment (from Figures 3.7a and b) are reported in Table 3.1 in

terms of copy number per cell and copy number per  $\mu\text{g}$  of cytosol and  $\mu\text{g}$  of membrane.

### 3.3.6 Levels of Syntaxin 16 and mVps45 in Fibroblasts

In section 3.3.3 it was reported that protein expression levels of Syntaxin 16 and mVps45 in fibroblasts differed greatly to those in differentiated adipocytes (see Figure 3.5). In an effort to understand and quantify these differences, the protein quantities in 20 and 50  $\mu\text{g}$  of fibroblast lysate was compared against a standard curve of recombinant Syntaxin 16 protein to assess the levels of Syntaxin 16 in fibroblasts and to then compare this amount to what was seen in differentiated 3T3-L1 adipocytes. Quantitative data from this experiment is listed in Table 3.1 as copies per  $\mu\text{g}$  of fibroblast lysate.

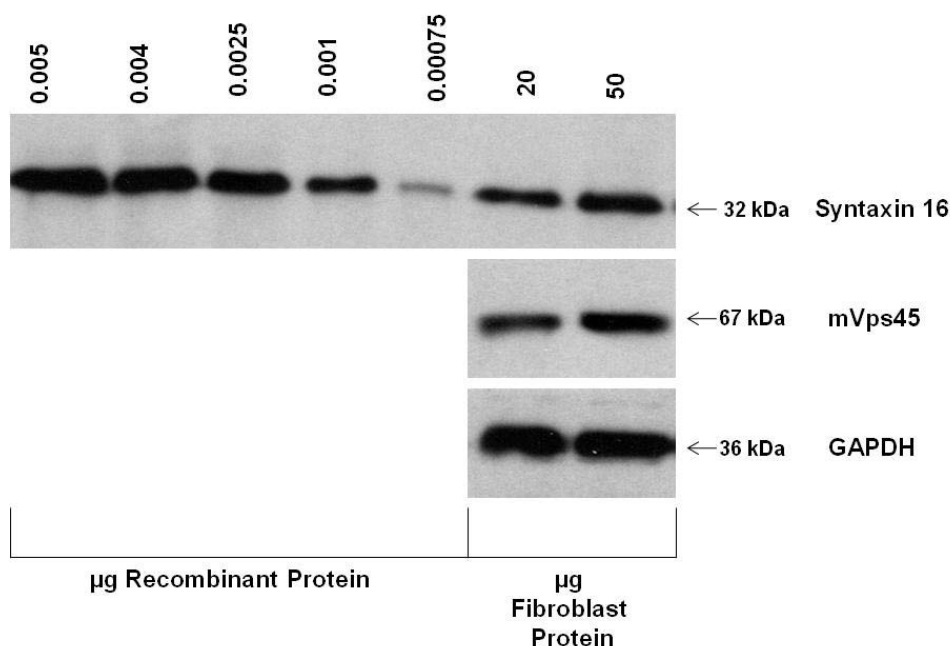


#### Figure 3.8a Quantification of the levels of Syntaxin 16 in 3T3-L1 fibroblast cells

Syntaxin 16 recombinant protein was purified as previously described and loaded in known amounts onto SDS-PAGE gels in a dose-dependent manner. This standard curve was later used to quantify the amount of Syntaxin 16 present in 3T3-L1 fibroblast cells. Also shown are representative immunoblots of known amounts of 3T3-L1 fibroblast lysate. The antibodies used are indicated along with the approximate position of the molecular weight marker at the right of the figure. Data from one representative immunoblot with each antibody is shown, repeated three times with different samples of 3T3-L1 fibroblast lysate.

Similarly, the levels of mVps45 in fibroblasts were assessed by comparison of 20 and 50  $\mu\text{g}$  quantities of fibroblast lysate against a standard curve of recombinant mVps45 protein (shown below in Figure 3.8b). The quantitative

results of this experiment are shown in Table 3.1 as copies per  $\mu\text{g}$  of fibroblast lysate.

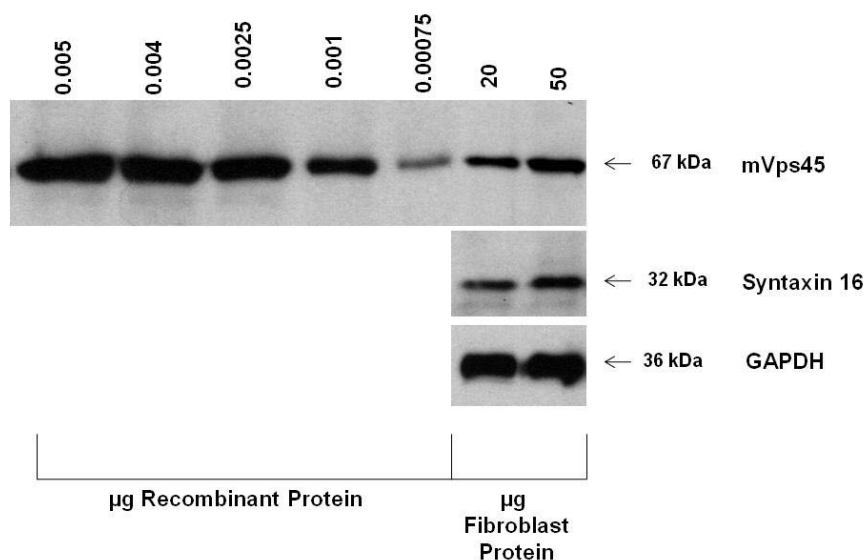


### Figure 3.8b Quantification of the levels of mVps45 in 3T3-L1 fibroblast cells

mVps45 recombinant protein was purified as previously described and loaded in known amounts onto SDS-PAGE gels in a dose-dependent manner. This standard curve was later used to quantify the amount of mVps45 present in 3T3-L1 fibroblast cells. Also shown are representative immunoblots of known amounts of 3T3-L1 fibroblast lysate. The antibodies used are indicated along with the approximate position of the molecular weight marker at the right of the figure. Data from one representative immunoblot with each antibody is shown, repeated three times with different samples of 3T3-L1 fibroblast lysate.

### 3.3.7 Levels of Syntaxin 16 and mVps45 in Rat Primary Cells

So far in this study, protein expression in adipocytes has been analysed using cultured 3T3-L1 adipocytes. It is possible that results may differ in primary cells. In order to determine if there are differences in protein levels between the use of an immortalized cell line in an in-vitro system and isolated primary cells, rat adipocytes were isolated from male Sprague-Dawley (SD) rats and whole cell lysates were prepared (as described in Materials and Methods). These lysates (20 and 50  $\mu\text{g}$ ) were first compared against a standard curve of known quantities of recombinant Syntaxin 16 protein (as shown in Figure 3.9a). The quantitative results of this experiment are shown in Table 3.1 as copies per  $\mu\text{g}$  of rat adipocyte lysate. Next, 20 and 50  $\mu\text{g}$  of these lysates were compared against a standard curve of known quantities of recombinant mVps45 protein (shown in Figure 3.9b). The quantitative results of this experiment are shown in Table 3.1 as copies per  $\mu\text{g}$  of rat adipocyte lysate.

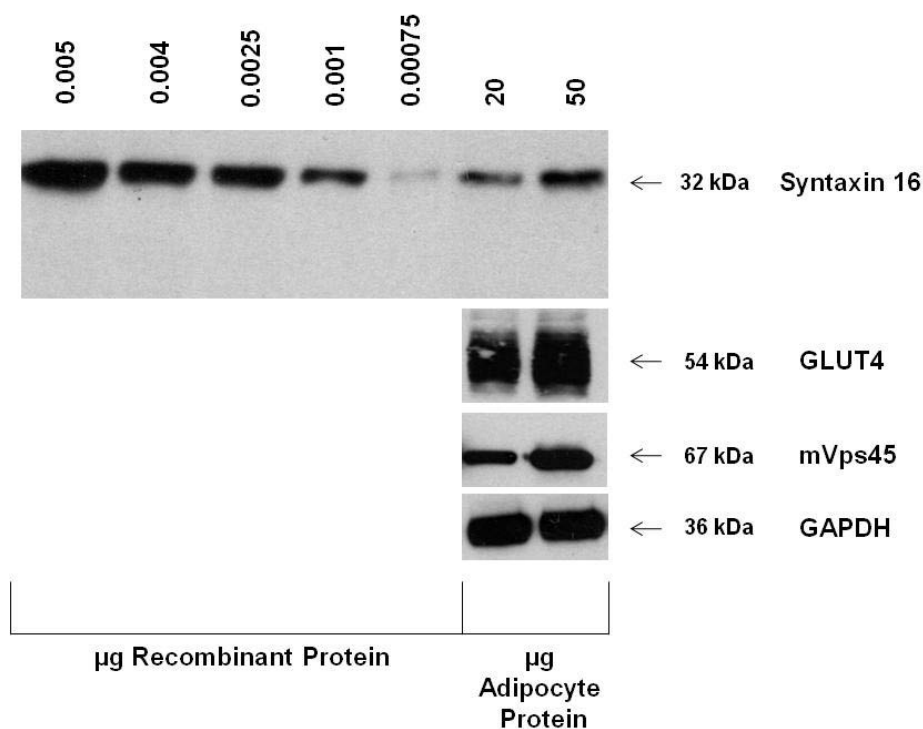


**Figure 3.9a Quantification of the levels of Syntaxin 16 in rat primary adipocytes**

Syntaxin 16 recombinant protein was purified as previously described and loaded in known amounts onto SDS-PAGE gels in a dose-dependent manner. This standard curve was later used to quantify the amount of Syntaxin 16 present in primary rat adipocytes. These adipocytes were isolated from SD rats and whole cell lysates were prepared as described in Materials and Methods. Also shown are representative immunoblots of known amounts of rat primary adipocytes. The antibodies used are indicated along with the approximate position of the molecular weight marker at the right of the figure. Data from one representative immunoblot with each antibody is shown, repeated three times with different samples of rat primary lysate.

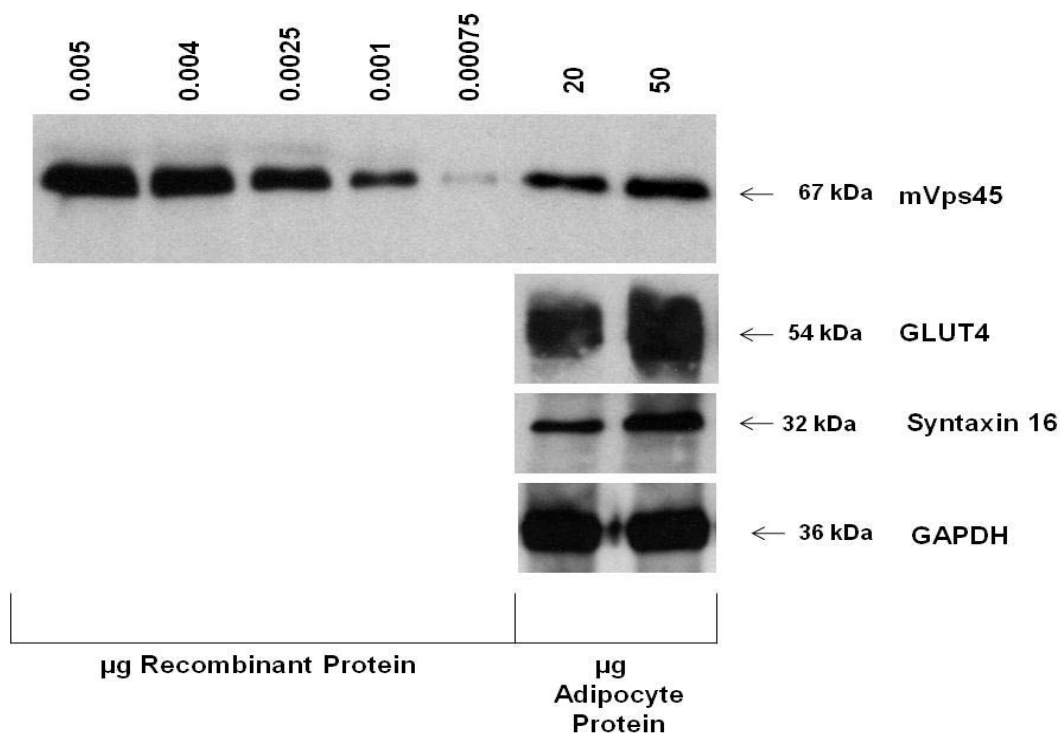


### Figure 3.9b Quantification of the levels of mVps45 in rat primary adipocytes

mVps45 recombinant protein was purified as previously described and loaded in known amounts onto SDS-PAGE gels in a dose-dependent manner. This standard curve was later used to quantify the amount of mVps45 present in primary rat adipocytes. These adipocytes were isolated from SD rats and whole cell lysates were prepared as described in Materials and Methods. Also shown are representative immunoblots of known amounts of rat primary adipocytes. The antibodies used are indicated along with the approximate position of the molecular weight marker at the right of the figure. Data from one representative immunoblot with each antibody is shown, repeated three times with different samples of rat primary lysate.

### 3.3.8 Analysis of Endogenous Syntaxin 16 and mVps45 expression using the Standard Curve Method and Calculation of Copy Number per Cell

Once all of the samples had been compared to their corresponding standard curves, the immunoblots were analysed and densitometric data was collected (See Materials and Methods, Section 2.3.6).

Protein	Copies per cell	Copies per $\mu\text{g}$ Lysate	Copies per $\mu\text{g}$ Membrane	Copies per $\mu\text{g}$ Cytosol
Syntaxin 16 Basal Membrane	635, 238		$6.35 \times 10^{11}$	
mVps45 Basal Membrane	202, 264		$3.85 \times 10^{11}$	
mVps45 Insulin- Stimulated membrane	247, 212		$4.10 \times 10^{11}$	
mVps45 Basal Cytosol	92, 142			$2.38 \times 10^{12}$
mVps45 Insulin- Stimulated Cytosol	224, 738			$3.73 \times 10^{12}$
Syntaxin 16 Fibroblast	115, 872	$1.92 \times 10^{12}$		
mVps45 Fibroblast	44, 947	$7.46 \times 10^{13}$		
Syntaxin 16 Rat Adipocyte		$3.59 \times 10^{12}$		
mVps45 Rat Adipocyte		$2.79 \times 10^{12}$		

**Table 3.1 Quantification of SNARE protein levels**

Estimated levels of the indicated proteins are shown above. In this analysis the diameter of the dishes employed was 100 mm, and these contained  $\sim 1 \times 10^7$  cells per dish.

Densitometry values for each lane of the standard curve were used to plot the 20 and 50  $\mu\text{g}$  values for each experiment. After this value was determined, approximations of the amount of protein in the samples (2500  $\mu\text{g}$  for membrane, cytosol and adipocytes, 1250  $\mu\text{g}$  for fibroblasts) was divided against the quantity of protein blotted (20 or 50  $\mu\text{g}$ ). This value was converted to the amount in 10 million cells before being divided by the molecular weight of the protein (32,000 for Syntaxin 16 and 67,000 for mVps45). This value was reported as the copies per microgram. To obtain the copies per cell, this number was multiplied by Avogadro's number and divided by the estimated number of cells in the sample (10 million). The

quantification results of the experiments shown in Figures 3.6-3.9 are listed in Table 3.1 above.

These data reveal that the total mVps45 levels (i.e. copies per cell in membrane fraction + copies per cell cytosol) are broadly similar to that of Sx16, as would be predicted if this SM protein acts together with the cognate syntaxin. Levels of Sx16 are clearly increased during differentiation from fibroblasts to adipocytes, as is also the case for mVps45. Interestingly, the levels of mVps45 and Sx16 expressed per microgram of membrane are broadly similar in rat adipocytes, consistent with the notion that these two proteins interact functionally.

### 3.3.9 The Co-Immunoprecipitation of Syntaxin 16 and mVps45

While quantification of the levels of Syntaxin 16 and mVps45 tested the hypothesis that they were present in roughly stoichiometric amounts, it was imperative to discover whether there is a binding interaction between Syntaxin 16 and mVps45. In order to test the second part of the hypothesis co-immunoprecipitation experiments were performed. These experiments shed light on the hypothesis that in basal conditions mVps45 binds to Syntaxin 16 thereby allowing Glut4 into the slow cycle and upon insulin stimulation mVps45 does not bind Syntaxin 16 and therefore cannot enter into the slow recycling pathway.

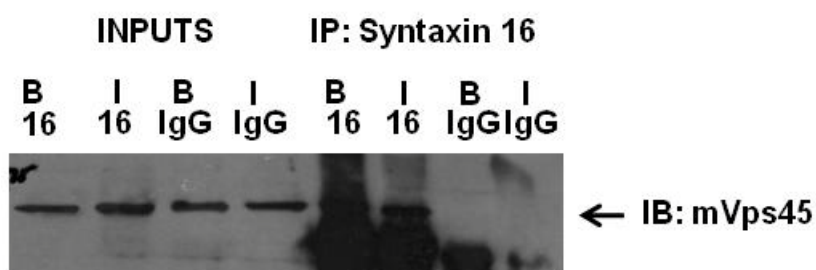


#### Figure 3.10a Syntaxin 16 Co-Immunoprecipitates with mVps45

Immunoprecipitation lysates were prepared from basal and insulin-stimulated 3T3-L1 differentiated adipocytes as described in Materials and Methods. These lysates were incubated with Syntaxin 16 antibody and immunoblotted with an antibody against mVps45. Inputs are lysate supernatants. Random IgG antibody was also incubated with basal and insulin-stimulated lysates as a control for binding.

In Figure 3.10a, shown above, basal and insulin-stimulated lysates were immunoprecipitated with Syntaxin 16 antibody and immunoblotted against an antibody specific to mVps45. In these experiments random IgG was used as a control for binding. It is clear from this experiment that Syntaxin 16 and mVps45 interact under basal conditions.



#### Figure 3.10b mVps45 Co-Immunoprecipitates with Syntaxin 16

Immunoprecipitation lysates were prepared from basal and insulin-stimulated 3T3-L1 differentiated adipocytes as described in Materials and Methods. These lysates were incubated with mVps45 antibody and immunoblotted with an antibody against syntaxin 16. Random IgG antibody was also incubated with basal and insulin-stimulated lysates as a control for binding

When the converse co-immunoprecipitation experiment was performed (as shown in Figure 3.10b above), it is clear that Syntaxin 16 and mVps45 are able to bind in basal conditions, once again validating the hypothesis that mVps45 can bind Syntaxin 16. Insulin did not appear to modulate these interactions.

### 3.4 Discussion

In this first chapter, the hypothesis that mVps45 and Syntaxin 16 are present in stoichiometric amounts and that mVps45 can bind to Syntaxin 16 was tested.

Shewan and colleagues found that Syntaxin 16 was upregulated significantly during adipocyte differentiation (Shewan et al., 2003). In Figure 3.5, we confirm these results since there is an increase in Syntaxin 16 protein levels as fibroblasts are differentiated into adipocytes. We also show that mVps45 levels appear to be upregulated in tandem with Syntaxin 16. These data are consistent, and suggest that mVps45 and Sx16 function is enhanced during the adipocyte differentiation process by increasing the absolute levels of these two proteins.

We then quantified the levels of Syntaxin 16 and mVps45 in adipocytes. Hickson and colleagues examined the SNARE complex involved in exocytosis of GLUT4 in response to insulin to determine whether any of the associated proteins were rate limiting to the formation of a SNARE complex and subsequent fusion of GLUT4 vesicles with the plasma membrane (Hickson et al., 2000). In this study, we quantified the t-SNARE associated with GLUT4 intracellular trafficking (Syntaxin 16) and its cognate SM protein mVps45 in order to test whether one of these proteins was present in significantly disproportionate amounts and was thus rate limiting to the sorting of GLUT4 into GSVs. When we quantified these levels (Figures 3.6-3.9) we found that levels of Syntaxin 16 and mVps45 were present in roughly stoichiometric amounts and also the levels in rat primary adipocytes were similar.

When we quantified the levels of Syntaxin 16 in basal membranes we calculated a cell copy number of over 600,000 molecules of Syntaxin 16 per 3T3-L1 adipocyte. This value is broadly in keeping with the membrane fusion t-SNARE values that Hickson obtained (Hickson et al., 2000). When this value is compared with the values calculated for mVps45 (which is present in both basal membrane and cytosol) in 3T3-L1 adipocytes, it shows that these two molecules are present in stoichiometric quantities which suggests that their interaction is important for membrane fusion in adipocytes.

Quantification of the levels of Syntaxin 16 and mVps45 in fibroblasts (as reported in Table 3.1) indicate when compared to values reported for adipocytes that the copies of both Syntaxin 16 and mVps45 increase upon adipocyte differentiation. This result confirms the qualitative findings in Figure 3.5 that show that both Syntaxin 16 and mVps45 increase upon adipocyte differentiation and is in keeping with the findings of Shewan et al which found that Syntaxin 16 increased upon adipocyte differentiation (Shewan et al., 2003). The increase in copy number for both Syntaxin 16 and mVps45 suggests that these two proteins are important in differentiated adipocytes.

When we quantified the levels of Syntaxin 16 and mVps45 in isolated rat primary adipocytes we found that they were present in similar levels, which is consistent with the data from differentiated 3T3-L1 adipocytes indicating that

they are present in roughly similar amounts. The idea that Syntaxin 16 and mVps45 are present in stoichiometric amounts in both 3T3-L1 adipocytes and primary cells suggests that they interact functionally in adipocytes.

In this chapter we also examined the hypothesis that Syntaxin 16 and mVps45 interact in the basal state but are dissociated when 3T3-L1 adipocytes are insulin-stimulated. We tested this binding interaction between Syntaxin 16 and mVps45 by performing immunoprecipitation experiments. In these experiments we showed that in basal conditions Syntaxin 16 and mVps45 are able to bind, indicating that the first portion of this hypothesis may be correct. In lanes which show Syntaxin 16 and mVps45 interaction in insulin-stimulated conditions, we found that there is a clear interaction still present upon insulin-stimulation and so it appears that insulin does not modulate this interaction, or if it does, then the modulation is too subtle to be revealed using this approach.

## **Chapter 4: The Yeast Model in Understanding mVps45 Function**

## Chapter 4: The Yeast Model in Understanding mVps45 Function

### 4.1 Introduction

#### 4.1.1 Homology between Yeast and Mammalian Vps45

Yeast can be used as a model system to study the function of mVps45. Yeast work is experimentally tractable and membrane trafficking has been conserved in both yeast and mammalian cells. Although mVps45 was identified as a mammalian homologue of Vps45, it remains unknown whether mVps45 can complement the Vps45 deletion, and is therefore a true functional homologue. This chapter sets out to determine whether this is the case. If so, then mutants of mVps45 could be generated, based upon known mutations in the yeast isoform.

#### 4.1.2 Complementation between the behaviour of Vps45p and mVps45

To test if mVps45 is a functional homologue of Vps45p, mammalian Vps45 was expressed in yeast cells lacking endogenous Vps45p and tested for complementation. If the yeast cells could function as expected using the mammalian Vps45 and thus complement for the loss of the endogenous yeast Vps45 then mVps45 would be considered to be a functional homologue of Vps45p.

Several studies in this lab have employed the use of the yeast expression vector pVT102u to drive expression of various proteins of interest. In this study, however, we have used a plasmid containing a less strongly expressing promoter than pVT102u since over-expression of mVps45 might mask true functional differences in complementation. pVT102u uses the *ADH1* promoter which is constitutively active and thus would generate very high expression levels which could lead to excessive levels of Vps45 being produced.

### 4.1.3 Use of yeast mutants to screen for mVps45 function

Mutants of mVps45 can be generated based upon homology modeling with yeast Vps45p. Vps45p binds Tlg2p via an NH<sub>2</sub>-terminal peptide of the syntaxin inserting into a hydrophobic pocket on the outer face of domain I of Vps45p. In the related SM protein, Sly1p, this hydrophobic pocket is formed by five residues of Sly1p (L137, L140, A141, I153, and V156) that surround F10 of Sed5p (the cognate syntaxin) (Munson and Bryant, 2009). Sequence alignment of Vps45p and Sly1p indicates that four of these residues are conserved, with the fifth residue, I153, being replaced by a valine in Vps45p. Mutation of these residues results in a pocket-fill mutant that abrogates Vps45p function (Carpp et al., 2006). In addition, a version of Vps45p carrying a single amino acid substitution (W244R) exerts a dominant-negative effect on the sorting of CPY (Carpp et al., 2006). This chapter also describes the generation of mutants of the equivalent residues in mVps45, and an analysis of their phenotypes when expressed in yeast lacking Vps45p (*VPS45Δ*).

## 4.2 Aims

Vps45p and mVps45 are thought to be functional homologues and this chapter aims to investigate whether this is the case using a variety of methods. *S. cerevisiae* depleted of Vps45 are unable to correctly sort the vacuolar hydrolase carboxypeptidase Y (CPY), and, instead, a precursor form of the protease is secreted from the cell. This sorting event involves yeast syntaxin Tlg2p, the yeast homologue of Syntaxin 16. In this chapter, we determine whether mammalian Vps45 can complement the *VPS45Δ* by expressing recombinant mammalian mVps45 in yeast from a centromeric plasmid and assaying CPY secretion.

## 4.3 Results

### 4.3.1 Construction of the rat recombinant

To express mVps45 in yeast, the mVps45 ORF was placed downstream of the *VPS45* yeast promoter with approximately 1 kb of flanking sequence both upstream and downstream for recombination stability. Homologous

recombination was performed by the standard gap repair method as shown in Figure 5.1.

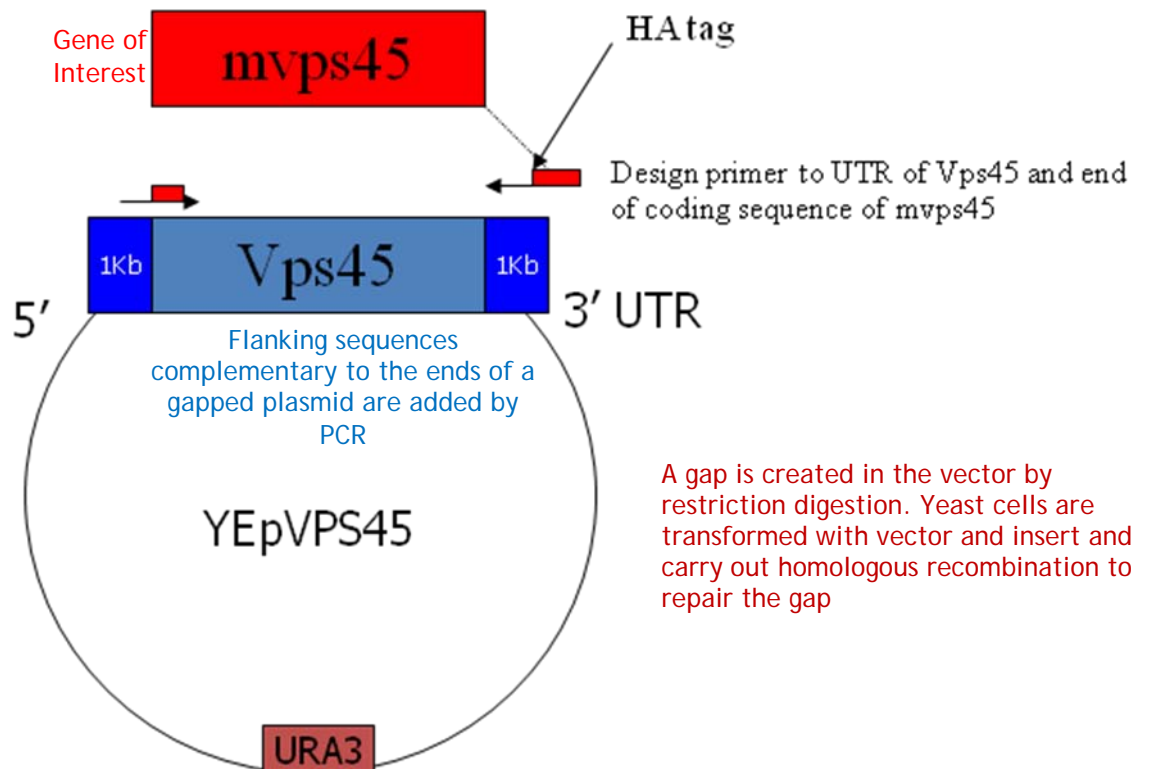


**Figure 4.1 The method of Homologous Recombination allows mammalian Vps45 to be expressed in yeast**

The yeast expression vector pCog70, here in this diagram labelled as YEpVPS45 to denote that YEplac195 was subcloned with a Vps45p fragment and the vector contains the VPS45 promoter, is 'gapped' by restriction digestion also removing the endogenous Vps45 (shown in blue). The PCR product, created by designing primers to amplify the gene of interest (here in red) and 1 Kb of additional sequence (royal blue) is co-transformed with the vector in yeast cells so that the yeast machinery can replace the missing Vps45 (in blue, excised before transformation by restriction digestion) with the mammalian copy of Vps45 (red, the gene of interest). The expression plasmid contains a *URA3* selection marker (dark red) allowing the transformed recombinant to grow on media deficient in uracil.

As described in Materials and Methods, YEpVPS45 (pCog70), is a 2 micron yeast expression plasmid containing an endogenous version of yeast Vps45p tagged with the HA epitope and containing a *URA3* selection marker which allows growth on uracil deficient media. This vector was linearized by restriction digestion, a process which also excised the endogenous coding sequence of the yeast Vps45 (Vps45p). This gapped yeast expression vector was co-transformed into SF838-9D (9Da) cells with the PCR amplified mammalian ORF encoding mVps45. This PCR product also contained flanking sequences homologous to the 3' end of the *VPS45* promoter and the 5' end of the 3' UTR of pCog70. The gap repair machinery within the yeast cells homologously

recombined the mammalian sequence with the expression plasmid and successful transformants grew into colonies on solid media lacking uracil (SD-ura -met). Colonies were selected and underwent plasmid rescue after which they were transformed into *E. coli* cells. Resulting colonies were then selected and the DNA isolated and sent for sequencing. (See Materials and Methods)

#### 4.3.2 Expression of the recombinant in yeast cells

Once sequencing confirmed that the plasmid contained mammalian Vps45, protein extracts from yeast containing the resulting plasmid, YEpmVps45, were used to perform immunoblots and these are shown below in Figure 5.2.

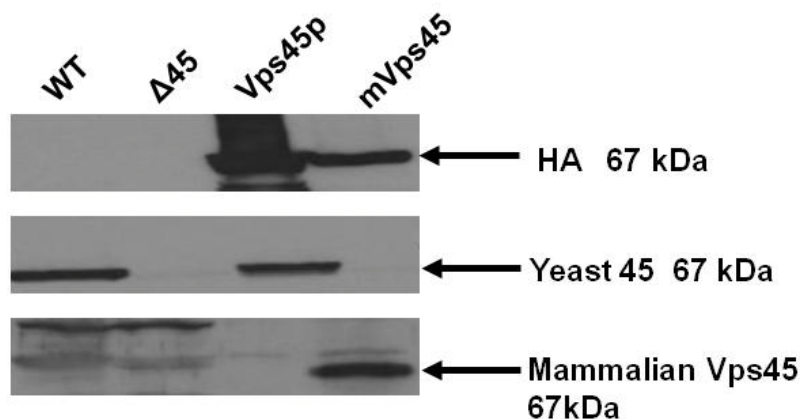


#### Figure 4.2 Mammalian Vps45 expression in transformed yeast cells

Whole cell lysates (1 O.D.<sub>600</sub> equivalent) prepared from 9Dα (SF838-9D) and 9DαΔ45 (LCY008) cells and 9DαΔ45 cells co-transformed with either empty vector or recombinant plasmid were screened for expression of protein levels using immunoblot analysis. Lane 1: 9Dα cells not transformed with any plasmid. Lane 2: 9DαΔ45 cells not transformed with any plasmid. Lane 3: 9DαΔ45 cells containing the yeast expression plasmid pCog70 (HA-Vps45p). Lane 4: 9DαΔ45 cells containing the mVps45 insert that had previously undergone homologous recombination, plasmid rescue and sequencing as described.

In the upper panel, lysates were subjected to immunoblot analysis using a mouse monoclonal antibody against HA (see Antibody table, Materials and Methods). In lane 1, no HA expression is detected in empty 9Dα cells. Similarly, in lane 2, no HA is detected in empty 9DαΔ45 cells. These two lanes contained lysates from cells that were not transformed with any plasmid so that no HA antigen would be present. However, in lane 3, these delete cells (9DαΔ45) contained the expression vector pCog70, which contained an HA-tagged version of endogenous yeast Vps45 (Vps45p) and do show HA expression. Lane 4 shows the signal from yeast expressing HA-tagged mVps45.

In the middle panel, lysates were immunoblotted using a rabbit antibody against the yeast Vps45 (as described in Materials and Methods, an antibody specific to yeast Vps45p). In lane 1, Vps45p expression in these 9D $\alpha$  wildtype cells is shown. These wildtype cells harbour endogenous Vps45p and the level of protein expression from these cells is shown. In lane 2, the 9D $\alpha$  $\Delta$ 45 cells have their copy of Vps45p deleted and so there is no expression of Vps45p when immunoblotted with the antibody. Because these yeast delete cells do not contain Vps45p, when they are transformed with plasmids containing Vps45p, as in Lane 3, expression levels are detected upon immunoblot analysis. Importantly, in lane 4, delete cells not containing Vps45p but transformed with the recombinant containing the mammalian copy of Vps45 (mVps45) do not show expression of the yeast Vps45. This shows that the recombinant did truly lose the copy of endogenous Vps45p contained in the yeast expression plasmid pCog70 when it was removed by digestion before recombination. In the last blot, lysates were immunoblotted using a rabbit antibody against the mammalian mVps45 (see Materials and Methods for description, an antibody specific for mammalian mVps45). A strong band at 67 kDa is detected in Lane 4 which contains the recombinant harbouring the mammalian copy of Vps45. This band is not detected in wildtype cells containing Vps45p (Lane 1), delete cells which do not contain Vps45 (Lane 2), delete cells 'rescued' with yeast Vps45p (Lane 3).

### 4.3.3 Construction of yeast mutants

Site-directed mutagenesis was used to construct mutants using YEpmVps45 as a template (as described in Materials and Methods). A pocket-fill arginine mutant, pHA-mVps45-V107R, was constructed using primers Vps45 V107R that replaced two base pairs (GTG to CGG) in the Vps45 sequence from a valine residue to an arginine. Similarly, a dominant negative mutant, pHA-mVps45-W230R, was constructed using primers Vps45 W230R replacing one base pair (TGG to CGG) in the sequence from a tryptophan to an arginine residue. Also, a double mutant (pHA-mVps45-Double) containing both mutations was constructed using pHA-mVps45-V107R as a template and using the W230R primers to mutate the tryptophan. The mutations were sequenced using sequence primers listed in Table 2.1.3, Materials and Methods and subsequent expression blots were performed to test the validity of these mutants.

#### 4.3.4 Expression of the recombinant and yeast mutants in wildtype and delete cells

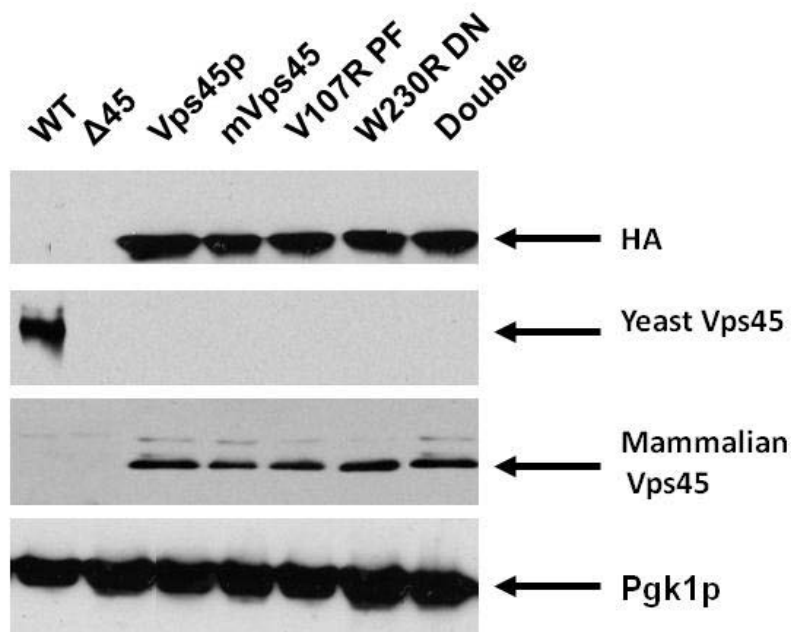


**Figure 4.3 HA-tagged Mammalian Vps45 expresses in yeast delete cells**

Whole cell lysates (1 O.D.<sub>600</sub> equivalent) prepared from 9D $\alpha$  (SF838-9D) and 9D $\alpha\Delta 45$  (LCY008) cells and 9D $\alpha\Delta 45$  cells co-transformed with either empty vector or recombinant plasmid were screened for expression of protein levels using immunoblot analysis. Lane 1: 9D $\alpha$  cells not transformed with any plasmid. Lane 2: 9D $\alpha\Delta 45$  cells not transformed with any plasmid. Lane 3: 9D $\alpha\Delta 45$  cells containing the yeast expression plasmid pCog70 (HA-Vps45p). Lane 4: 9D $\alpha\Delta 45$  cells containing the mVps45 insert that had previously undergone homologous recombination, plasmid rescue and sequencing as described. Lane 5: 9D $\alpha\Delta 45$  cells containing the pocket-fill arginine mutant V107R (PF). Lane 6: 9D $\alpha\Delta 45$  cells containing the dominant negative mutant W230R (DN). Lane 7: The double mutant in delete cells expresses protein levels for HA, Vps45p and mVps45 in a similar manner to the other two mutants.

As in the expression blots showing the initial construction of the mammalian recombinant, the mutants express the appropriate levels of HA tag and the correct version of Vps45. The upper panel, assessing the levels of HA protein expression, shows that empty wildtype and delete cells are a negative control for HA expression (see Antibodies, Materials and Methods). The last 4 lanes, all containing lysates from delete cells transformed with plasmids harbouring an HA-tag, show appropriate and relatively even levels of protein expression for all of the mutants of mVps45 generated. In an immunoblot demonstrating the levels of yeast Vps45, it is clear that only the wildtype cells, with their copy of endogenous Vps45p, show protein expression when immunoblotted with a polyclonal rabbit Vps45 antibody. Mammalian Vps45 protein levels were assessed in these mutants by subjecting the lysates to immunoblot analysis with a commercial rabbit mVps45 antibody. This blot clearly shows

that mammalian Vps45 is only detected in delete cells (cells not containing a copy of Vps45) transformed with plasmids containing the mammalian copy of Vps45. These lanes (4-7) correspond to the YEpmVps45 plasmid and subsequent mutants. The lower panel shows a loading control which was also employed when assessing the level of protein expression in these lysates.

#### 4.3.5 CPY Assay- TCA Precipitation

Normal CPY trafficking is a receptor-mediated event. In wildtype cells, CPY is synthesized as a prepro form and is transported across the endoplasmic reticulum membrane (Bowers and Stevens, 2005). In the ER it is cleaved to produce the 67 kDa p1 form. CPY binds the receptor Vps10p and this complex is sorted from the late Golgi to the late endosome (Bowers and Stevens, 2005). CPY then dissociates from Vps10p at the late endosome and is transported back to the vacuole where it is cleaved into mature CPY from the Golgi-modified p2 form (Bowers and Stevens, 2005). Vps mutants secrete the soluble hydrolase CPY. Vps45, a class D mutant, exhibits defective vacuolar morphology because it forms a single large vacuole that does not extend into daughter bud cells. Vacuoles in the mother cells of these mutants appear as single large spheres that fail to form segregation structures and buds appear to receive little or no vacuolar material from mother cells (Raymond et al., 1992). This suggests that nascent vacuolar material produced in these cells transiently accumulates as unfused vesicles. The fact that nearly all mother cells possess vacuoles raises the possibility that vacuoles can arise from unassembled vacuole precursors in a de novo fashion within daughter cells (Raymond et al., 1992). These mutants are unable to generate a pH gradient across the vacuolar membrane and fail to assemble peripheral membrane subunits of V-ATPase onto the cytoplasmic surface of the vacuole (Raymond et al., 1992). Class D mutants also affect genes that are thought to control anterograde vesicular traffic between the late Golgi and the late endosome (Horazdovsky et al., 1995). In Vps mutant cells such as this, a portion of the p2 form of CPY is secreted from the cell (Bowers and Stevens, 2005).

Since Vps45 mutants contain this secretion defect, this forms a useful model in which to test complementation. The CPY secreted from wildtype cells (SF-838, 9Da) transformed with empty vector was compared to that of cells

lacking the endogenous copy of Vps45p (LCY008, 9D $\alpha$ Δ45) transformed with empty vector, the mammalian copy of Vps45 (mVps45), the mammalian pocket-fill, dominant-negative or double mutant. TCA precipitation was used to collect the secreted proteins from selective media (SD -ura -met) and these proteins were subjected to immunoblot analysis using an antibody specific to CPY.

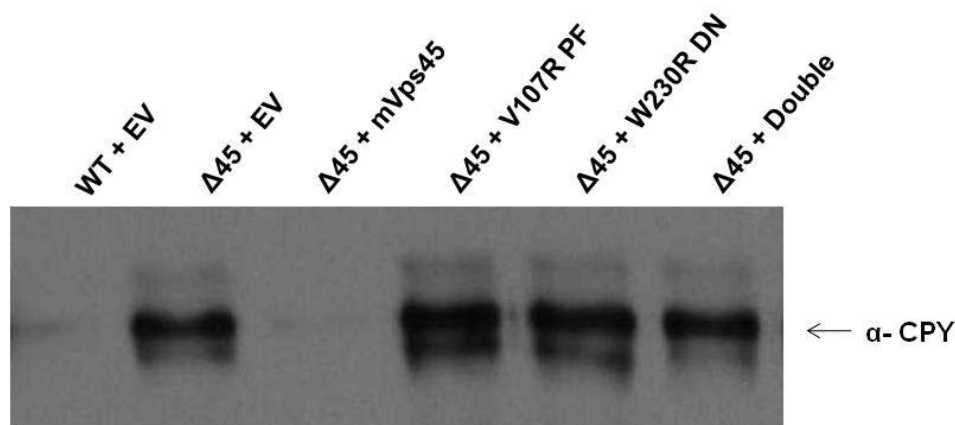


**Figure 4.4 The TCA Secretion Assay**

TCA precipitation was performed as described in Materials and Methods. Wildtype and 9D $\alpha$ Δ45 cells were allowed to double, consequently secreting CPY protein in the process. Cell cultures containing the conditioned media were precipitated for protein content by incubating them with TCA. Collected protein pellets were then normalized for protein levels and immunoblotted for  $\alpha$ -CPY levels using a mouse monoclonal (Clone 10A5) anti-CPY antibody. (Roederer and Shaw, 1996) Lane 1: Wildtype cells containing yeast Vps45 transformed with empty vector (EV). Lane 2: 9D $\alpha$ Δ45 cells deleted for Vps45 transformed with empty vector (EV). Lane 3: 9D $\alpha$ Δ45 delete cells transformed with the plasmid containing mVps45 (mVps45). Lane 4: Delete cells transformed with pHA-mVps45-V107R, the pocket-fill mutant (PF). Lane 5: Delete cells transformed with pHA-mVps45-W230R, the dominant negative mutant (DN). Lane 6: Delete cells transformed with pHA-mVps45-V107R/W230R, the double mutant (Double).

Figure 4.4 reveals that wildtype cells traffic CPY correctly and the CPY has been converted to the mature form. In comparison, the delete cells in lane 2 which lack *VPS45* clearly secrete the p2 form of CPY from the cell. The expression of the mammalian Vps45 reduces CPY secretion of Vps45 delete cells to levels seen in wildtype cells. However, mutants lacking the ability to express a functional copy of Vps45, such as the pocket-fill mutant V107R and the dominant-negative mutant W230R as well as a double mutant of both of these forms display defective CPY trafficking. In these lanes (4-6), CPY has been secreted out of the cell at levels similar to delete cells transformed with empty vector. This assay shows that mVps45 complements for the loss of Vps45p with respect to trafficking of the vacuolar hydrolase CPY and that mVps45 mutants cannot restore this function.

### 4.3.6 CPY Invertase Assay- Colorimetric Assay

Invertase ( $\beta$ -D-fructofuranoside fructohydrolase) in *S. cerevisiae* hydrolyzes sucrose into glucose and fructose (Darsow et al., 2000). The invertase gene (*SUC2*) encodes two transcripts with the longer sequence translocating to the cell surface from the ER through the Golgi where it is heavily glycosylated and the shorter sequence staying in the cytoplasm (Darsow et al., 2000). Vacuolar protein trafficking can be studied by measuring this invertase enzymatic activity. This method measures invertase glycosylation as indicative of ER to Golgi transport (Darsow et al., 2000) and because invertase secretion is not vital to cell survival cells mutant for CPY sorting secrete CPY-invertase allowing these cells to function through sucrose fermentation. Use of the liquid invertase assay quantitates the amount of glucose released by the hydrolysis of sucrose by comparing the invertase levels in the secreted population with the levels in total cell lysates.

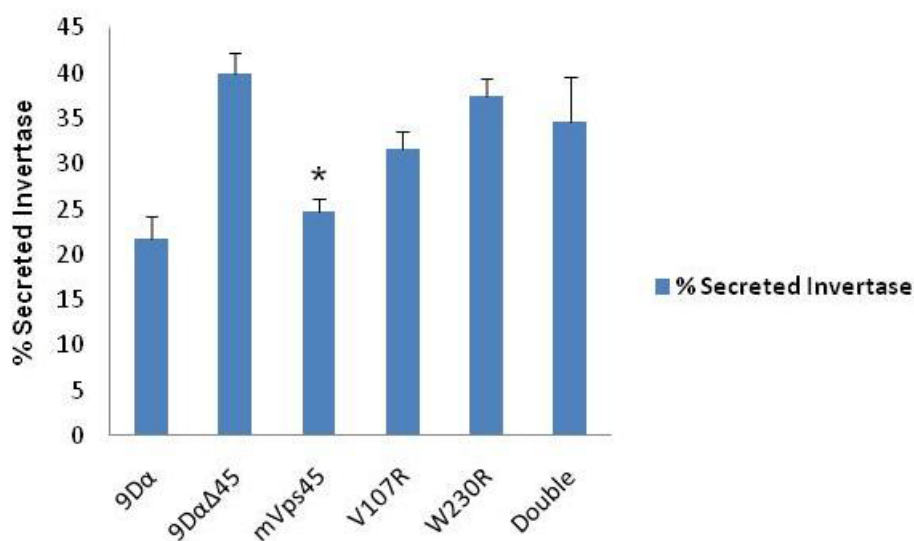


**Figure 4.5 Secretion of Invertase**

Wildtype yeast cells transformed with empty vector and delete cells transformed with empty vector, the mammalian copy of Vps45, the mammalian pocket-fill mutant, the mammalian dominant-negative mutant and the mammalian double mutant were grown in selective media (SD -ura -met) to mid-log phase and were harvested and diluted as described in Materials and Methods. Cells were incubated in 0.5 M sucrose, stopped in  $K_2HPO_4$  and then incubated in glucostat reagent before being read at 540 nm. Data shown represent the mean % Invertase secretion  $\pm$  SEM from 5 independent experiments. \* $p < 0.05$  by one-way ANOVA compared to delete cells.

In this assay, glucose oxidase was used to oxidize the glucose released by hydrolysis. This hydrolysis reaction produced hydrogen peroxide which was used by peroxidase to oxidize the chromogen *o*-dianisidine. The chromogenic product was read at 540 nm and the ratios of secreted and total fractions were estimated as a percentage of secreted invertase. As Figure 4.5 shows, cells lacking a copy of *VPS45* (*9D $\alpha$  $\Delta$ 45*) are defective in CPY-Invertase sorting and secrete nearly double the amount of invertase as wildtype cells. In contrast, delete cells transformed with the mammalian copy of *VPS45* (*mVps45*) showed reduced secretion of invertase approximating the levels in wildtype. This ability to rescue CPY-Invertase sorting showed complementation of function. Mammalian mutants however, transformed into these delete cells, showed abnormal CPY-Invertase secretion. Delete cells transformed with the mammalian pocket-fill mutant (*V107R*) showed increased secretion compared to the mammalian recombinant (*mVps45*) but functioned better than the dominant-negative mutant (*W230R*). Interestingly in this assay, the double mutant seems to show a closer phenotype to the pocket-fill mutant and shows lower levels of invertase secretion than the dominant-negative. This is not necessarily unexpected, since the role of *Vps45p* in protein sorting is likely to be pleiotropic.

#### 4.3. 7 Spot Plate Complementation

Yeast grown on media with higher than normal salt concentrations are sensitive to osmotic stress when they lack the ability to traffic CPY normally (Banta et al., 1988). In this study, normal growth media (SD -ura -met) was supplemented with an additional 1.5M concentration of potassium chloride. In order to test whether *mVps45* mutants can complement the function of *Vps45p*, yeast cells harbouring both yeast and mammalian genes were grown to mid-log phase in selective medium (SD -ura -met) and were spotted onto plates containing selective media supplemented with 1.5 M KCl. Wildtype SF-8389D (*9D $\alpha$* ) cells were transformed with empty vector and were shown to grow normally. Likewise, delete cells lacking the endogenous *Vps45p*, LCY008 (*9D $\alpha$  $\Delta$ 45*), were transformed with the yeast copy of *Vps45*, HA-*Vps45p*, and grew at a similar rate to the wildtype. The addition of the mammalian copy of *Vps45*, *mVps45*, in these delete cells was able to rescue the ability of the

yeast to grow on altered media and shows complementation of function. As expected, delete cells transformed with empty vector displayed an inability to cope with added salt and grew poorly in the face of such osmotic stress. As Figure 4.6 shows, the yeast pocket-fill mutant, L117R, transformed into these delete cells also showed an inability to grow in a hyperosmotic environment. As others have shown, the mutation of the hydrophobic pocket in these mutants causes Vps45p to lose binding ability and thus perturbs the function of vacuolar sorting (Carpp et al., 2006). Interestingly however, the mammalian version of this mutant, V107R, when transformed into delete cells, grows at a similar rate to wildtype.

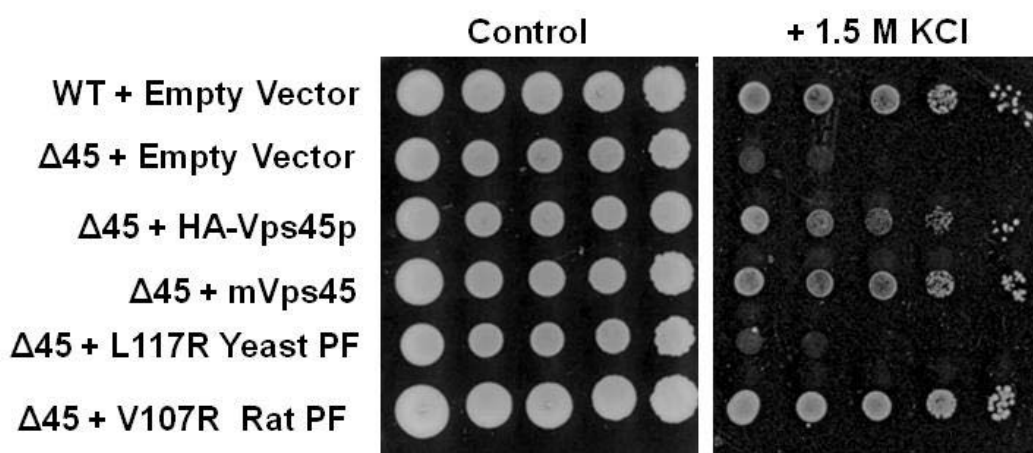


**Figure 4.6 Expression of mVps45 pocket-fill mutants complement the osmotic sensitivity phenotype of Vps45 mutants**

An empty vector was transformed into both wildtype and Vps45 delete cells as a control for growth activity. Delete cells were also transformed with endogenous Vps45, the mammalian construct mVps45p, the yeast pocket fill mutant L117R or the mammalian pocket-fill mutant, V107R to assess complementation. Cells were grown to mid-log phase in selective medium (SD -ura -met) and were then harvested and resuspended at an OD<sub>600</sub> of 10 in sterile water. Serial dilutions were performed generating cultures with an OD<sub>600</sub> of 10, 1, 0.1, 0.01 and 0.001. 5 μl of each culture was spotted onto an SD -ura -met plate containing 1.5 M KCl and grown for 3 days at 30°C.

In addition to the pocket-fill mutant, the dominant-negative mutant was also assayed for complementation using the spot plate method. In figure 4.7, the ability of the mammalian Vps45 recombinant, mVps45, to complement the function of the yeast HA-Vps45p was confirmed. The yeast dominant-negative, W244R, shows loss of function in high salt conditions. However, the mammalian dominant-negative grows well in hyperosmotic conditions.

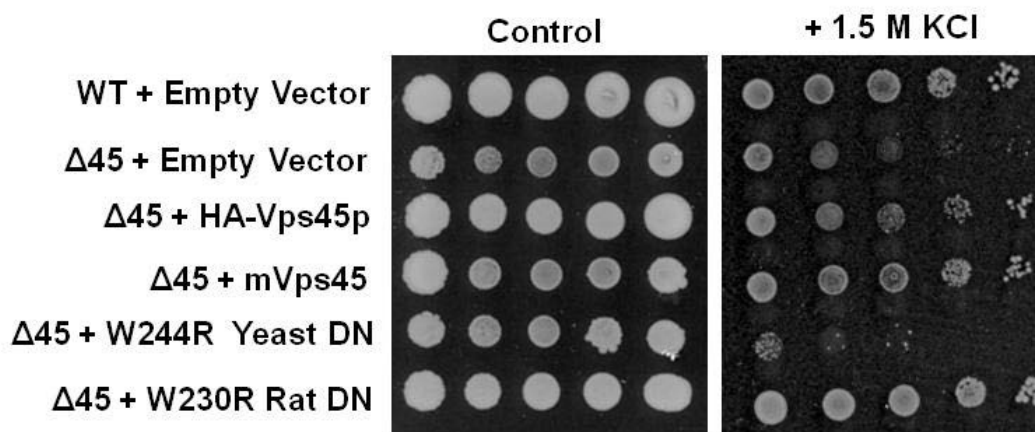


**Figure 4.7 Expression of mVps45 dominant-negative mutants complement the osmotic sensitivity phenotype of Vps45 mutants**

An empty vector was transformed into both wildtype and Vps45 delete cells as a control for growth activity. Delete cells were also transformed with endogenous Vps45, the mammalian construct mVps45p, the yeast dominant-negative mutant W244R or the mammalian dominant-negative mutant, W230R to assess complementation. Cells were grown to mid-log phase in selective medium (SD -ura -met) and were then harvested and resuspended at an OD<sub>600</sub> of 10 in sterile water. Serial dilutions were performed generating cultures with an OD<sub>600</sub> of 10, 1, 0.1, 0.01 and 0.001. 5 μl of each culture was spotted onto an SD -ura -met plate containing 1.5 M KCl and grown for 3 days at 30°C.

A double mutant was also assayed on spot plates and as figure 4.8 shows, the yeast double mutant again loses function when faced with additional salt while the mammalian double mutant grows well on hyperosmotic media.

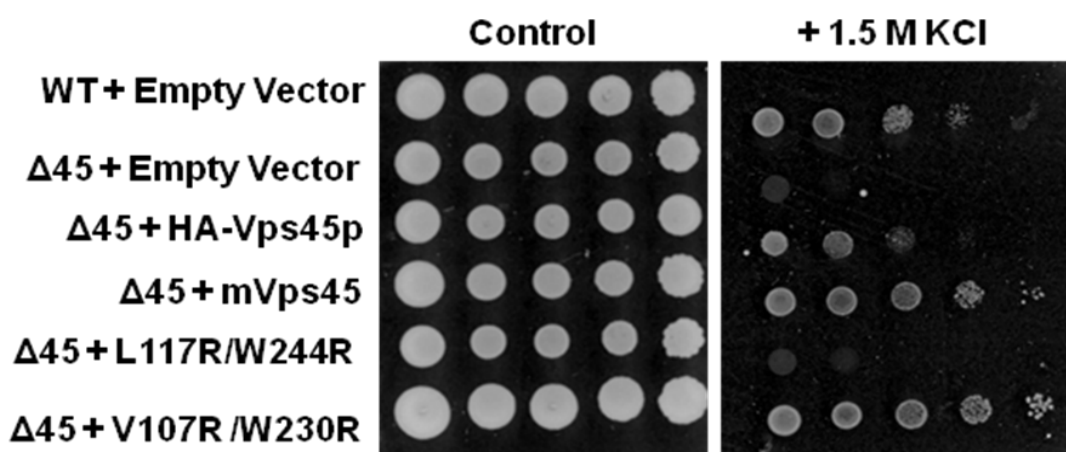


**Figure 4.8 Expression of mVps45 double mutants complement the osmotic sensitivity phenotype of Vps45 mutants**

An empty vector was transformed into both wildtype and Vps45 delete cells as a control for growth activity. Delete cells were also transformed with endogenous Vps45, the mammalian construct mVps45p, the yeast double mutant L117R/W244R or the mammalian double mutant, V107R/W230R to assess complementation. Cells were grown to mid-log phase in selective medium (SD -ura -met) and were then harvested and resuspended at an OD<sub>600</sub> of 10 in sterile water. Serial dilutions were performed generating cultures with an OD<sub>600</sub> of 10, 1, 0.1, 0.01 and

0.001. 5  $\mu$ l of each culture was spotted onto an SD -ura -met plate containing 1.5 M KCl and grown for 3 days at 30°C.

These results indicate that under hyperosmotic conditions, the mammalian Vps45 (mVps45) complements the function of yeast Vps45 (Vps45p). The mammalian mutants (V107R, W230R and double) however, do not show a similarity in behaviour and grow well on media supplemented with 1.5 M KCl. This lack of complementation can be explained in several ways. Firstly, it is thought that Vps45 acts in different steps in endocytosis and the complementation by mVps45 may not be identical in the pathway that is assayed in this experiment. Also, the residues chosen for mutation in the mammalian mutants were based on sequence homology to the yeast Vps45 and it may be that different or additional residues need to be replaced in order to show proper complement using this assay.

Similarly, temperature sensitivity was assayed using this experimental method. As Figure 4.9 shows, the mammalian Vps45 complements the phenotype of the yeast Vps45 at a non-permissive temperature. These results demonstrate the ability of mVps45 to complement for the loss of Vps45p by correcting the trafficking defects displayed in  $\Delta$ 45 mutant cells.

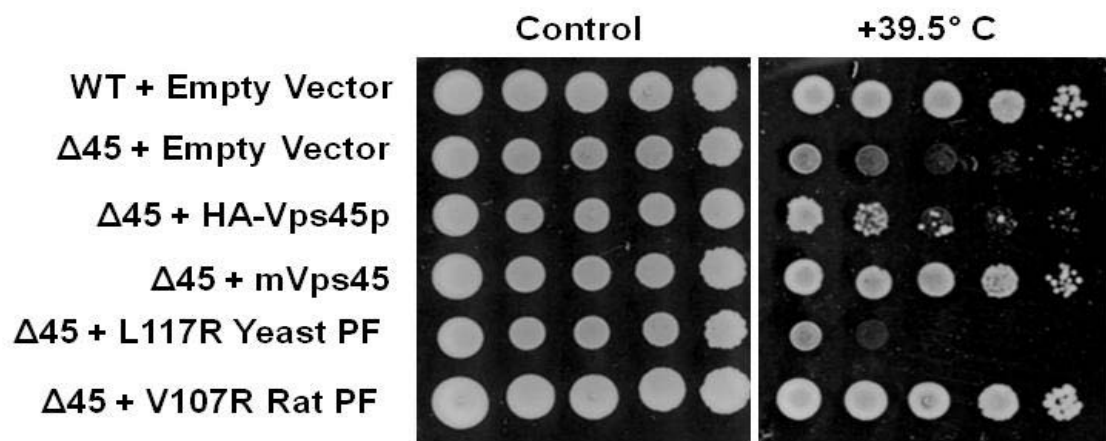


**Figure 4.9 Expression of mVps45 pocket-fill mutants complement the temperature sensitivity phenotype of Vps45 mutants**

An empty vector was transformed into both wildtype and Vps45 delete cells as a control for growth activity. Delete cells were also transformed with endogenous Vps45, the mammalian construct mVps45p, the yeast pocket fill mutant L117R or the mammalian pocket-fill mutant, V107R to assess complementation based on the fact that Vps45 has the ability to grow temperature sensitive mutants. Cells were grown to mid-log phase in selective medium (SD -ura -met) and were then harvested and resuspended at an OD<sub>600</sub> of 10 in sterile water. Serial dilutions were performed generating cultures with an OD<sub>600</sub> of 10, 1, 0.1, 0.01 and 0.001. 5  $\mu$ l of each culture was spotted onto an SD -ura -met plate and grown for 3 days at 39.5°C.

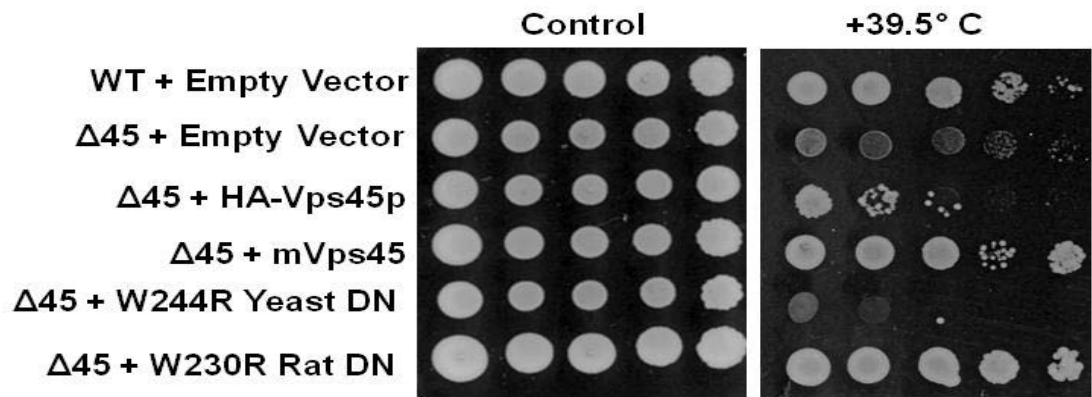


**Figure 4.10 Expression of mVps45 dominant-negative mutants complement the temperature sensitivity phenotype of Vps45 mutants**

An empty vector was transformed into both wildtype and Vps45 delete cells as a control for growth activity. Delete cells were also transformed with endogenous Vps45, the mammalian construct mVps45p, the yeast dominant-negative mutant W244R or the mammalian pocket-fill mutant, W230R to assess complementation. Cells were grown to mid-log phase in selective medium (SD -ura -met) and were then harvested and resuspended at an  $OD_{600}$  of 10 in sterile water. Serial dilutions were performed generating cultures with an  $OD_{600}$  of 10, 1, 0.1, 0.01 and 0.001. 5  $\mu$ l of each culture was spotted onto an SD -ura -met plate and grown for 3 days at 39.5°C.

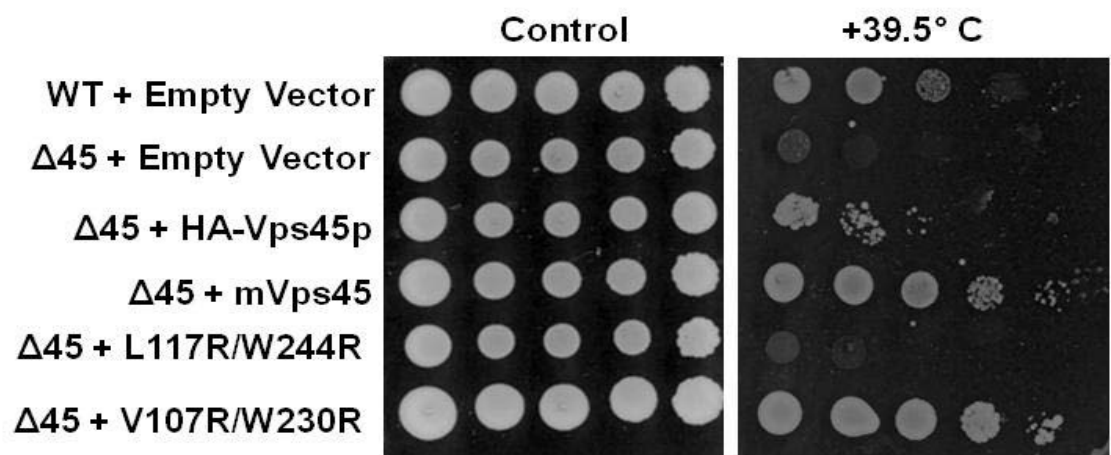


**Figure 4.11 Expression of mVps45 double mutants complement the temperature sensitivity phenotype of Vps45 mutants**

An empty vector was transformed into both wildtype and Vps45 delete cells as a control for growth activity. Delete cells were also transformed with endogenous Vps45, the mammalian construct mVps45p, the yeast double mutant L117R/W244R or the mammalian double mutant, V107R/W230R to assess complementation. Cells were grown to mid-log phase in selective medium (SD -ura -met) and were then harvested and resuspended at an  $OD_{600}$  of 10 in sterile water. Serial dilutions were performed generating cultures with an  $OD_{600}$  of 10, 1, 0.1, 0.01 and 0.001. 5  $\mu$ l of each culture was spotted onto an SD -ura -met plate and grown for 3 days at 39.5°C.

Expression of the dominant-negative and double mutants at non-permissive temperatures exhibited the same phenotype as the pocket-fill mutant. As figures 4.10 and 4.11 clearly illustrate, mVps45 is able to complement for the function of Vps45p. The mammalian mutants however, do not match the phenotype of the yeast mutants and this mismatch in complementation can be explained by possibly altering the residues mutated, but even this may not remedy the differences in function as it is not a given that mammalian and yeast mutants will work in exactly the same way in all assays.

#### 4.3.8 Expression of Tlg2p in mVps45 Mutants

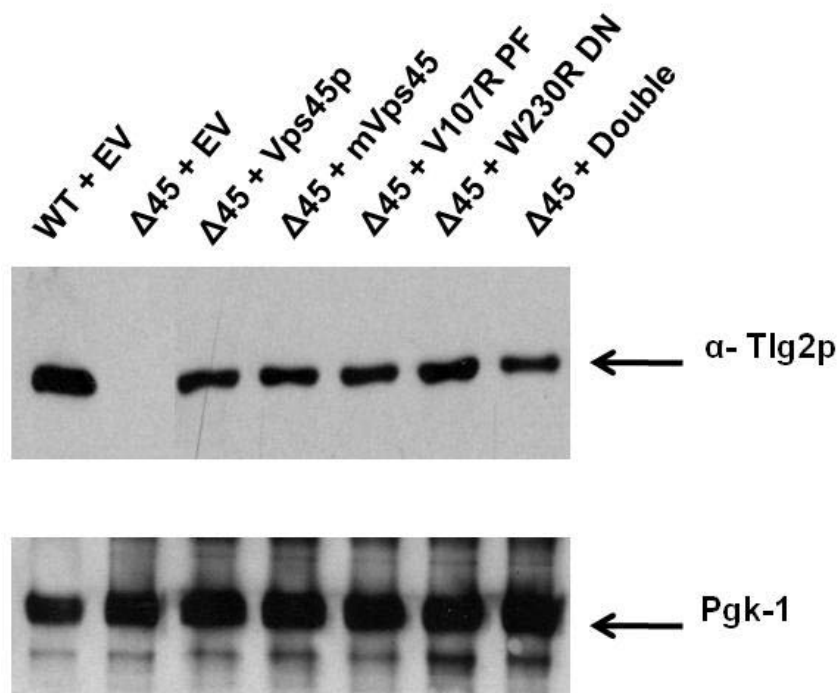


**Figure 4.12 Expression of mammalian Vps45 stabilises cellular levels of Tlg2p, the yeast homologue of Syntaxin 16**

Cell lysates were prepared from wild-type yeast (SF838-9D $\alpha$ ) harbouring empty vector YEpURA3 (Lane 1) and a congenic  $\Delta$ vps45 yeast strain (LCY008-9D $\alpha$  $\Delta$ 45) harbouring empty vector YEpURA3 (Lane 2), or producing an HA-tagged version of yeast Vps45p (Vps45-HA) (Lane 3), an HA-tagged version of the mammalian homologue of Vps45 (mVps45-HA) (Lane 4), a putative 'pocket-filled' mutant of mVps45-HA (mVps45-HA-V107R) (Lane 5), a putative 'dominant-negative' mutant of mVps45-HA (mVps45-HA-W230R) (lane 6) and a version of mVps45-HA containing both 'pocket-filled' and 'dominant-negative' mutations (mVps45-HA-V107R/W230R) (Lane 7). Proteins within the cell lysates were separated using SDS-PAGE before being subjected to immunoblot analysis using antibodies specific for Tlg2p and Pgk1p. Pgk1p was used as a loading control.

Mutation of residues within the hydrophobic pocket of Vps45 disrupts the interaction of this SM protein with its cognate syntaxin and results in a decrease in Tlg2p cellular levels to ~15 % of wild-type levels (Carpp et al., 2007).

In order to assess functional complementation of mammalian Vps45p (mVps45) in yeast lacking *VPS45* and functionally characterise putative 'pocket-filled' and 'dominant negative' versions of mVps45, yeast cells were transformed with mVps45 mutant constructs and lysates prepared for immunoblot analysis and probed for the presence of Tlg2p (Figure 4.12). Pgc1p (phosphoglycerate kinase) was used as a loading control. In wild-type yeast cells transformed with an empty vector (lane 1, Figure 4.12), Tlg2p is stable and runs at approximately 49 kDa. In  $\Delta vps45$  yeast transformed with empty vector, Tlg2p is rapidly degraded and is not detectable (lane 2). Expression of an HA-tagged version of yeast Vps45p in  $\Delta vps45$  yeast stabilises Tlg2p cellular levels (lane 3), although not to the levels seen in wild-type yeast. Expression of an HA-tagged version of mVps45 in  $\Delta vps45$  yeast stabilises Tlg2p cellular levels (lane 4) to a similar extent as the yeast HA-Vps45p construct, indicating that the mammalian version of Vps45 can protect Tlg2p from degradation and suggests a conserved mode of interaction. In yeast, a Vps45p pocket-filled mutant (Vps45p-L117R) which causes a disruption of the hydrophobic residues that form a pocket on the outer-face of the protein, is unable to interact with the N-terminal peptide of Tlg2p (Carpp et al., 2006) and consequently has greatly reduced cellular levels of Tlg2p compared to the cells containing wild-type Vps45p. In contrast, the mVps45 'pocket-filled' mutant (mVps45-V107R) which was designed to mimic the yeast mutation appears to bind and stabilise Tlg2p to a similar level as the wild-type mVps45p and yeast Vps45p (lane 5). This suggests that the mutation of residue V107 to R107 may not be enough to disrupt the hydrophobic pocket of mVps45 and does not abrogate the binding interaction between mVps45p and Tlg2p. In yeast, a dominant negative version of Vps45p (Vps45-W244R) can bind and stabilise Tlg2p but cannot functionally complement trafficking defects of  $\Delta vps45$  yeast (Carpp et al., 2007). Expression of a putative dominant-negative version of mVps45p (mVps45-W230R) in  $\Delta vps45$  yeast stabilises cellular levels of Tlg2p (lane 6) (to a greater extent than wild-type versions of mVps45 and yeast Vps45p). The double mutant of mVps45 expressed in  $\Delta vps45$  yeast (lane 7), interestingly

shows a lower Tlg2p binding stability than the other mutants. Anti-Pgk1p antiserum was used as a loading control.

#### 4.4 Discussion

The data in this chapter demonstrated that mVps45 can functionally complement the *VPS45* deletion. This conclusion is supported by data from the TCA precipitation experiment (Figure 4.4) which showed the complementation between mVps45 and Vps45p and also that the mammalian mutants did not traffic CPY and could not correct the trafficking defects displayed in yeast mutants. Likewise, data from the secreted invertase assay showed the ability of mVps45 to secrete reduced levels of invertase approximating the levels secreted by the wildtype.

The data reveal that the behaviour of the mVps45 mutants in some CPY assays (osmotic shock and temperature sensitivity) differ from the corresponding yeast *VPS45* mutants. There are several potential explanations for this. Firstly, it is important to note that mVPS45 functions in several stages of trafficking, and thus is likely to exert distinct phenotypes on each of these processes, reflecting different consequences for the different functional assays. It is clear from the CPY secretion data (and the osmotic shock and temperature sensitivity data) that mVps45 can functionally complement the *VPS45* deletion. The different behaviour of the mVps45 mutants from the corresponding yeast mutants therefore likely reflects differing affinities for interaction of mVps45 with Tlg2p compared to the yeast counterpart: there is no prior reason to assume that these affinities will be the same, and so the different data between the yeast and mammalian mutants probably reflects this. Future work will involve biochemical measurement of the interactions and affinities of mVps45 (and its mutants) to Tlg2p (and Sx16).

Also, since the Tlg2p open/closed transition may be controlled by Vps45p, it is not a given that each of the mVps45 species (wildtype or mutants) will mediate this transition in exactly the same manner.

It is, however, important to note that in all of the assays shown in this chapter, mVps45 complements for the functional loss of Vps45p, and that thus allowed us to rationally design mutants of mVps45 to study the role of this

protein in adipocytes. The fact that the mammalian mutants have shown complement in the TCA precipitation assay by failing to traffic CPY properly corresponds to what Carpp et al. have shown in yeast mutants (Carpp et al., 2007).

Future experiments will focus on determining whether these mutants can bind Tlg2p in a similar manner to yeast mutants. In the event that this data can be obtained, it will then be reasonable to generate these mVps45 constructs in an adenovirus vector to allow gene delivery into differentiated adipocytes and examine the consequences for glucose transport (see Chapter 5).

**Chapter 5: Generation of mVPS45 Knockdown and  
Expression of Intracellular Factors in  
3T3L1 Adipocytes**

## Chapter 5: Generation of mVPS45 Knockdown and Expression of Intracellular Factors in 3T3L1 Adipocytes

### 5.1 Introduction

A key to determining the function of genes is the ability to target specific genes for knockout, such approaches provide the ability to determine whether a particular gene is essential and what functions are perturbed by its loss. Post-translational gene silencing by the process of RNA interference (RNAi) is now widely used to study the role(s) of a given gene product (Rossi, 2008). RNAi is activated by introducing a double-stranded (ds) RNA whose sequence is homologous to the target gene transcript. The exogenous RNA is digested into small interfering RNAs (siRNA) which bind a nuclease complex to an RNA-induced silencing complex (RISC). This RISC then targets the endogenous gene transcripts by base-pairing and cleaves the mRNA. This chapter employs small hairpin siRNA molecules (shRNA) to achieve knockdown of the mammalian Vps45 gene in adipocytes, and to examine the consequences of this knockdown on cellular function.

mVps45, a member of the Sec1 family, modulates assembly of SNARE complexes by competitively binding to the t-SNARE Syntaxin 16. It has been shown that loss of Sec1 in yeast blocks the fusion of transport vesicles with the plasma membrane (Tellam et al., 1997). Here, we will examine the role of mVps45 by studying the effects of depleting 3T3-L1 adipocytes of this SM protein and determine if there are any effects on glucose transport, the levels of SNAREs associated with GLUT4 sorting, (chiefly Syntaxins 16, 6 and 4) and the effect of depletion of mVps45 on Glut4 translocation.

It has been widely suggested that Syntaxin 16 functions to control the sorting of GLUT4 in the slow recycling pathway of adipocytes and acts in concert with Syntaxin 6 to regulate the intracellular trafficking of GLUT4 in adipocytes. How Syntaxin 16 is regulated has not been definitively determined, so understanding how this SNARE is regulated will further our understanding into

how GLUT4 traffic into the slow cycle is controlled. The most likely candidate is the cognate Sec/Munc (SM) protein for Syntaxin16, mVps45.

## 5.2 Aims

The aim of this chapter is to investigate how the depletion of mVps45 alters cellular function, proteins levels and transport. This study uses shRNA methodology as well as glucose transport assays to determine whether depletion of mVps45 alters the rate, sensitivity or extent of insulin stimulation as well as whether there is a reduction in total GLUT4 levels and a reduced ability of insulin to translocate GLUT4.

## 5.3 Results

### 5.3.1 Construction of shRNA targets

In order to generate a knockdown of mVps45 in 3T3-L1 adipocytes, shRNA targets were constructed and viral particles were generated from a packaging cell line. This virus was later used to infect the 3T3-L1 adipocytes leading to suppression of mVps45 expression (and the knockdown effect). This knockdown was achieved by using a pSIREN retroviral expression vector (See Appendix for plasmid map) which uses the cells' own RNA Polymerase III to transcribe a specifically designed shRNA using the human U6 promoter which provides a high level of expression in cells resulting in target gene suppression. The mechanism includes initiator and effector steps. In the initiator step, input dsRNA is digested into siRNAs (21-23 nucleotides in length) by the action of the enzyme Dicer (an RNase III family specific dsRNA ribonuclease) in an ATP-dependent manner yielding siRNA duplexes (19-21 bp). In the effector step, these siRNA duplexes bind to a nuclease complex and form RISC. RISC is activated by the ATP-dependent unwinding of the siRNA duplex. Active RISC then targets the native, homologous transcript by base pairing and cleaves the mRNA.

In mammalian cells, RNAi can be difficult because of non-specific gene silencing (McIntyre and Fanning, 2006). Also, use of nucleotides longer than 30 bp causes an anti-viral response (Chang et al., 2006). In this study, target sequences of 21-23 bp were synthesized using the coding region of the mVps45 gene. The full details of oligonucleotide selection are available in

Materials and Methods, however some considerations are important to emphasize. Sequences were chosen away from the start codon and UTRs so that any regulatory protein binding sites in these regions or translation initiation complexes would not interfere with the binding of RISC. The oligonucleotide was also checked for GC content, AT content (A and T residues at the end of the sense sequence increase knockdown efficiency), secondary structure and long base runs (both of which interfere with proper annealing). These sequences were cloned into the pSIREN retroviral vector (see Materials and Methods for details). This vector is self-inactivating (by deletion of the 3' LTR enhancer region) and designed to eliminate promoter interference from the upstream LTR in the integrated provirus. The CMV promoter in the 5' LTR produces sufficient viral titers in the HEK 293 based packaging cell line used (EcoPack2-293, which contain adenoviral E1A(1-4)). Virus containing conditioned media from these packing cells was then used to infect the target cell line (3T3-L1). These viral particles are replication incompetent (as they lack *gag*, *pol* and *env*) and are integrated systematically to ensure that replication-competent virus was not produced during recombination events during cell proliferation.

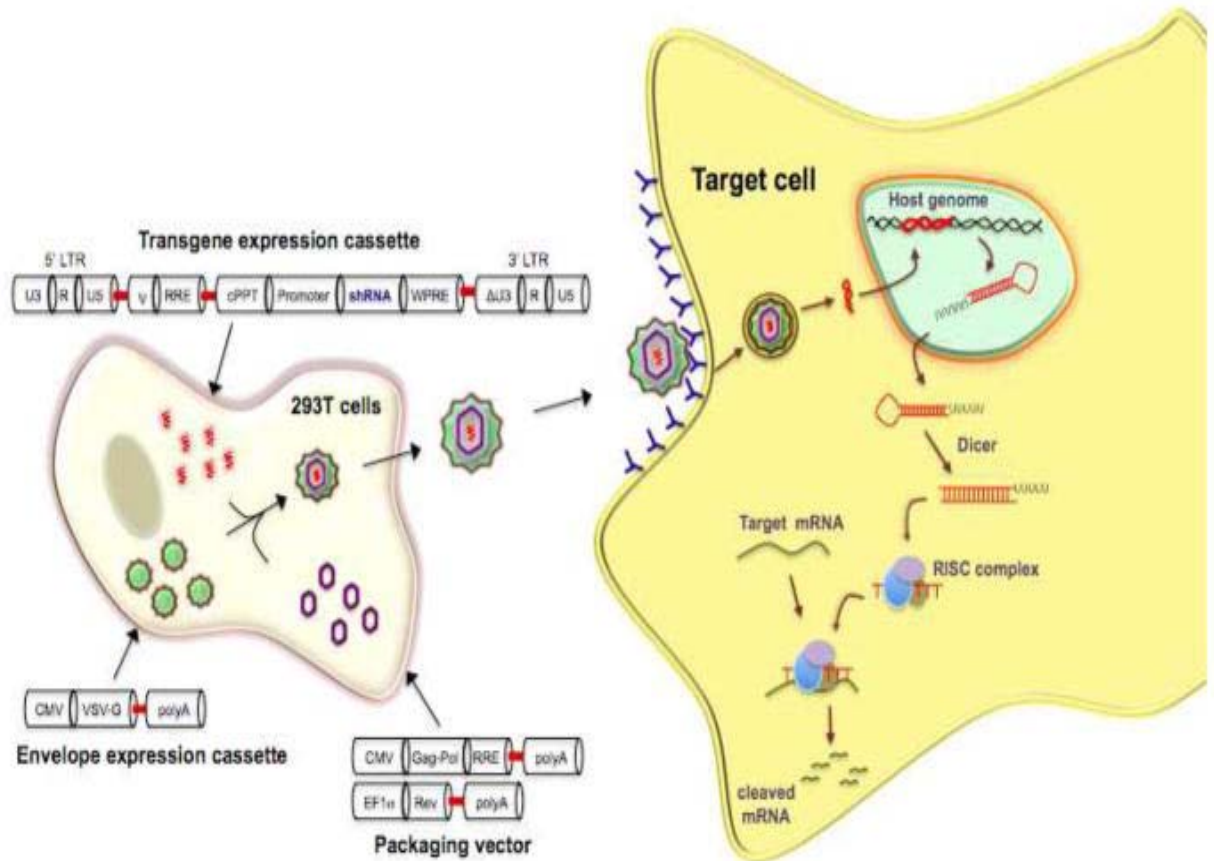


**Figure 5.1 Packaging of the shRNA virus using EcoPack2-293 cells**

DNA targets were silenced using a shRNA system of RNAi. Each sequence was cloned into the pSIREN RetroQ vector (vector information provided in Appendix) and transfected into EcoPack2-293 viral packaging cells. These cells then released viral particles into their conditioned media that were used to infect the target 3T3-L1 cells transiently. (Manjunath et al., 2009)

As Figure 5.1 illustrates, the retroviral construct is transfected into the viral packaging cell line which integrates the sequence, transcribing it and then synthesizing viral proteins. These proteins are packaged into viral particles which are then collected and used to infect the target cells. While this process is highly optimized, it was still necessary to validate it by the use of a GFP-tagged retroviral vector.

### 5.3.1.1 GFP control of transfection

After shRNA vectors had been constructed, a test for transfection efficiency in the viral packaging cell line EcoPack-2 293 cells was performed. This transfection was undertaken to ensure the effective delivery of the viral construct into the 293 cell line for efficient formation of viral particulate in which to infect the target cells. As described in Figure 5.1, the retroviral vector constitutively expressing *Zoanthus sp* green fluorescent protein (GFP)

was transfected using the Lipofectamine method (see Materials and Methods) into packaging cells where non-replicating infectious particles were generated. The ability of the retroviral vector to express GFP was extremely useful in proving that the retrovirus was delivered correctly to the packaging cell and that the construct was properly integrated into the cell for transcription to take place. Figure 5.2 shows that the cells incorporated the vector and that the vector was able to express GFP.

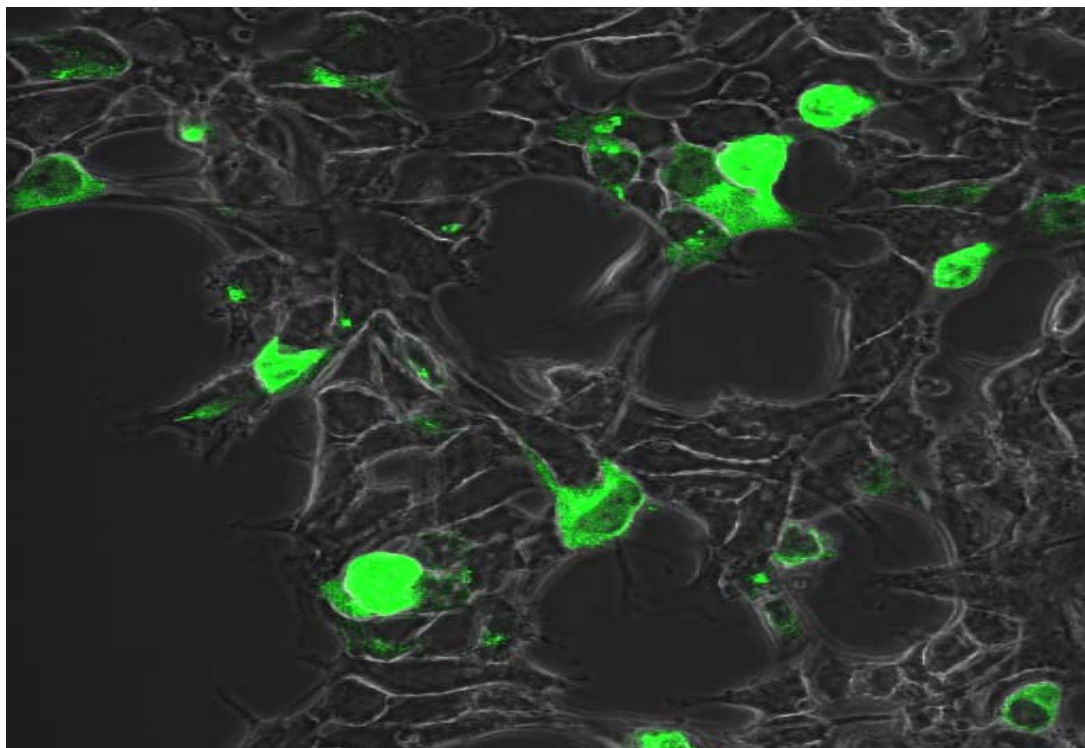


**Figure 5.2 Viral packaging cells are analysed for transfection efficiency using a GFP reporter plasmid**

pSIREN-RetroQ-Zs Green vector was used to assess transfection efficiency in EcoPack2- 293 cells. This vector constitutively expresses *Zoanthus* sp. green fluorescent protein and shows the efficient delivery of the construct by examination under a fluorescent microscope. In this figure, shRNA delivering silencing of mVps45 was prepared as described in Materials and Methods using the Zs Green vector and transfected into the packaging cell line. The fluorescence emitted from the GFP tag is shown to be largely in the perinuclear region of these fibroblasts indicating the successful incorporation of the silencing vector.

### 5.3.2 Immunoblots of mVps45 knockdown

In order to knockdown mVps45, 3T3-L1 fibroblasts were infected with virus and later differentiated using the standard method (see Materials and Methods for description of the differentiation process). Whole cell lysates from these cells were prepared and subjected to immunoblot analysis. The results of a typical experiment are shown in Figure 5.3, with quantification of several experiments of this type shown in Figure 5.3 bottom panel.

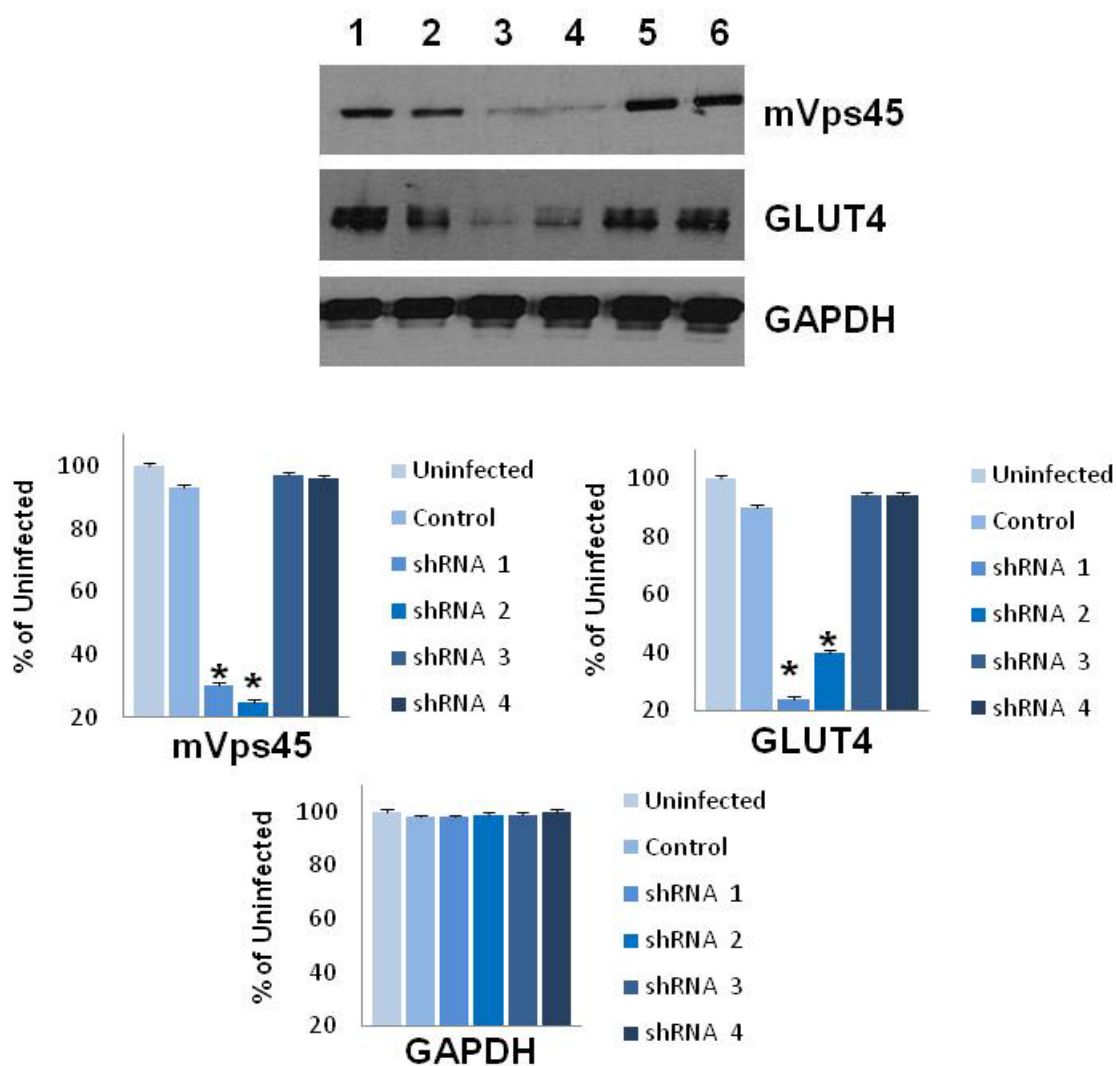


### Figure 5.3 mVps45 is knocked down in 3T3-L1 Adipocytes

3T3-L1 fibroblasts were grown to 70% confluence and infected with shRNA virus. These targets were selected for using puromycin and later differentiated as described previously. Whole cell lysates were then prepared and immunoblotted for mVps45 and GLUT4. Lane 1: No Virus, Lane 2: Luciferase Control, Lane 3: shRNA Target 1, Lane 4: shRNA Target 2, Lane 5: shRNA Target 3, Lane 6: shRNA Target 4. GAPDH was used as a loading control. Immunoblots above show the results of one representative experiment. Three separate experiments were performed and densitometric analysis was performed on the results, here shown as the mean of three experiments +/- SEM. \* $p < 0.05$  by one-way ANOVA compared to uninfected.

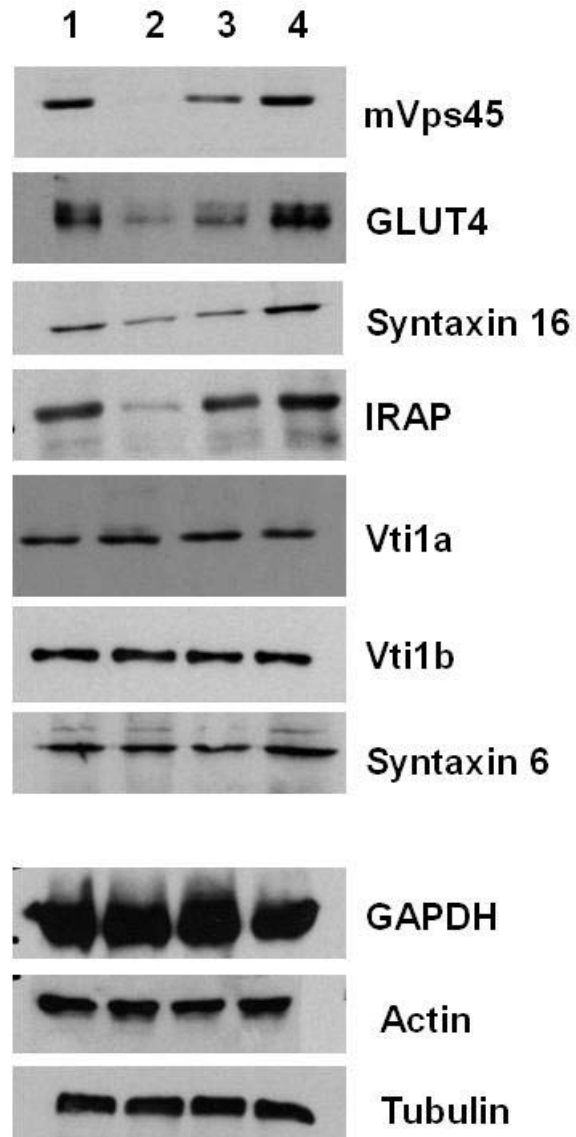
Because not all sequences in a given mRNA are equally sensitive to siRNA, it was necessary to choose four potential target sequences along rat Vps45 mRNA. Figure 5.3 shows these four targets compared with control virus and uninfected 3T3-L1 adipocytes. In the upper panel, immunoblots for mVps45 indicated that shRNA targets 1 and 2 were most effective in suppressing mVps45 expression. These two targets were also best at reducing the levels of GLUT4 protein. Quantification of these blots by densitometry in the bottom panel shows that mVps45 and GLUT4 are reduced by 80% by these

targets. In comparison, targets 3 and 4, entailing sequences that were farther along the mRNA than either target 1 or 2, fail to have much of an effect on silencing mVps45. In fact, shRNA targets 3 and 4 produced similar results to control virus or uninfected cells.

### **5.3.3 Immunoblots of the intracellular environment**

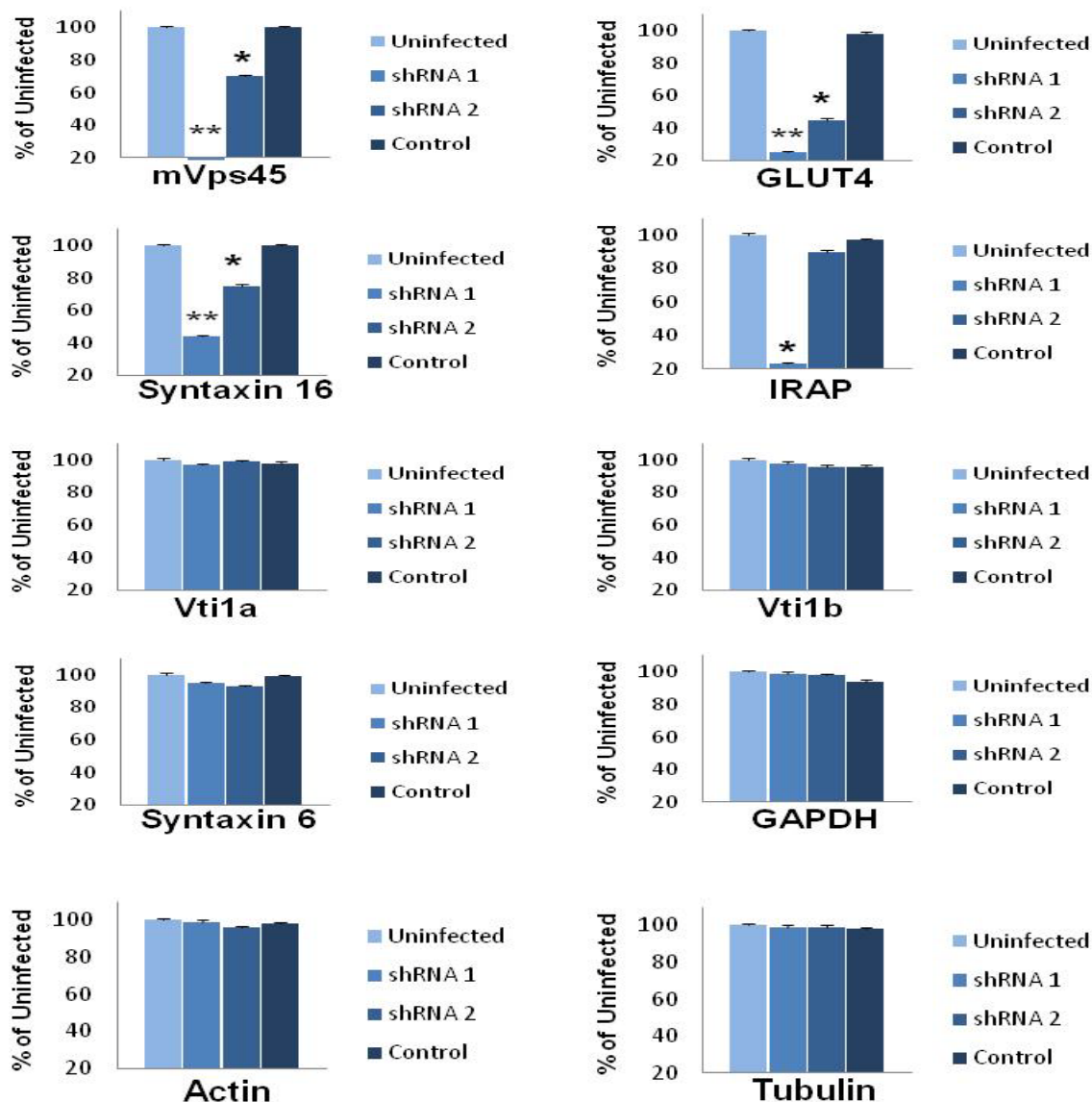
Initial immunoblots showed that shRNA targets 1 and 2 were best at reducing protein expression levels in 3T3-L1 adipocytes. Using this knowledge, lysates from 3T3-L1 cells infected with control virus or either shRNA target 1 or 2 virus were prepared and immunoblotted using antibodies specific for proteins known to act in GLUT4 translocation. As shown in Figure 5.4a, shRNA 1 reduces mVps45 and GLUT4 protein levels most effectively compared to control and uninfected lysates. shRNA2 also shows a reduction in protein expression, however this effect is less dramatic than in Target 1.

Densitometric analysis in Figure 5.4b shows that while shRNA 1 decreases the levels of mVps45 more than 90% and GLUT4 around 80%, shRNA2 only decreases expression approximately 50-60% for these proteins.



**Figure 5.4a The effect of mVps45 depletion on intracellular proteins**

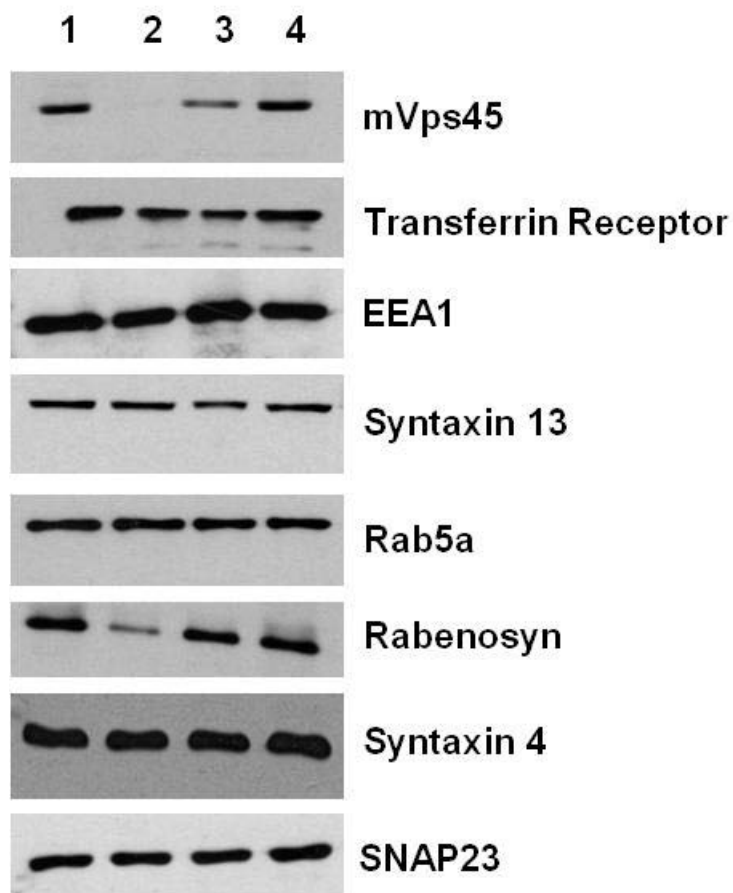
3T3-L1 fibroblasts were grown to confluence, infected with viral targets and differentiated as described in Materials and Methods. Lane 1: Uninfected cells, Lane 2: shRNA Target 1, Lane 3: shRNA Target 2, Lane 4: Luciferase control. This figure shows the effect of depletion on endosomal to TGN proteins involved in the GLUT4 sorting pathway. GAPDH, Actin and Tubulin were used as loading controls.



**Figure 5.4b Densitometric analysis of the effect of mVps45 depletion on intracellular Proteins**

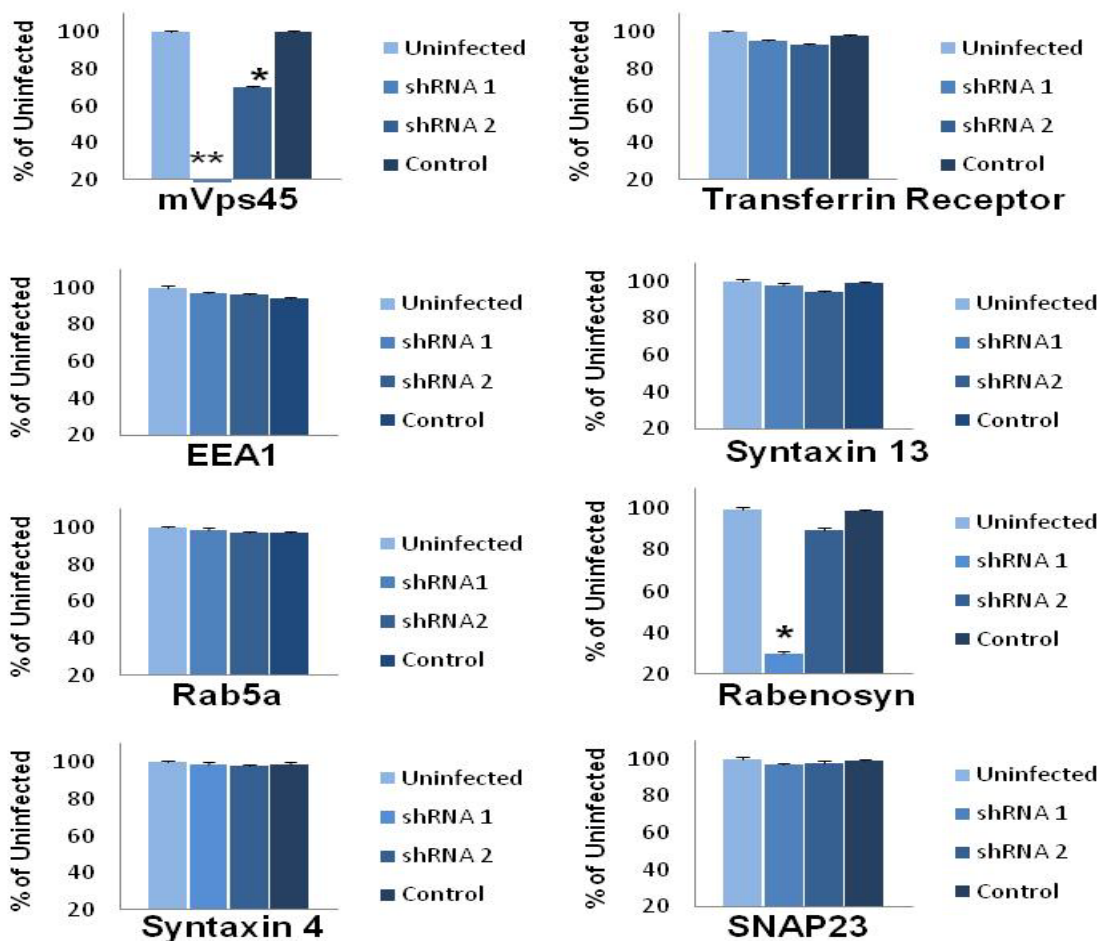
Three separate preparations of 3T3-L1 lysates from uninfected cells, cells depleted of mVps45 using shRNA1 or shRNA2, and control infected cells were immunoblotted using the antibodies indicated in Figure 5.4a. Those results were subjected to densitometric analysis using Image J software and are shown above as the mean of three experiments +/- SEM. \*= $p < 0.05$ , \*\*= $p < 0.02$  by one-way ANOVA compared to Uninfected.

Similarly, Syntaxin 16 is reduced by ~60% by shRNA 1 while shRNA 2 reduced protein levels by only approximately 30%. Interestingly, shRNA 1 is able to reduce IRAP protein levels by 75% while shRNA 2 reduced levels by only 15%. There was no change in protein expression levels in Syntaxin 6, Vti1a or Vti1b.



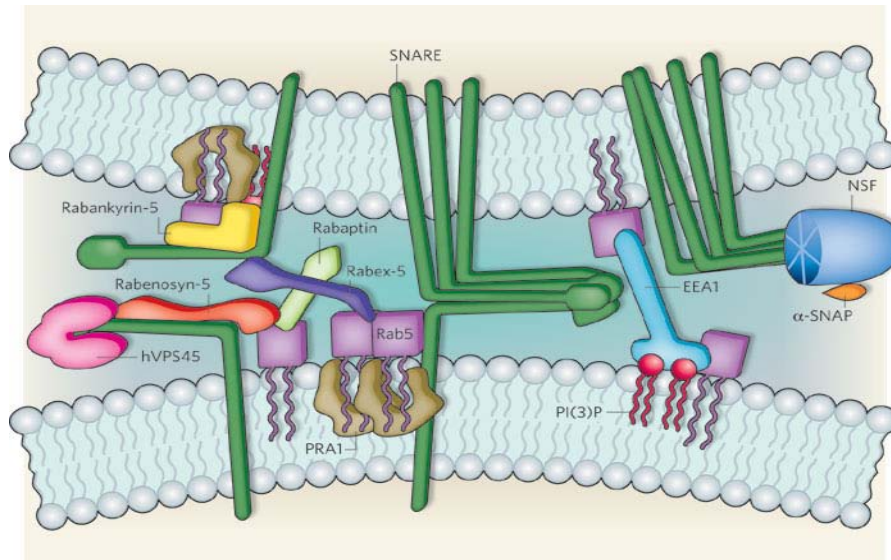
**Figure 5.5a The effect of mVps45 depletion on proteins involved in membrane fusion**  
 3T3-L1 fibroblasts were grown to confluence, infected with viral targets and differentiated as described in Materials and Methods. Lane 1: Uninfected cells, Lane 2: shRNA Target 1, Lane 3: shRNA Target 2, Lane 4: Luciferase control. This figure shows the effects of mVps45 depletion on proteins regulating membrane fusion from one representative experiment.

Figure 5.5 shows the effect of mVps45 knockdown on other proteins involved in GLUT4 sorting and membrane fusion. Figure 5.5a shows immunoblot analysis of cell lysate knocked down for mVps45. Densitometric analysis of protein levels in Figure 5.5b shows that only Rabenosyn in shRNA 1 is decreased. Figure 5.6 shows the action of Rabenosyn and its interaction with Rab5 and EEA1. It has been shown that Vps45 interacts with Rabenosyn-5 and others have reported that human Vps45 depletion causes a reduction in Rabenosyn-5 expression (Rahajeng et al., 2009).



**Figure 5.5b Densitometric Analysis of the effect of mVps45 depletion on proteins involved in membrane fusion**

Three separate preparations of 3T3-L1 lysates from uninfected cells, cells depleted of mVps45 using shRNA1 or shRNA2, and control infected cells were immunoblotted using the antibodies indicated in Figure 5.5a. Those results were subjected to densitometric analysis using Image J software and are shown above as the mean of three experiments  $\pm$  SEM.  $*=p<0.05$  by one-way ANOVA compared to wildtype.



**Figure 5.6 Proteins involved in membrane fusion**

Rab5 and Rabenosyn as well as EEA1 are involved in membrane fusion. (Collins and Zimmerberg, 2009.)

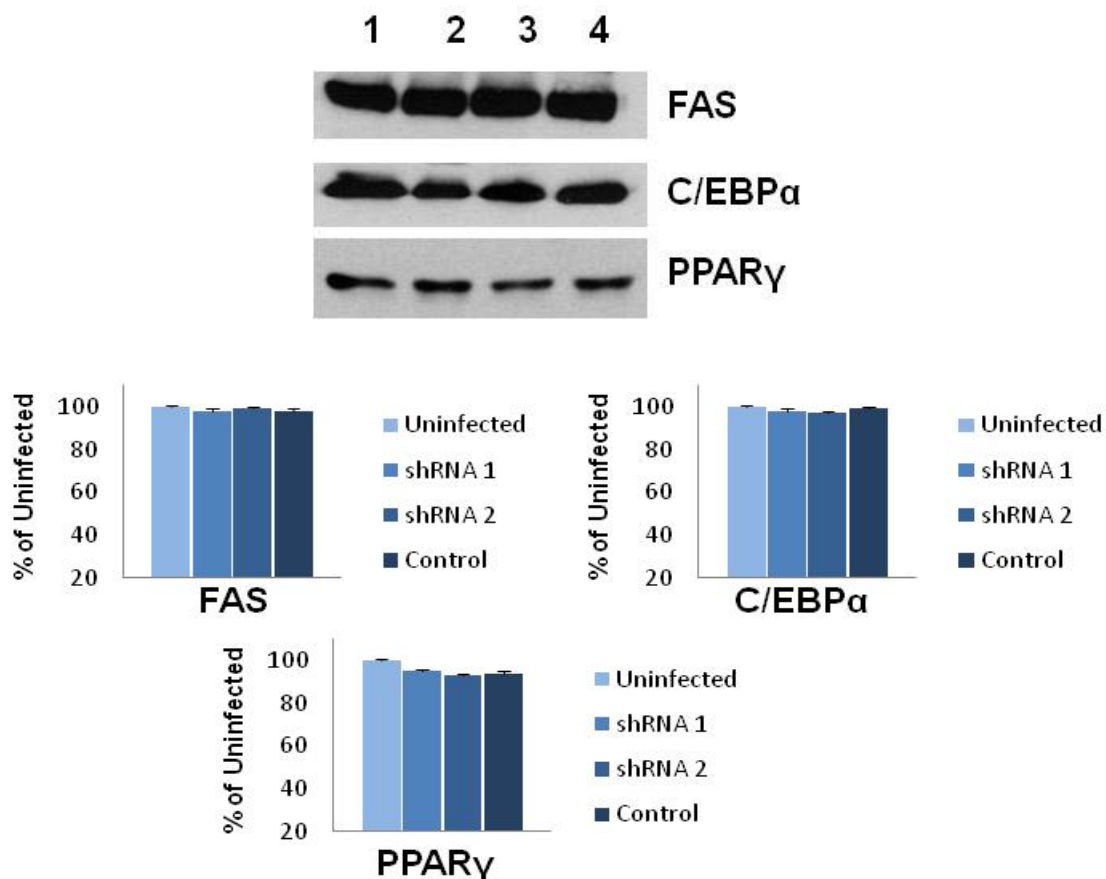


**Figure 5.7 The effect of mVps45 depletion on differentiation proteins**

3T3-L1 fibroblasts were grown to confluence, infected with viral targets and differentiated as described in Materials and Methods. Lane 1: Uninfected cells, Lane 2: shRNA Target 1, Lane 3: shRNA Target 2, Lane 4: Luciferase control. This figure shows the effect of mVps45 depletion on proteins involved in the conversion of fibroblasts to adipocytes. These immunoblots represent the results of one representative experiment. The results from three separate experiments were subjected to densitometric analysis using Image J software and are shown above as the mean of three experiments  $\pm$  SEM. There were no statistically significant differences between lanes.

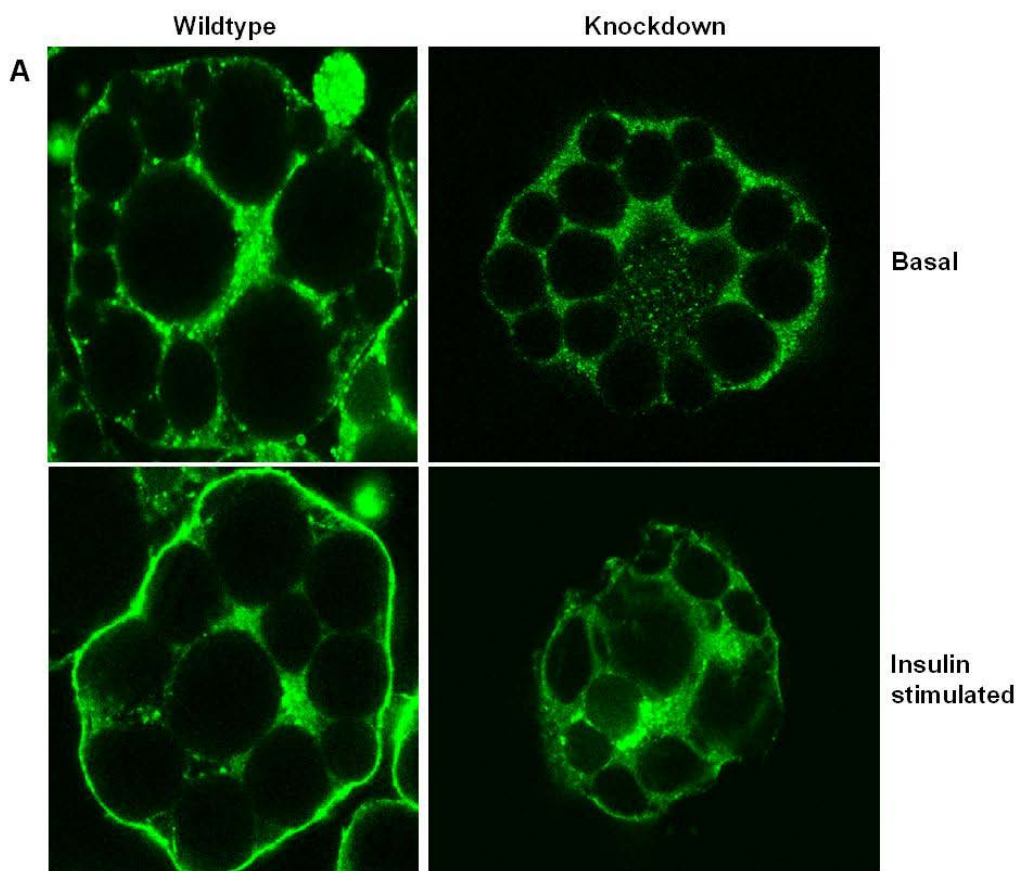
We used shRNA technology to look at whether depletion of mVps45 alters cellular levels of GLUT4 and other proteins involved in trafficking. The main reason to use this shRNA system as opposed to siRNA techniques is that this method is more uniform and knockdown is not as variable or as expensive. Another advantage of this system is that it can be used to infect fibroblasts which can be selected as clones expressing the shRNA which can then be differentiated into mature adipocytes. The mature adipocyte is difficult to transfect or electroporate because of its large fat vacuole and this method gets around this limitation.

In Figure 5.7, we assess proteins activated by adipocyte differentiation. Depletion of mVps45 does not affect the protein expression levels of FAS,

C/EBP $\alpha$  or PPAR $\gamma$ . These results indicate that mVps45 does not have a role in adipocyte differentiation, and provide good evidence that the 3T3-L1 adipocytes generated using this approach have differentiated well and are thus a suitable model for the analysis of GLUT4 trafficking.

### 5.3.4 Confocal Images of GLUT4 Translocation

Adipocytes are notoriously difficult to image because of their unique structural limitations with their large central triglyceride storage droplets and thin ring of cytoplasm. Using confocal microscopy optical sectioning allows the in situ localization of proteins and the changes in response to different stimuli to be seen. These experiments used single and double labelling to examine staining with a fluorescence microscope equipped with a confocal laser scanning system. Confocal imaging allows precise visualization of fluorescent signals within a narrow plane of focus (Malide, 2001).



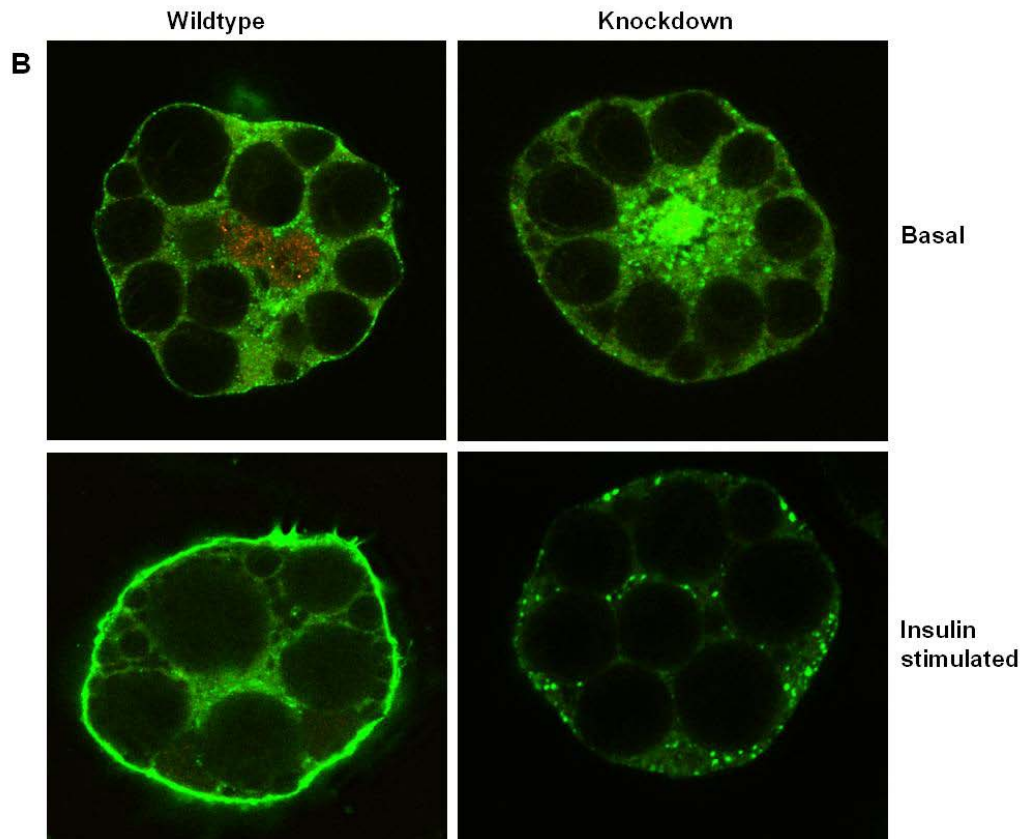


**Figure 5.8 GLUT4 is translocated to the plasma membrane in response to insulin-stimulation**

These images show that upon insulin stimulation, the amount of GLUT4 translocated to the surface of the cell in wildtype cells is markedly increased over basal in wildtype cells. A: 3T3-L1 adipocytes stably expressing HA-GLUT4-GFP were either left in the basal state and or stimulated with insulin. 63X Oil magnification. B: 3T3-L1 adipocytes stably expressing HA-GLUT4-GFP were either left in the basal state or insulin stimulated and were later stained for mVps45 (Red). 63X Oil magnification.

In these experiments, HA-GLUT4-GFP (details of which can be found in Muretta et al., 2008, but briefly contain an exofacial HA-tag and GFP on the C-terminus of GLUT4) cells were used to show GLUT4 translocation in response to insulin-stimulation in wildtype and mVps45 (knockdown) depleted cells. In the first set of images (Panel A, Figure 5.8) insulin-stimulation causes GLUT4 translocation to the plasma membrane in control cells. GLUT4 molecules are seen to leave centralized peri-nuclear GSVs and translocate to the PM in response to insulin-stimulation. On the right side of Panel A, cells depleted of mVps45 show that in response to insulin stimulation, this GLUT4 does not translocate to the PM. In insulin-stimulated knockdown cells, GLUT4 stays predominantly in the perinuclear region in GSVs. Although descriptive, these data clearly suggest that depletion of mVps45 has altered GLUT4 trafficking to an extent that insulin-responsiveness is lost. This is consistent

with our hypothesis that mVps45 may act to control GLUT4 sorting from cycle 1 into cycle 2 (i.e. into GSVs).

In panel B, these cells are co-stained with an antibody specific to mVps45. In wildtype basal cells, mVps45 can be seen to conglomerate in areas rich in GLUT4. However upon insulin stimulation, this centralized collection of mVps45 molecules disperses and appears to move with GLUT4 toward the PM (the intensity of the GLUT4 signal at the PM in the bottom left image occludes mVps45 staining, which can be seen faintly next to the bright green ring).

### 5.3.5 Glucose Transport Assays

Here, we set out to determine whether the maximal rate of glucose transport, the insulin sensitivity of glucose transport, or the rate of reversal of insulin-stimulated glucose transport were altered upon mVps45 knockdown.

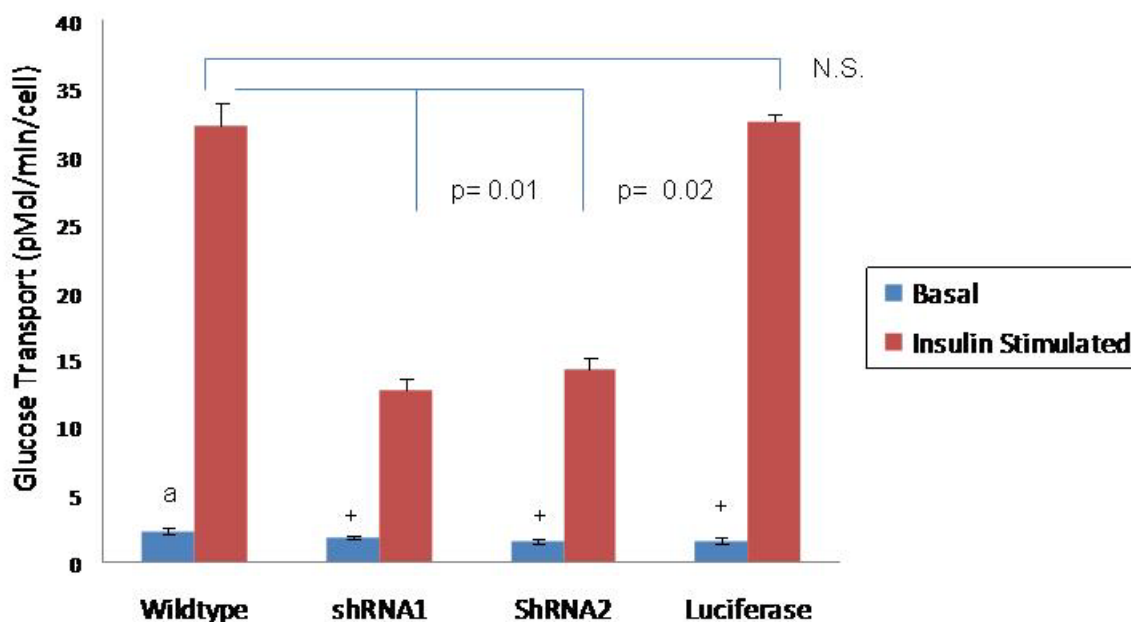


**Figure 5.9a Effect of mVps45 depletion by viral targeting on basal and insulin-stimulated deoxyglucose uptake in 3T3-L1 adipocytes.**

3T3-L1 adipocytes were grown under standard conditions (see Materials and Methods) in triplicate wells and transfected with either no virus (Wildtype), virus designed to knockdown mVps45, or virus designed to knockdown luciferase (as a control for viral infection: Luciferase). Four different viral constructs were designed to target mVps45 depletion and the most effective two are represented (shRNA1 and ShRNA2). Cells were then differentiated and treated with either no Insulin (Basal) or 1uM Insulin for 30 minutes (Insulin-stimulated). Glucose transport was then measured by the uptake of 2-Deoxy-D-Glucose for 5 minutes as described in *Materials and Methods*. Shown is the data averaged from three separate experiments. Data are represented as the mean fold increase relative to basal (wild-type) cells +/- SEM. += not significant to a by Students unpaired t-test.

In this assay, glucose uptake is measured using radioactive 2-deoxyglucose that cannot be metabolized by the cells. This label is phosphorylated but cannot be used by the cell and is trapped, making it a measure of unidirectional transport. The cells are washed in cold PBS and lysed to measure the amount of radioactive 2-deoxyglucose taken up by the cells incubated with (insulin-stimulated glucose uptake resulting from translocation of GLUT4) and without insulin (basal glucose uptake resulting from the GLUT1 transporter). These values are subtracted to give the true insulin-stimulated glucose uptake value.

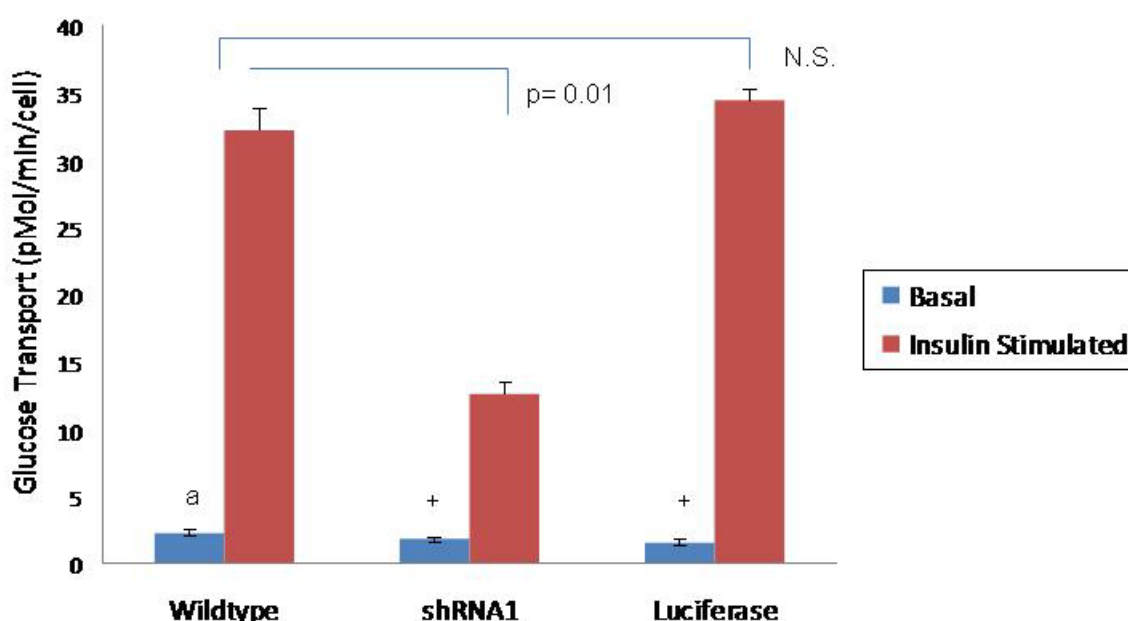


**Figure 5.9b Effect of mVps45 depletion by best viral construct on basal and insulin-stimulated deoxyglucose uptake in 3T3-L1 adipocytes.**

3T3-L1 adipocytes were grown under standard conditions (see Materials and Methods) in triplicate wells and transfected with either no virus (Wildtype), virus designed to knockdown mVps45 (shRNA1, the most effective viral construct), or virus designed to knockdown luciferase (as a control for viral infection: Luciferase). Cells were then differentiated and treated with either no Insulin (Basal) or 1  $\mu$ M Insulin for 30 minutes. Glucose transport was then measured by the uptake of 2-Deoxy-D-Glucose for 5 minutes as described in Materials and Methods. Shown is the data averaged from three separate experiments. Data are represented as the mean fold increase relative to basal (wild-type) cells  $\pm$  SEM. + = not significantly different to a by unpaired Students t-test.

Cytoscholasin B binds to glucose transporters and inhibits glucose transport. Subtracting the uptake value of Cytocholasin B removed non-specific transport from the equation.

Glucose transport assays were performed initially using both shRNA1 and 2 targets. 3T3-L1 adipocytes were left as wildtype cells or infected with either shRNA1, shRNA2 or Luciferase control virus.

The first glucose transport figure (Figure 5.9a) shows that insulin stimulates glucose uptake ~7-fold in wildtype. Control (Luciferase) cells also show a similar stimulation. When cells are depleted of mVps45 however, this effect is decreased to only approximately 3-fold. shRNA target 2 shows a slight increase in insulin-stimulated glucose uptake compared to shRNA1. In the beginning of the chapter, it was shown that shRNA1 is the more effective knockdown target for mVps45 depletion and this can explain the increase in uptake in shRNA2. shRNA1 is the more effective knockdown target and cells in these wells were depleted of more mVps45 and the effect on glucose uptake was more substantial than in cells infected with shRNA2. Cells infected with shRNA 1 show less than a 3-fold increase in insulin-stimulated glucose transport. It is important to note that basal rates of glucose transport were not significantly different between the groups studied.

Once shRNA 1 was established to be the best target for mVps45 depletion (as confirmed by immunoblot analysis, Section 5.1) and showed the most promising effect on glucose uptake (as shown in Figure 5.9a) glucose transport assays were confirmed by performing the same assay again this time only using shRNA 1 as the target for knocking down mVps45. As Figure 5.9b shows, 3T3-L1 adipocytes infected with shRNA 1 virus clearly demonstrate a decrease in insulin-stimulated glucose uptake when compared to wildtype and control (Luciferase) cells. While cells not depleted of mVps45 showed a more than 7-fold increase in glucose transport in response to insulin-stimulation, mVps45 depleted cells only showed a less than 3-fold increase.

We next analysed the dose-dependence of insulin in glucose transport. In this set of experiments, glucose transport assays were performed with varying concentrations of insulin.

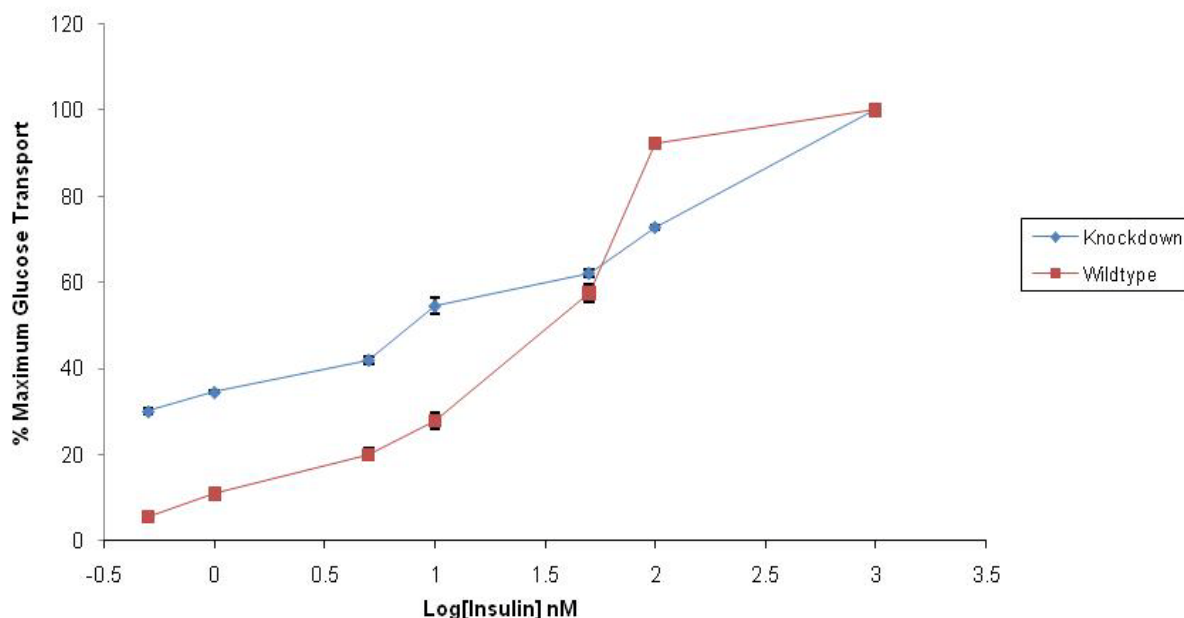


**Figure 5.10a Analysis of the maximum glucose transport in Wildtype and mVps45 depleted 3T3-L1 adipocytes.**

3T3-L1 adipocytes were grown under standard conditions (see Materials and Methods) in triplicate wells and transfected with either no virus (uninfected Wildtype), or virus designed to knockdown mVps45. Cells were then differentiated and treated with varying concentrations of Insulin for 30 minutes as indicated on the graph. Glucose transport was then measured by 2-Deoxy-D-Glucose uptake for 3 minutes as described in Materials and Methods. Shown is the data averaged from three separate experiments of this type. Data are expressed as the maximum percentage insulin-stimulated deoxyglucose uptake for each of four sets of cells. Note that the cells depleted of mVps45 exhibited a significant reduction in this value.

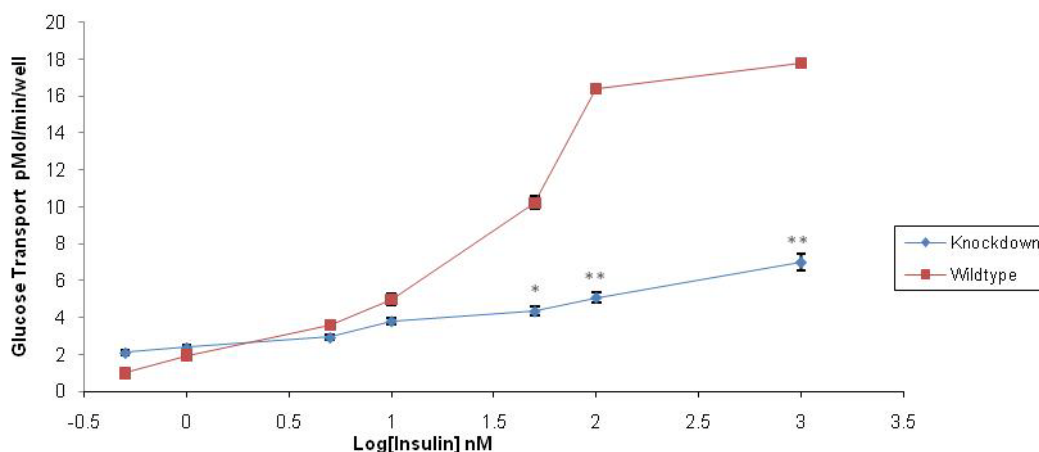


**Figure 5.10b Analysis of the maximal concentration-dependence of insulin-stimulated deoxyglucose uptake in Wildtype and mVps45 depleted 3T3-L1 adipocytes.**

3T3-L1 adipocytes were grown under standard conditions (see Materials and Methods) in triplicate wells and transfected with either no virus (uninfected Wildtype), or virus designed to knockdown mVps45. Cells were then differentiated and treated with varying concentrations of Insulin for 30 minutes as indicated on the graph. Glucose transport was then measured by 2-Deoxy-D-Glucose uptake for 3 minutes as described in Materials and Methods. Shown is the data averaged from three separate experiments of this type. Data are expressed as a percentage of the maximal insulin-stimulated deoxyglucose uptake rates for each of the two sets of cells. Note that the cells depleted of mVps45 exhibited a significant reduction in this

maximal value, see previous figure. \* $p = 0.05$  vs wildtype, \*\* $p < 0.01$  vs wildtype by unpaired Students t-test.

In these assays, mVps45 depleted cells (knockdown) show a more linear response to varying insulin concentration than wildtype. As shown in Figure 5.9, glucose transport in response to insulin-stimulation is decreased in knockdown cells compared to wildtype. It would appear that the half maximal concentration of insulin required to elicit a maximal response has increased upon mVps45 knockdown, but as the graph has not reached a clear plateau, this is difficult to ascribe with accuracy.

Next, glucose transport assays were performed to test the ability of cells to reverse insulin-stimulated glucose transport. Cells were stimulated with  $0.1 \mu\text{M}$  insulin for 30 min and reversed for various amounts of time before being assayed for glucose transport. Figure 5.11 shows that the rates of reversal in knockdown cells are rather complex. For example, the knockdown is more effective in reversing insulin-stimulated glucose transport than wildtype at early time points. For example, after 5 minutes of reversal the percent of maximal glucose transport has decreased only 10% in the wildtype compared to 25% in the knockdown. After 15 min the wildtype cells decreased their uptake 20% while knockdown cells decreased uptake by nearly 40%. This effect was temporary however as by 30 min both cell types had decreased uptake by over 40% and then appeared to decline in tandem.

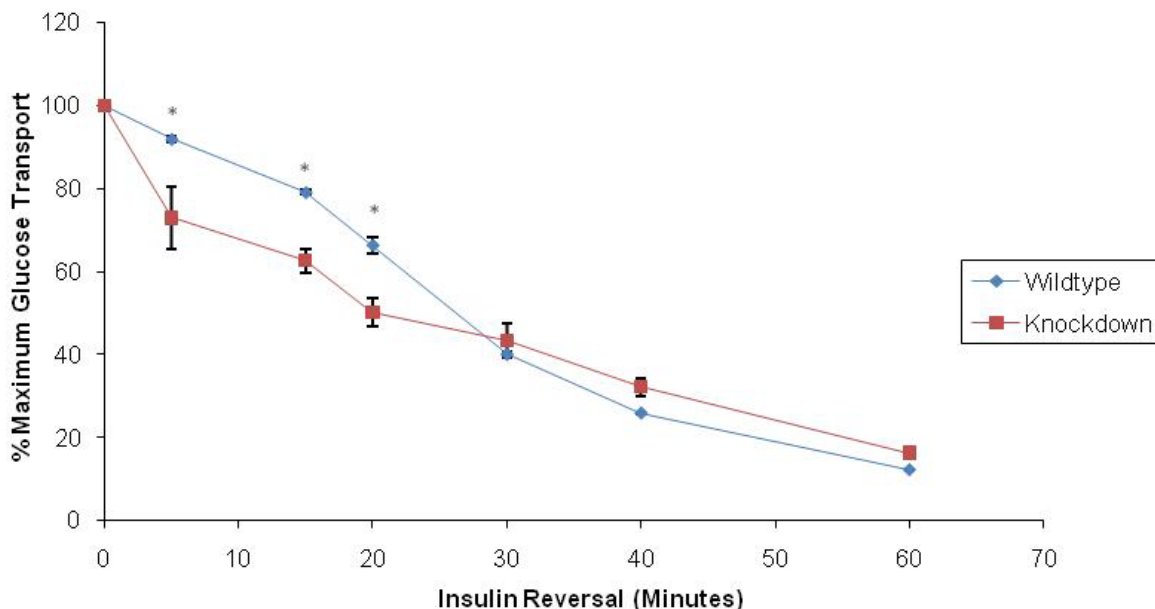


**Figure 5.11a Time course of the maximal percentage of the reversal of insulin-stimulated 2-Deoxy-D-Glucose Transport in control and mVps45 knockdown 3T3-L1 adipocytes**

3T3-L1 adipocytes were grown under standard conditions (see Materials and Methods) in triplicate wells and transfected with either no virus (uninfected Wildtype), or Knockdown virus for mVps45. Cells were then differentiated and treated with 100nM of Insulin for 30 minutes. Insulin reversal was initiated by washing in low pH buffer (see Materials and Methods) and deoxyglucose transport was assayed at different times following reversal (see graph) as described in Materials and Methods. Shown is the data averaged from three separate experiments of this type. Data are expressed as a percentage of maximal insulin-stimulated deoxyglucose uptake rates for each of the two sets of cells. Note that the cells depleted of mVps45 exhibited a significant reduction in this maximal value, see previous figure. \*  $p < 0.05$  vs knockdown in the corresponding points by unpaired Students t-test.

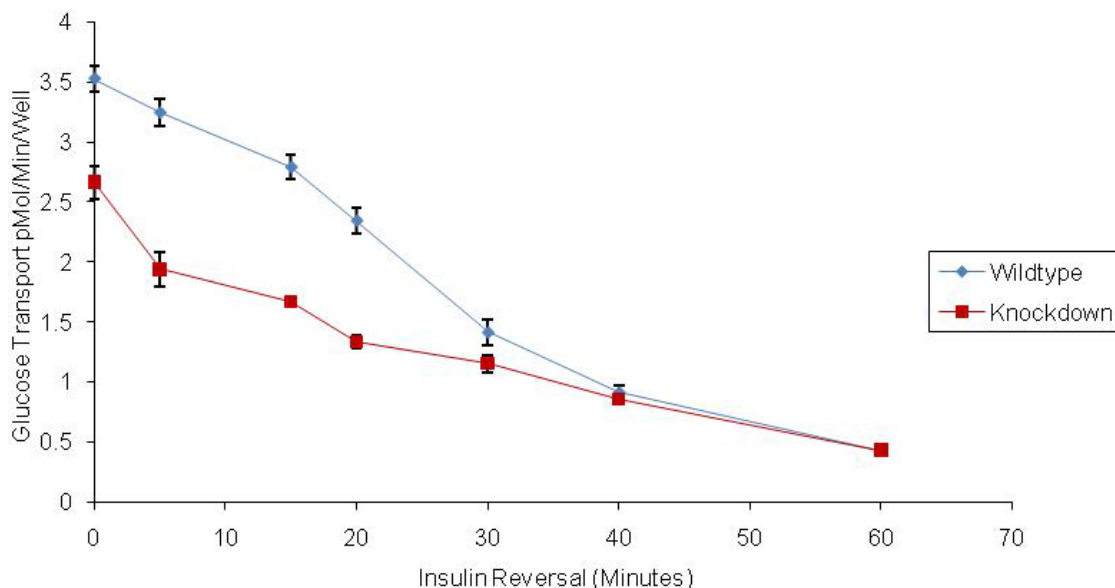


**Figure 5.11b Time course of the reversal of insulin-stimulated 2-Deoxy-D-Glucose Transport in control and mVps45 knockdown 3T3-L1 adipocytes**

3T3-L1 adipocytes were grown under standard conditions (see Materials and Methods) in triplicate wells and transfected with either no virus (uninfected Wildtype), or Knockdown virus for mVps45. Cells were then differentiated and treated with 100nM of Insulin for 30 minutes. Insulin reversal was initiated by washing in low pH buffer (see Materials and Methods) and deoxyglucose transport was assayed at different times following reversal (see graph) as

described in Materials and Methods. Shown is the data averaged from three separate experiments of this type. Data are expressed as the mean insulin-stimulated deoxyglucose uptake rate (pMol/Min/Cell) for each of the two sets of cells. Note that the cells depleted of mVps45 exhibited a significant reduction in this maximal value, see previous figure.

### 5.3.6 Budding Assay

In order to define molecules required for entry of Glut4 into the GSV compartment Kandror and colleagues described an *in vitro* budding assay which recapitulates the formation of GSVs. In brief, a membrane fraction (donor membranes) was prepared from a simple one-step 16,000 xg centrifugation of a homogenate of 3T3-L1 adipocytes. After washing, this fraction was incubated at 37°C with cytosol and ATP from 3T3-L1 adipocytes and incubated. After incubation, the donor membranes were sedimented at 16,000 xg, and any GSVs which were formed remain in the 16,000 xg supernatant. Using this method Kandror et al have shown that Glut4 is sorted from the donor membranes into GSVs in a time-, ATP- and cytosol-dependent manner, consistent with data from other groups (Xu and Kandror, 2002).

Here in Figure 5.12a, we used this assay to look at GSV formation in control and mVps45 depleted cells. Donor membrane and cytosol were prepared from 3T3-L1 adipocytes (as described in Materials and Methods) and combined with ATP in the combinations indicated at the bottom of the figure. These reactions were incubated at 37°C for either 20 or 40 minutes and the vesicle fraction was collected by high speed centrifugation. These fractions were immunoblotted with antibodies specific for GLUT4 and mVps45. When the donor membrane fraction was incubated with 1 mg/ml cytosol in the presence of ATP (since the formation of vesicles occurs in an ATP-dependent manner) vesicles formed in the period from initial mixing to 20 minutes of incubation as evidenced by the presence of GLUT4 protein in the top panel. After 40 minutes, the vesicle budding had increased. In the bottom two panels we analysed the presence of mVps45 in vesicular budding.

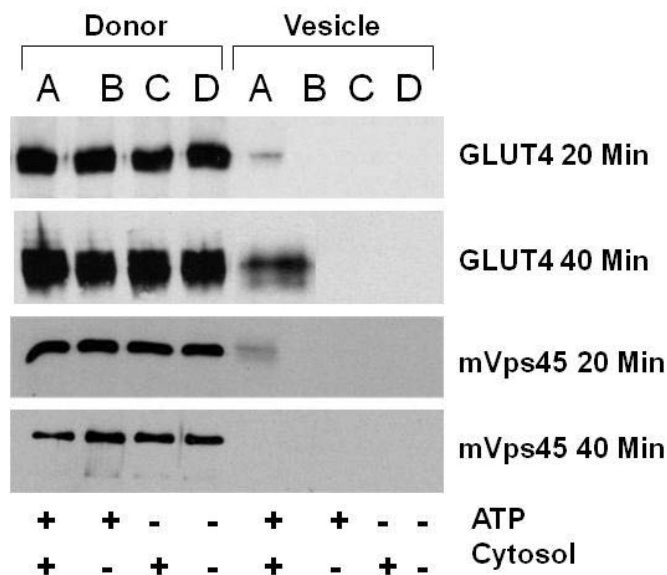


### Figure 5.12a Budding of Vesicles in Wildtype Cells

Cell lysates were prepared from wildtype 3T3-L1 adipocytes and centrifuged into membrane and cytosol fractions as described in Materials and Methods. Membrane and cytosol fractions were combined as indicated above with the addition of an ATP regeneration system and incubated at physiological temperature for 20 and 40 minutes before being centrifuged into donor and vesicle fractions and immunoblotted with GLUT4 and mVps45 antibody. Set A-D: The donor fraction. Set 2 A-D: The Vesicle Fraction. A: Membrane, Cytosol, ATP. B: No Cytosol, C: No ATP, D: No Cytosol, No ATP

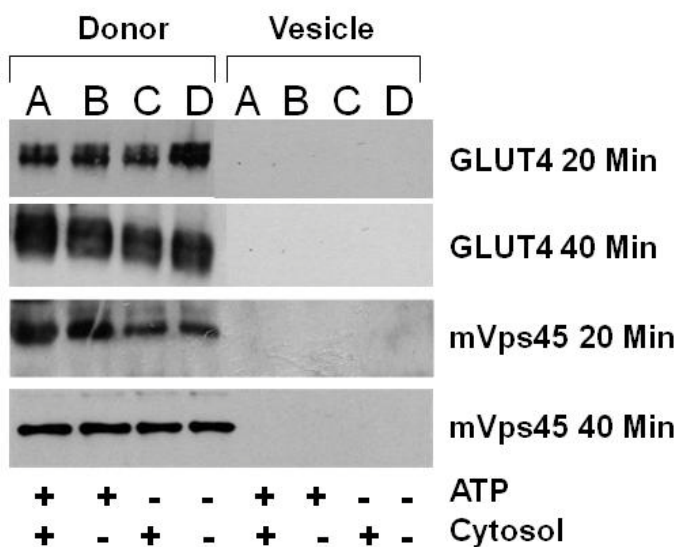


### Figure 5.12b Budding of Vesicles in Knockdown Cells

Cell lysates prepared from 3T3-L1 adipocytes infected with shRNA virus designed to knockdown levels of mVps45 were centrifuged into membrane and cytosol fractions as described in Materials and Methods. Membrane and cytosol fractions were combined as indicated above with the addition of an ATP regeneration system and incubated at physiological temperature for 20 and 40 minutes before being centrifuged into donor and vesicle fractions and immunoblotted with GLUT4 and mVps45 antibody. Set A-D: The donor fraction. Set 2 A-D: The Vesicle Fraction. A: Membrane, Cytosol, ATP. B: No Cytosol, C: No ATP, D: No Cytosol, No ATP

In cells depleted of mVps45, vesicular budding does not seem to occur (as shown in Figure 5.12b). This result is in keeping with the idea that mVps45 is necessary for GLUT4 sorting. When mVps45 is absent, GLUT4 does not enter into newly budded vesicles (Figure 5.12b, top two panels). The lack of mVps45 (Figure 5.12b, bottom two panels) suggests that mVps45 acts on the GLUT4 recycling pathway. However, these data are very preliminary, and require repeating and optimising to be certain of their veracity. They are included here to show the interesting result obtained, but it is important to stress that further work on this area is required and the data are not definitive.

### **5.3.7 Recycling Assay with HA-GLUT4-GFP**

One prediction from the experiments performed above is that in the absence of mVps45, Glut4 may not be trafficked into the slower cycle 2 pathway (see Figure 1.2). To test for this, we used cells expressing HA-GLUT4-GFP. The uptake of fluorescently labelled anti-HA monoclonal antibody into the cell reflects the trafficking of Glut4 through the plasma membrane. Hence, by incubating cells with anti-HA for increasing times, it is possible to measure the rate of accumulation of anti-HA inside the cells, reflecting the rate at which the total population of Glut4 trafficks through the PM. Figure 5.12 shows data from a typical experiment. In cells expressing control shRNA (targeted against luciferase), the half time for accumulation of anti-HA is of the order of 4h. In cells depleted of mVps45, this is significantly shortened to around 100 minutes.

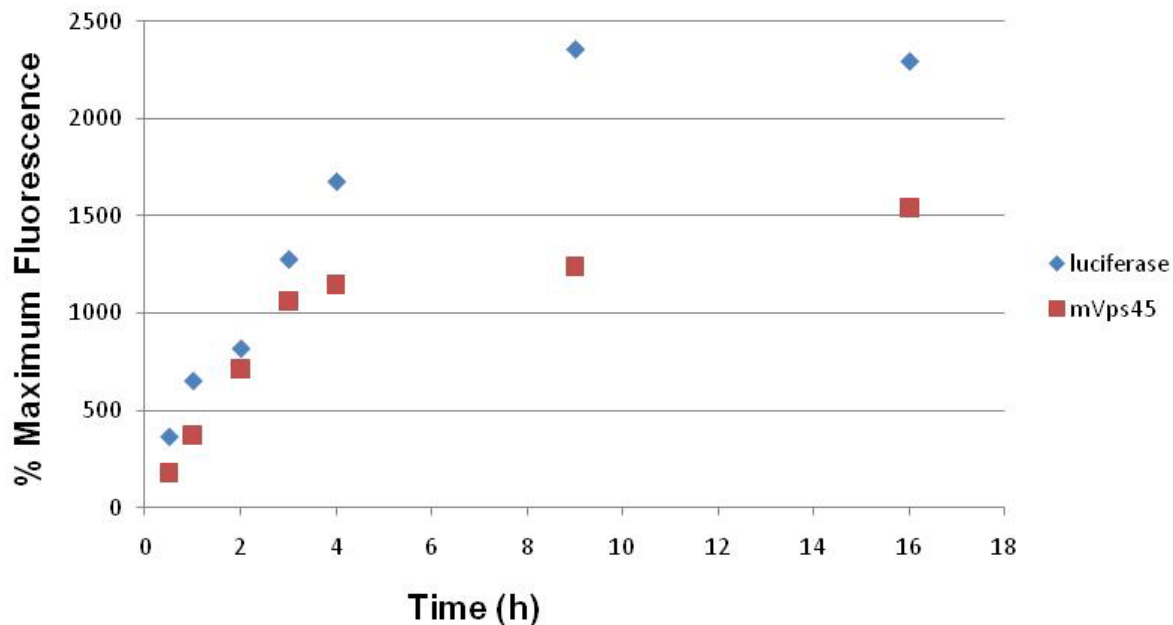


**Figure 5.13a The Recycling Assay**

The graph above shows increased fluorescence with time. Cells were infected with control (Luciferase) shRNA or mVps45 shRNA1. The data shows that in control cells, it takes about 4 h (240 min) for fluorescence to plateau, which shows that total GLUT4 in cells recycles through the PM with a half time of 4 h in control cells. In mVps45 knockdown, the half time is 100 min (1.75 h), so in the absence of mVps45, GLUT4 recycles faster. This can be explained by the possibility that GLUT4 is retained in cycle 1 and in the absence of mVps45 cannot enter cycle 2.

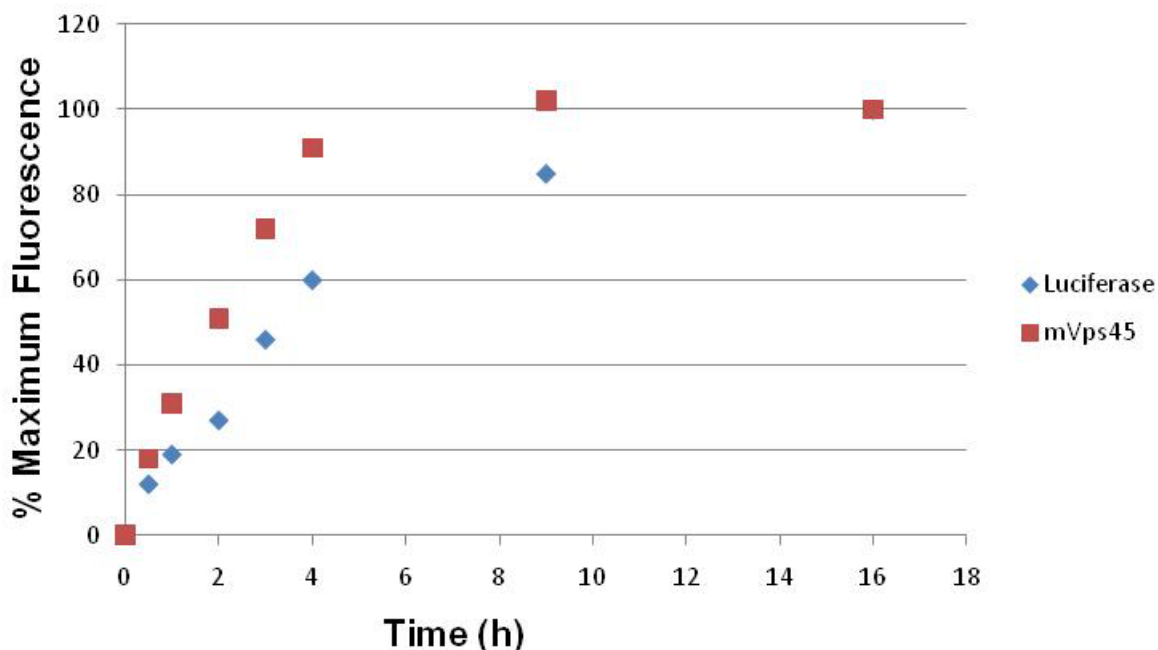


**Figure 5.13b The Recycling Assay normalized for HA-GLUT4-GFP Expression**

The graph above shows increased fluorescence with time. Cells were infected with control (Luciferase) shRNA or mVps45 shRNA1. The data shows that in control cells, it takes about 4 h (240 min) for fluorescence to plateau, which shows that total GLUT4 in cells recycles through the PM with a half time of 4 h in control cells. In mVps45 knockdown, the half time is 100 min (1.75 h), so in the absence of mVps45, GLUT4 recycles faster. This can be explained by the possibility that GLUT4 is retained in cycle 1 and in the absence of mVps45 cannot enter cycle 2. Note that the fluorescence value plotted has been normalised for HA-GLUT4-GFP expression by using the GFP fluorescence signal.

### 5.3.8 Subcellular Fractionation

As shown in Section 5.3.3, depleting 3T3-L1 adipocytes of mVps45 causes changes to the intracellular environment. Several proteins that may act with or are acted upon by mVps45 show decreased expression with depletion of mVps45 in whole cell lysates as analysed by immunoblotting. These interesting results prompted further characterization of protein distribution in 3T3-L1 adipocytes depleted of mVps45. To further examine the effects that mVps45 depletion might have on protein distribution in these adipocytes, an analysis of the subcellular fraction of proteins was undertaken on wildtype and knockdown adipocytes treated with or without insulin (Figure 5.14).

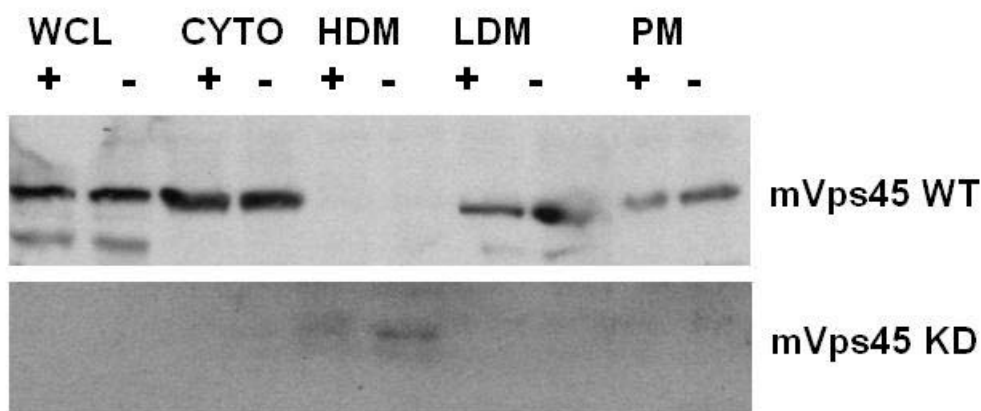


**Figure 5.14 The subcellular distribution of proteins in basal and Insulin-stimulated 3T3-L1 adipocytes depleted of mVps45**

Wildtype 3T3-L1 adipocytes and adipocytes that were depleted of mVps45 were either incubated in the presence of 1  $\mu$ M Insulin for 20 min or left in their basal state and crude lysates were prepared as described in Materials and Methods. Lysates were then subjected to a series of differential centrifugations and fractions containing the cytosol, High Density Microsomes (HDM), Low Density Microsomes (LDM) and Plasma Membranes (PM) were collected. These fractions were immunoblotted with an antibody specific to mVps45. The results shown are representative fractions from 5 preparations.

Through a series of sequential differential centrifugations, cell structures were separated into cytosolic, high density microsomes (HDM), low density microsomes (LDM) and plasma membrane (PM). Fractions were then subjected to immunoblot analysis with an antibody specific for mVps45. Whole cell lysate was immunoblotted as a protein control. 3T3-L1 adipocytes were used on Day 8 after differentiation because it is at this stage in adipocyte development that mRNA and protein levels along with the glucose transport response have reached a steady state for analysis. The intracellular pool of GLUT4 is localized to the LDM, and this fraction also contains

endosomes and the Golgi apparatus. The HDM fraction is enriched with endoplasmic reticulum (ER).

mVps45 is found in the cytosolic fraction in both basal and insulin-stimulated wildtype cells (as shown in figure 5.14, top panel) which confirms the findings in Chapter 3 which show that mVps45 is present in the cytosol of 3T3-L1 adipocytes in both basal and insulin-stimulated conditions. It is not found in the HDM which contains ER and other structures not associated with GLUT4 recycling. It is, however, found in the LDM fraction. The LDM contains the TGN which is where mVps45 is known to act. mVps45 is also found at the PM in both basal and insulin-stimulated conditions. mVps45 follows the pathway of GLUT4 and the presence of mVps45 in the PM of both basal and insulin-stimulated cells suggests that it may move with GSVs to the PM. This finding that mVps45 is found in the PM also confirms the results of Chapter 3 which shows that mVps45 is present in both basal and insulin-stimulated membranes.

As this study shows, depleting mVps45 from these cells removed any trace amounts of mVps45 from all fractions aside from the HDM and slight traces at the PM. This result indicates that with mVps45 depletion, the GSVs are not available for GLUT4 entry because shifting the fraction where mVps45 is present indicates that the proteins normally resident in Pool1 (the GSV pool in the two pool system) are no longer functional and proteins shift into Pool 2 (the TGN/endosomal pool). The results from Iodixanol sedimentation analysis, discussed below, also confirm this finding.

### **5.3.9 Iodixanol Gradients**

While the above data suggests differences in the movement of proteins in cellular compartments upon depletion of mVps45, resolving distinct subcellular compartments by sucrose density centrifugation has its difficulties. For example, proteins deriving from the same vesicle may be a similar density and size limiting the information available from this type of experiment. Also, the density of GLUT4-containing vesicles is the same density as hyper-osmotic sucrose (Hashiramoto and James, 2000) which detracts from its usefulness. In order to gain valuable data about the proteins contained in cellular fractions this study employed another method not

encumbered with the same limitations. Iodixanol (Optiprep: 5,5' [2-hydroxy-1-3propanediyl)-bis(acetylamino)] bis[N,N'-bis(2,3-dihydroxypropyl)-2,4,6-triiodo-1,3-benzenecarboxamide] ) is an iso-osmotic iodinated sedimentation media used in centrifugation analyses to segregate intracellular organelles of different densities from the LDM as prepared from cell lysates. In fact, the banding patterns of many membrane compartments are sufficiently distinctive in iodixanol gradients and provide information about the specific components and functions and the shift in location during cellular activity.

Here, we prepared lysates from wildtype 3T3-L1 adipocytes and adipocytes depleted of mVps45 and isolated the LDM fraction which was then used for iodixanol sedimentation analysis (see Materials and Methods), fractions were then immunoblotted for GLUT4 and mVps45 protein.

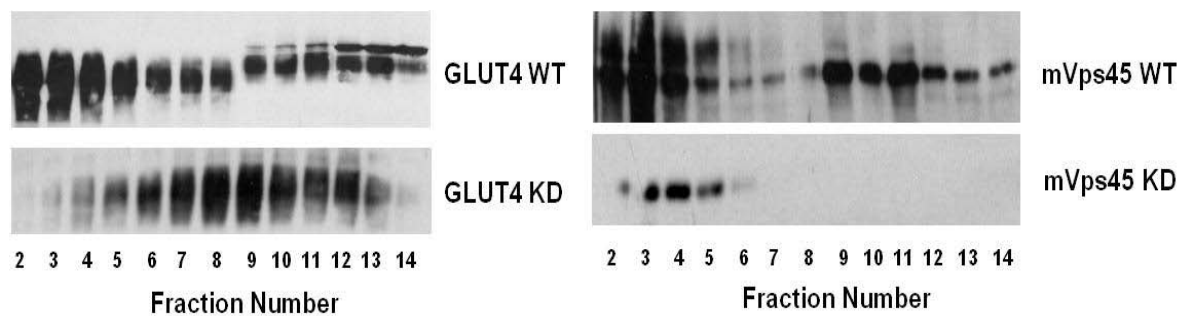


**Figure 5.15 Iodixanol equilibrium gradient sedimentation analysis of wildtype and Knockdown 3T3-L1 adipocytes**

Low density microsomes (LDM) were prepared from both wildtype 3T3-L1 cell lysates and those depleted of mVps45. These lysates were subjected to iodixanol equilibrium sedimentation analysis as described in Materials and Methods. The fractions were collected after sedimentation and immunoblotted for the distribution of GLUT4 and mVps45 proteins using antibodies specific to those proteins. The data shown omits the first two and last two fractions of the sixteen collected and are the results of a single experiment representing 5 experiments. Images have been intentionally overexposed for clarity of purpose.

In wildtype 3T3-L1 cells, two distinct peaks were resolved containing GLUT4 fractions. The first peak contains a significantly larger proportion of GLUT4 than the later peak. Other studies have shown similar results in 3T3-L1 adipocytes and skeletal muscle (Hashiramoto and James, 2000) indicating that in insulin-sensitive cells GLUT4 is targeted to GSVs and endosomal fractions. In the left side panel of Figure 5.15, LDM fractions were resolved through iodixanol sedimentation analysis and were found to contain the greatest

amount of GLUT4 in wildtype cells in the earlier fractions (fractions 2-5). In LDM fractions resolved by this method from cells depleted of mVps45, the GLUT4 profile changes and the fractions containing the most GLUT4 shifts (Fractions 7-10). This finding may indicate that GLUT4 cannot gain entry to the GSVs or that GSVs are absent or of a distinct density when mVps45 is no longer available. The shift of GLUT4 from a dense GSV pool (classically found in the first 5 fractions) to a pool that appears to be primarily endosomal suggests that mVps45 is necessary for GLUT4 to reside in the GSV fraction.

In the right hand panel of Figure 5.15, mVps in wildtype cells appears to mirror that of GLUT4, and can be found to reside in the earlier, dense GSV population (Fractions 2-5) of the first peak while, like GLUT4, also is present in the TGN/endosomal fractions (Fractions 9-12). This finding validates the knowledge that mVps45 acts at the TGN and interacts with membrane fusion proteins (most notably the t-SNARE Syntaxin 16) that sort GLUT4. However, in LDM fractions from cells depleted of mVps45, the profile changes and the little mVps45 which remains after knockdown, while still present in the first peak (Fractions 2-5) corresponding with the GSVs is present in much lower levels

## 5.4 Discussion

This chapter examines the effect of mVps45 knockdown on GLUT4 translocation using a variety of assays. First we used shRNA mediated knockdown to deplete 3T3-L1 adipocytes of mVps45. We used this method because lipid-based transfection methods transduce genes into 3T3-L1 adipocytes poorly. Once cells are differentiated they become refractory to standard methods of transfection and low efficiencies are achieved. Single cell microinjection does not allow for global populations of cells to be studied and electroporation can be only used on very early stage cells and may cause changes to cell function and viability. The advantage of shRNA is that the lentivirus integrates into the cell genome and thus the expression is permanent. Thus targeted gene knockdown can be achieved at any phase of the cell cycle and can be maintained indefinitely.

The effects of depleting mVps45 from adipocytes were analysed by the immunoblot analysis of several proteins known to act on the GLUT4 sorting pathway. We found that when mVps45 was knocked down, the cellular levels of its cognate t-SNARE Syntaxin 16 decreased giving evidence that there is a direct interaction between these two proteins. Data from this chapter suggests that mVps45 may have a role in GLUT4 sorting and support for this theory was given by the fact that when mVps45 was depleted in 3T3-L1 adipocytes, GLUT4 protein levels fell significantly in these cells. Also, protein levels of the GSV resident protein IRAP decreased in mVps45 depleted cells suggesting that mVps45 may have a role in regulating entry into the GSVs. Rahajeng et al have found that human vps45 binds to rabenosyn-5 and that depletion of this vps45 decreased the levels of rabenosyn-5 (Rahajeng et al., 2010). This observation is confirmed in our study which demonstrated that mVps45 depletion decreased the levels of rabenosyn-5.

We also studied the in-situ visualisation of GLUT4 translocation using HA-GLUT4-GFP cells. In these experiments, we found that depletion of mVps45 in these cells causes loss of insulin sensitivity. This loss of insulin sensitivity was evidenced by the fact that in mVps45 depleted cells, GLUT4 was not able to traffic to the PM in response to insulin-stimulation. The inability of GLUT4 to traffic to the PM in insulin-stimulated mVps45 depleted cells suggests a role for mVps45 in regulating GLUT4 sorting.

Glucose transport using 3T3-L1 adipocytes was measured and it was found that mVps45 depletion alters the rate and sensitivity of insulin-stimulated glucose transport. Experiments measuring basic glucose transport in mVps45 depleted cells showed that insulin-stimulated 2-deoxyglucose uptake was profoundly decreased in these cells compared to wildtype cells. Experiments measuring the sensitivity of mVps45 depleted cells to varying doses of insulin suggested more insulin was needed to elicit a response in knockdown cells compared to wildtype which suggests a decrease in insulin-sensitivity in these cells compared to wildtype. This decrease in glucose uptake suggests a role for mVps45 in regulating GLUT4 sorting. Experiments measuring the ability of mVps45 depleted cells to reverse insulin-stimulated glucose transport showed that initially these cells are able to reverse transport more effectively than wildtype cells. An explanation for these data is not immediately apparent, but

may reflect changes in the intracellular trafficking of Glut4 into a degradative pathway upon mVps45 depletion. Since GLUT4 levels decrease upon mVps45 knockdown, it may be speculated that depletion of mVps45 results in GLUT4 entering a degradative pathway; this pathway may allow faster movement of GLUT4 from cycle 1, so causing an apparent increase in reversal rates, at least at early times. Clearly, further work will be required to address this.

We performed a budding assay designed to recapitulate the formation of GSVs in-vitro in an effort to understand the effect mVps45 depletion might have on the creation of newly budded vesicles and to further investigate the role mVps45 might have on GLUT4 sorting. Xu and Kandror show the creation of newly budded vesicles by the presence of GLUT4 protein in immunoblots of the vesicle fraction (Xu and Kandror, 2002). In our study, newly budded vesicles were formed in wildtype cells as evidenced by the presence of GLUT4 protein on immunoblots of the vesicle fraction. The use of mVps45 depleted membrane and cytosol in this in-vitro budding assay suggested that new vesicles could not form when mVps45 was not present as evidenced by the lack of a GLUT4 band in immunoblots of the vesicle fraction. This suggests that GLUT4 isn't able to enter newly budding vesicles in mVps45 depleted cells which further gives rise to the possibility that mVps45 is necessary for GLUT4 sorting into the GSVs.

Measurement of GLUT4 trafficking by the use of a recycling assay that used HA-staining to track GLUT4 movement in HA-GLUT4-GFP cells showed differences between wildtype and mVps45 depleted cells. In wildtype cells, the total cycling of GLUT4 through the PM took nearly 4 hours, however, in mVps45 knockdown cells this rate was much more rapid and was found to be around 100 minutes, less than half the time of wildtype. These findings suggest that the rate at which the total population of GLUT4 trafficks through the PM increases in the absence of mVps45 suggesting that in the absence of mVps45, GLUT4 may not enter the slow cycle. This suggestion supports the possibility that mVps45 controls entry into the slow cycle.

Subcellular fractionation experiments measuring the subcellular distribution of mVps45 protein showed that mVps45 normally resides at the TGN (as evidenced by the fact that it was found in the LDM fraction which is known to

contain the TGN) which is where it has been found to act. Depleting 3T3-L1 adipocytes of mVps45 showed the presence of traces of mVps45 in the HDM fraction but not the LDM fraction which indicates a shift of proteins from the GSV to the endosome pools. This shift indicates that in the absence of mVps45 GSVs are not available for GLUT4 entry.

Expanding upon the finding of the subcellular fractionation studies, iodixanol sedimentation analysis showed a shift from the GSV pool to the TGN/endosomal pool for GLUT4 proteins in 3T3-L1 adipocytes depleted of mVps45 as evidenced by the change in band patterns for GLUT4 from fractions 2-5 to fractions 7-10. This finding suggests that GLUT4 shifts to the second pool in the absence of mVps45 because mVps45 may be necessary for GLUT4 to enter the GSVs. Hashiramoto and James suggest that these endosomal vesicles may mediate withdrawal of GLUT4 from the recycling system and this might explain the unique insulin responsiveness of GLUT4 in adipocytes. Maier and colleagues also found two distinct intracellular pools of GLUT4, one that was endosomal and enriched with transferrin receptors and early endosomal rab proteins and a second pool that was denser and devoid of endosomal markers (Maier and Gould, 2000). They found that the earlier fractions correspond to GSVs and our study recapitulates this finding.

## **Chapter 6- Conclusions and Future Directions**

## Chapter 6: Conclusions and Future Directions

Insulin resistance is caused by the failure of insulin to stimulate the translocation of GLUT4 from internal GSV stores to the PM thereby internalizing glucose into muscle and fat cells (Bryant et al., 2002). In insulin responsive cells such as adipocytes, GLUT4 traffics between two inter-related endosomal cycles. Cycle 1 (the fast cycle) shuttles GLUT4 between the PM and early endosomes clearing it from the PM in the basal state while Cycle 2 (the slow cycle) recycles GLUT4 between recycling endosomes/TGN and GSVs (see Figure 6.1 for an illustration). Insulin mobilises GLUT4 to the PM from this slow recycling pathway (Bryant et al., 2002). This thesis seeks to understand how GLUT4 entry into the second cycle is controlled.

GLUT4 trafficking is a highly regulated process and is controlled by the formation of a specific SNARE complex, the formation of which ensures specificity of function. Syntaxin 16 is the t-SNARE shown to form a SNARE complex with Syntaxin 6 and Vti1a that facilitates the traffic of GLUT4 into GSVs (Shewan et al., 2003; Proctor et al., 2006). Regulation of this t-SNARE controls the SNARE complex which may regulate GLUT4 entry into the slow cycle. mVps45 is the SM protein thought to control Syntaxin 16 (Dulubova et al., 2002; Yamaguchi et al., 2002).

Data from several experiments appear to suggest that mVps45 may have a role in regulating GLUT4 sorting. It is assumed that mVps45 regulates GLUT4 sorting through the regulation of Syntaxin 16 and subsequently the formation of SNARE complexes involving Syntaxin 16 but precisely how this regulation occurs is not known. Data from this thesis suggest an interaction between Syntaxin 16 and mVps45 so this assumption may be correct.

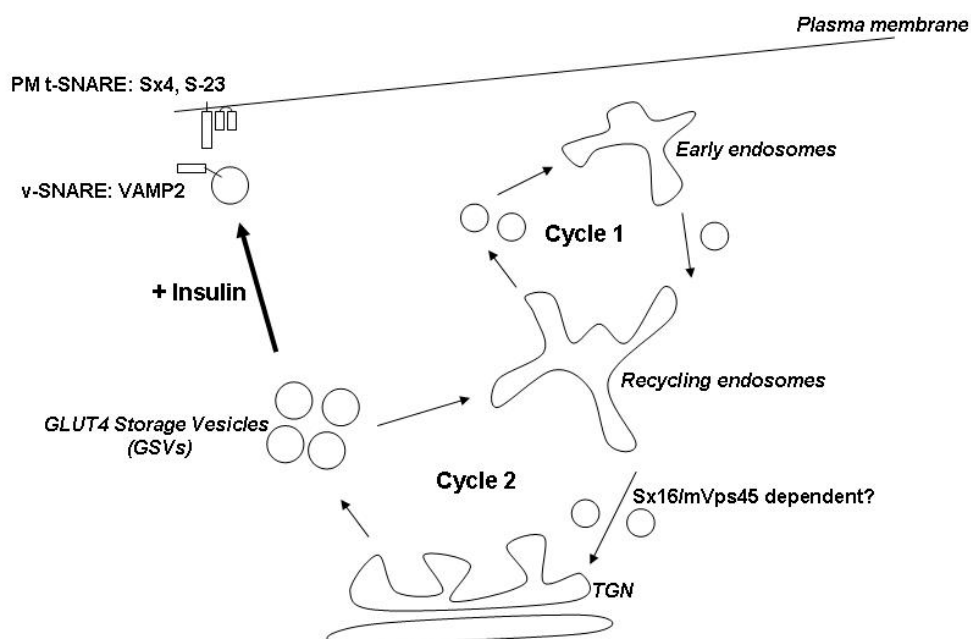


**Figure 6.1 The effect of mVps45 on GLUT4 sorting into the slow recycling pathway**  
 Data from this thesis suggests a role for mVps45 in regulating the entry of GLUT4 into the slow cycle (reproduced with permission from Gwyn Gould)

## 6.1 Endogenous levels and binding of Syntaxin 16 and mVps45

In chapter 3, the aim was to assess whether mVps45 and Syntaxin 16 were present in stoichiometric amounts and also to test whether insulin stimulation alters the interaction between Syntaxin 16 and mVps45.

Through quantification analysis using standard curve methodology, we found that mVps45 and Syntaxin 16 are present in roughly stoichiometric amounts which suggested that there is a functional interaction between Syntaxin 16 and mVps45. When these calculated values from 3T3-L1 adipocytes were compared to values obtained through the quantification of the levels of Syntaxin 16 and mVps45 in fibroblasts, it was found that the copy number of both proteins increase upon adipocyte differentiation. This finding suggested that both Syntaxin 16 and mVps45 are important in the functioning of adipocytes. When the copy number of Syntaxin 16 and mVps45 were compared between 3T3-L1 adipocytes and rat primary adipocytes, the levels

of both proteins appeared broadly similar which suggested that the roles of both Syntaxin 16 and mVps45 are important in adipocytes and that mVps45 and syntaxin 16 being present in proportional quantities were able to interact functionally. Further quantification work is necessary to quantify the levels of Syntaxin 16 from insulin-stimulated 3T3-L1 membranes in order to compare this to the data already obtained from quantifying the levels of mVps45 in 3T3-L1 membrane proteins. It is important to determine whether the expression of this complex is altered in insulin resistance so it would be interesting to quantify the levels of Syntaxin 16 and mVps45 from insulin resistant samples (ZDF rats or diabetic human samples).

We also tested the binding interaction between Syntaxin 16 and mVps45 through immunoprecipitation experiments. These experiments revealed that in basal conditions Syntaxin 16 and mVps45 bind. However, when immunoprecipitation experiments were performed using lysates from insulin-stimulated 3T3-L1 adipocytes, it appeared that the interaction between mVps45 and Syntaxin 16 remained, suggesting that insulin does not modulate this interaction. In other data from this thesis, the absence of mVps45 appears to alter the ability of insulin to modulate Syntaxin 16 action and it would be interesting to perform immunoprecipitation experiments using 3T3-L1 cells transduced with a dominant negative form of mVps45 to assess the ability of insulin to modulate this interaction.

## **6.2 Yeast Model of Vps45 mutants and Complementation**

In chapter 4, we aimed to determine whether Vps45p and mVps45 are functional homologues. We examined this question primarily through assessing whether mVps45 can complement for the deletion of Vps45p through a series of complementation assays.

When we performed CPY trafficking assays we found that mVps45 can complement for the loss of Vps45p with respect to the trafficking of CPY and that mVps45 mutants cannot restore this function. These data suggested that mVps45 is a functional homologue of Vps45p and mVps45 mutants in this assay may show homology to yeast mutants established in the lab previously (Carpp

et al., 2007). Similarly, Invertase secretion assays appeared to suggest that mVps45 shows functional homology to Vps45p by rescuing the ability of cells to sort invertase. These assays were performed with only mVps45 and mVps45 mutants and were not assayed at the same time as Vps45p and its corresponding mutants (although the data was confirmed by comparing the data from mVps45 and its mutants with published literature for Vps45p and its mutants- see Carpp et al., 2006; Carpp et al., 2007). Therefore, it would be advantageous to perform these experiments again with mVps45, the mutants described herein, Vps45p and its corresponding mutants in order to be able to directly compare the data in our assays at the same time.

We also examined the ability of yeast to grown on hyperosmotic media and at non-permissive temperatures. These assays assessed the ability of mVps45 to functionally complement for the loss of Vps45p in the face of osmotic shock and temperature sensitivity. Here, we found that mVps45 was clearly able to rescue the ability of yeast to grow on altered media (supplemented with 1.5M KCl) and at non-permissive temperatures throughout this series of experiments. Lastly, we performed Tlg2p expression assays which also suggested the functional complementation of mVps45 in yeast lacking *VPS45* by showing that mVps45 is able to stabilize Tlg2p cellular levels.

Future work will involve biochemical assays designed to measure the affinity of mVps45 to Tlg2p (the binding mode for which Dulubova et al., 2002 has already established) and also to its mammalian homologue Syntaxin 16. We will also perform assays to assess the interactions of mVps45 mutants with Tlg2p and Syntaxin 16.

### **6.3 Effects of mVps45 knockdown on the intracellular environment.**

In this last chapter, our aim was to discover how depletion of mVps45 alters the cellular function, protein levels and transport in 3T3-L1 adipocytes.

In order to do this, we first depleted cells for mVps45 and assessed the changes to the intracellular environment. In this series of knockdown experiments we found that levels of mVps45's cognate t-SNARE Syntaxin 16

were reduced as were the cellular levels of the GSV proteins GLUT4 and IRAP. These findings suggested a role for mVps45 in GLUT4 sorting. Data from this chapter suggested that in the absence of mVps45 the influence of insulin-stimulation is altered which affects glucose transport. These knockdown experiments were performed in basal cells and it would be interesting to note any changes to proteins involved in GLUT4 sorting in insulin-stimulated cells depleted of mVps45.

A series of glucose transport assays suggested that the absence of mVps45 alters the rate and sensitivity of glucose transport in insulin-stimulated 3T3-L1 adipocytes. While this data suggests a role for mVps45 in GLUT4 sorting, a more specific role might be assigned to mVps45 in assays that incorporated an inhibitor. It has been found that wortmannin inhibits insulin-stimulated GLUT4 translocation and glucose uptake in 3T3-L1 adipocytes in a dose-dependent manner (Hausdorff et al., 1999). The use of wortmannin also led to the conclusion that it is the p110 isoform of PI3-kinase that is involved in regulating GLUT4 translocation and that cell-surface exofacially exposed glucose transporters (such as GLUT4) require additional factors to maintain activity (Hausdorff et al., 1999). It would be interesting to include the use of wortmannin in future assays of glucose transport using these mVps45 depleted cells to see what effect PI3-kinase inhibition would have on our system.

Budding assays performed in this chapter indicated that in the absence of mVps45, GLUT4 may not be able to enter into newly budded vesicles. This finding suggests that mVps45 is necessary for GLUT4 sorting and possibly regulates the entry of GLUT4 into GSVs. It has been found that insulin can induce plasma membrane fusion of pre-formed vesicles and also stimulates the formation of new vesicles (Xu and Kandror, 2002). GLUT4 is found in small insulin-sensitive 60-70 S membrane vesicles that may derive from larger donor membranes in-vitro (Xu and Kandror, 2002). Xu and Kandror have demonstrated that small GLUT4-containing vesicles are formed from large rapidly sedimenting donor membranes in a cytosol-, ATP-, time- and temperature-dependent fashion (Xu and Kandror, 2002). This suggests that small insulin-responsive vesicles are where GLUT4 is stored and that fusion of these vesicles with the plasma membrane is the result of insulin-stimulation. Insulin may also stimulate formation of these vesicles and accelerate GLUT4

recycling to the plasma membrane (Xu and Kandrór, 2002). Vesicle budding requires GTP binding to Arf and GTP $\gamma$ S increases recruitment of the adaptor complex AP1 onto donor membranes, however GTP-bound Arf does not limit the budding reaction. Xu and Kandrór found that insulin stimulated the formation of GLUT4 vesicles in-vitro by ~50% and it would be interesting to insulin-stimulate wildtype and mVps45 depleted cells and test whether the same result is obtained in insulin-stimulated wildtype cells and what the effect of insulin-stimulation would be in mVps45 depleted cells.

Recycling experiments in HA-GLUT4-GFP cells suggested that in the absence of mVps45 the rate at which the total population of GLUT4 traffics through the PM increases, which may suggest that when mVps45 is not available GLUT4 may not be able to enter into the slow pathway and instead is trapped in the fast cycle. These experiments were performed in HA-GLUT4-GFP cells depleted of mVps45. Others in the lab have depleted these cells of Syntaxin 16. It will be interesting to see if similar results using this assay will be obtained in Syntaxin 16 depleted cells. If this is the case, it suggests that the SNARE complex regulates GLUT4 sorting into the slow pathway and validates the role of mVps45 in regulating the t-SNARE involved in the complex.

Subcellular fractionation and Iodixanol experiments identified a shift in cellular pool for GLUT4 in the absence of mVps45 from the GSV rich pool into the TGN/endosomal pool. These very preliminary findings suggest that in the absence of mVps45 GSVs may not be available for GLUT4 internalization. While these findings are initially interesting, they do not communicate the full story available from these experiments. It will be necessary to perform these experiments again and analyse the locations of other proteins involved in GLUT4 sorting, most notably GLUT4 protein itself in subcellular fractions to validate our assay against the established literature. Other proteins vital to analyse will be IRAP, to obtain information about the GSVs, Syntaxin 16, the cognate t-SNARE for mVps45 as well as Rab4, Mannose-6 phosphate and other markers testing for purity of each fraction.

Taken together, the findings in this thesis suggest a role for mVps45 in regulating GLUT4 sorting, probably through regulating the entry of GLUT4 into the GSVs

## Bibliography

- Abeliovich H, Grote E, Novick P, Ferro-Novick S. 1998. Tlg2p, a yeast syntaxin homologue that resides on the golgi and endocytic structures. *J Biol Chem.* 273(19): 11719-11727.
- Abeliovich H, Darsow T, Emr SD. 1999. Cytoplasm to vacuole trafficking of aminopeptidase I requires a t-SNARE-Sec1p complex composed of Tlg2p and Vps45p. *EMBO J.* 18(21): 6005-6016.
- Amessou M, Popoff V, Yelamos B, Saint-Pol A, Johannes L. 2006. Measuring Retrograde Transport to the *Trans*-Golgi Network. *Curr Protoc Cell Biol.* 2006 Oct (Chapter 15:Unit 15.10): 15.10.1-15.10.21.
- Amessou M, Fradagrada A, Falguieres T, Lord JM, Smith DC, Roberts LM, Lamaze C, Johannes L. 2007. Syntaxin 16 and syntaxin 5 are required for efficient retrograde transport of several exogenous and endogenous cargo proteins. *J Cell Sci.* 120(8): 1457-1468.
- Andre B. 1995. An overview of membrane transport proteins in *Saccharomyces cerevisiae*. *Yeast.* 11(16): 1575-611.
- Antonin W, Fasshauer D, Becker S, Jahn R, Schnieder TR. 2002. Crystal structure of the endosomal SNARE complex reveals common structural principles of all SNARES. *Nat Struct Biol.* 9: 107-11.
- Aran V, Brandie FM, Boyd AR, Kantidakis T, Rideout EJ, Kelly SM, Gould GW, Bryant NJ. 2009. Characterization of two distinct binding modes between syntaxin 4 and Munc18c. *Biochem J.* 419(3): 655-660.
- Armoni M, Harel C, Karnieli E. 2007. Transcriptional regulation of the GLUT4 gene: from PPAR-gamma and FOXO1 to FFA and inflammation. *Trends Endocrinol Metab.* 18(3): 100-107.
- Bai L, Wang Y, Fan J, Chen Y, Ji W, Qu A, Xu P, James DE, Xu T. 2007. Dissecting Multiple Steps of GLUT4 Trafficking and Identifying the Sites of Insulin Action. *Cell Metab.* 5(1): 47-57.
- Banta LM, Robinson JS, Klionsky DJ, Emr SD. 1988. Organelle assembly in yeast: characterization of yeast mutants defective in vacuolar biogenesis and protein sorting. *J Cell Biol.* 107(4): 1369-1383.
- Barzel A, Kupiec M. 2008. Finding a match: how do homologous sequences get together for recombination? *Nat Rev Genet.* 9(1): 27-37.
- Bennett MK. 1995. SNAREs and the specificity of transport vesicle targeting. *Curr Opin Cell Biol.* 7: 581-6.
- Berenguer M, Marchand-Brustel YL, Govers R. 2009. GLUT4 molecules are recruited at random for insertion within the plasma membrane upon insulin stimulation. *FEBS Lett.* 584(3): 537-542.

- Bethani I, Lang T, Geumann U, Sieber JJ, Jahn R, Rizzoli SO. 2007. The specificity of SNARE pairing in biological membranes is mediated by both proof-reading and spatial segregation. *EMBO J.* 26(17): 3981-3992.
- Bethani I, Werner A, Kadian C, Geumann U, Jahn R, Rizzoli SO. 2009. Endosomal Fusion upon SNARE Knockdown is Maintained by Residual SNARE Activity and Enhanced Docking. *Traffic.* 10(10): 1543-1559.
- Birnbaum M J, Haspel HC, Rosen OM. 1986. Cloning and characterization of a cDNA encoding the rat brain glucose-transporter protein. *Proc Natl Acad Sci USA.* 83(16): 5784-5788.
- Bimbaum MJ, Martin F, Mueckler M. 1992. The Insulin-Sensitive Glucose Transporter. *Int Rev Cytol.* Volume 137, Part 1: 239-297.
- Blot V, McGraw TE. 2008. Molecular Mechanisms Controlling GLUT4 Intracellular Retention. *Mol Biol Cell.* 19(8): 3477-3487.
- Blot V, McGraw TE. 2008. Use of quantitative immunofluorescence microscopy to study intracellular trafficking: studies of the GLUT4 glucose transporter. *Methods Mol Biol.* 457: 347-66.
- Bock JB, Klumperman J, Davanger S, Scheller R. 1997. Syntaxin 6 functions in trans-Golgi network vesicle trafficking. *Mol. Biol. Cell.* 8(7): 1261-1271.
- Bogan JS, Kandror KV. 2010. Biogenesis and regulation of insulin-responsive vesicles containing GLUT4. *Curr Opin Cell Biol.*
- Bonifacino JS, Weissman AM. 1998. Ubiquitin and the control of protein fate in the secretory and endocytic pathways. *Annu Rev Cell Dev Biol.* 14(1): 19-57.
- Bonifacino JS, Dell'Angelica EC, Springer TA. 2001. Immunoprecipitation. *Curr Protoc Protein Sci.* Chapter 9(Unit 9.8).
- Bonifacino JS, Rojas R. 2006. Retrograde transport from endosomes to the trans-Golgi network. *Nat Rev Mol Cell Biol.* 7(8): 568-579.
- Bonifacino JS, Hurley JH. 2008. Retromer. *Curr Opin Cell Biol.* 20(4): 427-436.
- Bose A, Guilherme A, Huang S, Hubbard AC, Lane CR, Soriano NA, Czech MP. 2005. The v-SNARE Vti1a Regulates Insulin-stimulated Glucose Transport and Acrp30 Secretion in 3T3-L1 Adipocytes. *J Biol Chem.* 280(44): 36946-36951.
- Bowers K, Stevens TH. 2005. Protein transport from the late Golgi to the vacuole in the yeast *Saccharomyces cerevisiae*. *Biochim Biophys Acta (BBA) - Mol Cell Res.* 1744(3): 438-454.
- Bracher A, Weissenhorn W. 2002. Structural basis for the Golgi membrane recruitment of Sly1p by Sed5p. *EMBO J.* 21(22): 6114-6124.
- Brandie FM, Aran V, Verma A, McNew JA, Bryant NJ, Gould GW. 2008. Negative regulation of Syntaxin 4/SNAP-23/VAMP-2-mediated membrane fusion by Munc18c in vitro. *PLoS One.* 3(12):e4074.

- Braun S, Jentsch S. 2007. SM-protein-controlled ER-associated degradation discriminates between different SNAREs. *EMBO Rep.* 8: 1176-82.
- Brozinick JT, Berkmeier BA, Elmendorf JS. 2007. "Acting" on GLUT4: Membrane & Cytoskeletal Components of Insulin Action. *Curr Diabetes Rev.* 3(2): 111-22.
- Brunger AT. 2006. Structure and function of SNARE and SNARE-interacting proteins. *Q Rev Biophys.* 38: 1-47.
- Bryant NJ, Stevens TH. 1997. Two Separate Signals Act Independently to Localize a Yeast Late Golgi Membrane Protein through a Combination of Retrieval and Retention. *J Cell Biol.* 136(2): 287-297.
- Bryant NJ, Piper RC, Weisman LS, Stevens TH. 1998. Retrograde Traffic Out of the Yeast Vacuole to the TGN Occurs via the Prevacuolar/Endosomal Compartment. *J Cell Biol.* 142(3): 651-663.
- Bryant NJ, Piper RC, Gerrard SR, Stevens TH. 1998. Traffic into the prevacuolar/endosomal compartment of *Saccharomyces cerevisiae*: A VPS45-dependent intracellular route and a VPS45-independent, endocytic route. *Eur J Cell Biol.* 76: 43-52.
- Bryant NJ, Stevens TH. 1998. Vacuole Biogenesis in *Saccharomyces cerevisiae*: Protein Transport Pathways to the Yeast Vacuole. *Microbiol Mol Biol Rev.* 62(1): 230-247.
- Bryant NJ, James DE. 2001. Vps45p stabilizes the syntaxin homologue Tlg2p and positively regulates SNARE complex formation. *EMBO J.* 20(13): 3380-3388.
- Bryant NJ, Govers R, James DE. 2002. Regulated transport of the glucose transporter GLUT4. *Nat Rev Mol Cell Biol.* 3(4): 267-277.
- Bryant NJ, James DE. 2003. The Sec1p/Munc18 (SM) protein, Vps45p, cycles on and off membranes during vesicle transport. *J Cell Biol.* 161(4): 691-696.
- Buchholz F, Kittler R, Slabicki M, Theis M. 2006. Enzymatically prepared RNAi libraries. *Nat Meth.* 3(9): 696-700.
- Burd CG, Peterson M, Cowles CR, Emr SD. 1997. A novel Sec18p/NSF-dependent complex required for Golgi-to-endosome transport in yeast. *Mol Biol Cell.* 8(6): 1089-104.
- Burkhardt P, Hattendorf DA, Weis W, Fasshauer D. 2008. Munc18a controls SNARE assembly through its interaction with the syntaxin N-peptide. *EMBO J.* 27(7): 923-933.
- Burri L, Varlamov O, Doege CA, Hofmann K, Beilharz T, Rothman JE, Sollner TH, Lithgow T. 2003. A SNARE required for retrograde transport to the endoplasmic reticulum. *Proc Natl Acad Sci USA.* 100(17): 9873-9877.
- Burri L, Lithgow T. 2004. A Complete Set of SNAREs in Yeast. *Traffic.* 5(1): 45-52.

- Cai H, Reinisch K, Ferro-Novick S. 2007. Coats, Tethers, Rabs, and SNAREs work together to mediate the intracellular destination of a transport vesicle. *Dev Cell*. 12(5): 671-82.
- Camp HS, Ren D, Leff T. Adipogenesis and fat-cell function in obesity and diabetes. *Trends Mol Med*. 8:442-7.
- Capilla E, Diaz M, Hou JC, Planas JV, Pessin JE. 2007. High basal cell surface levels of fish GLUT4 are related to reduced sensitivity of insulin-induced translocation toward GGA and AS160 inhibition in adipocytes. *Am J Physiol Endocrinol Metab*. 298(2): E329-336.
- Carpp LN, Ciufo LF, Shanks SG, Boyd A, Bryant NJ. 2006. The Sec1p/Munc18 protein Vps45p binds its cognate SNARE proteins via two distinct modes. *J Cell Biol*. 173(6): 927-936.
- Carpp LN, Shanks SG, Struthers MS, Bryant NJ. 2007. Cellular levels of the syntaxin Tlg2p are regulated by a single mode of binding to Vps45p. *Biochem Biophys Res Commun*. 363(3): 857-860.
- Carr CM, Grote E, Munson M, Hughson FM, Novick PJ. 1999. Sec1p binds to SNARE complexes and concentrates at sites of secretion. *J Cell Biol*. 146: 333-44.
- Castle JD. 2004. Overview of cell fractionation. *Curr Protoc Protein Sci*. Chapter 3(Unit 3.1): 3.1.1-3.1.9.
- Cavalli V, Corti M, Gruenberg J. 2001. Endocytosis and signaling cascades: a close encounter. *FEBS Lett*. 498(2-3): 190-196.
- Chang K, Elledge SJ, Hannon JG. 2006. Lessons from Nature: microRNA-based shRNA libraries. *Nat Meth*. 3(9): 707-714.
- Charron MJ, Brosius FC, Alper SL, Lodish HF. 1989. A glucose transport protein expressed predominately in insulin-responsive tissues. *Proc Natl Acad Sci USA*. 86: 2535-9.
- Cheatham B, Volchuk A, Khan CR, Wang L, Rhodes C, Klip A. 1996. Insulin-stimulated translocation of GLUT4 glucose transporters requires SNARE-complex proteins. *Proc Natl Acad Sci USA*. 93(26): 15169-15173.
- Cheatham B. 2000. GLUT4 and Company: SNAREing Roles in Insulin-regulated Glucose Uptake. *Trends Endocrinol Metab*. 11: 356-61.
- Chen YA, Scheller RH. 2001. SNARE-mediated membrane fusion. *Nat Rev Mol Cell Biol*. 2(2): 98-106.
- Chen Y, Gan BQ, Tang BL. 2010. Syntaxin 16: Unraveling Cellular Physiology through a Ubiquitous SNARE molecule. *J Cell Physiol*. 225: 326-32.
- Cheng Z-J, Singh RD, Wang T, Holicky EL, Wheatley CL, Bernlohr DA, Marks DL, Pagano RE. 2010. Stimulation of GLUT4 (glucose transporter isoform 4) storage vesicle formation by sphingolipid depletion. *Biochem J*. 427: 143-150.

- Chiang S-H, Baumann CA, Kanzaki M, Thurmond DC, Watson RT, Neudauer CL, Macara IG, Pessin JE, Saltiel AR. 2001. Insulin-stimulated GLUT4 translocation requires the CAP-dependent activation of TC10. *Nature*. 410(6831): 944-948.
- Christoforidis S, McBride HM, Burgoyne RD, Zerial M. 1999. The Rab5 effector EEA1 is a core component of endosome docking. *Nature*. 397(6720): 621-625.
- Coe JG, Lim AC, Xu J, Hong W. 1999. A role for Tlg1p in the transport of proteins within the Golgi apparatus of *Saccharomyces cerevisiae*. *Mol Biol Cell*. 10: 2407-23.
- Collins RN, Zimmerberg J. 2009. Cell Biology: A score for membrane fusion. *Nature*. 159:1065-1066.
- Collison M, James DJ, Graham D, Holman JD, Connell JMC, Dominiczak AF, Gould GW, Salt IP. 2005. Reduced insulin-stimulated GLUT4 bioavailability in stroke-prone spontaneously hypertensive rats. *Diabetologia*. 48(3): 539-546.
- Conibear E, Stevens TH. 1998. Multiple sorting pathways between the late Golgi and the vacuole in yeast. *Biochim Biophys Acta (BBA) - Mol Cell Res*. 1404(1-2): 211-230.
- Conibear E, Cleck JN, Stevens TH. 2003. Vps51p Mediates the Association of the GARP (Vps52/53/54) Complex with the Late Golgi t-SNARE Tlg1p. *Mol Biol Cell*. 14(4): 1610-1623.
- Cope DL, Lee S, Melvin DR, Gould GW. 2000. Identification of further important residues within the Glut4 carboxy-terminal tail which regulate subcellular trafficking. *FEBS Lett*. 481(3): 261-5.
- Cosson P, Ravazzola M, Varlamov O, Sollner TH, Di Liberto M, Volchuk A, Rothman JE, Orci L. 2005. Dynamic transport of SNARE proteins in the Golgi apparatus. *Proc Natl Acad Sci USA*. 102(41): 14647-14652.
- Cowles C, Emr SD, Horazdovsky BF. 1994. Mutations in the VPS45 gene, a SEC1 homologue, result in vacuolar protein sorting defects and accumulation of membrane vesicles. *J Cell Sci*. 107(12): 3449-3459.
- Cross BCS, Sinning I, Luirink J, High S. 2009. Delivering proteins for export from the cytosol. *Nat Rev Mol Cell Biol*. 10(4): 255-264.
- Cushman SW, Satoh S, Timmers KI, Malide D, Holman GD. 1997. Cell biology of insulin action on glucose transport. *Jpn J Physiol*. 47(Suppl 1): S39.
- Cushman SW, Wardzala LJ. 1980. Potential mechanisms of Insulin Action on Glucose Transport in the Isolated Rat Adipocyte. *J Biol Chem*. 255(10):4758-4762.
- Czech MP, Corvera S. 1999. Signaling mechanisms that regulate glucose transport. *J Biol Chem*. 274(4): 1865-8.
- Czech MP. 2002. Fat targets for insulin signaling. *Mol Cell*. 9(4): 695-6.

- Dacks JB, Peden AA, Field MC. 2009. Evolution of specificity in the eukaryotic endomembrane system. *Int J Biochem Cell Biol.* 41(2): 330-340.
- Darsow T, Odorizzi G, Emr SD. 2000. Invertase Fusion Proteins for Analysis of Protein Trafficking in Yeast. *Methods Enzymol.* 327: 95-106.
- DeFronzo RA. 1992. Pathogenesis of type 2 (non-insulin dependent) diabetes mellitus: a balanced overview. *Diabetologia.* 35(4): 389-97.
- DeFronzo RA. 1992. Pathogenesis of type 2 (non-insulin dependent) diabetes mellitus: a balanced overview. *Diabetologia.* 35(4): 389-97.
- DiAngelo JR, Birnbaum MJ. 2009. Regulation of Fat Cell Mass by Insulin in *Drosophila melanogaster*. *Mol Cell Biol.* 29(24): 6341-6352.
- Donaldson JG. 2001. Immunofluorescence staining. *Curr Protoc Cell Biol.* Chapter 21(Unit 21.3).
- Donaldson JG, Porat-Shliom N, Cohen LA. 2009. Clathrin-independent endocytosis: A unique platform for cell signaling and PM remodeling. *Cell Signal.* 21(1): 1-6.
- Donaldson JG, McPherson PS. 2009. Membrane trafficking heats up in Pavia. *EMBO Rep.* 10(2): 132-136.
- Doria A, Patti ME, Khan CR. 2008. The Emerging Genetic Architecture of Type 2 Diabetes. *Cell Metab.* 8: 186-200.
- Dugani CB, Klip A. 2005. Glucose transporter 4: cycling, compartments and controversies. *EMBO Rep.* 6(12): 1137-1142.
- Dulubova I, Sugita S, Hill S, Hosaka M, Fernandez I, Sudhof TC, Rizo J. 1999. A conformational switch in syntaxin during exocytosis: role of munc18. *EMBO J.* 18: 4372-82.
- Dulubova I, Yamaguchi T, Gao Y, Min S-W, Huryeva I, Sudhof TC, Rizo J. 2002. How Tlg2p/syntaxin 16 'snares' Vps45. *EMBO J.* 21(14): 3620-3631.
- Dulubova I, Yamaguchi T, Aras D, Li H, Huryeva I, Min S-W, Rizo J, Sudhof TC. 2003. Convergence and divergence in the mechanism of SNARE binding by Sec1/Munc18-like proteins. *Proc Natl Acad Sci USA.* 100(1): 32-37.
- El-Jack AK, Kandror KV, Pilch PF. 1999. The Formation of an Insulin-responsive Vesicular Cargo Compartment Is an Early Event in 3T3-L1 Adipocyte Differentiation. *Mol Biol Cell.* 10(5): 1581-1594.
- El-Husseini AE, Guthrie H, Snutch TP, Vincent SR. 1997. Molecular cloning of a mammalian homologue of the yeast vesicular transport protein vps45. *Biochim Biophys Acta.* 1325(1): 8-12.
- Elmendorf JS. 2002. Signals that regulate GLUT4 Translocation. *J Membr Biol.* 190: 167-74.
- Elmendorf JS. 2003. Fractionation Analysis of the Subcellular Distribution of GLUT-4 in 3T3-L1 Adipocytes. *Methods Mol Med.* 83: 105-11.

- Emr SD, Schauer I, Hansen W, Esmon P, Schekman R. 1984. Invertase beta-galactosidase hybrid proteins fail to be transported from the endoplasmic reticulum in *Saccharomyces cerevisiae*. *Mol Cell Biol.* 4: 2347-55.
- Emr S, Glick BS, Linstedt A, Lippincott-Schwartz J, Luini A, Malhotra V, Marsh BJ, Nakano A, Pfeffer SR, Rabouille C, Rothman JE, Warren G, Wieland FT. 2009. Journeys through the Golgi: "taking stock in a new era." *J Cell Biol.* 187(4): 449-453.
- Ezaki O, Kono T. 1982. Effects of temperature on basal and insulin-stimulated glucose transport activities in fat cells. Further support for the translocation hypothesis of insulin action. *J Biol Chem.* 257(23): 14306-14310.
- Fasshauer D, Sutton RB, Brunger AT, Jahn R. 1998. Conserved structural features of the synaptic fusion complex: SNARE proteins reclassified as Q- and R-SNAREs. *Proc Natl Acad Sci USA.* 95: 15781-6.
- Ferro-Novick S, Jahn R. 1994. Vesicle fusion from yeast to man. *Nature.* 370: 191-3.
- Foster LJ, Yeung B, Mohtashami M, Ross K, Trimble WS, Klip A. 1998. Binary interactions of the SNARE proteins Syntaxin 4, SNAP23, and VAMP-2 and their regulation by phosphorylation. *Biochemistry.* 37: 11089-96.
- Foster LJ, Klip A. 2000. Mechanism and regulation of GLUT-4 vesicle fusion in muscle and fat cells. *Am J Physiol Cell Physiol.* 279(4): C877-890.
- Foster LJ, Li D, Randhawa VK, Klip A. 2001. Insulin Accelerates Inter-endosomal GLUT4 Traffic via Phosphatidylinositol 3-Kinase and Protein Kinase B. *J Biol Chem.* 276(47): 44212-44221.
- Fujita H, Hatakeyama H, Watanabe TM, Sato M, Higuchi H, Kanzaki M. 2010. Identification of Three Distinct Functional Sites of Insulin-mediated GLUT4 Trafficking in Adipocytes using Quantitative Single Molecule Imaging. *Mol Biol Cell.* 21: 2721-2731.
- Fukuda R, McNew JA, Weber T, Parlati F, Engel T, Nickel W, Rothman JE, Sollner TH. 2000. Functional architecture of an intracellular membrane t-SNARE. *Nature.* 407(6801): 198-202.
- Furgason ML, MacDonald C, Shanks SG, Ryder SP, Bryant NJ, Munson M. 2009. The N-terminal peptide of the syntaxin Tlg2p modulates binding of its closed conformation to Vps45p. *Proc Natl Acad Sci USA.* 106(34): 14303-14308.
- Gallwitz D, Jahn R. 2003. The riddle of the Sec1/Munc-18 proteins- new twists added to their interactions with SNAREs. *Trends BiochemSci.* 28: 113-15.
- Ganley IG, Espinosa E, Pfeffer SR. 2008. A syntaxin 10-SNARE complex distinguishes two distinct transport routes from endosomes to the trans-Golgi in human cells. *J Cell Biol.* 180(1): 159-172.

- Gengyo-Ando K, Kuroyanagi H, Kobayashi T, Murate M, Fujimoto K, Okabe S, Mitani S. 2007. The SM protein VPS-45 is required for RAB-5-dependent endocytic transport in *Caenorhabditis elegans*. *EMBO Rep.* 8(2): 152-157.
- Gerber SH, Rah JC, Min SW, Liu X, de Wit H, Dulubova I, Meyer AC, Rizo J, Arancillo M, Hammer RE, Verhage M, Rosenmund C, Sudhof TC. 2008. Conformational switch of syntaxin-1 controls synaptic vesicle fusion. *Science.* 321(5895): 1507-10.
- Gerst GE. 1999. SNAREs and SNARE regulators in membrane fusion and exocytosis. *Cell Mol Life Sci.* 55(5): 707-34.
- Gesta S, Tseng YH, Khan CR. 2007. Developmental Origin of Fat: Tracking Obesity to its Source. *Cell.* 131: 242-256.
- Geumann U, Barysch SV, Hoopmann P, Jahn R, Rizzoli SO. 2008. SNARE Function Is Not Involved in Early Endosome Docking. *Mol Biol Cell.* 19(12): 5327-5337.
- Gietz RD, Sugino A. 1988. New yeast-Escherichia coli shuttle vectors constructed with in vitro mutagenized yeast genes lacking six-base pair restriction sites. *Gene.* 74(2): 527-34.
- Giraudo CG, Garcia.-Diaz A, Eng WS, Chen Y, Hendrickson WA, Melia TJ, Rothman JE. 2009. Alternative zippering as an on-off switch for SNARE-mediated fusion. *Science.* 323(5913): 512-6.
- Gonzalez E, McGraw TE. 2006. Insulin Signaling Diverges into Akt-dependent and -independent Signals to Regulate the Recruitment/Docking and the Fusion of GLUT4 Vesicles to the Plasma Membrane. *Mol Biol Cell.* 17(10): 4484-4493.
- Gottesman I, Mandarino L, Verdonk C, Rizza R, Gerich J. 1982. Insulin increases the Maximum Velocity for Glucose Uptake without Altering the Michaelis Constant in man. *J Clin Invest.* 70(6): 1310-1314.
- Gould GW, Bell GI. 1990. Facilitative glucose transporters: an expanding family. *Trends Biochem Sci.* 15(1): 18-23.
- Gould GW, Lippincott-Schwartz J. 2009. New roles for endosomes: from vesicular carriers to multi-purpose platforms. *Nat Rev Mol Cell Biol.* 10(4): 287-292.
- Grant BD, Donaldson JG. 2009. Pathways and mechanisms of endocytic recycling. *Nat Rev Mol Cell Biol.* 10(9): 597-608.
- Gregoire FM, Smas CM, Sul HS. 1998. Understanding Adipocyte Differentiation. *Physiol Rev.* 78: 783-809.
- Gregoire FM. 2001. Adipocyte Differentiation: From Fibroblast to Endocrine Cell. *Exp Biol Med.* 226: 997-1002.
- Gross DN, Farmer SR, Pilch PF. 2004. Glut4 Storage Vesicles without Glut4: Transcriptional Regulation of Insulin-Dependent Vesicular Traffic. *Mol Cell Biol.* 24(16): 7151-7162.
- Grosshans BL, Ortiz D, Novick P. 2006. Rabs and their effectors: Achieving

specificity in membrane traffic. *Proc Natl Acad Sci USA*. 103(32): 11821-27.

Gruenberg J. 2001. The endocytic pathway: a mosaic of domains. *Nat Rev Mol Cell Biol*. 2(10): 721-730.

Guilherme A, Emoto M, Buxton JM, Bose S, Sabini R, Theurkauf WE, Leszyk J, Czech MP. 2000. Perinuclear Localization and Insulin Responsiveness of GLUT4 Requires Cytoskeletal Integrity in 3T3-L1 Adipocytes. *J Biol Chem*. 275(49): 38151-38159.

Guilherme A, Virbasius JV, Puri V, Czech MP. 2008. Adipocyte dysfunctions linking obesity to insulin resistance and type 2 diabetes. *Nat Rev Mol Cell Biol*. 9(5): 367-377.

Gurunathan S, Marash M, Weinberger A, Gerst JE. 2002. t-SNARE phosphorylation regulates endocytosis in yeast. *Mol Biol Cell*. 13: 1594-607.

Hamm JK, El-Jack AK, Pilch PF, Farmer SR. 1999. Role of PPAR gamma in Regulating Adipocyte Differentiation and Insulin-Responsive Glucose Uptake. *Ann N Y Acad Sci*. 892(THE METABOLIC SYNDROME X: Convergence of Insulin Resistance, Glucose Intolerance, Hypertension, Obesity, and Dyslipidemias- Searching for the Underlying Defects): 134-145.

Hanahan D. 1983. Studies on transformation of Escherichia coli with plasmids. *J Mol Biol*. 166(4): 557-80.

Hashiramoto M, James DE. 2000. Characterization of Insulin-Responsive GLUT4 Storage Vesicles Isolated from 3T3-L1 Adipocytes. *Mol Cell Biol*. 20(1): 416-427.

Hashizume K, Cheng YS, Hutton JL, Chiu C, Carr CM. 2009. Yeast Sec1p Functions before and after Vesicle Docking. *Mol Biol Cell*. 20(22): 4673-4685.

Hausdorff S F, Fingar DC, Morioka K, Garza LA, Whiteman EL, Summers SA, Birnbaum MJ. 1999. Identification of Wortmannin-sensitive Targets in 3T3-L1 Adipocytes. *J Biol Chem*. 274(35): 24677-24684.

He A, Liu X, Liu L, Chang Y, Fang F. 2007. How many signals impinge on GLUT4 activation by insulin? *Cell Signal*. 19(1): 1-7.

Hickson GRX, Chamberlain LH, Maier VH, Gould GW. 2000. Quantification of SNARE Protein Levels in 3T3-L1 Adipocytes: Implications for Insulin-Stimulated Glucose Transport. *Biochem Biophys Res Commun*. 270(3): 841-845.

Hodgkinson CP, Mander A, Sale GJ. 2005. Protein kinase- $\zeta$  interacts with munc18c: role in GLUT4 trafficking. *Diabetologia*. 48: 1627-36.

Holman GD, Lo Leggio L, Cushman SW. 1994. Insulin-stimulated GLUT4 glucose transporter recycling. A problem in membrane protein subcellular trafficking through multiple pools. *J Biol Chem*. 269(26): 17516-24.

Holman GD, Cushman SW. 1994. Subcellular localization and trafficking of the GLUT4 glucose transporter isoform in insulin-responsive cells. *Bioessays*. 16(10): 753-9.

- Holman GD, and Sandoval IV. 2001. Moving the insulin-regulated glucose transporter GLUT4 into and out of storage. *Trends Cell Biol.* 11(4): 173-179.
- Horazdovsky BF, Busch GR, Emr SD. 1994. VPS21 encodes a rab5-like GTP binding protein that is required for the sorting of yeast vacuolar proteins. *EMBO J.* 13(6): 1297-1309.
- Horazdovsky B, DeWald DB, Emr SD. 1995. Protein transport to the yeast vacuole. *Curr Opin Cell Biol.* 7(4): 544-551.
- Hou JC, Pessin JE. 2007. Ins (endocytosis) and outs (exocytosis) of GLUT4 trafficking. *Curr Opin Cell Biol.* 19(4): 466-473.
- Huang S, Lifshitz LM, Jones C, Bellve KD, Standley C, Fonseca S, Corvera S, Fogarty KE, Czech MP. 2007. Insulin Stimulates Membrane Fusion and GLUT4 Accumulation in Clathrin Coats on Adipocyte Plasma Membranes. *Mol Cell Biol.* 27(9): 3456-3469.
- Huang S, Czech MP. 2007. The GLUT4 Glucose Transporter. *Cell Metab.* 5(4): 237-252.
- Im JY, Wollert T, Boura E, Hurley JH. 2009. Structure and Function of the ESCRT-II-III Interface in Multivesicular Body Biogenesis. *Dev Cell.* 17: 235-243.
- Ishiki M, Randhawa VK, Poon V, JeBailey L, Klip A. 2005. Insulin Regulates the Membrane Arrival, Fusion, and C-terminal Unmasking of Glucose Transporter-4 via Distinct Phosphoinositides. *J Biol Chem.* 280(31): 28792-28802.
- Ishiki M, Klip A. 2005. Minireview: Recent Developments in the Regulation of Glucose Transporter-4 Traffic: New Signals, Locations, and Partners. *Endocrinology.* 146(12): 5071-5078.
- Ishikura S, Koshkina A, Klip A. 2008. Small G proteins in insulin action: Rab and Rho families at the crossroads of signal transduction and GLUT4 vesicle traffic. *Acta Physiol.* 192(1): 61-74.
- Ito H, Fukuda Y. 1983. Transformation of intact yeast cells treated with alkali cations. *J Bacteriol.* 153(1): 163-8.
- Jackson CL. 2009. Mechanisms of transport through the Golgi complex. *J Cell Sci.* 122(4): 443-452.
- Jahn R. 2000. Sec1/Munc18 proteins: mediators of membrane fusion moving to center stage. *Neuron.* 27: 201-4.
- Jahn R, Lang T, Sudhof TC. 2003. Membrane Fusion. *Cell.* 112(4): 519-33.
- Jahn R, Scheller RH. 2006. SNAREs - engines for membrane fusion. *Nat Rev Mol Cell Biol.* 7(9): 631-643.
- James, DE. 2005. MUNC-ing around with insulin action. *J Clin Invest.* 89: 1367-74.

- Jedrychowski MP, Gartner CA, Gygi SP, Zhou L, Herz J, Kandror KV, Pilch PF. 2010. Proteomic Analysis of GLUT4 Storage Vesicles Reveals LRP1 to Be an Important Vesicle Component and Target of Insulin Signaling. *J Biol Chem.* 285(1): 104-114.
- Johannes L, Popoff V. 2008. Tracing the Retrograde Route in Protein Trafficking. *Cell.* 135(7): 1175-1187.
- Joost HG, Weber TM, Cushman SW. 1988. Qualitative and quantitative comparison of glucose transport activity and glucose transporter concentration in plasma membranes from basal and insulin-stimulated rat adipose cells. *Biochem J.* 249(1): 155-161.
- Joost HG, Schurmann A. 2001. Subcellular fractionation of adipocytes and 3T3-L1 cells. *Methods Mol Biol.* 155: 77-82.
- Joost HG, Thorens B. 2001. The extended GLUT-family of sugar/polyol transport facilitators: nomenclature, sequence characteristics, and potential function of its novel members. *Mol Membr Biol.* 18(4): 247-56.
- Jordens I, Molle D, Xiong W, Keller SR, McGraw TE. 2010. Insulin-regulated Aminopeptidase Is a Key Regulator of GLUT4 Trafficking by Controlling the Sorting of GLUT4 from Endosomes to Specialized Insulin-regulated Vesicles. *Mol Biol Cell.* 21(12): 2034-2044.
- Jordens I, Molle D, Xiong W, Keller SR, McGraw TE. 2010. IRAP Is a Key Regulator of GLUT4 Trafficking by Controlling the Sorting of GLUT4 from Endosomes to Specialized Insulin-regulated Vesicles. *Mol Biol Cell.* 21(12): E10-02-0158.
- Jung G, Ueno H, Hayashi R. 1999. Carboxypeptidase Y: Structural basis for Protein Sorting and Catalytic Triad. *J Biochem.* 126(1): 1-6.
- Kaestner KH, Christy RJ, McLenithan JC, Braiterman LT, Cornelius P, Pekala PH, Lane MD. 1989. Sequence, tissue distribution, and differential expression of mRNA for a putative insulin-responsive glucose transporter in mouse 3T3-L1 adipocytes. *Proc Natl Acad Sci USA.* 86: 3150-4.
- Kametaka S, Sawada N, Bonifacino JS, Waguri, S. 2010. Functional characterization of protein-sorting machineries at the trans-Golgi network in *Drosophila melanogaster*. *J Cell Sci.* 123(3): 460-471.
- Kanda H, Tamori Y, Shinoda H, Yoshikawa M, Sakaue M, Udagawa J, Otani H, Tashiro F, Miyazaki J, Kasuga M. 2005. Adipocytes from Munc18c-null mice show increased sensitivity to insulin-stimulated GLUT4 externalization. *J Clin Invest.* 115(2): 291-301.
- Kandror KV, Pilch PF. 1996. Compartmentalization of protein traffic in insulin-sensitive cells. *Am J Physiol.* 271(1 Pt 1): E1-14.
- Kandror KV, Pilch PF. 1998. Multiple endosomal recycling pathways in rat adipose cells. *Biochem J.* 331(3): 829-835.
- Kandror KV, Pilch PF. 2006. Isolation of GLUT4 Storage Vesicles. *Curr Protoc Cell Biol.* Chapter 3(Unit 3.20): 3.20.1-3.20.13.

- Kanzaki M, Pessin JE. 2001. Insulin-stimulated GLUT4 Translocation in Adipocytes Is Dependent upon Cortical Actin Remodeling. *J Biol Chem.* 276(45): 42436-42444.
- Kanzaki M. 2006. Insulin Receptor Signals Regulating GLUT4 Translocation and Actin Dynamics. *Endocr J.* 53(3): 267-293.
- Karylowski O, Zeigerer A, Cohen A, McGraw TE. 2004. GLUT4 Is Retained by an Intracellular Cycle of Vesicle Formation and Fusion with Endosomes. *Mol Biol Cell.* 15(2): 870-882.
- Kasahara T, Kasahara M. 1997. Characterization of rat GLUT4 glucose transporter expressed in the yeast *Saccharomyces cerevisiae*: comparison with Glut1 glucose transporter. *Biochim Biophys Acta.* 1324(1): 111-9.
- Kawaguchi T, Tamori Y, Kanda H, Yoshikawa M, Tateya S, Nishino N, Kasuga M. The t-SNAREs syntaxin4 and SNAP23 but not v-SNARE VAMP2 are indispensable to tether GLUT4 vesicles at the plasma membrane in adipocyte. *Biochem Biophys Res Commun.* 391(3): 1336-1341.
- Keller SR. 2003. The insulin-regulated aminopeptidase: a companion and regulator of GLUT4. *Front Biosci.* 8(s4): 10-20.
- Keller SR. 2004. Role of the Insulin-Regulated Aminopeptidase IRAP in Insulin Action and Diabetes. *Biol Pharm Bull.* 27(6): 761-764.
- Kienle N, Klopper TH, Fasshauer D. 2009. Phylogeny of the SNARE vesicle fusion machinery yields insights into the conservation of the secretory pathway in fungi. *BMC Evol Biol.* 9:19.
- Klip A. 2009. The many ways to regulate glucose transporter 4. *App Physiol Nutr Metab.* 34(3): 481-7.
- Konstantopoulos N, Molero-Navajas JC. 2009. The Measurement of GLUT4 Translocation in 3T3-L1 Adipocytes. Type 2 Diabetes: 111-135. Academic Press.
- Koumanov FB, Jin B, Yang J, Holman GD. 2005. Insulin signaling meets vesicle traffic of GLUT4 at a plasma-membrane-activated fusion step. *Cell Metab.* 2(3): 179-189.
- Krogh BO, Symington LS. 2004. Recombination proteins in yeast. *Annu Rev Genet.* 38(1): 233-271.
- Kuliawat R, Kalinina E, Bock J, Fricker L, McGraw TE, Kim SR, Zhong J, Scheller R, Arvan P. 2004. Syntaxin-6 SNARE Involvement in Secretory and Endocytic Pathways of Cultured Pancreatic Beta-Cells. *Mol Biol Cell.* 15(4): 1690-1701.
- Koumandou VL, Dacks JB, Coulson RMR, Field, MC. 2007. Control systems for membrane fusion in the ancestral eukaryote; evolution of tethering complexes and SM Proteins. *BMC Evol Biol.* 7:29.

- Lakshmanan J, Elmendorf JS, Ozcan S. 2003. Analysis of Insulin-Stimulated Glucose Uptake in Differentiated 3T3-L1 Adipocytes. *Methods Mol Med.* 83: 97-103.
- Lalioti V, Vergarajauregui S, Sandoval IV. 2001. Targeting motifs in GLUT4. *Mol Membr Biol.* 18: 257-64.
- Latham CF, Lopez JA, Hu SH, Gee CL, Westbury E, Blair DH, Armishaw CJ, Alewood PF, Bryant NJ, James DE, Martin JL. 2006. Molecular dissection of the Munc18c/Syntaxin 4 Interaction: Implications for regulation of Membrane Trafficking. *Traffic.* 7: 1408-19.
- Leabu M. 2006. Membrane fusion in cells: molecular machinery and mechanisms. *J Cell Mol Med.* 10: 423-7.
- Lee J, Pilch PF. 1994. The insulin receptor: structure, function, and signalling. *Am J Physiol.* 266(2): C319-34.
- Lemmon SK, and Traub LM. 2000. Sorting in the endosomal system in yeast and animal cells. *Curr Opin Cell Biol.* 12(4): 457-466.
- Leney SE, Tavare JM. 2009. The molecular basis of insulin-stimulated glucose uptake: signalling, trafficking and potential drug targets. *J Endocrinol.* 203(1): 1-18.
- Lewis MJ, Pelham HRB. 2002. A New Yeast Endosomal SNARE Related to Mammalian Syntaxin 8. *Traffic.* 3(12): 922-929.
- Li L, Bakirtzi VK, Watson RT, Pessin JE, Kandror KV. 2009. The C-terminus of GLUT4 targets the transporter to the perinuclear compartment but not to the insulin-responsive vesicles. *Biochem J.* 419(1): 105-112.
- Liao W, Nguyen MTA, Takeshi I, Singer O, Verma IM, Olefsky JM. 2006. Lentiviral Short Hairpin Ribonucleic Acid-Mediated Knockdown of GLUT4 in 3T3-L1 Adipocytes. *Endocrinology.* 147(5): 2245-2252.
- Liao W, Nguyen MTA, Yoshizaki T, Favellyukis S, Patsouris D, Imamura T, Verma IM, Olefsky JM. 2007. Suppression of PPAR-gamma attenuates insulin-stimulated glucose uptake by affecting both GLUT1 and GLUT4 in 3T3-L1 adipocytes. *Am J Physiol Endocrinol Metab.* 293(1): E219-227.
- Liewen H, Meinhold-Heerlein I, Oliveira V, Schwarzenbacher R, Luo G, Wadle A, Jung M, Pfreundschuh M, Stenner-Liewen F. 2005. Characterization of the human GARP (Golgi associated retrograde protein) complex. *Exp Cell Res.* 306(1): 24-34.
- Liu G, Hou JC, Watson RT, Pessin JE. 2005. Initial entry of IRAP into the insulin-responsive storage compartment occurs prior to basal or insulin-stimulated plasma membrane recycling. *Am J Physiol Endocrinol Metab.* 289(5): E746-752.
- Liu L, Jedrychowski MP, Gygi SP, Pilch PF. 2006. Role of Insulin-dependent Cortical Fodrin/Spectrin Remodeling in Glucose Transporter 4 Translocation in Rat Adipocytes. *Mol Biol Cell.* 17(10): 4249-4256.

- Livingstone C, James DE, Rice JE, Hanpeter D, Gould GW. 1996. Compartment ablation analysis of the insulin-responsive glucose transporter (GLUT4) in 3T3-L1 adipocytes. *Biochem J.* 315(2): 487-495.
- Lizunov VA, Matsumoto H, Zimmerberg J, Cushman SW, Frolov VA. 2005. Insulin stimulates the halting, tethering, and fusion of mobile GLUT4 vesicles in rat adipose cells. *J Cell Biol.* 169(3): 481-489.
- Lizunov VA, Lisinski I, Stenkul K, Zimmerberg J, Cushman SW. 2009. Insulin Regulates Fusion of GLUT4 Vesicles Independent of Exo70-mediated Tethering. *J Biol Chem.* 284(12): 7914-7919.
- Luzio JP, Pryor PR, Bright NA. 2007. Lysosomes: fusion and function. *Nat Rev Mol Cell Biol.* 8(8): 622-632.
- Ma H, Kunes S, Schatz PJ, Botstein D. 1987. Plasmid construction by homologous recombination in yeast. *Gene.* 58(2-3): 201-16.
- Macaulay SL, Grusovin J, Stoichevska V, Ryan JM, Castelli LA, Ward CW. 2002. Cellular munc18c levels can modulate glucose transport rate and GLUT4 translocation in 3T3L1 cells. *FEBS Lett.* 528: 154-160.
- MacDonald C, Munson M, Bryant NJ. 2010. Autoinhibition of SNAREcomplex assembly by a conformational switch represents a conserved feature of syntaxins. *Biochem Soc Trans.* 38(Pt 1): 209-12.
- Maianu L, Keller SR, Garvey WT. 2001. Adipocytes Exhibit Abnormal Subcellular Distribution and Translocation of Vesicles Containing Glucose Transporter 4 and Insulin-Regulated Aminopeptidase in Type 2 Diabetes Mellitus: Implications Regarding Defects in Vesicle Trafficking. *J Clin Endocrinol Metab.* 86(11): 5450-5456.
- Maier VH, Gould GW. 2000. Long-term insulin treatment of 3T3-L1 adipocytes results in mis-targeting of GLUT4: implications for insulin-stimulated glucose transport. *Diabetologia.* 43: 1273-1281.
- Malide D, Dwyer NK, Blanchette-Mackie EJ, Cushman SW. 1997. Immunocytochemical evidence that GLUT4 resides in a specialized translocation post-endosomal VAMP2-positive compartment in rat adipose cells in the absence of insulin. *J Histochem Cytochem.* 45: 1083-96.
- Malide D, St-Denis J-F, Keller SR, Cushman SW. 1997. Vp165 and GLUT4 share similar vesicle pools along their trafficking pathways in rat adipose cells. *FEBS Lett.* 409(3): 461-468.
- Malide D. 2001. Confocal microscopy of adipocytes. *Methods Mol Biol.* 155: 53-64.
- Mallard F, Tang BF. 2002. Early/recycling endosomes-to-TGN transport involves two SNARE complexes and a Rab6 isoform. *J Cell Biol.* 156(4): 653-64.
- Malsam J, Kreye S, Sollner T. 2008. Membrane traffic in the secretory pathway. *Cell Mol Life Sci.* 65(18): 2814-2832.

- Manjunath M, Haoquan W, Sandesh S, Premlata S. 2009. Lentiviral delivery of short hairpin RNAs. *Adv Drug Deliv Rev.* 61(9):732-745.
- Marsh BJ, Alm RA, McIntosh SR, James DE. 1995. Molecular regulation of GLUT-4 targeting in 3T3-L1 adipocytes. *J Cell Biol.* 130(5): 1081-1091.
- Marsh BJ, Martin S, Melvin DR, Martin LB, Alm RA, Gould GW, James DE. 1998. Mutational analysis of the carboxy-terminal phosphorylation site of GLUT-4 in 3T3-L1 adipocytes. *Am J Physiol Endocrinol Metab.* 275(3): E412-422.
- Martens S, McMahon HT. 2008. Mechanisms of membrane fusion: disparate players and common principles. *Nat Rev Mol Cell Biol.* 9(7): 543-556.
- Martin S, Millar CA, Lyttle CT, Meerloo T, Marsh BJ, Gould GW, James DE. 2000. Effects of insulin on intracellular GLUT4 vesicles in adipocytes: evidence for a secretory mode of regulation. *J Cell Sci.* 113(19): 3427-3438.
- Masters JR, Stacey GN. 2007. Changing medium and passaging cell lines. *Nat. Protoc.* 2(9): 2276-2284.
- Maxfield FR, McGraw TE. 2004. Endocytic recycling. *Nat Rev Mol Cell Biol.* 5(2): 121-132.
- Mayor S, Pagano RE. 2007. Pathways of clathrin-independent endocytosis. *Nat Rev Mol Cell Biol.* 8(8): 603-612.
- McBride HM, Rybin V, Murphy C, Giner A, Teasdale R, Zerial M. 1999. Oligomeric Complexes Link Rab5 Effectors with NSF and Drive Membrane Fusion via Interactions between EEA1 and Syntaxin 13. *Cell.* 98(3): 377-386.
- McGraw TE, Subtil A. 2001. Endocytosis: biochemical analyses. *Curr Protoc Cell Biol.* Chapter 15(Unit 15.3).
- McIntyre G, Fanning G. 2006. Design and cloning strategies for constructing shRNA expression vectors. *BMC Biotechnol.* 6(1): 1.
- McNew JA, Parlati F, Fukuda R, Johnston R J, Paz K, Paumet F, Sollner TH, Rothman JE. 2000. Compartmental specificity of cellular membrane fusion encoded in SNARE proteins. *Nature.* 407(6801): 153-159.
- McNiven MA, Thompson HM. 2006. Vesicle formation at the Plasma Membrane and Trans-Golgi Network: The same but different. *Science.* 313: 591-4.
- Melia TJ, Weber T, McNew JA, Fisher LE, Johnston RJ, Parlati F, Mahal LK, Sollner TH, Rothman JE. 2002. Regulation of membrane fusion by the membrane-proximal coil of the t-SNARE during zippering of SNAREpins. *J Cell Biol.* 158(5): 929-940.
- Miaczynska M, Pelkmans L, Zerial M. 2004. Not just a sink: endosomes in control of signal transduction. *Curr Opin Cell Biol.* 16(4): 400-406.
- Miller SE, Collins BM, McCoy AJ, Robinson MS, Owen DJ. 2007. A SNARE-adaptor interaction is a new mode of cargo recognition in clathrin-coated vesicles. *Nature.* 450(7169): 570-574.

- Mills I, Urbe S, Clague MJ. 2001. Relationships between EEA1 binding partners and their role in endosome fusion. *J Cell Sci.* 114(10): 1959-1965.
- Mima J, Wickner W. 2009. Complex Lipid Requirements for SNARE- and SNARE Chaperone-dependent Membrane Fusion. *J Biol Chem.* 284(40): 27114-27122.
- Mishra VS, Holt SM, Teodoro JM, Kingsmore SF. 1998. Genetic mapping of vacuolar protein sorting-45 (Vps45) on mouse chromosome 3. *Mamm Genome.* 9(1): 90-1.
- Mohammed A, John JR, Dongho K. 2005. Approaches for chemically synthesized siRNA and vector-mediated RNAi. *FEBS Lett.* 579(26): 5974-5981.
- Molero JC, Whitehead JP, Meerloo T, James DE. 2001. Nocodazole inhibits insulin-stimulated glucose transport in 3T3-L1 adipocytes via a microtubule-independent mechanism. *J Biol Chem.* 276(47): 43829-43835.
- Mora S, Pessin JE. 2002. An adipocentric view of signaling and intracellular trafficking. *Diabetes Metab Res Rev.* 18(5): 345-356.
- Morrison HA, Dionne H, Rusten TE, Brech A, Fisher WW, Pfeiffer BD, Celniker SE, Stenmark H, Bilder D. 2008. Regulation of Early Endosomal Entry by the Drosophila Tumor Suppressors Rabenosyn and Vps45. *Mol Biol Cell.* 19(10): 4167-4176.
- Mueckler M. The molecular biology of glucose transport: Relevance to insulin resistance and non-insulin-dependent diabetes mellitus. *J Diabetes Complicat.* 7(2): 130-141.
- Munson M, Chen X, Cocina AE, Schultz SM, Hughson FM. 2000. Interactions within the yeast t-SNARES Sso1p that control SNARE complex assembly. *Nat Struct Biol.* 7: 894-902.
- Munson M, Bryant NJ. 2009. A role for the syntaxin N-terminus. *Biochem J.* 418(1): e1-e3.
- Muretta JM, Romenskaia I, Mastick CC. 2008. Insulin Releases Glut4 from Static Storage Compartments into Cycling Endosomes and Increases the Rate Constant for Glut4 Exocytosis. *J Biol Chem.* 283(1): 311-323.
- Muretta JM, Mastick CC, Gerald L. 2009. Chapter 10 How Insulin Regulates Glucose Transport in Adipocytes. *Vitamins & Hormones.* Academic Press. Volume 80: 245-286.
- Negrel R, Dani C. 2001. Cultures of adipose precursor cells and cells of clonal lines from animal white adipose tissue. *Methods Mol Biol.* 155: 225-37.
- Ng Y, Ramm G, Lopez JA, James DE. 2008. Rapid activation of Akt2 is Sufficient to Stimulate Glut4 Translocation in 3T3-L1 Adipocytes. *Cell Metab.* 7(4): 348-356.
- Ng Y, Ramm G, Burchfield JG, Coster ACF, Stockli J, James DE. 2010. Cluster analysis of Insulin action in adipocytes reveals a key role for Akt at the plasma

membrane. *J Biol Chem.* 285(4): 2245-57.

Nichols BJ, Holthuis JC, Pelham HR. 1998. The Sec1p homologue Vps45p binds to the syntaxin Tlg2p. *Eur J Cell Biol.* 77(4): 263-8.

Niedenthal RK, Riles L, Johnston M, Hegemann JH. 1996. Green Fluorescent Protein as a Marker for Gene Expression and Subcellular Localization in Budding Yeast. *Yeast.* 12: 773-786.

Nielsen E, Severin F, Backer JM, Hyman AA, Zerial M. 1999. Rab5 regulates motility of early endosomes on microtubules. *Nat Cell Biol.* 1(6): 376-382.

Nielsen E, Christoforidis S, Uttenweiler-Joseph S, Miaczynska M, Dewitte F, Wilm M, Hoflack B, Zerial M. 2000. Rabenosyn-5, a Novel Rab5 Effector, Is Complexed with hvp45 and Recruited to Endosomes through a Fyve Finger Domain. *J Cell Biol.* 151(3): 601-612.

Nothwehr SF, Stevens TH. 1994. Sorting of membrane proteins in the yeast secretory pathway. *J Biol Chem.* 269(14): 10185-10188.

Novick P, Ferro S, Schekman R. 1981. Order of Events in the Yeast Secretory Pathway. *Cell.* 25(2): 461-9.

Novick P, Zerial M. 1997. The diversity of Rab proteins in vesicle transport. *Curr Opin Cell Biol.* 9(4): 496-504.

Ohya T, Miaczynska M, Coskun U, Lommer B, Runge A, Drechsel D, Kalaidzidis Y, Zerial M. 2009. Reconstitution of Rab- and SNARE-dependent membrane fusion by synthetic endosomes. *Nature.* 459(7250): 1091-1097.

Okada T, Kawano Y, Sakaibara T, Hazeki O, Ui M. 1994. Essential role of phosphatidylinositol 3-kinase in insulin-induced glucose transport and antilipolysis in rat adipocytes. Studies with a selective inhibitor wortmannin. *J Biol Chem.* 269(5): 3568-73.

Orme CM, Bogan JS. 2009. Cell Biology. Sorting out diabetes. *Science.* 324(5931): 1155-6.

Ostrowicz CW, Meiringer CTA, Ungermann C. 2008. Yeast vacuole fusion: A model system for eukaryotic endomembrane dynamics. *Autophagy.* 4(1): 5-19.

Patel N, Huang C, Klip A. 2006. Cellular location of insulin-triggered signals and implications for glucose uptake. *Pflügers Arch.* 451(4): 499-510.

Paumet F, Bruegger B, Parlati F, McNew JA, Sollner TH, Rothman JE. 2001. A t-SNARE of the endocytic pathway must be activated for fusion. *J Cell Biol.* 155(6): 961-968.

Pelham HRB. 1999. Intracellular membrane traffic: getting proteins sorted. The 1999 Croonian Lecture. *Philos Trans R Soc Lond B Biol Sci.* 354(1388): 1471-1478.

Perera HKI, Clarke M, Morris NJ, Hong W, Chamberlain LH, Gould GW. 2003. Syntaxin 6 Regulates Glut4 Trafficking in 3T3-L1 Adipocytes. *Mol Biol Cell.* 14(7): 2946-2958.

- Perez-Victoria FJ, Bonifacino JS. 2009. Dual Roles of the Mammalian GARP Complex in Tethering and SNARE Complex Assembly at the trans-Golgi Network. *Mol Cell Biol.* 29(19): 5251-5263.
- Pessin JE, Bell GI. 1992. Mammalian Facilitative Glucose Transporter Family: Structure and Molecular Regulation. *Annu Rev Physiol.* 54(1): 911-930.
- Pessin JE, Thurmond DC, Elmendorf JS, Coker KJ, Okada S. 1999. Molecular basis of insulin-stimulated GLUT4 vesicle trafficking. Location! Location! Location! *J Biol Chem.* 274(5): 2593-6.
- Peterson KF, Shulman GI. 2006. Etiology of Insulin Resistance. *Am J Med.* 119: 10S-16S.
- Peterson MR, Burd CG, Emr SD. 1999. Vac1p coordinates Rab and phosphatidylinositol 3-kinase signalling in Vps45p-dependent vesicle docking/fusion at the endosome. *Curr Biol.* 9(3): 159-62.
- Pevsner J, Hsu SC, Hyde PS, Scheller RH. 1996. Mammalian homologues of yeast vacuolar protein sorting (vps) genes implicated in Golgi-to-lysosome trafficking. *Gene.* 183(1-2): 7-14.
- Pilch, P. 2008. The mass action hypothesis: formation of Glut4 storage vesicles, a tissue-specific, regulated exocytic compartment. *Acta Physiol.* 192(1): 89-101.
- Piper RC, Whitters EA, Stevens TH. 1994. Yeast Vps45p is a Sec1p- like protein required for the consumption of vacuole-targeted, post-Golgi transport vesicles. *Eur J Cell Biol.* 65: 305-18.
- Piper RC, Bryant NJ, Stevens TH. 1997. The Membrane Protein Alkaline Phosphatase Is Delivered to the Vacuole by a Route That Is Distinct from the VPS-dependent Pathway. *J Cell Biol.* 138(3): 531-545.
- Piper RC, Whitters EA, Stevens TH. 1999. Yeast Vps45p is a Sec1p-like protein required for the consumption of vacuole-targeted, post-Golgi transport vesicles. *Eur J Cell Biol.* 65(2): 305-18.
- Piper RC, Luzio JP. 2001. Late Endosomes: Sorting and Partitioning in Multivesicular Bodies. *Traffic.* 2(9): 612-621.
- Poteryaev D, Datta S, Ackema K, Zerial M, Spang A. 2010. Identification of the Switch in Early-to-Late Endosome Transition. *Cell.* 141(3): 497-508.
- Prekeris RE, Klumperman J, Chen YA, Scheller RH. 1998. Syntaxin 13 Mediates Cycling of Plasma Membrane Proteins via Tubulovesicular Recycling Endosomes. *J Cell Biol.* 143(4): 957-971.
- Proctor KM, Miller SCM, Bryant NJ, Gould GW. 2006. Syntaxin 16 controls the intracellular sequestration of GLUT4 in 3T3-L1 adipocytes. *Biochem Biophys Res Commun.* 347(2): 433-438.

- Rahajeng J, Caplan S, Naslavsky N. 2010. Common and distinct roles for the binding partners Rabenosyn-5 and Vps45 in the regulation of endocytic trafficking in mammalian cells. *Exp Cell Res.* 316(5): 859-874.
- Ramm G, Slot JW, James DE, Stoorvogel W. 2000. Insulin recruits GLUT4 from specialized VAMP 2-carrying vesicles as well as from the dynamic endosomal/trans-golgi network in rat adipocytes. *Mol Biol Cell.* 11: 4079-91.
- Ramm G, James DE. 2005. GLUT4 trafficking in a test tube. *Cell Metab.* 2(3): 150-152.
- Raposo G, Stenmark H. 2008. Membranes and organelles. *Curr Opin Cell Biol.* 20(4): 357-359.
- Raymond CK, Howald-Stevenson I, Vater CA, Stevens TH. 1992. Morphological classification of the yeast vacuolar sorting mutants: evidence for a prevacuolar compartment in Class E Vps mutants. *Mol Biol Cell.* 3(12):1389-1402.
- Rea S, James DE. 1997. Moving GLUT4: the biogenesis and trafficking of GLUT4 storage vesicles. *Diabetes.* 46(11): 1667-77.
- Rizo J. 2003. SNARE function revisited. *Nat Struct Mol Biol.* 10(6): 417-419.
- Rizo J, Dai H. 2007. How much can SNAREs flex their muscles? *Nat Struct Mol Biol.* 14(10): 880-882.
- Rizo J, Sudhof TC. 2002. Snares and Munc18 in synaptic vesicle fusion. *Nat Rev NeuroSci.* 3(8): 641-53.
- Roberg KJ, Rowley N, Kaiser CA. 1997. Physiological Regulation of Membrane Protein Sorting Late in the Secretory Pathway of *Saccharomyces cerevisiae*. *J Cell Biol.* 137(7): 1469-1482.
- Robinson JS, Klionsky DJ, Banta LM, Emr SD. 1988. Protein sorting in *Saccharomyces cerevisiae*: isolation of mutants defective in the delivery and processing of multiple vacuolar hydrolases. *Mol Cell Biol.* 8(11): 4936-4948.
- Robinson MS, Watts C, Zerial M. 1996. Membrane dynamics in endocytosis. *Cell.* 84(1): 13-21.
- Roederer AD, Shaw JM. 1996. Vacuole portioning during meiotic division in yeast. *Genetics.* 144: 445-58.
- Rodkey TL, Liu S, Barry M, McNew JA. 2008. Munc18a Scaffolds SNARE Assembly to Promote Membrane Fusion. *Mol Biol Cell.* 19(12): 5422-5434.
- Rojas R, van Vlijmen T, Mardones GA, Prabhu Y, Rojas AL, Mohammed S, Heck AJR, Raposo G, van der Sluijs P, Bonifacino JS. 2008. Regulation of retromer recruitment to endosomes by sequential action of Rab5 and Rab7. *J Cell Biol.* 183(3): 513-526.
- Rose MD, Broach JR. 1991. Cloning genes by complementation in yeast. *Methods Enzymol.* 194: 195-230.

Rossi JJ. 2008. Expression Strategies for Short Hairpin RNA Interference Triggers. *Hum Gene Ther.* 19(4): 313-317.

Rothman JE, Wieland FT. 1996. Protein Sorting by Transport Vesicles. *Science.* 272(5259): 227-34.

Rothman JH, Stevens TH. 1986. Protein sorting in yeast: mutants defective in vacuole biogenesis mislocalize vacuolar proteins into the late secretory pathway. *Cell.* 47: 1041-51.

Rothman JH, Howland I, Stevens TH. 1989. Characterization of genes required for protein sorting and vacuolar function in the yeast *Saccharomyces cerevisiae*. *EMBO J.* 8(7): 2057-65.

Rubin BR, Bogan JS, Gerald L. 2009. Chapter 7: Intracellular Retention and Insulin-Stimulated Mobilization of GLUT4 Glucose Transporters. Vitamins & Hormones. Academic Press. Volume 80: 155-192.

Sadowski HB, Wheeler TT, Young DA. 1992. Gene expression during 3T3-L1 Adipocyte Differentiation. *J Biol Chem.* 266: 4722-31.

Sakamoto K, Holman GD. 2008. Emerging role for AS160/TBC1D4 and TBC1D1 in the regulation of GLUT4 traffic. *Am J Physiol Endocrinol Metab.* 295(1): E29-37.

Salaün C, James DJ, Greaves J, Chamberlain LH. 2004. Plasma membrane targeting of exocytic SNARE proteins. *Biochim Biophys Acta.* 1693(2): 81-89.

Saltiel AR, Kahn CR. 2001. Insulin signalling and the regulation of glucose and lipid metabolism. *Nature.* 414: 799-806.

San Filippo J, Sung P, Klein H. 2008. Mechanism of Eukaryotic Homologous Recombination. *Annu Rev Biochem.* 77(1): 229-257.

Sandy P, Ventura A, Jacks T. 2005. Mammalian RNAi: a practical guide. *Biotechniques.* 39(2): 215-24.

Sato TK, Rehling P, Peterson MR, Emr SD. 2000. Class C Vps protein complex regulates vacuolar SNARE pairing and is required for vesicle docking/fusion. *Mol Cell.* 6: 661-71.

Schmitt HD, Jahn R. 2009. A tethering complex recruits SNAREs and grabs vesicles. *Cell.* 139(6): 1053-5.

Schürmann A, Monden I, Joost HG, Keller K. 1992. Subcellular distribution and activity of glucose transporter isoforms GLUT1 and GLUT4 transiently expressed in COS-7 cells. *Biochim Biophys Acta.* 1131(3): 245-252.

Scita G, Di Fiore PP. The endocytic matrix. *Nature.* 463(7280): 464-473.

Shen J, Tareste DC, Paumet F, Rothman JE, Melia TJ. 2007. Selective Activation of Cognate SNAREpins by Sec1/Munc18 proteins. *Cell.* 128(1): 183-95.

Shewan AM, van Dam EM, Martin S, Luen TB, Hong W, Bryant NJ, James DE. 2003. GLUT4 Recycles via a trans-Golgi Network (TGN) Subdomain Enriched in

Syntaxins 6 and 16 But Not TGN38: Involvement of an Acidic Targeting Motif. *Mol Biol Cell*. 14(3): 973-986.

Shi J, Huang G, Kandror KV. 2008. Self-assembly of Glut4 Storage Vesicles during Differentiation of 3T3-L1 Adipocytes. *J Biol Chem*. 283(44): 30311-21.

Shi J, Kandror KV. 2008. Study of Glucose Uptake in Adipose Cells. Adipose Tissue Protocols: 307-315.

Shi X, Burkart A, Nicoloso SM, Czech MP, Straubhaar J, Corvera S. 2008. Paradoxical Effect of Mitochondrial Respiratory Chain Impairment on Insulin Signaling and Glucose Transport in Adipose Cells. *J Biol Chem*. 283(45): 30658-30667.

Shin H-W, Hayashi M, Christoforidis S, Lacas-Gervais S, Hoepfner S, Wenk MR, Modregger J, Uttenweiler-Joseph S, Wilm M, Nystuen A, Frankel WN, Solimena M, De Camilli P, Zerial M. 2005. An enzymatic cascade of Rab5 effectors regulates phosphoinositide turnover in the endocytic pathway. *J Cell Biol*. 170(4): 607-618.

Sikorski RS, Hieter P. 1989. A System of Shuttle Vectors and Yeast Host Strains Designed for Efficient Manipulation of DNA in *Saccharomyces cerevisiae*. *Genetics*. 122(1): 19-27.

Simonsen A, Bremnes B, Ronning E, Aasland R, Stenmark H. 1998. Syntaxin-16, a putative Golgi t-SNARE. *Eur J Cell Biol*. 75(3): 223-31.

Simpson F, Whitehead JP, James DE. 2001. GLUT4- At the Cross Roads Between Membrane Trafficking and Signal Transduction. *Traffic*. 2(1): 2-11.

Siolas D, Lerner C, Burchard J, Ge W, Linsley PS, Paddison PJ, Hanno GJ, Cleary MA. 2005. Synthetic shRNAs as potent RNAi triggers. *Nat Biotech*. 23(2): 227-231.

Slot JW, Geuze HJ. 1991. Immuno-localization of the insulin regulatable glucose Transporter in brown adipose tissue of the rat. *J Cell Biol*. 113(1): 123-35.

Snyder D, Kelly M, Woodbury D. 2006. SNARE complex regulation by phosphorylation. *Cell Biochem Biophys*. 45(1): 111-123.

Soldati T, Schliwa M. 2006. Powering membrane traffic in endocytosis and recycling. *Nat Rev Mol Cell Biol*. 7(12): 897-908.

Sollner T, Bennett MK, Whiteheart SW, Scheller RH, Rothman JE. 1993. A protein assembly-disassembly pathway in vitro that may correspond to sequential steps of synaptic vesicle docking, activation, and fusion. *Cell*. 75(3): 409-18.

Somwar A, Koterski S, Sweeney G, Sciotti R, Djuric S, Berg C, Trevillyan J, Scherer PE, Rondinone CM, Klip A. 2002. A dominant-negative p38 MAPK Mutant and Novel Selective Inhibitors of p38 MAPK reduce Insulin-stimulated glucose uptake in 3T3-L1 adipocytes without affecting GLUT4 translocation. *J Biol Chem*. 277: 50386-95.

Sorensen JB. 2009. Conflicting Views on the Membrane Fusion Machinery and the Fusion Pore. *Annu Rev Cell Dev Biol.* 25(1): 513-537.

Sorkin A, von Zastrow M. 2002. Signal transduction and endocytosis: close encounters of many kinds. *Nat Rev Mol Cell Biol.* 3(8): 600-614.

Sorkin A, von Zastrow M. 2009. Endocytosis and signalling: intertwining molecular networks. *Nat Rev Mol Cell Biol.* 10(9): 609-622.

Spang A. 2008. Membrane traffic in the secretory pathway. *Cell Mol Life Sci.* 65(18): 2781-2789.

Stack JH, Horazdovsky B, Emr SD. 1995. Receptor-Mediated Protein Sorting to the Vacuole in Yeast: Roles for a Protein Kinase, a Lipid Kinase and GTP-Binding Proteins. *Annu Rev Cell Dev Biol.* 11(1): 1-33.

St-Denis JF, Cushman SW. 1998. Role of SNAREs in the GLUT4 translocation response to insulin in adipose cells and muscle. *J Basic Clin Physiol Pharmacol.* 9(2-4): 153-65.

Stenmark H. 2009. Rab GTPases as coordinators of vesicle traffic. *Nat Rev Mol Cell Biol.* 10(8): 513-525.

Stockli J, Fazakerley DJ, Coster ACF, Holman GD, James DE. 2010. Muscling in on GLUT4 kinetics. *Commun Integr Biol.* 3(3): 260-2.

Struthers MS, Shanks SG, MacDonald C, Carpp LN, Drozdowska AM, Kioumourtzoglou D, Furgason MLM, Munson M, Bryant, NJ. 2009. Functional homology of mammalian syntaxin 16 and yeast Tlg2p reveals a conserved regulatory mechanism. *J Cell Sci.* 122(13): 2292-2299.

Sudhof TC, Rothman JE. 2009. Membrane Fusion: Grappling with SNARE and SM Proteins. *Science.* 323(5913): 474-7.

Tamori Y, Kawanishi M, Niki T, Shinoda H, Araki S, Okazawa H, Kasuga M. 1998. Inhibition of Insulin-induced GLUT4 Translocation by Munc18c through Interaction with Syntaxin4 in 3T3-L1 Adipocytes. *J Biol Chem.* 273(31): 19740-19746.

Taniguchi CM, Emanuelli B, Khan CR. 2006. Critical nodes in signalling pathways: insights into insulin action. *Nat Rev Mol Cell Biol.* 7(2): 85-96.

Tanti JF, Cormont M, Gremeaux T, Le Marchand-Brustel Y. 2001. Assays of glucose entry, glucose transporter amount, and translocation. *Methods Mol Biol.* 155: 157-65.

Tellam JT, Macaulay SL, McIntosh S, Hewish DR, Ward CW, James DE. 1997. Characterization of Munc-18c and Syntaxin-4 in 3T3-L1 Adipocytes. *J Biol Chem.* 272(10): 6179-6186.

Tellam J, James DE, Stevens TH, Piper RC. 1997. Identification of a Mammalian Golgi Sec1p-like Protein, mVps45. *J Biol Chem.* 272(10): 6187-6193.

Thong FSL, Dugani CB, Klip A. 2005. Turning Signals On and Off: GLUT4 Traffic in the Insulin-Signaling Highway. *Physiology*. 20(4): 271-284.

Thurmond DC, Ceresa BP, Okada S, Elmendorf JS, Coker K, Pessin JE. 1998. Regulation of Insulin-stimulated GLUT4 translocation by Munc18c in 3T3L1 adipocytes. *J Biol Chem*. 273: 33876-83.

Thurmond DC, Pessin JE. 2001. Molecular machinery involved in the insulin-regulated fusion of GLUT4-containing vesicles with the plasma membrane. *Mol Membr Biol*. 18(4): 237-45.

Thurmond DC, Gonelle-Gispert C, Furukawa M, Halban P A, Pessin JE. 2003. Glucose-Stimulated Insulin Secretion Is Coupled to the Interaction of Actin with the t-SNARE (Target Membrane Soluble N-Ethylmaleimide-Sensitive Factor Attachment Protein Receptor Protein) Complex. *Mol Endocrinol*. 17(4): 732-742.

Tishgarten T, Yin FF, Grant TR, Lipscomb LA, Faucher KM, Dluhy RA, Stevens TH, Von Mollard GF. 1999. Structures of yeast vesicle trafficking proteins. *Protein Sci*. 8(11): 2465-2473.

Togneri J, Cheng Y-S, Munson M, Hughson FM, Carr C M. 2006. Specific SNARE complex binding mode of the Sec1/Munc-18 protein, Sec1p. *Proc Natl Acad Sci*. 103(47): 17730-17735.

Toonen RF, Verhage M. 2003. Vesicle trafficking: pleasure and pain from SM genes. *Trends Cell Biol*. 13(4): 177-186.

Toonen RF, Kochubey O, de Wit H, Gulyas-Kovacs A, Konijnenburg B, Sorensen JB, Klingauf J, Verhage M. 2006. Dissecting docking and tethering of secretory vesicles at the target membrane. *EMBO J*. 25(16): 3725-3737.

Torrejón-Escribano B, Gómez de Aranda I, Blasi J. 2002. SNARE expression and distribution during 3T3-L1 adipocyte differentiation. *FEBS Lett*. 512(1-3): 275-281.

Tozzo E, Kahn BB, Pilch PF, Kandror KV. 1996. GLUT4 is targeted to specific vesicles in adipocytes of transgenic mice overexpressing GLUT4 selectively in adipose tissue. *J Biol Chem*. 271(18):10490-4.

Tran JH, Chen, C-J, Emr SD, Schekman R. 2009. Cargo sorting into multivesicular bodies in vitro. *Proc Natl Acad Sci*. 106(41): 17395-17400.

Umahara M, Okada S, Yamada E, Saito T, Ohshima K, Hashimoto K, Yamada M, Shimizu H, Pessin JE, Mori M. 2008. Tyrosine Phosphorylation of Munc18c Regulates Platelet-Derived Growth Factor-Stimulated Glucose Transporter 4 Translocation in 3T3L1 Adipocytes. *Endocrinology*. 149(1): 40-49.

Ungar D, Hughson FM. 2003. Snare protein structure and function. *Annu Rev Cell Dev Biol*. 19(1): 493-517.

Varlamov O, Volchuk A, Rahimian V, Doege CA, Paumet F, Eng WS, Arango N, Parlati F, Ravazzola M, Orci L, Sollner TH, Rothman JE. 2004. i-SNAREs. *J Cell Biol*. 164(1): 79-88.

- Verhey KJ, Hausdorff SF, Birnbaum MJ. 1993. Identification of the carboxy terminus as important for the isoform-specific subcellular targeting of glucose transporter proteins. *J Cell Biol.* 123(1): 137-147.
- Verhey KJ, Yeh JI, Birnbaum MJ. 1995. Distinct signals in the GLUT4 glucose transporter for internalization and for targeting to an insulin-responsive compartment. *J Cell Biol.* 130(5): 1071-1079.
- Vida TA, Emr SD. 1995. A new vital stain for visualizing vacuolar membrane dynamics and endocytosis in yeast. *J Cell Biol.* 128(5): 779-92.
- Watson RT, Pessin JE. 2000. Functional Cooperation of Two Independent Targeting Domains in Syntaxin 6 Is Required for Its Efficient Localization in the trans-Golgi Network of 3T3L1 Adipocytes. *J Biol Chem.* 275(2): 1261-1268.
- Watson RT, Pessin JE. 2001. Intracellular Organization of Insulin Signaling and GLUT4 Translocation. *Recent Prog Horm Res.* 56(1): 175-194.
- Watson RT, Kanzaki M, Pessin JE. 2004. Regulated Membrane Trafficking of the Insulin-Responsive Glucose Transporter 4 in Adipocytes. *Endocr Rev.* 25(2): 177-204.
- Watson RT, Pessin JE. 2006. Bridging the GAP between insulin signaling and GLUT4 translocation. *Trends Biochem Sci.* 31(4): 215-222.
- Watson RT, Pessin JE. 2007. GLUT4 translocation: The last 200 nanometers. *Cell Signal.* 19(11): 2209-2217.
- Watson RT, Hou JC, Pessin JE. 2008. Recycling of IRAP from the plasma membrane back to the insulin-responsive compartment requires the Q-SNARE syntaxin 6 but not the GGA clathrin adaptors. *J Cell Sci.* 121(Pt 8): 1243-51.
- Webb GC, Hoedt M, Poole LJ, Jones EW. 1997. Genetic interactions between a pep7 mutation and the PEP12 and VPS45 genes: evidence for a novel SNARE component in transport between the *Saccharomyces cerevisiae* golgi complex and endosome. *Genetics.* 147(2): 467-78.
- Weber T, Zemelman BV, McNew JA, Westermann B, Gmachl M, Parlati F, Sollner TH, Rothman JE. 1998. SNAREpins: minimal machinery for membrane fusion. *Cell.* 92(6): 759-72.
- Whitesell RR, Abumrad NA. 1986. Modulation of basal glucose transporter Km in the adipocyte by insulin and other factors. *J Biol Chem.* 261(32): 15090-15096.
- Whyte JRC, Munro S. 2002. Vesicle tethering complexes in membrane traffic. *J Cell Sci.* 115(13): 2627-2637.
- Wickner W, Haas A. 2000. Yeast homotypic vacuole fusion: a window on organelle trafficking mechanisms. *Annu Rev Biochem.* 69: 247-75.
- Wickner W, Schekman R. 2008. Membrane Fusion. *Nat Struct Mol Biol.* 15(7): 658-64.
- Wieczorke R, Dugai S. 2003. Characterisation of mammalian GLUT glucose

- transporters in a heterologous yeast expression system. *Cell Physiol Biochem.* 13(3): 123-34.
- Wiederhold K, Fasshauer D. 2009. Is Assembly of the SNARE Complex Enough to Fuel Membrane Fusion? *J Biol Chem.* 284(19): 13143-13152.
- Williams D, Pessin JE. 2008. Mapping of R-SNARE function at distinct intracellular GLUT4 trafficking steps in adipocytes. *J Cell Biol.* 180(2): 375-387.
- Wilson DW, Wilcox CA, Flynn GC, Chen E, Kuang WJ, Henzel WJ, Block MR, Ullrich A, Rothman JE. 1989. A fusion protein required for vesicle-mediated transport in both mammalian cells and yeast. *Nature.* 339: 355-9.
- Wit de H, Cornelisse LN, Toonen R FG, Verhage M. 2006. Docking of Secretory Vesicles Is Syntaxin Dependent. *PLoS ONE.* 1(1): e126.
- Wuestehube LJ, Duden R, Eun A, Hamamoto S, Korn P, Ram R, Schekman R. 1996. New Mutants of *Saccharomyces cerevisiae* Affected in the Transport of Proteins From the Endoplasmic Reticulum to the Golgi Complex. *Genetics.* 142(2): 393-406.
- Xiong W, Jordens I, Gonzalez E, McGraw TE. 2010. GLUT4 Is Sorted to Vesicles Whose Accumulation Beneath and Insertion into the Plasma Membrane Are Differentially Regulated by Insulin and Selectively Affected by Insulin Resistance. *Mol Biol Cell.* 21(8): 1375-1386.
- Xu J, Messina JL. 2009. Crosstalk between growth hormone and insulin signaling. *Vitam Horm.* 80: 125-53.
- Xu Y-K, Xu K-D, Li J-Y, Feng L-Q, Lang D, Zheng X-X. 2007. Bi-directional transport of GLUT4 vesicles near the plasma membrane of primary rat adipocytes. *Biochem Biophys Res Commun.* 359(1): 121-128.
- Xu Z, Kandror KV. 2002. Translocation of small preformed vesicles is responsible for the insulin activation of glucose transport in adipose cells. Evidence from the in vitro reconstitution assay. *J Biol Chem.* 277(50): 47972-5.
- Yamaguchi T, Dulubova I, Min SW, Chen X, Rizo J, Sudhof TC. 2002. Sly1 binds to Golgi and ER syntaxins via a conserved N-terminal peptide motif. *Dev Cell.* 2: 295-305.
- Yeh JI, Verhey KJ, Birnbaum MJ. 1995. Kinetic analysis of glucose transporter trafficking in fibroblasts and adipocytes. *Biochemistry.* 34(47): 15523-31.
- Yoon TY, Okumus B, Zhang F, Shin YK, Ha T. 2006. Multiple intermediates in SNARE-induced membrane fusion. *Proc Natl Acad Sci.* 103: 19731-36.
- Zaid H, Antonescu CN, Randhawa VK, Klip A. 2008. Insulin action on glucose transporters through molecular switches, tracks and tethers. *Biochem J.* 413(2): 201-15.
- Zaid H, Talior-Volodarsky I, Antonescu C, Liu Z, Klip A. 2009. GAPDH binds GLUT4 reciprocally to hexokinase-II and regulates glucose transport activity. *Biochem J.* 419(2): 475-484.

- Zerial M, McBride H. 2001. Rab proteins as membrane organizers. *Nat Rev Mol Cell Biol.* 2(2): 107-117.
- Zhao C, Matveeva EA, Ren Q, Whitehear SW. 2010. Dissecting the N-Ethylmaleimide-sensitive Factor. *J Biol Chem.* 285(1): 761-772.
- Zhao P, Yang L, Lopez JA, Fan J, Burchfield JG, Bai L, Hong W, Xu T, James DE. 2009. Variations in the requirement for v-SNAREs in GLUT4 trafficking in adipocytes. *J Cell Sci.* 122(19): 3472-3480.
- Zeigerer A, Lampson MA, Karlyowski O, Sabatini DD, Adesnik M, Ren M, McGraw TE. 2002. GLUT4 retention in adipocytes requires two intracellular insulin-regulated transport steps. *Mol Biol Cell.* 13(7): 2421-35.
- Zorzano A, Manuel Serrano R, José FC, Raffaele C, Gutiérrez Fuentes JA. 2005. Intracellular Signaling Mechanisms Involved in Insulin Action. The Metabolic Syndrome at the Beginning of the XXI Century. Madrid, Elsevier Espana: 15-42.
- Zwilling D, Cypionka A, Pohl WH, Fasshauer D, Walla, PJ, Wahl MC, Jahn R. 2007. Early endosomal SNAREs form a structurally conserved SNARE complex and fuse liposomes with multiple topologies. *EMBO J.* 26(1): 9-18.

